

# NASGRO®

## Fracture Mechanics and Fatigue Crack Growth Analysis Software



### Reference Manual

**Version 9.2 Final  
August 2021**

NASGRO® 9.2 is developed and distributed under the terms of a Space Act Agreement  
between NASA Johnson Space Center and Southwest Research Institute®





## DEVELOPMENT AND SUPPORT TEAM

NASGRO® 9.2 has been developed and distributed under the terms of a Space Act Agreement between NASA Johnson Space Center and Southwest Research Institute®, with additional support from the NASGRO Industrial Consortium, the Federal Aviation Administration, and the European Space Agency.

Additional background information and technical support are available on the NASGRO web site at [www.nasgro.swri.org](http://www.nasgro.swri.org).

### NASA Johnson Space Center Team

Joachim M. Beek  
Mohammad Zanganehgheshlaghi  
Randall C. Christian\*  
Yajun Guo\*  
Michael Baldauf\*  
Shakhrukh Ismonov\*  
\*JCLG Group

### Southwest Research Institute Team

R. Craig McClung  
Joseph W. Cardinal  
Yi-Der Lee  
James C. Sobotka  
Vikram Bhamidipati  
Luciano G. Smith  
Ghadir Haikal

### Previous Technical Contributors

Royce G. Forman  
Venkataraman Shivakumar  
Sambi R. Mettu  
Leonard C. Williams  
Susan M. Piotrowski  
Clyde A. Sapp  
Victor B. Lawrence  
Ben Nguyen  
Feng Yeh  
Brian M. Gardner  
James C. Newman, Jr.  
Mark E. Mear  
Chungchu Chang  
Arij U. de Koning  
Henk Jan ten Hoeve  
Torben K. Henriksen  
Mehmet I. Basci  
G. Graham Chell

### NASGRO Consortium Participants

(Cycle 6)  
Airbus  
Arconic  
Blue Origin  
Boeing  
Bombardier Aerospace  
Embraer  
GKN Aerospace  
Honda Aircraft Engines  
Honeywell  
IHI Corporation  
Israel Aerospace Industries  
Korea Aerospace Industries  
Leonardo  
Mitsubishi Aircraft Corporation  
Mitsubishi Heavy Industries  
Siemens Energy  
Sierra Nevada Corporation  
Sikorsky  
SpaceX  
United Launch Alliance  
UTC Aerospace Systems

### Other Technical Monitors

NASA Fracture Control Methodology Panel  
NASGRO Interagency Working Group  
Michael Reyer, FAA Small Airplane Directorate  
Kevin Stonaker, FAA Technical Center



## **NOTICE**

This documentation and the software it describes, hereinafter referred to as NASGRO®, are provided “as is” without warranty of any kind, either expressed or implied, with respect to accuracy, completeness, or usefulness of the information contained herein. NASA and Southwest Research Institute® (SwRI®) reserve the right to make changes to NASGRO without prior notice. Neither NASA, SwRI, nor any person or contractor acting on their behalf shall be liable for any damages, including consequential ones, caused by reliance on NASGRO or the use of any information, method, or process disclosed in this report. NASA and SwRI make no representations with respect to NASGRO, including without limitations, any implied warranties of fitness for a particular purpose or absence of typographical, arithmetic or listing errors. NASGRO software coding or the material database shall not be reproduced in whole or in part for use in other computer software without written approval from the NASGRO Consortium Project Manager at Southwest Research Institute.

This Reference Manual and the NASGRO 9.2 computer program are both Copyright © 2021 Southwest Research Institute. All rights reserved.

## TABLE OF CONTENTS

SYMBOLS.....	x
ABBREVIATIONS .....	xii
SUMMARY .....	1
1.0 Introduction .....	3
2.0 Fatigue Crack Growth Analysis .....	7
2.1 Theoretical Background .....	7
2.1.1 Crack Growth Relationship.....	7
2.1.2 Fatigue Crack Closure .....	9
2.1.3 Threshold Stress Intensity Factor Range .....	12
2.1.4 Fracture Toughness.....	17
2.1.5 Criteria for Failure .....	19
2.1.6 Yielding Checks.....	21
2.1.7 Crack Growth under Load Interaction .....	22
2.1.7.1 Generalized Willenborg Model.....	22
2.1.7.2 Modified Generalized Willenborg Model.....	23
2.1.7.3 Chang-Willenborg Model .....	24
2.1.7.4 Strip Yield Model .....	25
2.1.7.4a Strip Yield Model - Constant Constraint-loss option.....	29
2.1.7.4b Strip Yield Model - Variable Constraint-loss option .....	32
2.1.7.4c Strip Yield Model - Usage .....	33
2.1.7.5 Constant Closure Model .....	34
2.1.7.6 Notes on Using the Load Interaction Models .....	36
2.1.8 Cyclic Shakedown .....	44
2.1.9 Temperature Dependent Crack Growth Analysis .....	45
2.2 Details of Crack Growth Analysis .....	45
2.2.1 Choosing the Crack Geometry.....	50
2.2.2 Transition of Crack Geometry .....	50
2.2.3 Entering the Initial Flaw Size .....	91
2.2.4 Selecting the Material Properties .....	98
2.2.4.1 Entering Material Properties Data from File .....	100
2.2.4.2 Entering Material Properties Data Manually .....	101
2.2.4.3 Entering the Environmental FCG Factor .....	101
2.2.5 Entering the Load Spectrum .....	104
2.2.5.1 Defining the Block Cases.....	105
2.2.5.2 Setting the Keac Check .....	110
2.2.5.3 Scaling the Stresses.....	112
2.2.5.4 Setting the Limit Stress Checks .....	112
2.2.5.5 Combining the Block Cases to Form a Schedule.....	112
2.2.6 Spectrum Generation and Editing.....	113

2.2.6.1 Spectrum Generation from Time Series Data .....	114
2.2.6.2 Long Block Spectrum Editing .....	116
2.2.6.3 Examples of Spectrum Clipping and Truncation.....	120
2.2.6.3.1 Clipping.....	121
2.2.6.3.2 Truncation.....	125
2.2.7 Advanced Spectrum Editing .....	126
2.2.7.1 Conversion of Long Block Spectrum to Advanced Editing Format.....	127
2.2.7.2 Performing Advanced Spectrum Editing Analysis .....	130
2.2.8 Output Options.....	131
2.2.9 Computations and Post-processing Output.....	132
3.0 Critical Crack Size (CCS) Calculations .....	133
3.1 Critical Crack Size .....	133
3.2 Threshold Crack Size.....	133
3.3 Iteration Procedures .....	134
3.4 How to Run NASCCS .....	137
4.0 Stress Intensity Factor Calculations .....	140
4.1 Theoretical Background.....	140
4.2 How to Run a Stress Intensity Factor Calculation .....	140
4.2.1 SIF Calculations Using Linear Stresses .....	141
4.2.2 SIF Calculations Using Nonlinear Stresses .....	142
5.0 Sustained Stress (da/dt) Analysis of Glass (NASGLS).....	143
5.1 Theoretical Background.....	143
5.2 How to Run a Sustained Stress Analysis .....	143
5.2.1 Material Properties.....	145
5.2.2 Entering the Sustained Load Schedule .....	146
6.0 Crack Growth Data Analysis.....	147
6.1 Entering Crack Growth Data for Curve Fitting .....	147
6.2 Obtaining the Constants .....	151
6.3 Entering and Processing Fracture Toughness Data .....	154
6.4 Files created by NASMAT .....	156
7.0 Boundary Element Method Analysis .....	158
7.1 The Data Input Interface .....	158
7.2 The Philosophy of Building a NASBEM Model .....	159
7.2.1 Points.....	160
7.2.2 Boundary Segments .....	160
7.2.3 Boundaries .....	161
7.2.4 Zones .....	162
7.2.5 Crack Segments and Cracks.....	163
7.2.6 Boundary Conditions and Concentrated (or Point) Loads .....	164
7.2.7 Special Case Geometries.....	165
7.2.7.1 Circular Hole Boundaries .....	165
7.2.7.2 A Row of Holes of Uniform Diameter .....	166
7.2.7.3 An Arc Connected to One or Two Inclined Linear Sections .....	166
7.2.7.4 SIF Analysis of a Crack Evaluated at Multiple Lengths.....	167
7.2.8 Materials .....	167
7.2.9 Stress Analysis .....	167

7.3 The Drawing Toolbar .....	168
7.3.1 File Manipulation Buttons .....	168
7.3.2 Segment Drawing Tools and Mesh Assistants.....	170
7.3.3 Boundary Condition and Point Load Buttons.....	172
7.3.4 Crack Definition Button.....	174
7.4 Other Buttons not on the Drawing Toolbar.....	174
7.4.1 Mesh Assembly Buttons .....	174
7.4.2 Utility Buttons.....	176
7.4.3 Drawing Surface Information Windows and Settings .....	176
7.5 Information Tables .....	177
7.6 The Calculations Page .....	178
7.7 Operational Issues .....	179
7.7.1 Numerical Limits on Input Items - how big can the model be?.....	179
7.7.2 Program Output and Files Created During a Run.....	180
7.8 Theory of Stress Analysis .....	180
7.8.1 Stresses in the Interior.....	181
7.8.2 Stresses on the Boundary .....	182
7.8.3 Stresses in the Boundary Layer.....	183
ACKNOWLEDGMENTS .....	185
REFERENCES .....	186
 Appendix A – Crack Growth Calculation using Tabular da/dN Data .....	A-1
Appendix B – Net-section Stress Analysis .....	B-1
Appendix C – Stress Intensity Factor Equations and Tables .....	C-1
Appendix D – Crack Transition Analysis .....	D-1
Appendix E – NASFLA Data Files and Material File Structure .....	E-1
Appendix F – Interpolation Routines.....	F-1
Appendix G – Materials Tables .....	G-1
Appendix H – Loading Spectra for Acceptance Vibration Tests .....	H-1
H.1 Sinusoidal Sweep Vibration Test.....	H-1
H.1.1 Narrow band Response – Methodology and Results .....	H-1
H.1.2 Wide band Response – Methodology and Results.....	H-3
H.2 Sinusoidal Dwell Vibration Test.....	H-5
H.3 Random Vibration and Acoustic Tests .....	H-5
H.3.1 Methodology .....	H-5
H.3.2 Results .....	H-6
H.4 References.....	H-6
Appendix I – Installing NASGRO, System Requirements, and User Data Migration .....	I-1
I.1 Installation Entirely on a Local PC.....	I-1
I.1.1 Special Instructions for Installing a Secure Version .....	I-1
I.2 Installation in a Server Environment .....	I-2
I.3 Installation in a Windows Terminal Server Environment .....	I-3

I.4	General System Requirements.....	I-4
I.5	Folders Requiring “Write” Permissions.....	I-5
I.6	Migrating user data files from a prior NASGRO version to the current version.....	I-6
	Appendix J – Unit Conversion factors.....	J-1
	Appendix K – Stress Quantities in Fatigue Load Spectra.....	K-1
	Appendix M – Cyclic Shakedown Methodology.....	M-1
	Appendix O – Residual Strength and NASGRO .....	N-1
	Appendix P – Temperature Interpolation of Crack Growth .....	P-1
	Appendix Q – History of Materials File Changes .....	Q-1
	Appendix R – File Management Features .....	R-1
	Appendix S – Advanced Spectrum Editing .....	S-1
	Appendix T – NASBEM Examples.....	T-1
	Appendix U – Rules for Fracture Toughness .....	U-1
	Appendix V – Rules for Constraint Coefficient .....	V-1
	Appendix W – Using NASGRO for Sequential or “Batch” Computations.....	W-1
	Appendix X – Alternative Failure Criteria .....	X-1
	Appendix Y – Executing FASTRAN through NASGRO.....	Y-1
	Appendix Z – High Cycle Fatigue (HCF) Threshold Check .....	Z-1

## LIST OF FIGURES

Figure 1 - Curve fit to Eq. 2.1 for a Ti-6Al-4V Titanium Alloy .....	8
Figure 2 - Crack opening function vs. Stress ratio.....	12
Figure 3a - Definition of the small crack parameter $a_0$ .....	15
Figure 3b - Effect of crack size ratio $a/a_0$ on threshold behavior.....	15
Figure 4 - Crack growth threshold vs. Stress Ratio for Aluminum .....	16
Figure 5 - Curve fit of Eq. 2.14 for Be-Cu CDA172 .....	18
Figure 6 - $K_c$ vs. thickness showing R-curve effect for Aluminum 2219-T87 .....	19
Figure 7 - Surface crack fracture toughness curve fit.....	20
Figure 8 - Crack tip plastic zones .....	22
Figure 9 - Schematic of analytical crack-closure model under cyclic loading.....	27
Figure 10 - Schematic of the Strip Yield model .....	28
Figure 11 - Dugdale model: Superposition of two elastic solutions.....	29
Figure 12 - Flat to slant crack growth transition.....	30
Figure 13 - Illustration of constraint transition region.....	31
Figure 14 - Constraint factors in tension and compression.....	32
Figure 15 - Example of a 3-segment curve fit .....	35
Figure 16 - Through crack cases 1, 2, 3 & 4.....	55
Figure 17 - Through crack cases 5, 6, 7 & 8.....	56
Figure 18 - Through crack cases 9, 10, 11 & 12.....	57
Figure 19 - Through crack cases 13, 14, 15 & 16.....	58
Figure 20 - Through crack cases 17 & 18.....	59
Figure 21 - Through crack case 19, 23 & 24 .....	60
Figure 22 - Through crack cases 25, 26 & 27.....	61
Figure 23a - Through crack cases 28 & 30.....	62
Figure 23b - Through crack cases 31, 32, 33 & 34.....	63
Figure 23c - Through crack case 35.....	64
Figure 24 - Through crack 37, unrestrained cases .....	65
Figure 25a – Through crack 37, restrained cases .....	66
Figure 25a – Through crack 37, partially restrained cases .....	67
Figure 26 - Embedded crack cases 1, 2, 4 & 5 .....	68
Figure 27 - Corner crack cases 1, 2 & 3 .....	69
Figure 28a - Corner crack cases 4, 5, 7 .....	70
Figure 28b - Corner crack cases 8.....	71
Figure 29 - Corner crack cases 9, 10, 11 & 12 .....	72
Figure 30 - Corner crack cases 13 & 14 .....	73
Figure 31a - Corner crack cases 15, 16 & 17.....	74
Figure 31b - Corner crack case 18 .....	75
Figure 32a - Corner crack cases 19, 20, 21 & 22 .....	76
Figure 32b - Corner crack case 23 .....	77
Figure 33 - Surface crack cases 1, 2, 3 & 4 .....	78
Figure 34 - Surface crack cases 5, 6, 7 & 8 .....	79
Figure 35 - Surface crack cases 9, 10, 11 & 12 .....	80
Figure 36 - Surface crack cases 13 & 14 .....	81
Figure 37 - Surface crack cases 15, 17, 18 & 19 .....	82

Figure 38 - Surface crack cases 26 & 27 .....	83
Figure 39 - Surface crack cases 28, 29 & 30 .....	84
Figure 40 - Surface crack cases 31 & 32 .....	85
Figure 41a - Surface crack case 33 .....	85
Figure 41b - Surface crack case 34 & 35 .....	86
Figure 42 - Standard specimen crack cases 1, 2, 3 & 4 .....	87
Figure 43 - Standard specimen crack cases 5, 6, 7 & 8 .....	88
Figure 44 - Standard specimen crack cases 9 & 10 .....	89
Figure 45 - Standard specimen crack case 11 & 12.....	89
Figure 46 - Boundary element crack cases 2 & 3 .....	90
Figure 47 - Hybrid crack case 1 .....	90
Figure 48 - Crack plane orientations.....	99
Figure 49 - Load schedule example .....	105
Figure 50 - Spectrum File Generator dialog box .....	115
Figure 51 - Time series of points evaluated using filter level threshold.....	115
Figure 52 - Screen shot of Load Blocks tab with Edit Spectrum button .....	116
Figure 53 - Schematic of cycle removal in clipping algorithm .....	118
Figure 54 – Spectrum File Editor dialog window for ordering options.....	118
Figure 55 - Spectrum File Editor dialog window for cycle counting options .....	120
Figure 56 - Spectrum analysis for sample2c.lb spectrum file.....	121
Figure 57 - Screen shot of clipping by value with spectrum statistics for edited file.....	122
Figure 58 – Exceedance plots for clipping by value example (sample2.1.lb) .....	123
Figure 59 - Screen shot of clipping by percentage with spectrum statistics for edited file ...	124
Figure 60 - Exceedance plots for clipping by percentage example (sample2.1.lb) .....	124
Figure 61 - Screen shot of truncation by value with spectrum statistics for edited file.....	125
Figure 62 - Exceedance plots for truncation by value example (sample2.1.lb).....	126
Figure 63 - Screen shot of <i>Load Blocks</i> tab with <i>Edit Spectrum</i> button.....	127
Figure 64 - Screen shot of <i>Advanced spectrum editing</i> under <i>Cycle counting options</i> .....	128
Figure 65 - File selector for output filename – Advanced spectrum editing selected .....	128
Figure 66 - Spectrum statistics for advanced spectrum editing cycle counting.....	129
Figure 67 - Screen shot of Load Blocks tab – Advanced spectrum editing selected .....	129
Figure 68 - Sustained stress data with curve fits.....	144
Figure 69 - Element intersection types .....	184

## LIST OF TABLES

Table 1 – Effect of $R_{so}$ on Life Prediction for Generalized Willenborg model .....	39
Table 2 – Effect of $\phi_0$ on Life Prediction for Modified Generalized Willenborg model .....	40
Table 3 – Life Prediction for Zhang's Spectra.....	41
Table 4 – Comparison of Life Predictions for ASTM round robin Spectra .....	42
Table 5 – Life Predictions for ASTM round robin Spectra .....	43
Table 6a – Description of Crack Cases.....	51
Table 6b – Transition Relationship between Crack Cases.....	53
Table 7a – Changes from Previous to Current NASA NDE Standards, US Units .....	92
Table 7b – Changes from Previous to Current NASA NDE Standards, SI Units .....	92
Table 8a – Current NASA Standard NDE Flaw Sizes, US Units .....	94
Table 8b – Current NASA Standard NDE Flaw Sizes, SI Units .....	95
Table 9a – Obsolete NASA Standard NDE Flaw Sizes, US Units.....	96
Table 9b – Obsolete NASA Standard NDE Flaw Sizes, SI Units .....	97
Table 10 – Two-dimensional Interpolation Table .....	100
Table 11 – Launch and Landing Spectrum for STS Payloads .....	106
Table 12 – Keac Values for Several Metals.....	111
Table 13 – Summary of spectrum characteristics for sample2.1b .....	120
Table 14 – Sustained Stress Constants (US Units) .....	145
Table 15 – Sustained Stress Constants (SI Units).....	145



## SYMBOLS

$a$	Crack depth in thickness or diametral (e.g., for SC07) direction
$a_0$	Intrinsic crack length in Eq 2.12
$a_g$	Initial guess for critical crack size
$A$	Fit parameter in Eq 2.31 & Eq 5.2
$A_0, A_1, A_2, A_3$	Coefficients in crack opening function, Eq 2.4-2.7
$A_0$	Parameter given in Appendix H
$A_n$	Area of net section
$A_k, B_k$	Fit parameters in Eq 2.14
$c$	Crack length or half-crack length in width or peripheral direction
$C$	Crack growth rate constant in Eq 2.1
$C_{th}$	Fit exponent for threshold, Eqs 2.11a, 2.11b
$C_k$	Fit parameter in Eq 2.16
$f$	Crack opening function, Eq 2.3
$f$	Frequency
$f_n$	Resonant frequency
$f, f_c, f_i, f_w, f_x, f_0, f_l, f_\phi$	Functions given in Appendix C
$F_0, F_1, F_2, F_3, F_4$	Stress intensity magnification factors
$F_{th}$	Alternative exponent for threshold, Eqs 2.11c, 2.11d
$g, g_p, g_w, g_3, g_4$	Functions given in Appendix C or D, or both
$G, G_L, G_w, G_0, G_1$	Functions given in Appendix C or D, or both
$h, k$	Functions given in Appendix C
$H_c, H_1, H_2$	Functions given in Appendix C
$I, J$	Functions given in Appendix C
$I_n$	Moment of inertia of net section
$J_{Ic}$	Critical J-integral value (Mode I)
$K$	Stress intensity factor (Mode I)
$K_{(a)}$	Stress intensity factor at the a-tip
$K_{(c)}$	Stress intensity factor at the c-tip
$K_c$	Critical stress intensity as used in Eq 2.1
$K_{cr}$	Critical stress intensity factor for fracture
$K_{max}, K_{min}$	Maximum and minimum stress intensity factors in a load cycle
$K_{open}$	Opening stress intensity factor, above which the crack is open
$K_{Ic}$	Plane strain fracture toughness (Mode I)
$K_{Ie}$	Effective fracture toughness for part-through (surface/corner) crack
$K_{Ie(a)}$	$K_{Ie}$ value at the a-tip
$K_{Ie(c)}$	$K_{Ie}$ value at the c-tip
$K_{eac}$	Environmentally assisted cracking threshold

$\Delta K$	Stress intensity factor range ( $K_{\max} - K_{\min}$ )
$\Delta K_{\text{eff}}$	Effective stress intensity factor range ( $K_{\max} - K_{\text{open}}$ )
$\Delta K_{\text{th}}$	Threshold stress intensity factor range
$\Delta K_0$	Threshold stress intensity factor range at $R = 0$
$\Delta K_1$	Threshold stress intensity factor range at $R = 1.0$
$M$	Resultant moment in Eq 2.17
$M_0, M_1, M_2, M_3$	Functions given in Appendix C
$m$	Exponent in Chang-Willenborg (+ve R, Walker) Eq 2.28
$n, p, q$	Exponents in NASGRO Eq 2.1
$n, q$	Exponents in Chang-Willenborg (-ve R) Eq 2.29
$N$	Number of applied fatigue cycles
$P$	Resultant force in Eq 2.17
$Q$	Amplification factor for a sine sweep vibration test
$R$	Stress ratio ( $K_{\min}/K_{\max}$ )
$R_{\text{cut}^+}$	Positive cutoff stress ratio
$R_{\text{cut}^-}$	Negative cutoff stress ratio
$R_p$	Negative value of $R$ below which threshold is held constant
$R_{\text{SO}}$	Shutoff overload stress ratio
$R_U$	Current ratio of under-load to overload stress (or SIF), Eq 2.27
$S_0, S_1, S_2, S_3, S_4$	Nominally applied stresses
$S_{\max}$	Maximum applied stress
$S_n$	Nominal net section stress, Eq 2.17
$t$	Thickness of plate, sheet, extrusion, or forging
$t_0$	Thickness to meet plane strain condition, Eqs 2.14, 2.15
$V_0$	Fit parameter in Eq 5.1
$w$	Specimen width
$u, v, w, x, y, z$	Functions given in Appendix C
$Y$	Function given in Appendix C
$\alpha$	Plane stress/strain constraint factor
$\alpha, \beta, \delta, \lambda, \zeta$	Functions given in Appendix C
$\beta_R$	Crack closure factor correction for free surfaces, Eq 2.10
$\phi$	Parametric angle of the ellipse
$\phi$	Reduction factor in Willenborg model Eqs 2.24, 2.25
$\phi_0$	Material constant in Modified Willenborg model Eq 2.27
$\lambda$	Sweep rate of a sine sweep vibration test
$\eta$	Exponent in polynomial equations for $F_0, F_1, F_2, F_3$
$\nu$	Poisson's ratio
$\rho$	Crack tip plastic zone size, Eq 2.19
$\sigma_0$	Flow stress
$\sigma_{\text{ys}}$	Tensile yield strength

## ABBREVIATIONS

1-D .....	One dimensional
2-D .....	Two dimensional
3-D .....	Three dimensional
Ann.....	Annealed
ASW.....	Aircraft sump water environment
ASTM .....	American Society for Testing and Materials
A(T).....	Arc-shaped tension specimen
BA .....	Beta annealed
C1.....	Class
CR .....	Cold-rolled
CRT.....	Cold-rolled and tempered
C(T).....	Compact tension specimen
CW .....	Cold-worked
DA.....	Dry air environment
DC(T).....	Disc-shaped compact tension specimen
DW.....	Distilled water environment
Dyn.....	Dynamic
EB .....	Electron beam
ELI .....	Extra-low interstitial
Eq.....	Equation (number)
ESA .....	European Space Agency
FAD.....	Failure Assessment Diagram
Extr.....	Extrusion
Forg.....	Forging
Grd .....	Grade
GMA .....	Gas metal arc
GN2.....	Gaseous nitrogen environment
GSFC.....	Goddard Space Flight Center
GTA .....	Gas tungsten arc
GUI .....	Graphical user interface
HAZ .....	Heat affected zone
HHA.....	High humidity air environment
HPD.....	Hole preparation defect
JP-4 .....	JP-4 jet fuel environment
LA .....	Laboratory air environment
LH2 .....	Liquid hydrogen environment
LHe .....	Liquid helium environment
LN2 .....	Liquid nitrogen environment
MA .....	Mill annealed
M(T).....	Middle (center)-cracked tension specimen
NASA.....	National Aeronautics and Space Administration
NDE .....	Nondestructive evaluation
NLR.....	National Lucht-En Ruimtevaartlaboratorium

Nom.....	Nominal
OA.....	Over-aged
PA .....	Peak-aged
PAR.....	Parallel to weld-line
Plt.....	Plate
RA .....	Recrystallization annealed
Rc .....	Rockwell table C hardness
Rnd.....	Round rod
RTN.....	Return
SA .....	Submerged arc
SCT .....	Sub-cooled and tempered
SD .....	Standard deviation
SE(B).....	Single edge cracked three-point bend specimen
SE(T).....	Single edge cracked tension specimen
Sht .....	Sheet
SIF.....	Stress intensity factor
SMA.....	Shielded metal arc
SR.....	Stress relieved
SSF .....	Stress scaling factor
ST .....	Solution treated
STA.....	Solution treated and aged
STS.....	Space transportation system
SW.....	Seawater environment
Thk .....	Thickness
UTS .....	Ultimate tensile strength
VAR .....	Vacuum arc remelted
YS .....	Tensile yield strength



## SUMMARY

This document is a comprehensive reference on the theory and operation of the NASGRO 9.2 suite of software programs. It provides details of the theory of fatigue crack propagation behavior and the related empirical equations used in the various software modules. Other details supplied include description of the crack geometries, design and operation of the material database and the theory and operation of the boundary element method. Several appendices provide further details of computing net-section stresses and stress intensity factors. A list of materials for which properties are provided with the software is also found in the appendices. More information is provided here than is typical in a user's guide, since this manual is intended to be a comprehensive reference on the methods that form the basis of the software. Because of the interactive nature of the graphical user interface, only a few of the operational details are discussed. On-line help (i.e., from within the software) is provided on selected topics. However, time spent in reading this manual will be greatly rewarded, especially for the beginning user.

NASGRO is a suite of computer programs comprised of eight modules named NASFLA, NASSIF, NASCCS, NASFAD, NASGLS, NASBEM, NASMAT and NASFORM. The NASFLA program is based on fracture mechanics principles that can be used to compute crack growth under fatigue loading. The NASSIF module is used to calculate stress intensity factors. The NASCCS module is used to compute critical crack sizes. The NASFAD module provides the capability to use the Failure Assessment Diagram (FAD) to assess the criticality of crack-like flaws. The NASGLS module is used to perform sustained-load crack growth analyses for glass-like materials. These analyses may be done in a fully interactive mode using graphical user interfaces for each module. In the NASFLA module, material properties for crack growth can be obtained from a large database supplied with the program by selection from a menu of choices. Once the properties are displayed, any of them can be changed at will. Crack growth properties may also be entered either as a 1-D table or a 2-D table. The fatigue loading spectra can be input easily from a standard file or individual files. User-defined materials properties and fatigue spectra may also be supplied manually and saved for future use.

The NASMAT module is used to enter, edit and curve-fit fracture toughness and fatigue crack growth data obtained in a laboratory. It is designed to conveniently store and retrieve data and obtain curve fits to the NASGRO equation and the Walker equation. The NASBEM module incorporates the boundary element method for solving complex two-dimensional geometries with or without cracks to obtain stress intensity factors and stresses. The NASFORM module is used to analyze the initiation or formation of cracks in structures. A separate manual provides the theory and operation of this module.

The NASSIF module is useful in computing stress intensity factors or their normalized values i.e., geometry factors or beta factors) for any of the available crack configurations. The NASCCS module allows computation of critical crack size or threshold crack size for a specified geometry, loading and a given fracture toughness or threshold value. NASFAD allows the user to specify a crack geometry and loading to determine whether or not it is within the safe zone of the Failure Assessment Diagram. It also provides the ability to calculate a critical crack size using the FAD approach. The NASGLS module is applicable to glass-like

materials subjected to sustained loading over a certain period of time. NASGLS includes a small database of time-dependent crack growth properties for a few glass materials..

The NASMAT module is used to enter, edit and curve fit fatigue crack growth rate data ( $dN$  vs  $\Delta K$ ). Options to curve fit data to the NASGRO equation, the Walker equation and Spline equations are available. The data have been organized using an identification code (ID) and header information. The header consists of specimen type, environment, heat treatment and other relevant information. Specification of curve fit options is done using the various windows-style input dialog boxes and menus. Fracture toughness data and fatigue crack growth data are the two types of data stored in the database. These can be quickly retrieved from the database by using the proper ID code. The program allows the user to build the ID codes step by step and provides a number of options to retrieve the desired data. Once a set of data is retrieved, it can be edited, plotted and curve-fitted. NASMAT also provides the capability for a user to enter and fit their own sets of material data and save the results into a user database. This module thus provides a means to organize and process fracture mechanics properties generated in a laboratory. As more data becomes available, the database will be updated. This module is particularly useful in a laboratory environment where new materials are being characterized.

The boundary element module NASBEM is used to analyze two-dimensional geometries with holes and cracks. Stress analysis and computation of stress intensity factors at the tips of straight or curved cracks can be done using NASBEM. The graphical user interface for this module uses the WxWidgets class library. Geometric parameters such as points, lines and surfaces can be input easily using various geometry-building tools, pull-down menus and dialog boxes. The geometry can be plotted immediately on a canvas to check for errors. Once all the problem data have been entered, the data can be checked and processed to obtain the solution. Necessary changes to data can be made quickly and the problem can be reanalyzed. Output can also be viewed using the pull-down menu. The stress analysis portion of the software has been separated so that once the solutions for displacements and tractions are solved the user can input the locations of interest for stress computation. The stress analysis module can then be executed using a command from the GUI. The stresses along a specified line segment can be computed and plotted.

## 1.0 Introduction

---

The NASGRO computer software was originally developed to provide easy-to-use analytical tools for fracture control analysis of NASA space flight hardware and launch support facilities. It can also be used for stress and fracture mechanics analysis of aerospace and other structures or hardware and may be used as a learning and research tool in fracture mechanics. It is used by NASA and its support contractors as well as by many other companies worldwide. The primary capability of the program is to calculate fatigue crack growth and crack instability of cyclically or statically loaded structures that contain initial crack-like defects.

The original version of NASGRO (NASA/FLAGRO) was released in August. General distribution of the program was initiated in 1990 by COSMIC, the agency that formerly distributed NASA-developed computer software. Version 2.0 was first distributed in May 1994, and Version 3.0 was released to the general public via a web site in September 1998. Revisions of Version 3 were placed on the web site as needed, the last one being version 3.0.18 released in December 2001. That service is no longer available. Version 9.2, the present release, like all versions released after 3.0.18, has been jointly developed by NASA and Southwest Research Institute® (SwRI®) under the terms of a Space Act Agreement between NASA/JSC and SwRI. As part of this agreement, SwRI has formed and is managing a consortium of industrial NASGRO users, who are providing additional guidance and financial support.

New features in this version include:

- The following crack cases:
  - SC34, univariant weight function solution for an external circumferential surface crack in a hollow cylinder
  - SC35, univariant weight function solution for a circumferential surface crack in a solid cylinder
  - CC18, bivariant weight function model for a part-elliptical corner crack at a 135° angled corner
- Other crack-case related improvements and changes include:
  - Addition of end restraint options for multiple crack cases (TC12, TC15, TC17, TC19, TC25, TC31, TC32, TC37)
  - Revisions to SC09 and SC13
  - Expanded solution limits for TC28, CC08 and SC06
  - Added compounding to TC31, TC32 and TC37
  - Implemented  $\beta_R$  for CC09, CC11 and CC12
  - Implemented option to allow  $\beta_R$  to be turned off for all crack cases
- Miscellaneous improvements and changes include:
  - Implemented the new NASFAD module
  - Many GUI upgrades for improved display flexibility
  - Revisions and overhauls to Appendices C, G, and I

- Appendix N merged into Appendix C
- Appendix L merged into Appendix G
- New Appendix L for the new NASFAD module
- Default to most recent file path for file open or file save options

The software has been designed in a modular fashion, in order to allow for systematic continuing revisions and portability. The material files that store the crack growth properties are encrypted such that users cannot view or modify them directly. Users are able to input their own data and provision is made to save it to user-defined files. More information on these user-defined files is given in Appendix E.

In the Microsoft Windows environment, when NASGRO (the top-level menu program) is executed (typically by double-clicking on an icon set up on the desk top) four groups of buttons are presented. The first, “Crack Propagation and Fracture Mechanics Analysis Modules”, contains five radio-box choices for the five modules of which this group is comprised. These modules are NASFLA for crack propagation analysis, NASSIF for computing stress intensity factors, NASCCS for computing critical crack size, NASFAD for flaw assessment using the failure assessment diagram, and NASGLS for analyzing crack growth in glass-like materials. The second main option is the NASMAT module, which is a database of crack-growth data and tools for processing them. The third and fourth radio-box options will select, respectively, NASBEM, the Boundary Element module, and NASFORM, for crack formation analysis. Other buttons include one which brings up the manual in PDF format. First a Table of Contents is displayed from which one can select the main reference manual for NASFLA and related modules or the section on elastic-plastic analysis or the NASFORM module or one of the appendices. If one wants to directly run any of the eight individual modules, it can be executed by locating the appropriate executables (flague4.exe etc.,) in their respective folders and double-clicking on them. Once the graphical user interface for any of the eight modules is activated and running, a set of tabbed dialog boxes guides the user to input the problem data, analyze the data and view the results.

Using the NASFLA module for crack growth analysis, critical crack size calculation, and stress intensity factor computation will be covered in sections 2 through 4. The sustained stress analysis option will be described in section 5. NASFAD operation is discussed in Appendix L. Discussion of the NASMAT module for processing and storing of fracture mechanics data is contained in section 6, and the boundary element module NASBEM is covered in section 7. Additional help is available in the GUI in the form of pop-up files based on the context as well as in a general way. Whenever the cursor is placed over them, some of the boxes and grids display a message indicating their function to guide the user. Another very useful feature is the menu that appears when the user right-clicks on grids. By selecting items from this menu, several useful functions can be accomplished.

Several appendices at the end of the manual are provided with detailed information on topics such as net-section stress computations (Appendix B), the stress intensity factor formulations (Appendix C), list of materials for which NASGRO or Walker equation constants are available (Appendix G), and a host of other topics [Please see the Table of Contents for the full list].

Appendix I provides detailed information and instructions on the installation of NASGRO on Windows machines including general system requirements for operating systems, disk space and RAM, and graphics settings, etc. A set of error messages that may occur after installation and how to diagnose and resolve them is also contained in Appendix I.

Additional information about NASGRO and the NASGRO Consortium is available on the NASGRO web site at [www.nasgro.swri.org](http://www.nasgro.swri.org). This web site includes Bug Reporting and Feedback forms for questions and comments from NASGRO users.



## 2.0 Fatigue Crack Growth Analysis

---

### 2.1 Theoretical Background

This section provides the theoretical background for the equations used in NASGRO. It is generally assumed that the user has a basic understanding of the principles of fracture mechanics and fatigue crack growth. Comprehensive treatment of fracture mechanics applications and the underlying theory may be found in references [1 - 4].

#### 2.1.1 Crack Growth Relationship

Crack growth rate calculations in NASGRO use a relationship called the NASGRO equation. Different elements of this equation were developed by Forman and Newman of NASA, Shivakumar of Lockheed Martin, de Koning of NLR and Henriksen of ESA and was initially documented by Forman and Mettu [5]. It is given by:

$$\frac{da}{dN} = C \left[ \left( \frac{1-f}{1-R} \right) \Delta K \right]^n \frac{\left( 1 - \frac{\Delta K_{th}}{\Delta K} \right)^p}{\left( 1 - \frac{K_{max}}{K_c} \right)^q} \quad (2.1)$$

where  $N$  is the number of applied fatigue cycles,  $a$  is the crack length,  $R$  is the stress ratio,  $\Delta K$  is the stress intensity factor range, and  $C$ ,  $n$ ,  $p$ , and  $q$  are empirically derived constants. Explanations of the crack opening function,  $f$ , the threshold stress intensity factor,  $\Delta K_{th}$  and the critical stress intensity factor,  $K_c$  are presented in sections 2.1.2 through 2.1.4. Equation 2.1 produces  $da/dN-\Delta K$  curves that are similar to those obtained from the equation used in the initial (1989) version of NASGRO, but it provides a more direct formulation of the stress-ratio effect. Also, with Eq 2.1, variations in  $K_c$  and  $\Delta K_{th}$  values can have a reduced effect on the linear region of the curve (by a suitable choice of  $K_{max}$ ), which produces a better fit to data. Figure 1 shows crack growth data ( $da/dN-\Delta K$ ) for a Ti-6Al-4V Titanium alloy plotted together with a curve fit to Eq 2.1. The fit is slightly conservative for  $R = 0.33$  but otherwise very good for various  $R$  ratios.

ED13AB1: Ti-6Al-4V; ST(1750F) + A(1000F/4h)  
Envir: LA; Spec: C(T); Chien: T-L; Freq: 0.1  
STA(1750F/1HR/WQ1000F/4HR/AC)+SR(1C)

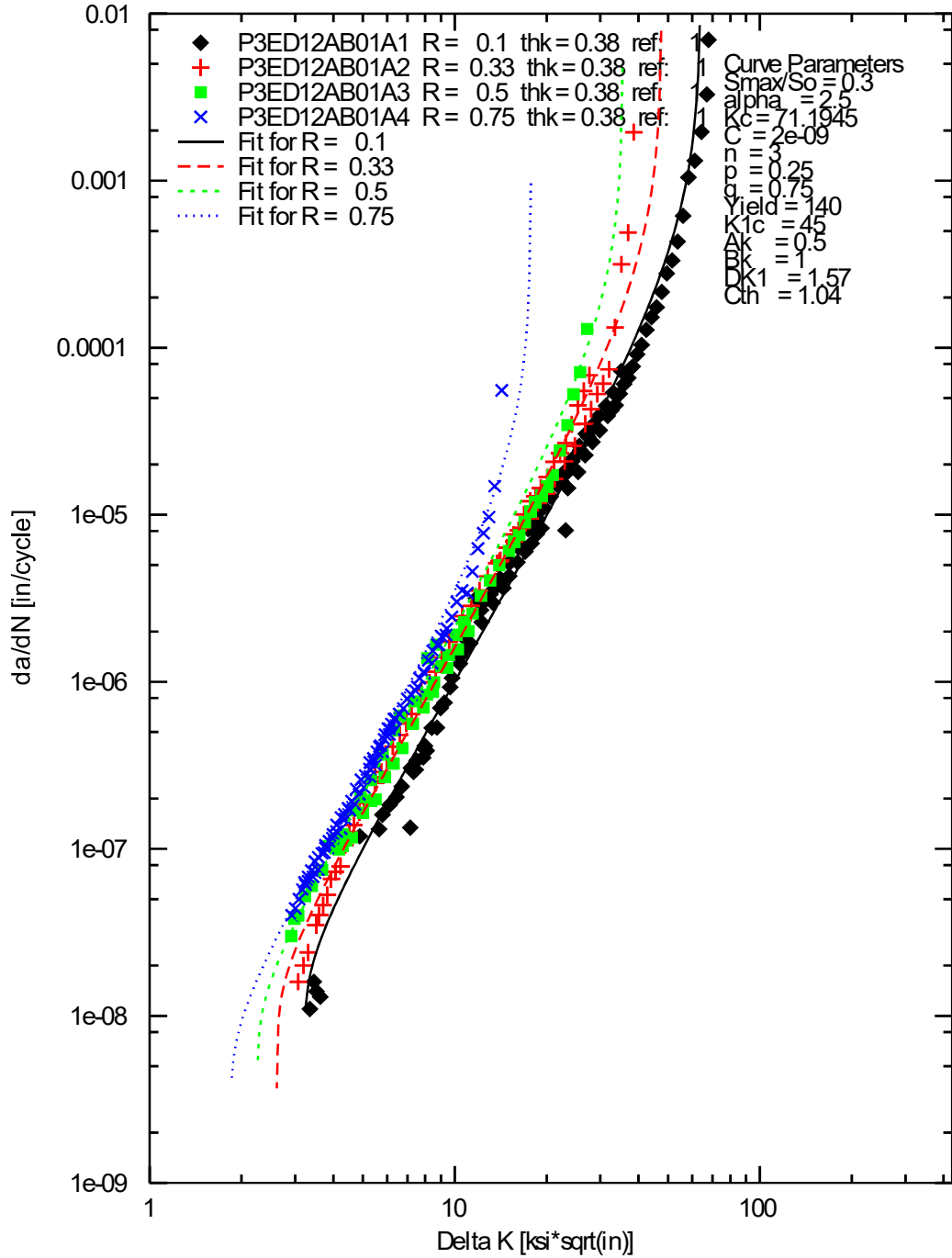


Figure 1 – Curve fit to Eq. 2.1 vs Data for a Titanium Alloy

To analyze cracked bodies under combined loading, the stress intensity factor is expressed as:

$$K = [S_0 F_0 + S_1 F_1 + S_2 F_2 + S_3 F_3 + S_4 F_4] \sqrt{\pi a} \quad (2.2)$$

The stress quantities  $S_0$ ,  $S_1$ ,  $S_2$ , and  $S_3$  are the applied tension/compression, bending in the thickness and width directions, and pin bearing pressures. For the crack case TC05, which has biaxial tension or compression loading, the term  $S_4$  is used for the stress in the lateral direction. For crack case SC03,  $S_4$  is used to denote the internal pressure in a sphere. The  $F_i$  values are geometric correction factors applicable to each type of applied stress and derived specifically for each crack case. Details of these factors are given in Appendix-C.

The program incorporates fatigue crack closure analysis for calculating the effect of the stress ratio on crack growth rate under constant amplitude loading. The crack opening function,  $f$ , for plasticity-induced crack closure has been defined by Newman [6] as:

$$f = \frac{K_{op}}{K_{\max}} = \begin{cases} \max(R, A_0 + A_1 R + A_2 R^2 + A_3 R^3) & R \geq 0 \\ A_0 + A_1 R & -2 \leq R < 0 \end{cases} \quad (2.3)$$

and the coefficients are given by:

$$A_0 = (0.825 - 0.34\alpha + 0.05\alpha^2) [\cos(\frac{\pi}{2} S_{\max} / \sigma_0)]^{1/\alpha} \quad (2.4)$$

$$A_1 = (0.415 - 0.071\alpha) S_{\max} / \sigma_0 \quad (2.5)$$

$$A_2 = 1 - A_0 - A_1 - A_3 \quad (2.6)$$

$$A_3 = 2A_0 + A_1 - 1. \quad (2.7)$$

In these equations,  $\alpha$  is a plane stress/strain constraint factor, and  $S_{\max} / \sigma_0$  is the ratio of the maximum applied stress to the flow stress. Selection of values for these parameters will be discussed in the next section. The closure function has been programmed to be non-negative everywhere in its domain of definition from NASGRO 6.2 onwards, reducing the earlier over-conservatism and keeping in line with the ideas of the author.

### 2.1.2 Fatigue Crack Closure

The plane stress/strain constraint factor,  $\alpha$ , has been treated as a constant for the purposes of curve fitting the crack growth data for each particular material system. Values range from 1, which corresponds to a plane stress condition, to 3, which corresponds to a condition of plane strain. Materials, such as high-strength steels, for which the  $K_{Ic}/\sigma_{ys}$  ratio is fairly low, are assigned relatively high  $\alpha$  values (2.5 or higher), while materials with higher  $K_{Ic}/\sigma_{ys}$  ratios usually have  $\alpha$  values ranging from 1.5 to 2.0. While better correlation with experimental

results may be obtained by allowing  $\alpha$  to vary with  $K_{\max}$  [6], reasonable agreement has been obtained by using it strictly as a fitting parameter.

In addition,  $S_{\max}/\sigma_0$ , the ratio of the maximum applied stress to the flow stress, is assumed to be constant. Using this parameter as a constant has been shown to produce acceptable results for positive stress ratios, where the effect of  $S_{\max}/\sigma_0$  on the crack opening function is relatively small [5]. Most materials that were curve fit for NASGRO use a value of  $S_{\max}/\sigma_0 = 0.3$ , which was chosen because it is close to an average value obtained from fatigue crack growth tests using various specimen types.

Some materials, however, exhibit only a very small stress ratio effect, and therefore may be evaluated without considering the effects of crack closure. In these special cases, a curve-fitting option that allowed the crack opening function to be bypassed was chosen. The parameters for this bypass option are  $\alpha = 5.845$ ,  $S_{\max}/\sigma_0 = 1.0$ . These values were selected in order that  $f$  in Eq 2.3 would be equal to zero for negative stress ratios and would be equal to R ( $K_{op} = K_{min}$ ) for  $0 \leq R < 1$ . Thus, for positive stress ratios, the crack growth relationship Eq 2.1 reduces to:

$$\frac{da}{dN} = \frac{C \Delta K^n \left(1 - \frac{\Delta K_{th}}{\Delta K}\right)^p}{\left(1 - \frac{K_{\max}}{K_c}\right)^q} \quad (2.8)$$

where the entire  $\Delta K$  range contributes to crack propagation, and, for negative stress ratios, reduces to:

$$\frac{da}{dN} = \frac{C K_{\max}^n \left(1 - \frac{\Delta K_{th}}{\Delta K}\right)^p}{\left(1 - \frac{K_{\max}}{K_c}\right)^q} \quad (2.9)$$

since  $\Delta K/(1-R) = K_{\max}$ . Figure 2 shows the opening function,  $f$ , as a function of the stress ratio for  $S_{\max}/\sigma_0 = 0.3$  and  $\alpha=2.5$ , typical for many steels, together with the  $S_{\max}/\sigma_0 = 1.0$ ,  $\alpha=5.845$  closure bypass option. Note that  $f$ , which reflects the amount of plasticity-induced crack closure that is present in a material, approaches the closure bypass option at the higher stress ratios (around  $R = 0.7$ ). However, for negative stress ratios, the  $S_{\max}/\sigma_0$  ratio greatly influences the amount of closure present in the material. Therefore, non conservative life predictions may be obtained from NASGRO analyses of structures such as over-wrapped pressure vessels, which are cycled to a relatively high compressive stress, with a negative stress ratio on the order of  $R = -1$  to  $-2$ . In such cases, better correlation with test results may be achieved by substituting the absolute value of  $S_{\min}$  in place of  $S_{\max}$  and calculating an appropriate  $S_{\max}/\sigma_0$  value.

It should also be noted that Eq 2.8 (the closure bypass option for  $R>0$  with  $\alpha = 5.845$ ,  $S_{\max}/\sigma_0 = 1.0$ ) may be further reduced to the Paris equation ( $da/dN=C\Delta K^n$ ) by setting the parameters  $p$  and  $q$  equal to zero. Similarly, Eq 2.1 may be reduced to a closure-corrected Paris equation by setting  $p$  and  $q$  equal to zero. In either case,  $K_c$  is retained as a cut-off value for failure, but the threshold ( $\Delta K_{th}$ ) cut-off for growth is present only if  $p > 0$ . Eq 2.1 can be used with  $p$  and  $q$  set to zero, but only if the constants  $C$ ,  $n$ , were originally properly fitted to the Paris equation.

For constant amplitude fatigue loading, Newman and Raju [7] have shown that multiplying  $\Delta K$  by a crack-closure factor,  $\beta_R$ , produces more accurate crack growth predictions for semi-elliptical surface cracks and quarter-elliptical corner cracks. This  $\beta_R$  factor is only applied at points where the part-through crack front intersects a free surface, and it is a function of the stress ratio. For  $R > 0$ ,  $\beta_R$  is given by:

$$\beta_R = 0.9 + 0.2R^2 - 0.1R^4 \quad (2.10)$$

and for  $R \leq 0$ ,  $\beta_R$  is assumed to have a value of 0.9. In NASGRO,  $\Delta K$  is multiplied by  $\beta_R$  for many, but not all, corner crack and surface crack models. A complete listing of which crack cases use or do not use the  $\beta_R$  factor is provided in Appendix C, Section C15. It is important to be aware that this near-surface correction is applied only in NASFLA (to  $\Delta K$  for crack growth calculations) and is not used in NASSIF.

Beginning with version 9.2, users have the option of completely turning off the Beta-R correction for all crack cases in the “Options” menu. This will generally result in shorter calculated lifetimes.

As a final note on crack closure in NASGRO, it should be remembered that the crack opening function was derived from an analysis of center-cracked panels, subjected to a constant amplitude load condition, in which the crack front advances through a zone of plastically deformed material. This means that the effect of bending was not included in the analysis and that the crack opening equation (Eq 2.3) accounts for plasticity-induced crack closure, but not necessarily other effects, such as extensive oxide-induced or roughness-induced crack closure.

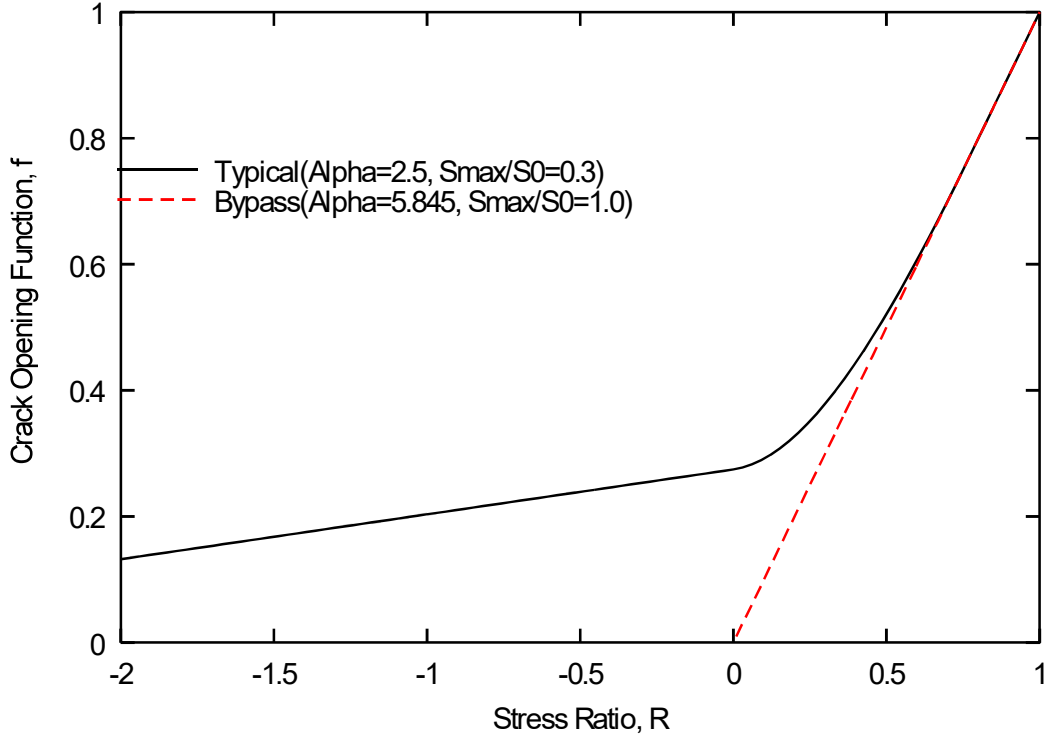


Figure 2 – Crack opening function vs. stress ratio

### 2.1.3 Threshold Stress Intensity Factor Range

The threshold stress intensity factor range in Eq 2.1,  $\Delta K_{th}$ , is approximated by the following empirical equations:

$$\Delta K_{th} = \Delta K_1^* \left[ \frac{1-R}{1-f[R]} \right]^{(1+RC_{th}^p)} / (1-A_0)^{(1-R)C_{th}^p}, \quad R \geq 0 \quad (2.11a)$$

$$\Delta K_{th} = \Delta K_1^* \left[ \frac{1-R}{1-f[R]} \right]^{(1+RC_{th}^m)} / (1-A_0)^{(C_{th}^p - RC_{th}^m)}, \quad R < 0 \quad (2.11b)$$

in which

$$\Delta K_1^* = \Delta K_1 \left[ \frac{a}{a+a_0} \right]^{1/2} \quad (2.12a)$$

where  $R$  is the stress ratio,  $f$  is the Newman closure function,  $A_0$  is a constant(Eq 2.4) used in  $f$ ,  $\Delta K_1$  is the threshold stress intensity factor range as  $R \rightarrow 1.0$ ,  $C_{th}$  is an empirical fit constant with different values for positive(superscript p) and negative(superscript m) R ratios,  $a$  is the crack length, and  $a_0$  is a small crack parameter(typical value of 0.0015 inch). The present form of the equation is preferred to the  $\Delta K_{th}$  formulation used in NASGRO 3.0

(where  $\Delta K_0$  was used as the basis) because it uses a threshold  $\Delta K_1$  (at a high R ratio) that is independent of crack closure. The spread between the da/dN curves (fanning at the lower end) for various R ratios can be controlled much better using the parameter  $C_{th}$ . Values of  $C_{th}^p$  for positive values of R, and  $\Delta K_1$  are stored as constants in the NASGRO materials files. The value of  $C_{th}^m$  for negative R ratios is set to a default of 0.1, but can be changed by the user. Also, while computing the threshold as per eqs. 2.11a, 2.11b, the Newman closure function f and the constant  $A_0$ , were based on average values of the fit constants  $\alpha$  and  $S_{max}/\sigma_0$  of 2.0 and 0.3 respectively. Use of the closure bypass option (with  $\alpha = 5.845$  and  $S_{max}/\sigma_0 = 1.0$ , dashed line in Figure 2) results in a constant value of threshold for  $R \geq 0$  while values for  $R < 0$  do show an inverse dependence (Eqs 2.11a and 2.11b).

An alternative expression for threshold, with a new fanning exponent,  $F_{th}$ , was introduced in v7.1b to overcome certain difficulties with the use of  $C_{th}$ :

$$\Delta K_{th} = \Delta K_{1f}^* \left[ \frac{1-R}{1-f[R]} \right]^{1+F_{th}^p}, \quad R \geq 0 \quad (2.11c)$$

$$\Delta K_{th} = \Delta K_{1f}^* \left[ \frac{1-R}{1-f[R]} \right]^{1+F_{th}^m} \frac{1}{(1-A_0)^{F_{th}^p - F_{th}^m}}, \quad R < 0 \quad (2.11d)$$

in which

$$\Delta K_{1f}^* = \Delta K_{1f} \left[ \frac{a}{a+a_0} \right]^{1/2} \quad (2.12b)$$

This alternative is described at the end of this section, [2.1.3].

Recent work by Forth, Newman and Forman [8, 9] shows the strong dependence of threshold on the test methods used, specifically on how a specimen is loaded to generate the threshold data. The traditional ASTM standard test method[10] has been shown to produce anomalous data due to the crack closure associated with the load-shedding procedure. The K-increasing tests are more reliable because they produce closure-free conditions during the test. At any given R ratio, the constant  $C_{th}$  can be used to model the threshold value for different degrees of crack closure. Setting a value of zero for  $C_{th}$  has the effect of using a low threshold leading to relatively conservative life predictions. This setting is suitable for the load-interaction crack growth models provided in NASGRO and has been implemented as such. Since the load interaction provides some crack growth retardation, it is desirable not to have the additional beneficial effect due to a higher threshold. Using a nonzero value for  $C_{th}$  such as the one stored in the NASGRO material database has the effect of using a higher threshold leading to relatively less conservative life predictions. Relative to this, the non-interaction model in NASGRO is now provided with three options: 1) to start with a zero value but allowing it to rise to the file value if the load level falls such that the normalized K-gradient is lower than  $-1 \text{ in}^{-1}$ , 2) to use zero values throughout for a conservative life estimation, 3) to use non-zero file values throughout for the least conservative life estimation. Note however that the option pertains solely to  $C_{th}$ , and that  $C_{th}^m$  (or Cth-, as displayed in the GUI) always retains its input cell value. In the case of spectrum loading, these options are expected to give

the user greater flexibility in modeling crack growth realistically. For general use, the most conservative (option 2) choice is recommended. As such, this is the default choice in the current version. In general, no “fanning out” behavior ( $C_{th} = 0$ ) at low R ratios is observed in M(T) specimens while C(T) specimens display it to some degree.

The criterion for option 1) is shown in some more detail below:

Only when the stress ratio  $R > -0.25$  the following condition is checked during computation:

$$\left( \frac{2}{K_1 + K_2} \right) \left( \frac{K_2 - K_1}{a_2 - a_1} \right) \leq -1 \text{ inch}^{-1} \quad (2.12a)$$

[The subscript 2 is understood to refer to values from the immediately previous crack growth increment; subscript 1 to values from the preceding call.]

If the check returns a YES,  $C_{th}$  is raised to its materials-file value – and retained for the remainder of the computation; the check is stopped at this point. This check is performed only when there is more than one cycle in the step having higher load.

The formulation also accounts for the small crack effect demonstrated by Tanaka, et al. [11]. This is accomplished via the small crack correction factor:  $[a/(a + a_0)]^{1/2}$  in Eq. 2.12. The intrinsic crack size  $a_0$  has a suggested value of 0.0015 in. (0.0381 mm), but can be changed to a different value by the user. The small crack correction factor becomes significant whenever the crack size  $a$  is comparable to  $a_0$  and can be optionally limited to a lower bound. This lower bound, equivalent to the ratio of short crack threshold to long crack threshold, has a suggested value of 0.2 but can be changed by the user.

While some researchers have proposed models for  $a_0$  based on grain size, others have not assigned any physical significance to the  $a_0$  parameter [11 - 13]. Fig. 3a shows the engineering basis for using  $a_0$  as an intrinsic crack size. It corresponds to the crack size which when combined with the endurance stress level will yield the threshold stress intensity factor. If the expression in Fig. 3a is used to calculate  $a_0$ , it should be noted that the threshold term shown in the figure, corresponding to  $a/a_0 = 1$ , equals 0.7 times the long-crack value, corresponding to  $a/a_0 \gg 1$ , of the threshold. The factor 0.7 is a consequence of the presence of the Tanaka factor, and it should be noted that since it is being applied to the long-crack threshold, a loop of self-reference to the short-crack value of the threshold is avoided in Eqs 2.11 and 2.12. It should also be noted that in NASFLA we are generally only concerned with crack growth starting from an NDE flaw size, and so are operating at values of  $a/a_0 \gg 1$ , where  $\Delta K_1^*$  is indistinguishable from  $\Delta K_1$ .

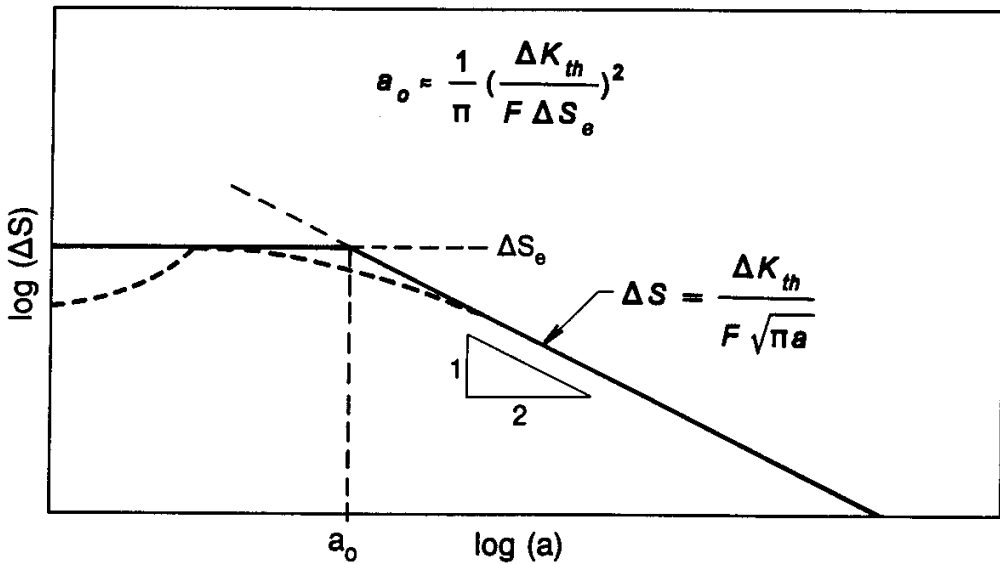
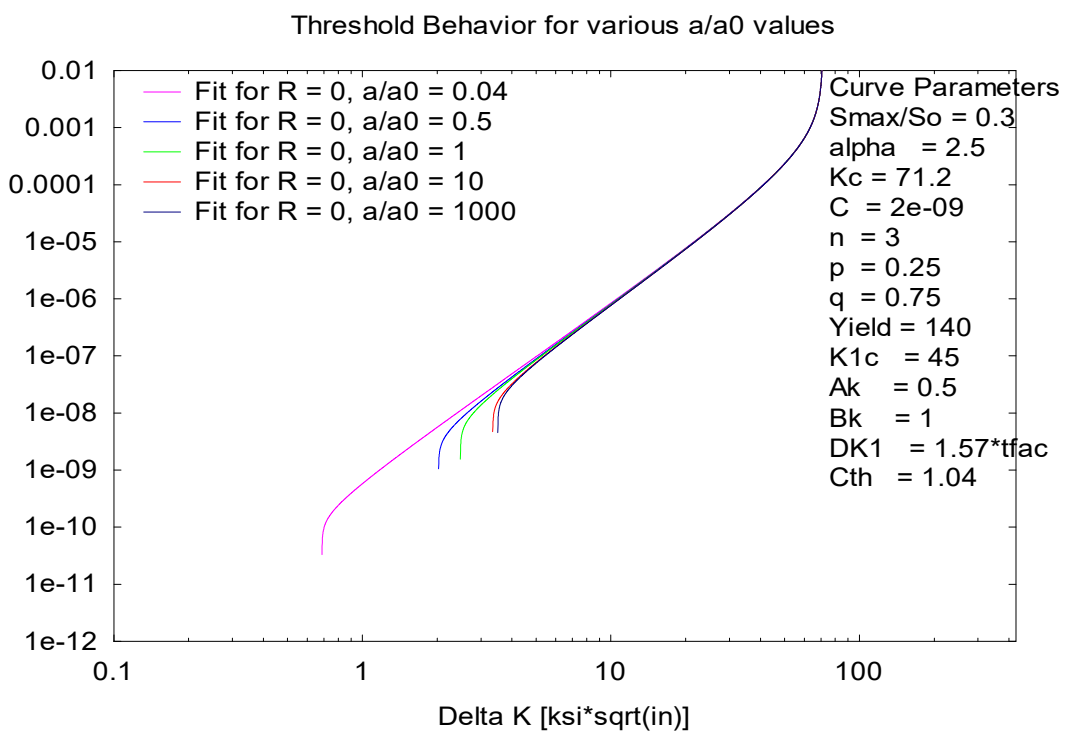
Fig. 3a – Definition of the small crack parameter  $a_0$ Fig. 3b - Effect of crack size ratio  $a/a_0$  on crack growth curves.

Figure 3b shows the influence of crack size on the threshold behavior at a stress ratio of  $R=0$ .

To increase the flexibility with which data can be fitted, provision has been made to use independent value of  $C_{th}$  for negative and positive  $R$  values. Fig 4 shows a fit of data for 2219-T6 Aluminum alloy. The values of constants chosen to obtain this fit are shown on the figure. For negative R ratios, a value of  $R$  ( $=R_p$ ) at which the threshold stress intensity factor reaches a maximum value is computed; for all values of  $R$  less than  $R_p$ , the threshold is assumed to be constant.

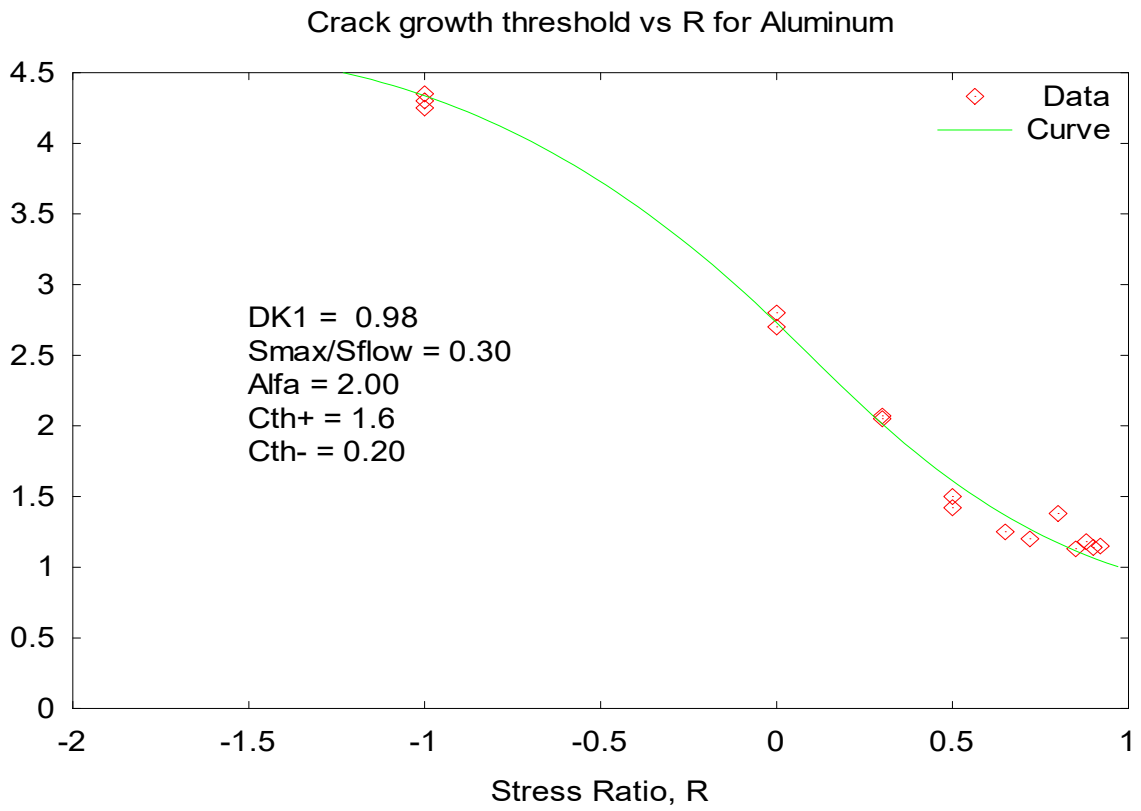


Figure 4 – Crack growth threshold vs. R for Aluminum

For the version 4.0 release, the values of  $\Delta K_1$  were computed based on the  $\Delta K_0$  values in the version 3.0 database using the following equation.

$$\Delta K_1 = \Delta K_0 (1 - A_0)^{(1+C_{th}^P)} \quad (2.13)$$

In future, these values of  $\Delta K_1$  will be revised based on original test data as per the methods suggested in [8, 9].

It is observed that use of the threshold expression, Eqns (2.11a & b), in which  $C_{th}^p$  is set to the NASFLA default of 0, after having been fitted originally with  $C_{th}^p > 0$  in NASMAT, causes not only the threshold regions of low-R crack growth curves to be shifted leftward (or decrease) as expected, but the threshold regions of high-R curves to be shifted leftward as well. This is so because threshold values based on Eqns (2.11a & b) approach their limit,  $\Delta K_1$ , i.e.,  $\Delta K_{th}$  as  $R \rightarrow 1$ , with non-zero slopes (except when  $C_{th}^p = 0$ ).

To solve this problem, a threshold expression was sought with the property,  $\lim_{R \rightarrow 1} \frac{\partial \Delta K_{th}}{\partial R} = 0$ , for all levels of fanning. This is the essential requirement for high-R thresholds to stay nearly invariant when changes to R and the fanning factor are made. The alternative threshold expression, Eqns (2.11c & d) was introduced in v7.1b to fulfill this requirement.

Values of the threshold constants,  $F_{th}^p$ ,  $F_{th}^m$ , and  $\Delta K_{1f}$  (the last being distinct from  $\Delta K_1$ , which is based on  $C_{th}^p$ ), provided in v7.1 were based on equivalence, approximating threshold values obtained earlier through  $C_{th}$ -based fitting. It is expected that fits for materials introduced post-v7.1 will be based on *ab initio* fitting of laboratory data in NASMAT, and likely to show bigger differences in threshold values between  $C_{th}$ - and  $F_{th}$ -based fitting.

#### 2.1.4 Fracture Toughness

Fracture toughness properties of a material are essential for reliable crack growth analyses. These include plane strain fracture toughness ( $K_{Ic}$ ) values, part-through fracture toughness ( $K_{Ic}$ ) values, and any other available fracture toughness ( $K_c$ ) values as a function of thickness.  $K_{Ic}$  values are especially important because flaws in real structures are often part-through (surface or corner) cracks. The main reason that fracture toughness depends on thickness is that differences in constraint produce changes in the stress state in the material. Thin structures, where the constraint is small, experience a plane stress condition, whereas thicker structures that are in plane strain have more constraint.

The following relationship has been adopted, for through crack problems, to describe the  $K_c$  - vs.-thickness behavior for various materials:

$$K_c / K_{Ic} = 1 + B_k e^{-(A_k t_0)^2} \quad (2.14)$$

where

$$t_0 = 2.5 \left( K_{Ic} / \sigma_{ys} \right)^2. \quad (2.15)$$

This is a generalization of the relationship proposed by Vroman [15], which can be obtained from Eq 2.14 and 2.15 by letting  $A_k = 5$  and  $B_k = 1$ . These equations are used by NASGRO to calculate a  $K_c$  value to substitute into Eq 2.1 for all through crack geometries (TCxx and SSxx crack cases). The one-dimensional surface crack cases (SC06, SC09, and SC10) also use Eq 2.14 and 2.15 for  $K_c$  determination. Figure 5 shows a plot of this curve for beryllium-copper alloy CDA172 [16]. When valid plane strain fracture data were not available for a curve fit,  $K_{Ic}$  was estimated, based either on  $K_{Ic}$  data for a similar material or  $J_{Ic}$  data

whenever possible, or derived from  $K_c$  values that were estimated from the asymptotes of the  $da/dN-\Delta K$  curves.

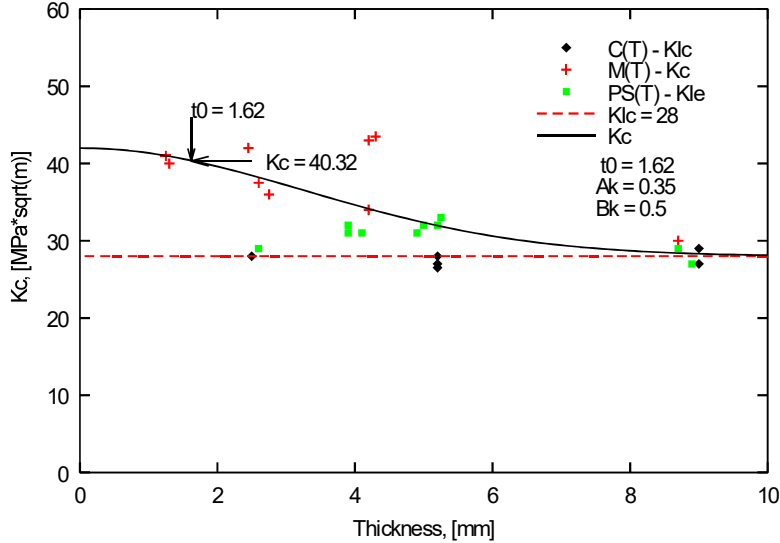


Figure 5 – Curve fit of Eq. 2.14 for Be-Cu CDA172

In addition to being a function of thickness, fracture toughness depends on crack length, or more directly, on stress level. This commonly known R-curve effect is especially prominent in thin structures. Figure 6 shows  $K_c$  data, obtained from 2219-T87 aluminum specimens, plotted as a function of thickness for different crack lengths. It should be noted that the  $K_c$  - vs.-thickness curve fit for a given material in the NASGRO database currently represents an average of the data points and does not account for the effect of stress level/crack size on fracture toughness. Therefore, the user should be cautioned that a crack growth analysis of a particularly high stress, low cycle fatigue condition could produce unconservative results at shorter crack lengths. Fracture toughness data obtained from part-through cracked PS(T) specimens can also show a variation in toughness with crack size and stress level, but demonstrate little dependence on thickness. For the part-through crack geometries (CCxx and two-dimensional SCxx crack cases),  $K_c$  in Eq 2.1 is set equal to a constant value of  $K_{le}$ , taken from the NASGRO material properties files. During the curve-fitting process,  $K_{le}$  for a given material/ environment combination was selected, based on available fracture toughness data from PS(T) or other surface-cracked specimens whenever possible. Otherwise,  $K_{le}$  was approximated by the following equation [17]:

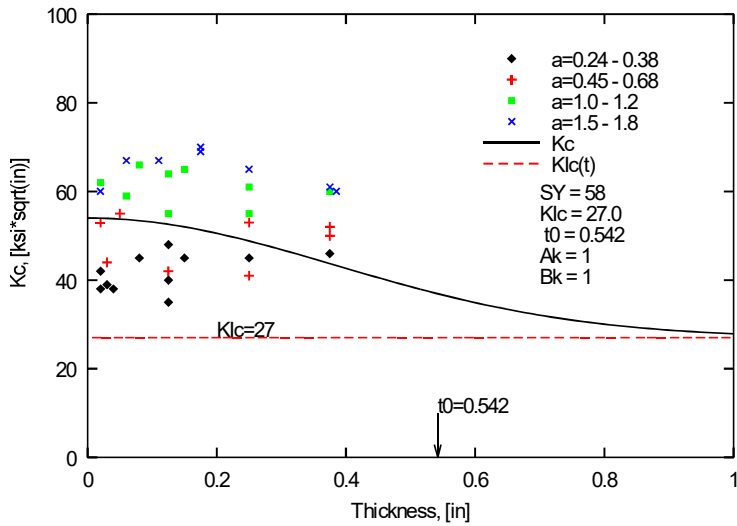


Figure 6 –  $K_c$  vs. thickness showing R-curve effect for Aluminum 2219-T87

$$K_{le} = K_{lc} \left( 1 + C_k K_{lc} / \sigma_{ys} \right) \quad (2.16)$$

where  $C_k$  is an empirical constant with units of length $^{-1/2}$ . The value of  $C_k$  is 1 for US units, 6.275 for MPa  $\sqrt{m}$  units, and 0.19842 for MPa  $\sqrt{mm}$  units. This relationship holds reasonably well for a variety of materials, as shown in Figure 7. For materials which have a very high  $K_{lc}/\sigma_{ys}$  ratio,  $K_{le}$  values calculated by this equation are very large. In these cases, to be conservative, the  $K_{le}$  values entered into the NASGRO materials files have been limited to 1.4 times the  $K_{lc}$  values.

### 2.1.5 Criteria for Failure

In NASGRO, crack instability is usually assumed to occur if  $K_{max}$  exceeds the fracture toughness ( $K_c$  or  $K_{le}$ ) of a material. For through crack geometries,  $K_{max}$  is compared with  $K_c$  calculated from Eq 2.14 and 2.15. For most of the part-through crack geometries,  $K_{max}$  at both the a-tip and c-tip are compared with  $K_{le}$ . However, for the part-through crack cases that have free surfaces,  $K_{max}$  at the c-tip (SC01-SC05, SC11, SC12) or  $K_{max}$  at the corner points (CC01-CC04) is compared with 1.1 times  $K_{le}$ . Failure is also assumed to occur if the net section stress exceeds the flow stress of the specified material, assumed to be the average of the yield and ultimate strengths.

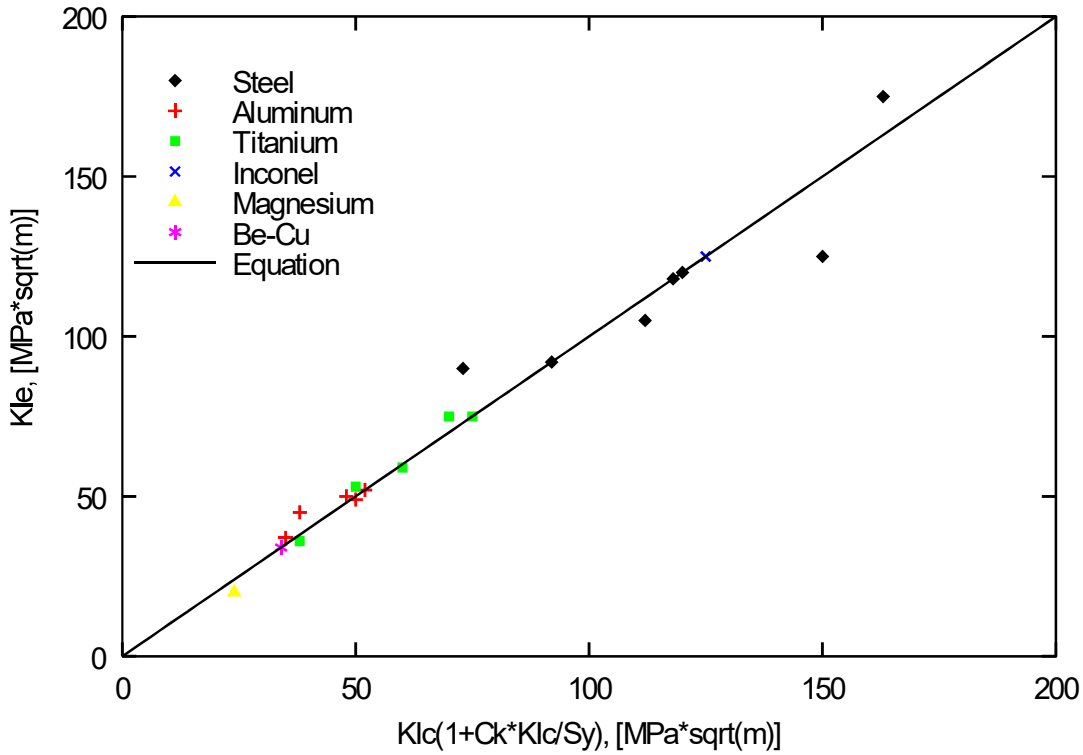


Figure 7 – Surface crack fracture toughness curve fit

In addition, there are two optional conditions for failure that may be specified by the user. The first is that the user may select an option of checking  $K_{max}$  with the threshold for environmentally assisted (stress corrosion) crack growth ( $K_{eac}$ ) for some or all of the blocks entered in a schedule. If  $K_{max}$  exceeds a user-specified value of  $K_{eac}$ , fracture is assumed and the crack growth analysis is terminated. More details about setting the  $K_{eac}$  check may be found in section 2.2.4.2. The second failure condition involves the use of a “limit stress”, which can be specified during each block case entry. This procedure is described in section 2.2.4.4. Here, failure is assumed to occur if the value of  $K$  calculated using the “limit stress” (e.g., stress value at limit load) exceeds  $K_c$  for the specific material used. The  $K_c$  value selected depends on whether the crack is through or part-through, and is based on the criteria outlined in the previous paragraph. There is also an additional option to completely bypass the net-section failure criterion, thus using only the crack instability as a failure criterion.

Crack size limits provided by the user may also be used optionally to terminate analysis. In the case of multi-dimensional crack cases, the user has full flexibility in specifying which, if any, of the crack tips this termination criterion should be applied to, as well as in specifying the actual value(s) of the crack size limit. In all cases, this criterion is applied in conjunction with (and never in lieu of) the other criteria described in the paragraphs above.

### 2.1.6 Yielding Checks

A warning is given when the net-section stress exceeds the yield strength of the material, where the net-section stress is expressed generally as:

$$S_n = \frac{P}{A_n} + \frac{Mc}{I_n} \quad (2.17)$$

The calculation is terminated if net section stress exceeds the flow stress (average of yield and ultimate), unless the user opts to have the check bypassed altogether. In the above equation,  $A_n$  is the net area,  $P$  is the resultant force,  $M$  is the resultant moment,  $c$  is the distance to the outer fibers, and  $I_n$  is the moment of inertia of the net section. Appendix B contains the net section yielding equations that are applicable to each of the crack cases. Crack growth calculations continue after the first net section warning is issued, but the user should realize that the results may be non conservative. Therefore, in situations where a part must be analyzed above net section yield, suitable methods that take the plasticity into account should be used. NASFLA provides a limited number of geometries for this purpose under the elastic-plastic option, set from the options menu.

For most of the surface and embedded crack cases (but not for corner cracks, which do not undergo this particular check), both  $K_{Ic}$  and  $K_{Ie}$  data are required because checks are made for failure as a through crack when net ligament yielding occurs [18]. The ligament yielding check is made using the following criterion:

$$a + \rho \geq t \quad (2.18)$$

where the plastic zone size,  $\rho$ , is given by:

$$\rho = \frac{1}{2\pi} \left( \frac{K_{\max}}{\sigma_{ys}} \right)^2 . \quad (2.19)$$

Before the ligament yielding criterion is met,  $K_{\max}$  is compared to  $K_{Ie}$ , and after it is met, a second check is done comparing  $K_{\max}$  for the corresponding through crack (i.e., an imagined through-the-thickness crack of the same length as the current part-through crack) against  $K_c$ , calculated from Eq 2.14 and 2.15, with the computation terminating if  $K_{\max} > K_c$ .

Note that the ligament yielding criterion does not control transition to a through crack. Transition to a through crack occurs when the crack depth exceeds the thickness of the part ( $a > t$ ) if an appropriate through crack solution is available. A list of crack cases with the geometry they transition to is shown in Table 6b.

### 2.1.7 Crack Growth under Load Interaction

#### 2.1.7.1 Generalized Willenborg Model

The Generalized Willenborg model, based on Gallagher's [20] generalization of Willenborg's [19] original development, was incorporated into NASGRO. This model deals with crack retardation effects only and the formulation is as follows.

The effect of current loading on crack growth is known to be influenced by the load history; the term "load interaction" describes the interplay of these influences. The Generalized Willenborg model, utilizes a residual stress intensity,  $K_R$ , which determines the effective stress ratio due to a load interaction as follows:

$$R_{eff} = \frac{K_{min} - K_R}{K_{max} - K_R} = \frac{K_{min,eff}}{K_{max,eff}} \quad (2.20)$$

This value of  $R_{eff}$  is used instead of the actual stress ratio within the crack growth equation and has the effect of retarding the crack growth.

The retardation for a given applied cycle of loading depends on the loading and the extent of crack growth into the overload plastic zone. Gallagher [20, 21] expressed the Willenborg residual stress-intensity factor as

$$K_R^W = K_{max}^{OL} \left( 1 - \frac{\Delta a}{Z_{OL}} \right)^{\frac{1}{2}} - K_{max} \quad (2.21)$$

where  $K_{max}^{OL}$  is the maximum stress intensity for the overload cycle, and  $\Delta a$  is the crack growth between the overload cycle and the current cycle as shown in Figure 8. The overload plastic zone size is given by

$$Z_{OL} = \frac{\pi}{8} \left( \frac{K_{max}}{\alpha_g \sigma_{ys}} \right)^2 \quad (2.22)$$

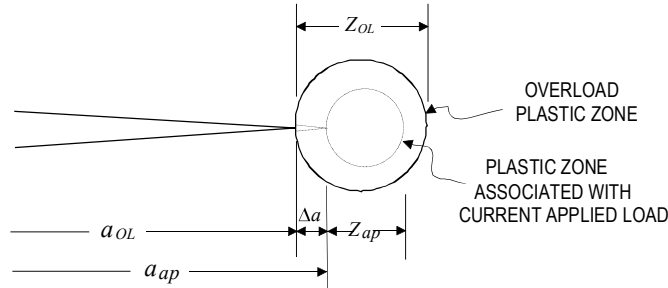


Figure 8 - Crack tip plastic zones

The constraint factor  $\alpha_g$  is taken from a fit developed by Newman [22] and is given by

$$\alpha_g = 1.15 + 1.4 e^{-0.95 \left( \frac{K_{\max}}{\sigma_{ys} \sqrt{t}} \right)^{1.5}} \quad (2.23)$$

This expression is used for one-dimensional crack models; for two-dimensional cases, limit values of 1.15 or 2.55 are used for  $\alpha_g$  depending on whether the crack tip under consideration emerges through the free surface (plane stress) or is buried (plane strain).

$K_R^W$  represents the difference between the stress intensity required to produce a plastic zone equal to  $Z_{OL} - \Delta a$  and the current maximum applied stress intensity  $K_{\max}$ . In the original development, retardation is considered to occur if  $K_R^W > 0$ . In the Generalized Willenborg model, a modified residual stress-intensity  $K_R$  is used, related to  $K_R^W$  by

$$K_R = \phi K_R^W \quad (2.24)$$

where

$$\phi = \frac{1 - \frac{\Delta K_{th}}{\Delta K}}{(R_{SO} - 1)} \quad (2.25)$$

$R_{SO}$  is the shut-off value of the stress ratio,  $K_{\max}^{OL} / K_{\max}$ . When this value is exceeded,  $K_{\max,eff}$  is set equal to  $\Delta K_{th} / (1 - R)$  and crack growth is arrested. Since  $\Delta K_{th}$  in Eqn. (2.25) is itself a function of R, earlier NASGRO versions used an iterative predictor-corrector procedure to obtain  $R_{eff}$ , i.e. using the same value of R in Eqn. (2.25) as is obtained by going through the chain of calculations to obtain  $R_{eff}$  from Eqn. (2.20). However, this procedure was taken out in v8.1, and instead the applied stress ratio was used directly in  $\Delta K_{th}$ , eliminating an error present in the iterative scheme and bringing the model more nearly in line with the original intentions of the authors. The net effect of these changes on calculated life was found to be small. No special consideration is given to multiple overloads and their effect is taken to be the same as that for a single overload.

### 2.1.7.2 Modified Generalized Willenborg Model

A load interaction model termed the Modified Generalized Willenborg (MGW) model was developed by T. R. Brussat of Lockheed Martin [23]. Based on this formulation, a computer model was developed and incorporated into NASGRO. The following description is based on his private communication and lecture notes [23].

The MGW model extends the Generalized Willenborg load interaction model [20] by taking into account the reduction of retardation effects due to underloads. The MGW model (like the Generalized Willenborg), utilizes a residual stress intensity,  $K_R$ , which determines the effective maximum and minimum stress due to a load interaction. The equations are:

$$\begin{aligned} K_{\max}^{eff} &= K_{\max} - K_R \\ K_{\min}^{eff} &= \text{Max}\{(K_{\min} - K_R), 0\}, \quad \text{for } K_{\min} > 0 \\ &= K_{\min} \quad \text{for } K_{\min} \leq 0 \end{aligned} \tag{2.26}$$

These effective stress intensity factors are used instead of the actual  $K_{\max}, K_{\min}$  within the crack growth equation and have the effect of retarding the crack growth. In addition, an underload (i.e., a compressive or tensile load that is lower than the previous minimum load subsequent to the last overload cycle) can reduce such retardation. The ratio  $R_U$  given by  $K_{UL}/K_{\max}^{OL}$  (the ratio of current underload\* to overload stress intensity factor) is used to adjust the factor  $\phi$ . This reduction is achieved by means of Eqn. (2.24). The factor  $\phi$  in that equation is now given by

The parameter  $\phi_0$  is the value of  $\phi$  for  $R_U = 0$ . Parameter  $\phi_0$  is a material dependent parameter that can be determined, ideally, by conducting a series of typical aircraft spectrum tests. The value of  $\phi_0$  ranges typically from 0.2 to 0.8.

### 2.1.7.3 Chang-Willenborg Model

Another load interaction model implemented into NASGRO is the Chang-Willenborg model developed at Rockwell. Chang and Engle [24] developed a version of the Generalized Willenborg model which takes into account the acceleration due to negative loads. The formulation was computerized into a code named CRKGRO at Rockwell under contract from US Air Force. They used the Walker equation for positive stress ratios and an equation developed by Chang for negative stress ratios. The retardation effects are modeled as in the case of Generalized Willenborg. The following set of equations defines this model.

For  $\Delta K > \Delta K_{th}$ ,  $R \geq 0$

$$da / dN = C \left[ \Delta K / (1 - \bar{R})^{1-m} \right]^n$$

$$R < R_{cut}^+, \bar{R} = R \quad (2.28)$$

$$R > R_{cut}^+, \bar{R} = R_{cut}^+$$

For  $\Delta K > \Delta K_{th}$ ,  $R < 0$

\* Proper rainflow cycle counting will pair the underload minimum with the overload maximum as part of the reordering process that precedes input of the spectra to NASGRO

$$\frac{da}{dN} = C \left[ (1 + \bar{R}^2)^q K_{\max} \right]^n$$

$$R \geq R_{cut}^+, \bar{R} = R \quad (2.29)$$

$$R < R_{cut}^+, \bar{R} = R_{cut}^-$$

For  $\Delta K < \Delta K_{th}$ ,

$$\frac{da}{dN} = 0 \quad (2.30)$$

In the above equations,  $R_{cut}^+$ ,  $R_{cut}^-$  are the cutoff values for positive and negative stress ratios. The threshold stress intensity factor range for this model is determined using

$$\Delta K_{th} = (1 - A R) \Delta K_o \quad (2.31)$$

To account for the reduction of the overload retardation effect, caused by compressive spike loads following tensile overload, the overload plastic zone size is modified as follows:

$$(Z_{ol})_{eff} = (1 + \bar{R}) Z_{ol} \quad (2.32)$$

where  $\bar{R}$  is as defined in Eq. 2.29 and  $Z_{ol}$  is the plastic zone size corresponding to maximum stress intensity factor.

Whenever the Willenborg load interaction model is invoked, the effective stress ratio  $R_{eff}$  is computed and used in the above equations (2.28, 2.29 2.31 and 2.32). Otherwise the stress ratio R used for crack growth in the non-interaction mode is directly used in the above equations.

#### 2.1.7.4 Strip Yield Model

This section describes the Strip Yield Model, one of the fatigue crack growth load interaction models in NASGRO. This model was developed by the European Space Agency (ESA) and the National Aerospace Laboratory (NLR) in the Netherlands in cooperation with the NASA Langley Research Center and the NASA Johnson Space Center. Reference [25] contains the details of the model and its implementation into NASGRO. Strip Yield is a mechanical model based on the assumption that a growing fatigue crack will propagate through the crack tip plastic region, and that this plastic deformation left in the wake of the crack will contribute to stress interaction effects such as stress-level dependence and crack growth rate acceleration and retardation. This section will first present an historical foundation for plasticity-induced fatigue crack closure and then give some insight into using this model.

Fatigue cracks can grow only when they are open, and historically cracks were assumed to open when the applied load increased from its minimum value, or passed from compression into tension in the case of reversed loading. The underlying assumption is that the crack tip plastic zone moves with and remains ahead of the tip as the crack grows. Extending linear elastic fracture mechanics principles to fatigue, the driving force for the crack growth rate was taken to be the stress-intensity factor range,

$$\Delta K = K_{\max} - K_{\min} \quad (2.33)$$

Plots of experimental data of crack growth rate  $da/dN$  versus  $\Delta K$  on log-log scales show a “sigmoidal” shape. The large central linear region suggests a power-law relationship, and the simplest such form was given by the Paris [26] equation

$$\frac{da}{dN} = C_1 (\Delta K)^{n_1} \quad (2.34)$$

where  $C_1$  and  $n_1$  are material constants. Since this equation is restricted to modeling the linear portion of such sigmoidal plots, in time, extensions were proposed to model the threshold and instability regions, for example equation (2.1) which is described in detail in section 2.1.1.

In the mid-sixties, Elber [27] discovered that fatigue cracks can remain closed during the loading step until a load substantially higher than minimum load (or zero load in the case of reversed loading), and close early during the unloading step before reaching minimum load (or zero load in the case of reversed loading). This was attributed to the permanent deformation that was left on the crack flanks as the crack propagated through the crack tip plastic zone, a phenomenon termed *plasticity-induced fatigue crack closure*. For such cases, Elber proposed modifying the basic Paris growth law by using an *effective* stress-intensity factor range

$$\frac{da}{dN} = C_2 (\Delta K_{\text{eff}})^{n_2} \quad (2.35)$$

where  $C_2$  and  $n_2$  are material constants,

$$\Delta K_{\text{eff}} = K_{\max} - K_{\text{open}} \quad (2.36)$$

and  $K_{\text{open}}$  is the stress-intensity factor value at which the crack opens. In general the stress-intensity factor values at which the crack opens and closes are not identical, but the difference is small. For the case when  $K_{\text{open}}$  is less than  $K_{\min}$ , Eq. (2.36) reverts to Eq. (2.33)

The benefit of accounting for crack closure is that events such as spike overloads lead to considerable permanent deformation on the crack flanks and thus to an elevated  $K_{\text{open}}$  and a reduced (or retarded) crack growth rate.

The stress interaction occurs as follows. Overloads cause large plastic zones and previously virgin material yields; this is called primary plasticity. As the crack grows the large amount of permanent deformation will be on the crack flanks, causing a rise in the opening stress and thus a decrease in the crack growth rate. This lower rate is sustained if subsequent cycles have smaller maximum loads than the overload, and the new plastic zones will be wholly contained within the overload plastic zone. This is termed secondary plasticity. Eventually the crack grows through the primary plastic zone, the region of large plastic deformation is well back in the crack wake. At this point, the material returns to primary plasticity and the crack growth rate increases, perhaps to stabilize at its original pre-overload value.

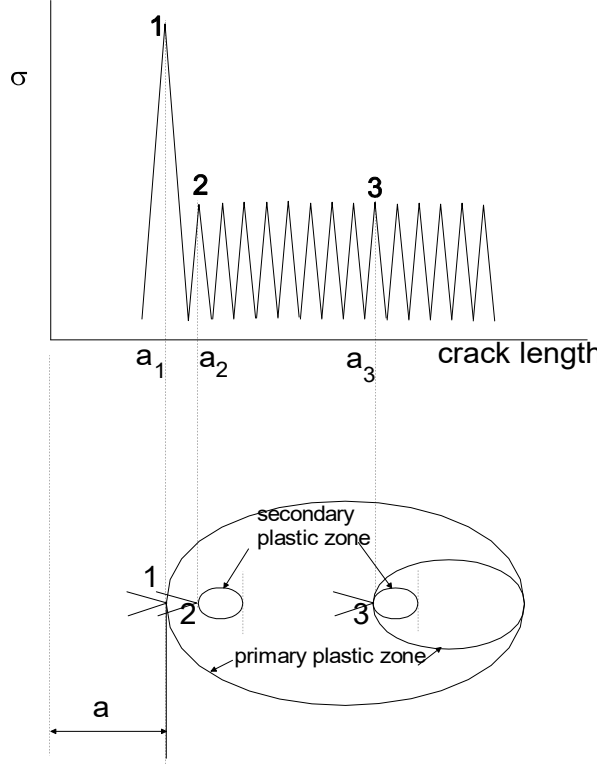


Figure 9 - Schematic of analytical crack-closure model under cyclic loading

It remains to discuss how to calculate  $K_{open}$ , the stress at which the crack opens and begins to grow. There exist empirical curve-fits in which the opening stress ratio  $K_{open}/K_{max}$  is cast as a function of applied stress ratio  $R$ , the maximum-stress-to-flow-stress ratio  $S_{max}/\sigma_o$ , and constraint factor  $\alpha$ . One such fit is used for the function  $f$  in the NASGRO equation (2.1). These fits are derived from experimental data or finite-element predictions for constant-amplitude fatigue tests. As such they can account for stress level effects in constant amplitude fatigue data by collapsing  $da/dN - \Delta K$  curves for multiple  $R$  values, but they cannot account for stress-interaction effects such as growth rate retardation or acceleration after overloads or underloads.

The Strip Yield model in NASGRO calculates a value for  $K_{open}$  by using a crack-opening model based on the Dugdale strip-yield model [28] but modified to leave plastically deformed material in the crack wake. In this strip-yield model it is assumed that all plastic deformation is contained within an infinitesimally thin strip located along the crack line in an infinite thin sheet. The material within the strip is represented by a series of finite-width rigid-perfectly plastic bar elements. These bar elements are either intact (in the plastic zone ahead of the crack tip, region 2 in figure 10) or broken (in the crack wake, region 3 in Figure 10). Elements in the plastic zone can carry tensile and compressive stresses, while the crack wake elements in

contact can only carry compressive stresses. Outside this strip, in the elastic continuum (region 1 in Figure 10), the material is perfectly elastic.

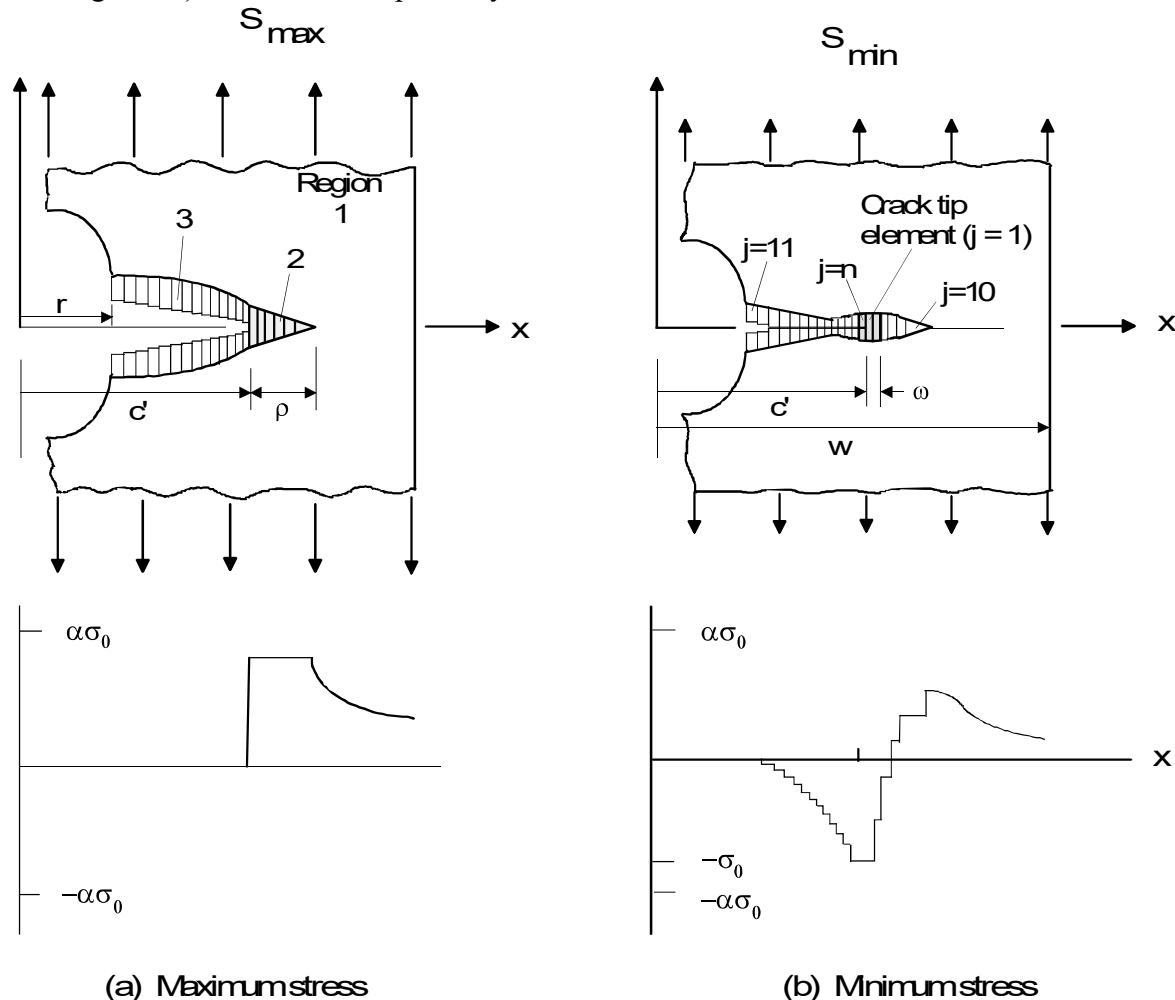


Figure 10 - Schematic of the Strip Yield Model

In simple terms, the strip-yield computations generally proceed as follows: a crack growth increment size is determined based on factors such as load step size and previous crack growth rate. During the current increment, the opening stress is assumed to be a constant equal to the value from the previous increment. At maximum applied load the plastic deformation in elements ahead of the crack tip is calculated and the crack is grown this increment by releasing an appropriate number of elements. At minimum load the contact stress is calculated for elements now in contact due to the recent plastic deformation at maximum load. This in turn gives rise to a new opening stress and crack growth rate for the next increment, and the number of load cycles expended in the current increment.

The advantage of using a strip yield model is that the stress and deformation solution can be obtained by superposition of two elastic solutions: a crack in a plate subjected to remote

uniform stress and a crack in a plate subjected to uniform stress acting along a portion of the crack surface, as shown in Figure 11 below.

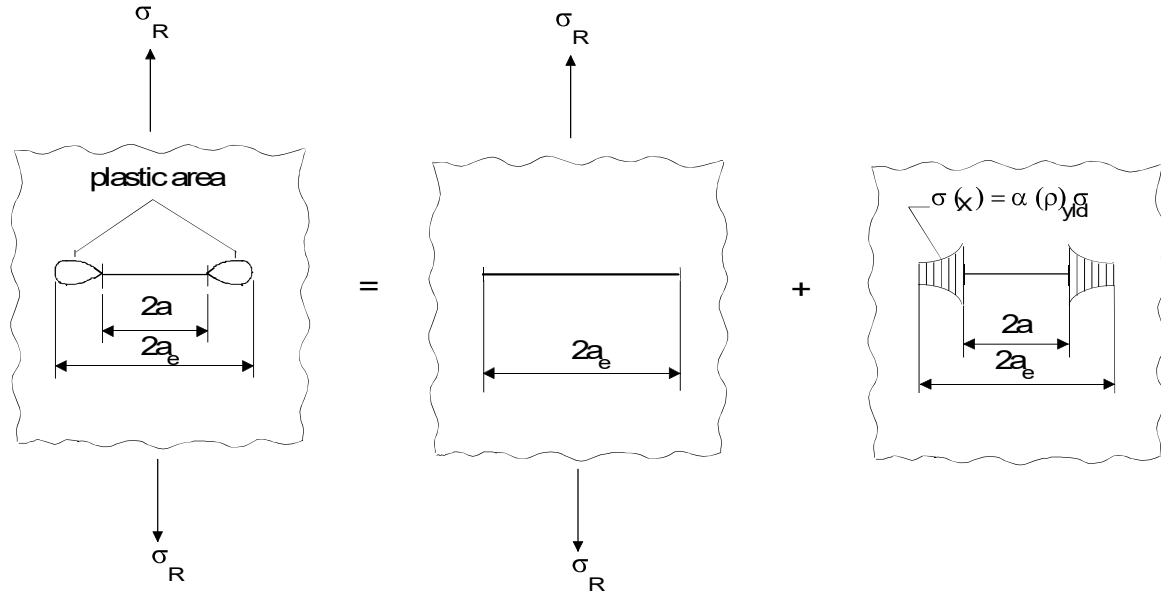


Figure 11 - Dugdale Model: Superposition of two elastic solutions

Dugdale's original strip-yield model was defined only for thin sheets, i.e., under plane stress conditions. To accommodate a more general state of stress in modern strip-yield models, the local yield stress is elevated by a constraint factor  $\alpha$ , where  $\alpha=1$  for plane stress and  $\alpha=3$  for plane strain. In practice, though, it is difficult to find fully plane strain or plane stress conditions, and  $\alpha$  ranges between 1.15 and 2.5. In compression the constraint factor is taken to be unity.

#### 2.1.7.4.a Strip Yield Model - Constant constraint-loss option

NASGRO contains two distinct implementations of the Strip Yield model. In one the constraint distribution ahead of the crack tip is spatially constant, while the other features a spatially parabolically decaying constraint; both feature a constraint-loss mechanism by which the current state of stress, ranging from plane strain to plane stress, can be accounted for.

The first model, used predominantly by NASA, FAA, their contractors, and airframe manufacturers, is the so-called constant constraint-loss option. In this option, the tensile constraint factor  $\alpha$  is constant along the elements of the plastic zone, but its value depends on the state of stress, ranging from plane strain to plane stress. This constraint loss is based on the observation that cracks which start initially with a flat face eventually grow in a slant face mode, as shown in Figure 12.

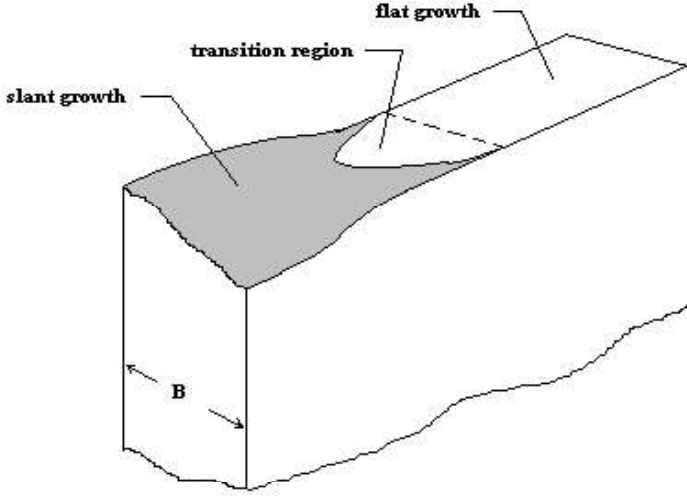


Figure 12 - Flat to slant crack growth transition

This transition is a manifestation of changing constraint: at low crack growth rates the flat crack growth indicates plane strain constraint, while at high rates the slant crack growth indicates plane stress constraint. In many materials the transition from flat to slant crack growth appears to end at the same crack growth rate and is independent of applied stress ratio. Because the crack closure concept can be used to collapse crack growth rate data to a single  $da/dN - \Delta K_{eff}$  relation, the effective stress intensity factor can be used to control the transition from flat to slant growth, i.e. determine which constraint value is appropriate. Newman proposed that the transition occurs when the cyclic plastic zone size (calculated from  $\Delta K_{eff}$ ) reaches a percentage of the specimen thickness:

$$(\Delta K_{eff})_T = \mu \sigma_0 \sqrt{B} \quad (2.37)$$

where  $\mu$  is the proportionality coefficient,  $\sigma_0$  is the flow stress (average of yield and ultimate),  $B$  is the specimen thickness, and  $(\Delta K_{eff})_T$  is the effective stress intensity factor at transition. He found that a value of 0.5 for  $\mu$  was suitable for a range of materials within a  $\pm 20\%$  scatter band for thin sheet; values tend to be lower for larger thickness values and higher for smaller thickness values. The constraint value does not change abruptly when the effective SIF crosses its transition value. Rather, there is a region starting at this transition value in which the constraint varies linearly from its plane strain value to its plane stress value. The extent of this transition region has been estimated conservatively at 1.0 decades of rate, as shown in Figure 13 below. Note that this has changed slightly from earlier versions of NASGRO wherein the transition point marked the *center* of the transition region, and the extent of the region was 1.5 decades. The extent of this transition region is not well-understood, and is subject to further study and refinement.

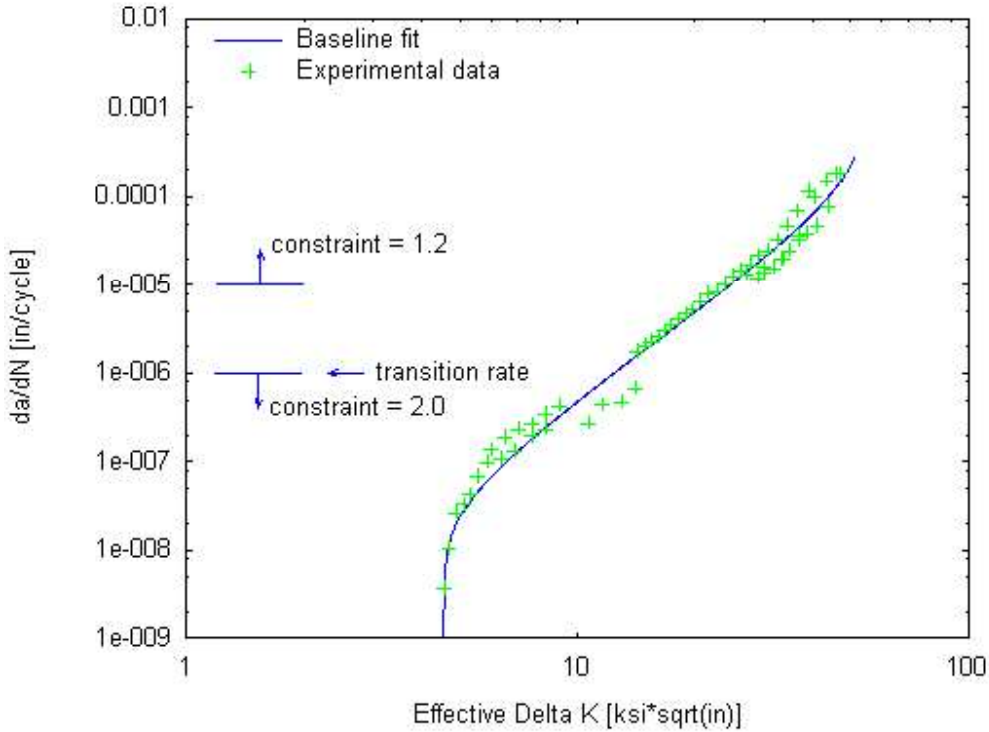


Figure 13 - Illustration of constraint transition region

Operationally the procedure is as follows. The Strip-Yield model initially calculates the transition value of  $\Delta K_{eff}$  from Eq 2.37 above, and uses it to determine the transition crack growth rate. Then it calculates the crack growth rate corresponding to the constraint value and opening stress for the current increment of crack growth. If this value of rate is greater than the upper limit of the transition band, then the constraint factor for the next crack growth increment is set to the appropriate plane stress value. If the rate is below the transition band, the constraint factor for the next crack growth increment is set to the appropriate plane strain value. This implementation is very similar to Newman's FASTRAN fatigue crack closure model.

This model is now available for both the NASGRO crack growth rate equation and the crack growth rate table look-up option, and tensile constraint factor values are chosen by material category. For example, plane strain values for aluminum alloys are generally taken to be 1.9, for steel alloys it is 2.1, and for titanium alloys it is 2.5. Plane stress values are assumed to be 1.2 for all materials, while compressive constraint factors both in the plastic zone and in the crack wake are assumed to be unity for all materials. Future research may refine these assumptions.

The NASGRO materials database contains such look-up tables for a number of materials, and they can be augmented by user-supplied data. To set the value of the tensile constraint factor, the user would run a number of constant-amplitude crack-growth rate predictions with this model and fix the value of  $\alpha$  to give the best fit.

### 2.1.7.4.b Strip Yield Model - Variable constraint-loss option

The second option, used predominantly by the European Space Agency (ESA) and their contractors, is the so-called variable constraint-loss option. In this option, the tensile constraint factor  $\alpha$  varies along the elements of the plastic zone according to a parabolic expression derived from finite-element analyses. The constraint decays spatially from its value at the crack tip ( $\alpha_{tip}$ ) to a plane stress value of 1.15 at the forward end of the plastic zone. Constraint loss is also built into this option, but in contrast to the model above, the plane strain or plane stress tensile value of  $\alpha_{tip}$  is calculated from the ratio of plastic zone size to specimen thickness. This relates the constraint loss to  $K_{max}$ , whereas the model described in the previous section relates it to  $\Delta K_{eff}$ . Furthermore, as seen in Figure 14, the compressive constraint factors in the plastic zone and in the crack wake are spatially constant, and their values are given by  $\alpha_{tip}/\alpha_{new}$  and  $1/\alpha_{new}$ , respectively, where the material parameter  $\alpha_{new}$  characterizes the ratio of tensile tip constraint to compressive constraint.

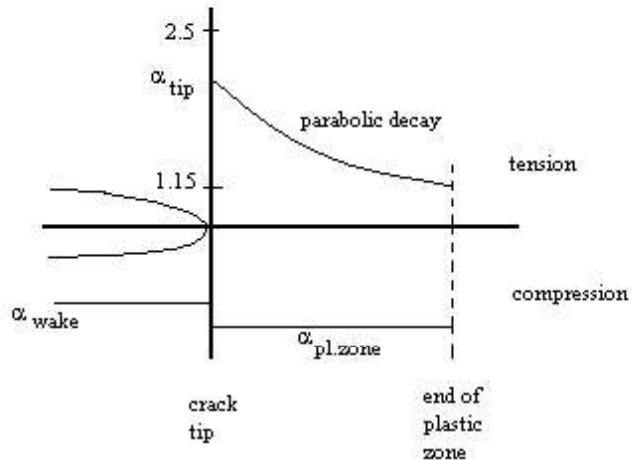


Figure 14 - Constraint factors in tension and compression

Operationally the procedure is as follows. The Strip-Yield model calculates the plastic zone size to thickness ratio for the current increment of crack growth; for small values of this ratio (less than 0.1),  $\alpha_{tip}$  is set to its plane strain value of 2.35. For large values (greater than 1.5),  $\alpha_{tip}$  is set to its plane stress value of 1.15. Intermediate values are determined from piece-wise linear interpolation. The compressive constraint factors are then calculated from  $\alpha_{tip}$  and  $\alpha_{new}$ .

This model is available for both the equation and table look-up options of crack growth rate description. The equation description is available for the traditional NASGRO equation (equation 2.1) as well as an enhanced version of this equation, developed by NLR (Dutch National Aerospace Laboratory), in which growth due to spike overloads is treated via a tearing

analogy. The NASGRO materials database contains equation parameters for a number of materials provided by ESA and NLR, and they can be augmented by user-supplied data. To set the value of the tensile-to-compressive constraint ratio  $\alpha_{new}$ , two or three different  $\alpha_{new}$  values are chosen for Strip-Yield comparisons to selected constant-amplitude and spike load sequences. Engineering judgment and interpolation then gives the best fit for  $\alpha_{new}$ . This final value is then used to set the remaining equation constants if they are needed.

#### 2.1.7.4.c Strip Yield Model - Usage

Use of either implementation of the Strip Yield module is virtually transparent to the user. After selecting the strip-yield model from the menu of interaction models and choosing the appropriate constraint model option (“spatially constant constraint variation” or “spatially variable constraint variation”), the user is presented with a choice of computation speed modes: full or fast. In the “full” mode, the strip-yield model is used to calculate the opening stress throughout the entire analysis. The “fast” mode makes use of the fact that for some load spectra the opening stress may stabilize and oscillate about some average value at some point in the load spectrum; the model is used only until a cycle-averaged value of opening stress is stabilized (within a user-specified tolerance, generally about 1%) within a load schedule. Subsequent load schedules then bypass the strip-yield calculations and use this stabilized value directly in crack growth equation (2.1). At this point the Strip Yield model mimics the non-interaction model, albeit with a computationally derived closure level.

In the Strip Yield model, the crack growth increments are chosen on the basis of load step size and crack growth rate from the previous increment. The first cycle of any load step is always analyzed separately and a minimum number of five increments to span the rest of the load step is guaranteed. For the case of aircraft load spectra or variable-amplitude load spectra, where load steps tend to contain very few cycles or frequently only one cycle, this basis of choosing the increment size would quickly force a cycle-by-cycle analysis, an accurate analysis but at a great expense of computer time. If the user wishes to analyze aircraft or variable-amplitude spectra but avoid cycle-by-cycle analyses, then there are two additional parameters to specify. These parameters govern an algorithm in which only the most severe load cycles are considered for the computations, where “severe” is effectively determined by the user input for these parameters. The first parameter is the difference in applied stress,  $\Delta S_{max}$ , from one significant maximum load (or minimum load) to the next that is required to trigger a calculation. This ensures that significant overloads or underloads are captured by the algorithm and that the increment size is set appropriately. The second parameter is the maximum number of cycles  $\Delta N_{max}$  that can be expended in an increment before another calculation is triggered. This ensures that spectra containing long constant-amplitude steps use enough increments to give good results.

The user then chooses the initial defect type: closed crack, such as in the case of fatigue cracks, or open crack, such as in the case of saw-cuts.

Diagnostic messages are printed at the end of the analysis giving information on constraint type and value, computation speed mode, initial defect type, and cycle-averaged opening stress

values (these are used in the “fast” computation mode but may be of general statistical interest for the “full” mode as well.)

Note: at this writing, there is a condition that will cause a program crash. This condition occurs under the combination of using a 2-D crack case with an initial  $a/c > 1$  and a first cycle that has both the maximum and minimum stress values less than zero. This problem is under study, but a work-around is to add a dummy tension-tension cycle with small stress values at the beginning of the block.

### 2.1.7.5 Constant Closure Model

This crack growth model was originally developed in early 1990s by Matt Creager for Boeing/Northrop. It is a simplified closure model based on the empirical observation that for some load spectra the crack closure level does not deviate substantially from some stabilized value. A requirement for this condition to occur is that the applied load spectrum contains a “controlling overload” (COL) and a “controlling underload” (CUL) which occur often enough to keep the residual stresses in the crack wake, and thus the opening stress, constant. The value of this stabilized closure level is a function of the material, and the controlling overload and underload, which are defined as follows:

$COL = 95\%$  of the peak load value that has at least 20 exceedances per lifetime

$CUL =$  the valley load that has the same number of exceedances as the COL

By taking advantage of these observations, the crack opening stress need be calculated only once for the entire spectrum rather than for each cycle. This model is available for the NASGRO equation and  $da/dN-\Delta K$  1-D table look-up.

The constant value of the opening stress  $S_{open}$  can be calculated from the stabilized closure level  $CF_{spec}$ , where  $CF_{spec}$  is defined as  $CF_{spec} = S_{open} / COL$  and is determined by one of the following:

1. direct entry of  $CF_{spec}$ ,
2. 3-region empirical curve-fit of the closure level  $CF$  in terms of  $R$ , evaluated at the spectrum stress ratio  $R_{spec}$  to give  $CF_{spec}$ , or
3. Newman's opening stress function evaluated at  $R_{spec}$  to give  $CF_{spec}$

where the applied load spectrum's stress ratio  $R_{spec}$  is defined as  $R_{spec} = CUL / COL$  and is calculated from user-supplied values of  $CUL$  and  $COL$ .

Note: both  $CUL$  and  $COL$  are required input for all three options in order to calculate  $R_{spec}$ . While  $R_{spec}$  is required in calculating  $CF_{spec}$  for options 2 and 3, it is used for informational purposes only in the output for option 1.  $COL$  is also used to calculate the stabilized opening stress value from  $CF_{spec}$  for all three options, as described in a subsequent paragraph.

The 3-region curve fit is shown in Figure 15: in the  $R < 0$  region  $CF$  is given by a linear, least-squares curve fit of test data for complex spectra with negative  $R$ -ratios:

$$CF = m \cdot R + b \quad (2.38)$$

where  $m$  and  $b$  (the slope, and intercept at  $R = 0$ , respectively) are user-supplied constants.

In the mid-range region ( $0 < R < R_i$ ) it is assumed that the Walker equation is valid for modeling stress ratio effects, and thus  $CF$  can be related to the Walker exponent  $M$  by the equation

$$CF = 1 - (1 - b) \cdot (1 - R)^M \quad (2.39)$$

In the high- $R$  region ( $R > R_i$ )  $CF$  is assumed to be equal to  $R$ . The value of  $R_i$  is obtained from simultaneously solving the  $CF$  equations for the Walker and high- $R$  regions.

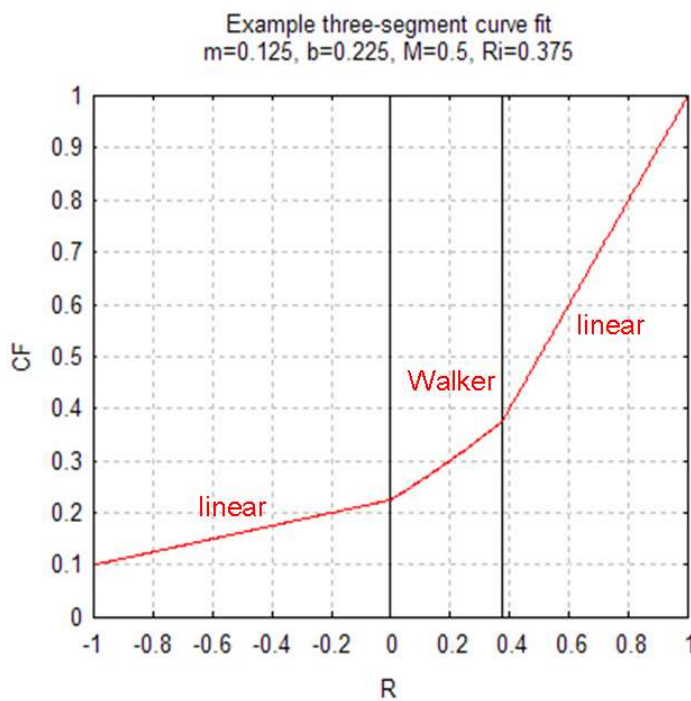


Figure 15 Example of a 3-segment curve fit

Newman's opening stress function  $f$  (where  $f = S_{open} / S_{max}$ ) for plasticity-induced crack closure is described in detail in section 2.1.1 of this manual, and a typical representation of this function was shown in Figure 2. Values of this function's fitting parameters (e.g. the constraint parameter  $\alpha$  and the applied stress ratio  $S_{max} / \sigma_o$ , where  $\sigma_o$  is the average between yield and ultimate strengths) are taken from the NASGRO or user material database files, or are user-supplied.

As mentioned in a previous paragraph, the stabilized opening stress  $S_{open}$  is calculated from the stabilized spectrum closure level  $CF_{spec}$ ; this opening stress value is then used to calculate  $\Delta K_{eff}$  for use in the crack growth rate equation or in the  $da/dN-\Delta K$  table look-up procedure. The computational procedure is as follows:

1. Input phase:
  - a. The stabilized closure level  $CF_{spec}$  is calculated (or supplied by the user) using one of the three options described above
  - b. The stabilized opening stress  $S_{open}$  is calculated using  $CF_{spec} = S_{open} / COL$ ; this opening stress value applies to every cycle in the spectrum
  - c. In addition, if  $da/dN-\Delta K$  tables rather than the NASGRO equation are to be used in the crack growth calculation phase, then input of  $CF_{data}$  and  $R_{data}$  values describing  $CF$  and  $R$  for the spectrum used in generating the  $da/dN$  tables is also required
2. Crack growth calculation phase:
  - a. If using the NASGRO crack growth rate equation: the spectrum's stabilized opening stress  $S_{open}$  and the current cycle's maximum applied load  $S_{max}$  are used to calculate  $\Delta K_{eff}$  and thence  $da/dN$  for the current crack growth calculation increment
  - b. If using  $da/dN-\Delta K$  tables: the spectrum's stabilized opening stress  $S_{open}$  and the current cycle's maximum applied load  $S_{max}$  are used to calculate  $\Delta K_{eff}$ ; this value of  $\Delta K_{eff}$  is used in interpolating a  $da/dN$  value within the table for the current crack growth calculation increment, with the table's  $\Delta K$  values converted to  $\Delta K_{eff}$  by multiplying by  $(1-CF_{data}) / (1-R_{data})$

#### **2.1.7.6 Notes on using the Load Interaction Models**

This section is meant to indicate to users, based on experience here at JSC, when to use the load interaction models. In general, caution should be exercised when these models are used because they can be less conservative compared to the non-interaction model. This is so because the dominant effect modeled is retardation, even if accelerated growth is predicted in a few cases. Before applying these models for life predictions, it is recommended that the user gain sufficient experience and fine-tune the various model parameters based on comparisons with test data for the kind of spectra relevant to the usage. Certain special structural features might cause the predictions from NASGRO to be in disagreement with test data. An example of this would be a crack growing out of a hole in a plate that has been subjected to considerable yielding. Such a crack would exhibit a lot of retardation in experiments but none of the NASGRO models accounts for the presence of such yielding.

In the case of the Generalized Willenborg model, the only parameter that can be varied is the overload shutoff ratio  $R_{so}$ . Table 1 shows the effect of this parameter on life prediction for Zhang's spectra. Table 2 shows the effect of  $\phi_0$  on life prediction using the modified generalized Willenborg model. These are the spectra with single or multiple overloads applied after several constant amplitude cycles. A trend of decreasing values of predicted life with increasing values of  $R_{so}$  was found. For the Modified Generalized Willenborg model, because  $\phi_0$  appears in the denominator, the opposite trend, i.e., increased life with increasing values of  $\phi_0$  was found. Table 3 summarizes life predictions using various growth models for Zhang's spectra.

Tables 4, 5 show life predictions using the various models for ASTM round robin spectra [29] that are typical aircraft spectra. In Table-4, comparison of current predictions is made with results from Chang [29]. For the case of non interaction model, using Walker growth rate equation with one segment, exact matching of results was obtained (see columns 6, 7), except for transport spectrum(M-93, M-94). The spectra given in [29] were cycle-counted using range-pair method, using a FORTRAN routine supplied by D. Ball[30]. These spectra were then used in the crack growth analysis. The exact matching verifies the coding of Walker equation in NASGRO as well as the cycle-counting algorithm. The next step was to look for agreement when the Chang-Willenborg load interaction model is used. Columns 11, 12 should have agreed, but as can be seen from the table, they don't match exactly. The reason is not clear as yet, but the numbers are not too far apart. The other columns in the table were shown because, in [24], the equation for negative stress ratios was modified and also two-segment fit was used for Walker equation. Table 5 summarizes the predictions by other methods, such as the Generalized and Modified Willenborg. The later two methods do somewhat better job in predicting the crack growth. Overall, the load interaction models are not as conservative as the non interaction models. It is found to be generally true that the predictions are more conservative at higher stress levels for a given load spectrum. There is one very conservative prediction for M-94 for non interactive Walker model which stands out from rest of the table. The analysis was double-checked and it is not clear why the ratio is so high compared to the rest of the values in the table.



**Generalized Willenborg Predictions ( $N_{\text{test}} / N_{\text{pred}}$ ) for Zhang's Spectra  
(Material :7475-T7351), December 2004**

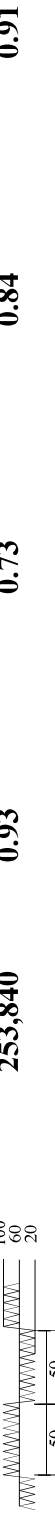
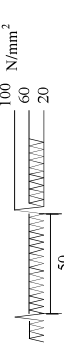
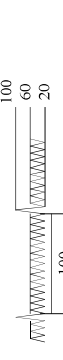
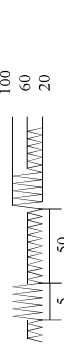
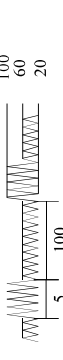
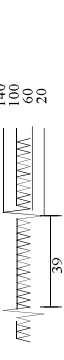
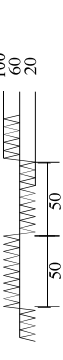
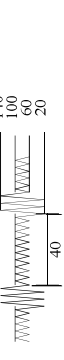
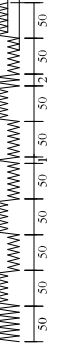
<b>Zhang's Test</b>	<b>Loading History</b>	<b>Test Life (Cycles)</b>	<b>Non-Interaction</b>	<b>Generalized Willenborg Model</b>	
			$(R_{SO} = 2.3)$	$(R_{SO} = 3.0)$	$(R_{SO} = 4.0)$
<b>1</b>		<b>474,240</b>	<b>1.50</b>	<b>0.68</b>	<b>1.10</b>
<b>2</b>		<b>637,730</b>	<b>1.93</b>	<b>0.82</b>	<b>1.38</b>
<b>3</b>		<b>251,210</b>	<b>1.05</b>	<b>0.67</b>	<b>0.87</b>
<b>4</b>		<b>409,620</b>	<b>1.46</b>	<b>0.79</b>	<b>1.14</b>
<b>5</b>		<b>179,320</b>	<b>0.96</b>	<b>0.86</b>	<b>0.91</b>
<b>6</b>		<b>251,050</b>	<b>1.42</b>	<b>1.32</b>	<b>1.38</b>
<b>7</b>		<b>253,840</b>	<b>0.93</b>	<b>0.73</b>	<b>0.84</b>
<b>8</b>		<b>149,890</b>	<b>1.16</b>	<b>1.12</b>	<b>1.15</b>
<b>10</b>		<b>57,680</b>	<b>1.20</b>	<b>1.18</b>	<b>1.18</b>

Table 1 Effect of R<sub>SO</sub> on life prediction for Generalized Willenborg Model

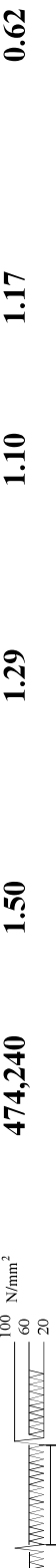
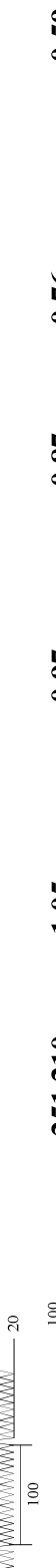
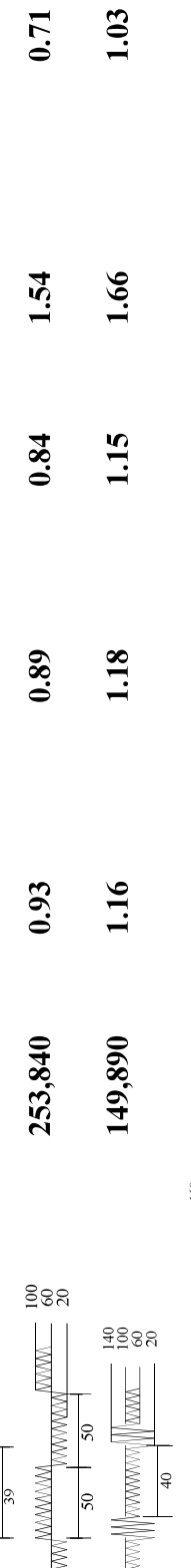
**Modified Generalized Willenborg Predictions ( $N_{test} / N_{pred}$ ) for Zhang's Spectra  
(Material :7475-T7351), December 2004**

Zhang's Test	Loading History	Test Life (Cycles)	Non-Interaction		Modified Generalized Willenborg Retardation Model	
			$(\Phi_0)^* = 0.2$	$(\Phi_0) = 0.4$	$(\Phi_0) = 0.2$	$(\Phi_0) = 0.6$
<b>1</b>		<b>474,240</b>	<b>1.50</b>	<b>1.29</b>	<b>0.70</b>	<b>0.31</b>
<b>2</b>		<b>637,730</b>	<b>1.93</b>	<b>1.64</b>	<b>0.85</b>	<b>0.31</b>
<b>3</b>		<b>251,210</b>	<b>1.05</b>	<b>0.97</b>	<b>0.68</b>	<b>0.49</b>
<b>4</b>		<b>409,620</b>	<b>1.46</b>	<b>1.30</b>	<b>0.81</b>	<b>0.48</b>
<b>5</b>		<b>179,320</b>	<b>0.96</b>	<b>0.95</b>	<b>0.90</b>	<b>0.83</b>
<b>6</b>		<b>251,050</b>	<b>1.42</b>	<b>1.42</b>	<b>1.37</b>	<b>1.29</b>
<b>7</b>		<b>253,840</b>	<b>0.93</b>	<b>0.89</b>	<b>0.74</b>	<b>0.63</b>
<b>8</b>		<b>149,890</b>	<b>1.16</b>	<b>1.18</b>	<b>1.15</b>	<b>1.11</b>
<b>10</b>		<b>57,680</b>	<b>1.20</b>	<b>1.18</b>	<b>1.21</b>	<b>1.18</b>

\*  $\Phi_0$  = Retardation parameter

Table 2 -Effect of  $\phi_0$  on Life Prediction for Modified Generalized Willenborg Model

NASGRO Predictions ( $N_{\text{test}} / N_{\text{pred}}$ ) for Zhang's Spectra  
(Material :7475-T7351 Al, Case TC01) December 2004

Zhang's Test	Loading History	Test Life (Cycles)	Non-Interaction ( $\Phi_0 = 0.2$ )	Interaction Models		
				Generalized Willenborg (modified) ( $\Phi_0 = 0.2$ )	Constant Closure(5) ( $R_{SO}^* = 3.0$ )	Strip Yield
1		474,240	1.50	1.29	1.10	0.62
2		637,730	1.93	1.64	1.38	0.72
3		251,210	1.05	0.97	0.87	0.59
4		409,620	1.46	1.30	1.14	1.10
5		179,320	0.96	0.95	0.91	0.87
6		251,050	1.42	1.42	1.38	2.58
7		253,840	0.93	0.89	0.84	1.54
8		149,890	1.16	1.18	1.15	1.66
10		57,680	1.20	1.18	1.18	23.4

$\Phi_0 = \text{retardation parameter for } R_U(\text{underload-to-overload ratio})=0$ ,  $R_{SO} = \text{shut-off overload ratio}$

Table 3 Life predictions for Zhang's Spectra

( $N_{\text{test}}/N_{\text{pred}}$ ) for ASTM Round Robin Spectra (Material: 2219-T851 Alum, L-T Orient.)  
 (Date: December 2004 - using Range-Pair counting)

Spec. No.	Loading Spectrum	Stress ksi	Test Cycles	Non Int. Walker 2 segments	Non Int. Walker 1 segment	Non Int. Jim Chang Ref.[29]	Interaction Walker,[24] 2 segments R <sub>SO</sub> = 3.0	Interaction Walker,[24] 1 segment R <sub>SO</sub> = 3.0	Chang-Wbreg Walker,[29] 1 segment R <sub>SO</sub> = 3.0	Chang-Wbreg Walker,[29] 1 segment R <sub>SO</sub> = 3.0	Interaction Chang-Wbreg Walker,[29] 1 segment R <sub>SO</sub> = 3.0
M-81	Air-Air	20	115700	0.81	0.82	0.83	0.58	0.57	0.62	0.68	
M-82		30	58585	1.05	1.32	1.32	0.75	0.90	0.98	1.10	
M-83		40	18612	0.93	1.27	1.27	0.65	0.88	0.94	1.08	
M-84	Air-Ground	20	268908	0.87	0.90	0.88	0.58	0.58	0.66	0.73	
M-85		30	95642	1.10	1.31	1.30	0.73	0.81	0.92	1.04	
M-86		40	36397	1.17	1.55	1.56	0.77	0.94	1.08	1.25	
M-88	Ins-Navigation	30	380443	1.33	1.37	0.94	0.68	0.70	0.77	0.72	
M-89		40	164738	1.53	1.74	1.74	0.76	0.82	0.91	0.89	
M-90	Fighter-Comp.	20	218151	0.89	0.95	0.94	0.59	0.61	0.67	0.75	
M-91	Fighter-Comp.	30	65627	1.03	1.26	1.26	0.67	0.78	0.87	0.99	
M-92	Fighter-Comp.	40	22187	0.95	1.30	1.30	0.63	0.79	0.89	1.02	
M-93	Transport	14	1354024	0.88	1.01	0.56	0.67	0.54	0.60	0.76	
M-94	Transport	19.6	279000	1.03	0.99	0.65	0.80	0.71	0.78	0.88	

Table 4 Comparison of life predictions for ASTM round robin spectra

(N<sub>test</sub>/N<sub>pred</sub>) for ASTM Round Robin Spectra (Material: 2219-T851 Alum, L-T Orient.)

(Date: December 2004 - using Range-Pair counting)

Spec. No.	Loading Spectrum	Stress ksi	Test Cycles	Non Int. NASGRO	Non Int. Walker 2 segments	Chang-Wbrg Walker 2 segments	G.Willenborg NASGRO R <sub>SO</sub> = 3.0	M. Willenborg NASGRO phi0=0.4
<b>M-81</b>	<b>Air-Air</b>	<b>20</b>	<b>115700</b>	<b>1.35</b>	<b>0.81</b>	<b>0.58</b>	<b>0.88</b>	<b>1.02</b>
<b>M-82</b>		<b>30</b>	<b>58585</b>	<b>2.02</b>	<b>1.05</b>	<b>0.75</b>	<b>1.35</b>	<b>1.56</b>
<b>M-83</b>		<b>40</b>	<b>18612</b>	<b>1.95</b>	<b>0.93</b>	<b>0.65</b>	<b>1.32</b>	<b>1.54</b>
<b>M-84</b>	<b>Air-Ground</b>	<b>20</b>	<b>268908</b>	<b>1.45</b>	<b>0.87</b>	<b>0.58</b>	<b>0.85</b>	<b>0.96</b>
<b>M-85</b>		<b>30</b>	<b>95642</b>	<b>1.95</b>	<b>1.10</b>	<b>0.73</b>	<b>1.14</b>	<b>1.33</b>
<b>M-86</b>		<b>40</b>	<b>36397</b>	<b>2.28</b>	<b>1.17</b>	<b>0.77</b>	<b>1.37</b>	<b>1.60</b>
<b>M-88</b>	<b>Ins-Navigation</b>	<b>30</b>	<b>380443</b>	<b>2.25</b>	<b>1.33</b>	<b>0.68</b>	<b>0.90</b>	<b>1.02</b>
<b>M-89</b>		<b>40</b>	<b>164738</b>	<b>2.71</b>	<b>1.53</b>	<b>0.76</b>	<b>1.07</b>	<b>1.26</b>
<b>M-90</b>	<b>Fighter-Comp.</b>	<b>20</b>	<b>218151</b>	<b>1.53</b>	<b>0.89</b>	<b>0.59</b>	<b>0.90</b>	<b>1.05</b>
<b>M-91</b>	<b>Fighter-Comp.</b>	<b>30</b>	<b>65627</b>	<b>1.91</b>	<b>1.03</b>	<b>0.67</b>	<b>1.15</b>	<b>1.35</b>
<b>M-92</b>	<b>Fighter-Comp.</b>	<b>40</b>	<b>22187</b>	<b>1.98</b>	<b>0.95</b>	<b>0.63</b>	<b>1.20</b>	<b>1.40</b>
<b>M-93</b>	<b>Transport</b>	<b>14</b>	<b>1354024</b>	<b>0.92</b>	<b>0.88</b>	<b>0.67</b>	<b>0.80</b>	<b>0.89</b>
<b>M-94</b>	<b>Transport</b>	<b>19.6</b>	<b>279000</b>	<b>1.08</b>	<b>1.03</b>	<b>0.80</b>	<b>0.95</b>	<b>1.06</b>

Table 5 Life predictions for ASTM round robin spectra

One of the choices the user makes while using Strip Yield is the “full” mode, which has better accuracy at the expense of computation time, or the “fast” mode, which provides faster results at the expense of accuracy. It is advised that if this “fast” option is chosen, several analyses be done at different tolerances to gauge their effect and to ensure convergence. It may be noted that the “fast” option is useful in the case of load spectra where the opening stress stabilizes. This usually occurs in spectra where the mean stress stays relatively constant for many load steps. The fast option is not suitable for spectra producing opening stresses that fluctuate greatly rather than stabilize.

Additional user input to Strip Yield are the two parameters used to prevent Strip Yield from analyzing aircraft spectra by default on a cycle-by-cycle basis. As mentioned in the previous section, the first parameter  $\Delta S_{\max}$  is the change in applied stress from one significant load to the next before triggering a  $K_{open}$  calculation. The second parameter  $\Delta N_{\max}$  is the maximum number of cycles expended between  $K_{open}$  calculations. Larger values chosen for both parameters mean a larger crack increment size and fewer  $K_{open}$  calculations, possibly resulting in lower accuracy. However, the effect on the speed of computations is of opposite nature, i.e., larger values result in faster execution. For example, for single-spike overloads  $\Delta N_{\max}$  would be chosen small enough to ensure that each spike is captured in a separate  $K_{open}$  calculation. An analogy to  $\Delta S_{\max}$  is the stress level clipping used in cycle counting of sequential loading. For example, for random loading  $\Delta S_{\max}$  would be chosen small enough to ensure that large deviations in loading trigger separate  $K_{open}$  calculations. These two parameters are highly load spectrum dependent, and only experience in using the program will allow one to make reasonable “educated” assessments.

### 2.1.8 Cyclic Shakedown

In some situations the calculated local elastic stresses in a component may exceed the yield strength of the material, especially near a stress concentration such as a hole or slot. When this happens, the most common result is for yielding to occur locally. This local yielding usually causes a local decrease in the stresses from their calculated elastic values, as well as some local redistribution of stresses to maintain equilibrium (and the stress redistribution may cause some local stress values to increase). If the calculated local elastic stress range exceeds twice the yield strength (for example, when applied stresses are fully reversed and the maximum stresses exceed the yield strength), then reversed yielding may occur (and may occur repeatedly).

A cyclic shakedown algorithm is available in NASGRO to calculate approximately the local elastic-plastic stress redistribution and relaxation resulting from local yielding, based on the calculated elastic stress distribution in the region of interest. The new stress gradients are then used as input to univariant weight function stress intensity factor solutions. The NASGRO shakedown algorithm can accommodate reversed yielding on subsequent fatigue cycles, and so it is called a “cyclic” shakedown algorithm.

Further information about shakedown module availability, shakedown model options, stress input options, and required material input is provided in Section 11.7 of Appendix C. The methodology used in cyclic shakedown analysis is described and illustrated in Appendix M.

### 2.1.9 Temperature dependent crack growth analysis

An option has been added in a recent version of the NASFLA module introducing temperature as an input parameter into crack growth analysis. This option is invoked by choosing the data source of material properties as “NASGRO material file, incl. temperature data”. Properties for a set of temperatures are then chosen from a limited database provided with the software. In the load spectrum input, provision is made to enter a temperature value for each step of the load block. More details are given in Appendix P.

## 2.2 Details of Crack Growth Analysis

When the crack growth module is selected from the top level menu, the GUI for the NASFLA module is activated. Under the “Options” pull-down menu, the following three “Calculation Modes” are possible:

- 1) Calculate crack growth, given initial flaw size  
(Forward life prediction analysis)
- 2) Calculate initial flaw size, given target life  
(Inverse life prediction analysis)
- 3) Calculate scale factor multiplier, given target life  
(Inverse life prediction analysis)

If option 1 (default) is selected, the user enters data for the crack case, the initial flaw size, the material properties, and the load schedule. The program will then apply the load schedule to the crack case until the schedule has been repeated the desired number of times or until a failure condition is met, whichever occurs first. At that time, both fatigue life and final flaw size will be reported.

If option 2 is selected, the user is prompted for the crack case, the material properties, the target fatigue life, and the load schedule. The program will then iteratively calculate the initial flaw size needed to cause failure at the specified target life.

If option 3 is selected, the user is prompted for the crack case, the material properties, the target fatigue life, and the load schedule. The program will then iteratively calculate the stress scale factor multiplier needed to cause failure at the specified target life.

The solution of option 2 or 3 is an inverse calculation to determine the initial flaw size or stress scale factor multiplier for which the fatigue life is equal to the user-specified target life; i.e.,

$$N(x) - N_T = 0 \quad (2.40a)$$

or

$$y(x) = \frac{N(x) - N_T}{N_T} = 0 \quad (2.40b)$$

where  $x$  is the initial flaw size or stress scale factor multiplier,  $N(x)$  is the fatigue life, a function of  $x$ , and  $N_T$  is the target life. In NASFLA inverse calculation,  $y(x)$  is usually steep when  $x$  is small, and becomes shallow as  $x$  increases, as illustrated in the figure below. Generally, the curve has two asymptotes, i.e.  $x = x_T$  and  $y = -1$ , where  $x_T$  is the threshold for fatigue crack growth.

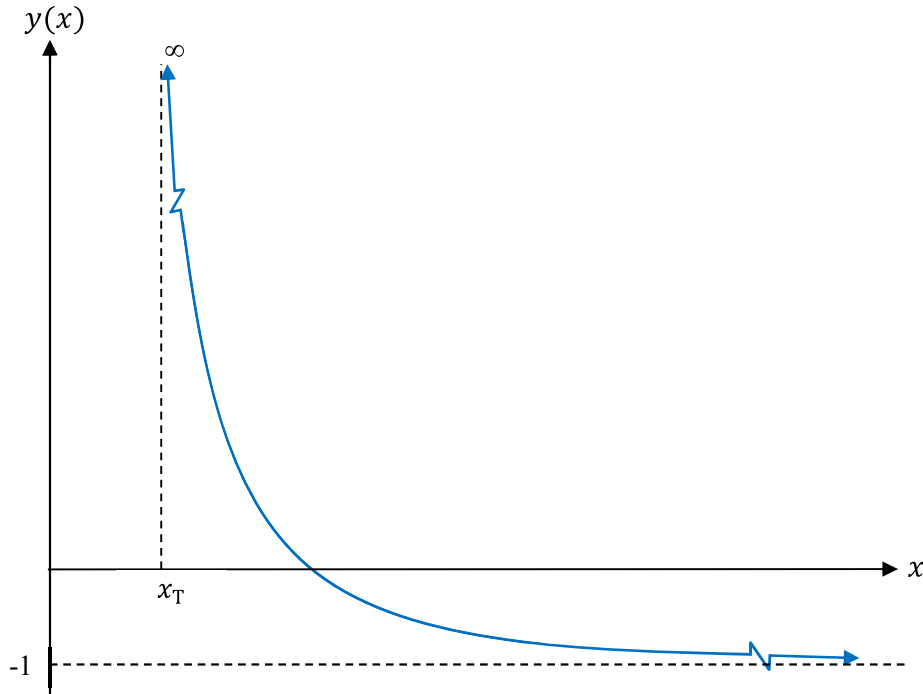


Illustration of the typical fatigue-life curve as a function of initial flaw size or stress scale factor

Since  $N(x)$  is a non-linear and implicit function of  $x$ , numerical methods have to be employed to solve eq. (2.40a) or (2.40b). The bisection method and the regula falsi method are two commonly-used methods to find the roots of non-linear equations. Both methods are guaranteed to converge to a root of  $y(x)$  if  $y(x)$  is a continuous function. The bisection method can handle a large root bracket efficiently, but convergence can be slow in the vicinity of the root. The regula falsi method exhibits the opposite features: it may be inefficient to handle a large root bracket, but it converges quickly near the root. Based on the above characteristics of the curve  $y(x)$ , a two-stage iteration scheme, called bisection/Pegasus iteration procedure, was developed to solve eq.(2.40b). The Pegasus method is an improved regula falsi method. During iteration, the bisection method is employed first, and the Pegasus method is triggered when the

function values of the current root bracket fall into a certain range, e.g. [-0.8, 4]. The solution is found when the fatigue life converges to the target life within the given tolerance, i.e.

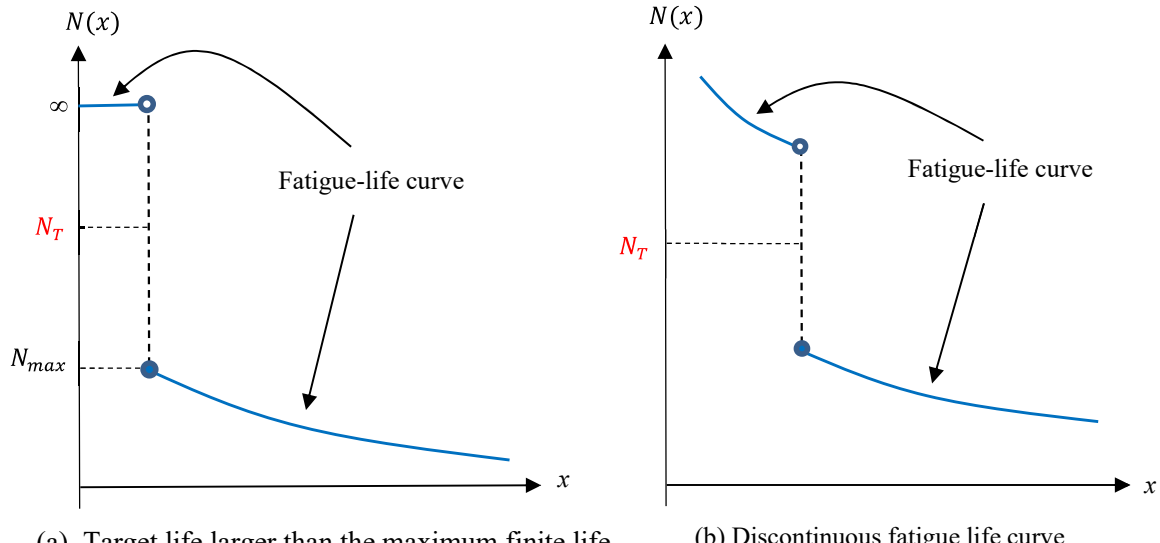
$$\frac{|N(x) - N_T|}{N_T} \leq 0.1\% \quad (2.41)$$

In order to employ the bisection or Pegasus method, the initial root bracket  $[x_{\min}, x_{\max}]$  has to be set.

For initial flaw size calculation, the initial root bracket is  $[x_{\min}, x_{\max}] = [a_{\min}, a_{\max}]$ , where  $a_{\min}$  and  $a_{\max}$  are the lower and upper limits of crack size, respectively, for the given crack case.

For stress scale factor multiplier calculation, the initial root bracket is  $[x_{\min}, x_{\max}] = [0, 10^6]$ , where an artificial upper limit ( $10^6$ ) of stress scale factor multiplier is adopted, which implies that NASGRO will search for the root up to  $x = 10^6$ .

As mentioned before, the bisection/Pegasus method is guaranteed to converge if the function  $y(x)$  is continuous at the point of the target life. Otherwise, the solution may not exist or cannot be found. In NASFLA inverse calculations, the fatigue-life curve can have two types of discontinuity, as shown in the figure below. The first type of discontinuity is that the target life is larger than the maximum finite fatigue life, which means the target life is actually in the threshold zone. The second type of discontinuity is that the target life is at a real discontinuous point of the fatigue-life curve. This sort of discontinuity could occur, for example, for a variable amplitude load history in which failure always occurs due to an infrequent peak load.



Two typical situations where the target life is at a discontinuous point

In order to avoid excessive iteration and non-convergence for the above two special cases, NASGRO performs a discontinuity check at every iteration step using the following two conditions:

$$\text{Condition 1: } \frac{|x_L - x_R|}{(x_L + x_R)/2} \leq 0.01\% \text{ and } \frac{|N_L - N_T|}{N_T} > 1\% \text{ and } \frac{|N_R - N_T|}{N_T} > 1\% \quad (2.42a)$$

$$\text{Condition 2: } \frac{|x_L - x_R|}{(x_L + x_R)/2} \leq 0.0001\% \text{ and } \frac{|N_L - N_T|}{N_T} > 0.1\% \text{ and } \frac{|N_R - N_T|}{N_T} > 0.1\% \quad (2.42b)$$

where  $(x_L, N_L)$  and  $(x_R, N_R)$  are the two closest points during iteration which straddle the target life  $N_T$ .

Condition 1 [(2.42a)] states that if the target life is straddled in a small region (0.01% tolerance) and the closest fatigue lives straddling the target life differ from the target life by more than 1%, the curve is discontinuous at the point of the target life.

Condition 2 [(2.42b)] states that if the target life is straddled in a tiny region (0.0001% tolerance) and the fatigue life has not converged to the target life (0.1% tolerance), the curve is discontinuous at the point of the target life.

If either of the two conditions [(2.42a) or (2.42b)] is met, the target life is at a discontinuous point of the fatigue-life curve. The computation will be terminated and the corresponding messages will be printed to the output file.

The quantitative convergence criteria in Conditions 1 and 2 are designed to encourage convergence according to the primary criterion (target life) whenever possible but to stop the calculation before an excessive (time-consuming) number of iterations is performed. Convergence of the secondary criteria (initial flaw size or stress scale factor multiplier) may indicate a “successful” iteration convergence when a fatigue life discontinuity is detected. The user will be provided with the necessary information to determine if the “converged” answer is satisfactory for their purposes.

The fatigue life convergence [eq.(2.41)] and the discontinuity [eqs. (2.42a) and (2.42b)] are both checked at every iteration step, as shown below by the pseudocode for initial flaw size calculation.

```

      .....
10  CONTINUE    ! Iteration loop starts here
    i = i+1    ! i is the iteration index
    Determine the trial value (xi) at step i by bisection/Pegasus method
    Calculate the fatigue life (Ni) at xi
    IF |Ni-NT|/NT<=0.1%, THEN    ! Fatigue life has converged to NT
        The solution is found -- it is xi. Stop.
    ELSE    ! Fatigue life has not converged to NT yet

```

```

IF (Condition1 or Condition2), THEN ! Fatigue-life curve at NT is discontinuous
IF (NL == ∞ .OR. NR == ∞), THEN ! NT is in the threshold zone
Print out the following messages, then stop:
The target life value has not converged within the 0.1% convergence
criterion. However, the initial crack size has converged with a
0.01% (or 0.0001%) convergence criterion. The target life is larger than
the maximum possible finite fatigue life. A smaller initial crack size is
below the threshold for fatigue crack growth, and hence gives infinite life.
Convergence of the target life is not possible for this particular problem.
Further details are available in the table of iteration results.
ELSE ! NT is straddled at a discontinuous point
Print out the following messages, then stop:
The target life value has not converged within the 0.1% convergence
criterion, possibly because the life response in the vicinity of the
target life is not continuous. However, the initial crack size has
converged with a 0.01% (or 0.0001%) convergence criterion. It is unlikely
that convergence of the target life is possible for this particular problem.
Further details are available in the table of iteration results.
ENDIF
ELSE ! Fatigue-life curve at NT is continuous
IF i>100, THEN ! The maximum number of iteration steps has reached
    Print message of no convergence within 100 steps. Stop.
ELSE ! The maximum number of iteration step has not reached
    GO TO 10 ! Go for next iteration
END IF
END IF
.....

```

Please note that the total fatigue stresses in calculation of stress scale factor multiplier are the product of: 1) stress gradients, 2) stress values in the load spectrum, 3) stress scale factors, and 4) stress scale factor multiplier. However, the limit stresses (if applied) are not scaled by the stress scale factor multiplier. The stress scale factor multiplier scales fatigue load only.

### 2.2.1 Choosing the Crack Geometry

The user selects the desired crack geometry from among the many configurations built into NASGRO by clicking on the “Select Geometry” tab and then using drop-down boxes. The current version features several improvements to the stress intensity factor solutions that existed in the previous releases. These include the use of finite element analyses to verify earlier approximate solutions and extension of the valid range of dimensions for several crack cases. In addition, several surface-crack cases have been extended to include general loading. Up to four nonlinear stress distributions may now be combined and applied to the SC02, SC04, and SC06 crack cases. An example of how to apply a nonlinear stress distribution to crack case SC04 may be found in example 2. In order to provide a consistent approach,  $S_0$  is reserved for tension and compression,  $S_1$  and  $S_2$  are bending stresses in through-the-thickness (out of plane) and width (in plane) directions,  $S_3$  is the bearing stress, and  $S_4$  is reserved for the second tension/compression stress for cases that have biaxial loading.

The stress intensity factor solutions that have been incorporated into NASGRO are listed in Table 6a, and the geometries for the crack cases are shown in Figures 16 through 47 (beginning on page 51). Through crack (TC) geometries are shown in Figures 16 through 23 and the embedded crack (EC) cases are shown in Figure 26. The corner crack (CC) geometries are depicted in Figures 27 through 32, the surface-crack (SC) cases are presented in Figures 33 through 38, and ASTM and other standard specimen (SS) geometries are shown in Figures 42 through 45. The boundary element crack cases are shown in Figure 46. The hybrid crack cases (HC) are shown in Figure 44. Three data table (DT) cases and one polynomial solution (PS01) have also been included. The menu for selecting the crack geometry is as follows: first, the general class such as through cracks, corner cracks, surface cracks etc., is chosen and then the particular geometry within that class. After selecting the appropriate crack case, the figure is displayed in a graphical window and the user can enter dimensional information such as width, thickness, diameter, etc. in the text boxes provided. Additional information regarding the stress intensity factor solutions may be found in Section 4 and Appendices C and D. The details of nonlinear stress input for cases SC02, SC04, SC06, SC15, CC05 and CC06 are also given in Appendix-C. Crack cases TC03 and CC02 allow user-defined tables (1-d for TC03; 1-d or 2-d for CC02) representing superimposed solutions to be compounded with the built-in solutions.

### 2.2.2 Transition of Crack Geometry

Crack growth analysis is usually conducted on part-through cracks, such as surface or corner crack in a plate. As the crack grows, the depth of the crack may exceed the thickness before the crack becomes unstable. In such instances, growth will continue using the corresponding through crack and then the crack will grow some more before becoming critical. Table 6b shows the transition relation between crack cases (with details given in Appendix D).

Table 6a – Description of Crack Cases

<b>Through Cracks:</b>	
TC01:	Through crack at center of plate
TC02:	Through crack at edge of plate
TC03:	Through crack from an offset hole in a plate
TC04:	Through crack from hole in a lug
TC05:	Through crack from hole in a plate with a row of holes
TC06:	Through crack in a sphere
TC07:	Through crack in a cylinder (longitudinal direction)
TC08:	Through crack in a thin cylinder (circumferential direction)
TC09:	Through crack from hole in a plate under combined loading
TC10:	Through crack from hole in a cylinder (circumferential direction)
TC11:	Through crack in center of plate – weight function solution
TC12:	Through crack at edge of plate – weight function solution
TC13:	Through crack(s) from hole in a plate (nonlinear stress)
TC14:	Through crack at edge of plate – remote displacement loading
TC15:	Through crack at edge of variable thickness plate – weight function solution
TC16:	Through crack in curved panel with bulging
TC17:	Through crack at angled or elliptical edge notch
TC18:	Through crack at embedded slot or elliptical hole
TC19:	Through crack at hole with broken ligament
TC23:	Through crack(s) (of equal or unequal length) at a hole
TC24:	Through crack at plate center – Displacement control
TC25:	Through crack at edge rectangular cutout with rounded corners
TC26:	Through crack at offset internal rectangular cutout with rounded corners
TC27:	Through crack at hole in lug – univariant weight function solution
TC28:	Curved through crack at edge of plate
TC30:	Through crack at hole in obliquely loaded and tapered lug (in short or in long ligament)
TC31:	Through crack (pre-corner) in L-section
TC32:	Through crack (post-corner) in L-section
TC33:	Through crack approaching a hole
TC34:	Two collinear through cracks of unequal length
TC35:	Through crack in plate with single symmetric step change in thickness
TC37:	Through crack in C-section under remote loading
<b>Embedded Cracks:</b>	
EC01:	Embedded crack in a plate
EC02:	Embedded crack, offset, in a plate
EC04:	Embedded crack, offset, in a plate subjected to bivariant stress
EC05:	Embedded crack, offset, in a plate subjected to univariant stress
<b>Corner Cracks:</b>	
CC01:	Corner crack in a rectangular plate
CC02:	Corner crack from offset hole in a plate
CC03:	Corner crack from hole in a lug
CC04:	Corner crack from hole in a plate (one or two cracks)
CC05:	Corner crack in a rectangular plate subjected to bivariant stress
CC07:	Corner crack from hole in a plate (new soln for one crack, tension and pin loads)
CC08:	Corner crack(s) from hole in a plate subjected to nonlinear stress
CC09:	Corner crack in a rectangular plate subjected to bivariant stress – new SwRI solution
CC10:	Corner crack from hole in a plate subjected to bivariant stress
CC11:	Corner crack in a plate subjected to univariant stress
CC12:	Corner crack from chamfered edge of plate subjected to bivariant stress
CC13:	Corner crack at elliptical or angled edge notch
CC14:	Corner crack at embedded slot or elliptical hole
CC15:	Corner crack at round hole with broken ligament
CC16:	Corner crack at hole (offset) / Two symmetric corner cracks at central hole in plate
CC17:	Two unequal corner cracks at hole (offset) in plate
CC18:	Part-elliptical Corner Crack at Angled Corner – Bivariant WF
CC19:	Corner crack at hole in lug – univariant weight function solution

CC20:	Corner crack at hole in lug – displacement control
CC21:	Corner crack at rectangular cutout at edge of plate
CC22:	Corner crack at internal (offset) rectangular cutout in plate
CC23:	Corner crack at hole in obliquely loaded and tapered lug (in short or in long ligament)
<b>Surface Cracks:</b>	
SC01:	Surface crack in a rectangular plate – tension and/or bending
SC02:	Surface crack in a rectangular plate – nonlinear stress
SC03:	Surface crack in a spherical pressure vessel
SC04:	Longitudinal surface crack in a hollow cylinder – nonlinear stress
SC05:	Thumbnail crack in a hollow cylinder
SC06:	Circumferential crack in a hollow cylinder – nonlinear stress
SC07:	Thumbnail crack in a solid cylinder
SC08:	Semi-elliptical surface crack (circumferential) in threaded solid cylinder
SC09:	Constant-depth surface crack (circumferential) in threaded solid cylinder
SC10:	Constant-depth surface crack (circumferential) in threaded hollow cylinder
SC11:	Surface crack from hole in a plate (one or two cracks)
SC12:	Surface crack from hole in a lug (one or two cracks)
SC13:	Surface crack in bolt head fillet - Shear bolt
SC14:	Surface crack in bolt head fillet - Tension bolt
SC15:	Surface crack in a plate subjected to bivariant stress
SC17:	Surface crack in a rectangular plate – nonlinear stress
SC18:	Surface crack(s) from hole in a plate – nonlinear stress
SC19:	Surface crack in a plate, bivariant weight function solution
SC26:	Surface crack at elliptical or angled edge notch
SC27:	Surface crack at embedded slot or elliptical hole
SC28:	Surface crack at round hole with broken ligament
SC29:	Surface crack at off-center hole in plate - bivariant weight function solution
SC30:	Surface crack (offset) in plate – univariant weight function
SC31:	Surface crack (offset) in a plate – bivariant weight function solution
SC32:	Surface crack at hole in lug – univariant weight function solution
SC33:	Semi-elliptical surface crack at center of plate subjected to remote bivariant displacement
SC34:	External surface crack in a hollow cylinder – univariant WF
SC35:	Semi-elliptical surface crack in a solid cylinder – univariant WF
<b>Standard Specimens:</b>	
SS01:	Center-cracked tension specimen M(T)
SS02:	Compact tension specimen C(T)
SS03:	Disc-shaped compact tension specimen DC(T)
SS04:	Arc-shaped tension specimen A(T)
SS05:	Three-point bend specimen SE(B)
SS06:	Edge cracked tension specimen SE(T) – constrained ends
SS07:	Notched round bar specimen R-bar(T) – circumferential crack
SS08:	Notched plate with a surface crack
SS09:	Notched plate with a corner crack
SS10:	Notched plate with a through crack
SS11:	Corner crack in a plate from symmetric hole
SS12:	Eccentrically-loaded single edge crack tension specimen ESE(T)
SS13:	Same as SC01, for use by NASMAT only
SS14:	Same as SC17, for use by NASMAT only
<b>Data Tables:</b>	
DT01:	One-dimensional data table for a through crack (one tip)
DT02:	Two-dimensional data table for a through crack (one tip)
DT03:	Two-dimensional data table for part-through cracks (two tips)
DT04:	Two-dimensional data table for one or two through cracks (two tips)
<b>Stress-Intensity Factor Data Tables:</b>	
KT01:	One-dimensional stress intensity factor table for a through crack (one tip)
KT02:	Two-dimensional stress intensity factor table for a through crack (one tip)
KT03:	Two-dimensional stress intensity factor table for part-through cracks (two tips)
KT04:	Two-dimensional stress intensity factor table for one or two through cracks (two tips)
<b>Polynomial Series:</b>	

PS01:	$F_0 = C_0 + C_1 u + C_2 u^2 + \dots + C_5 u^5$ where $u = (a/D)^m$
<b>Boundary Element Models:</b>	
BE02:	Two through cracks from either side of an offset hole in a plate
BE03:	One through crack, one corner crack on either side of an offset hole in a plate
<b>Hybrid Cracks</b>	
HC01	Corner crack and Through crack at (offset) hole in plate

Table 6b – Transition Relationship between Crack Cases (Details in Appendix D)

From	To	Condition/Comment
TC03	TC02	
TC11	TC12	Either crack tip can set off the transition
TC23	TC19	Either crack tip can set off the transition
TC31	TC32	
CC01	TC02 (or TC28)	
CC02	TC03	
CC03	TC04	
CC04	TC03	Occurs only if number of cracks=1
CC05	TC12	Uses averaged unvariant stresses in TC12
CC07	TC03	Occurs only if number of cracks=1
CC08	TC13	
CC09	TC12 (or TC28)	
CC10	TC13	
CC11	TC12 (or TC28)	Either crack tip can set off the transition
CC12	TC12	
CC13	TC17	
CC14	TC18	
CC15	TC19	
CC16	TC03 or TC23	
CC17	HC01 or TC23	
CC19	TC27	
CC21	TC25	
CC22	TC26	
CC23	TC30	
SC01	TC01	
SC02	TC01	Uses equivalent stresses in TC01
SC03	TC06	$S_1$ should be zero
SC04	TC07	Uses equivalent stresses in TC07
SC05	TC08	Both external & internal cracks undergo transition
SC11	TC03	Occurs only if number of cracks=1
SC12	TC04	Occurs only if number of cracks=1
SC15	TC11	
SC17	CC11, TC11 or TC12	
SC18	CC08 or TC13	
SC19	CC09, TC11 or TC12	

SC26	CC13 or TC17	
SC27	CC14 or TC18	
SC28	CC15 or TC19	
SC30	CC11, TC11 or TC12	
SC31	CC09, TC11 or TC12	
SC32	CC19 or TC27	
EC01	TC01	
EC02	SC30	
EC04	SC31, CC09, TC11 or TC12	Either crack tip can set off the transition
EC05	SC30, CC11, TC11 or TC12	Either crack tip can set off the transition
SS08	SS10	
SS09	SS10	
SS11	TC03	
HC01	CC15 or TC23	

Whenever nonlinear stresses are present in a part-through crack model, the statically equivalent tension and bending loads are computed and the corresponding nominal stresses  $S_0, S_1$  are obtained for use in the through crack model to which the part-through crack transitions. Numerical integration is performed over the cross section of the geometry in use. In some cases such as CC05 to TC12, the bivariant stress field is integrated across the thickness but the variation along width is preserved.

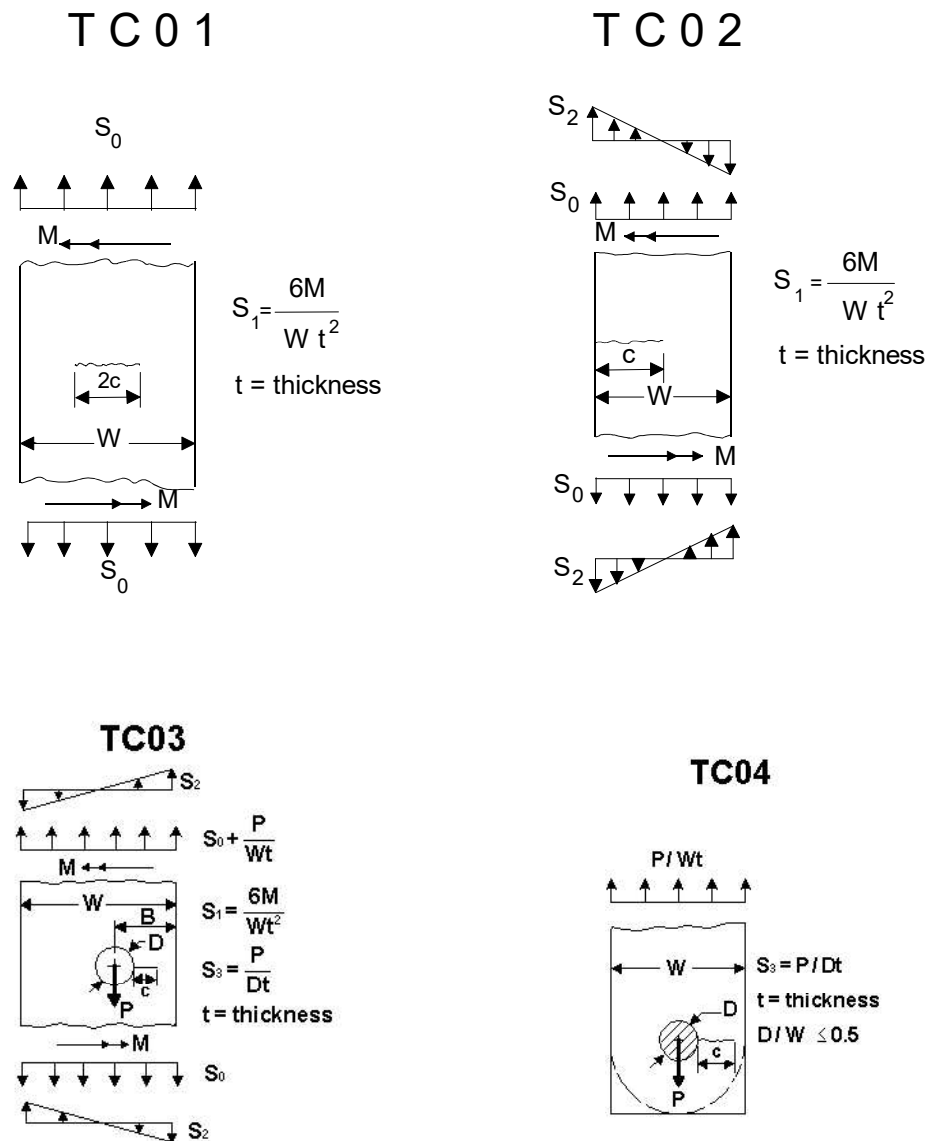


Figure 16 – Through crack cases 1, 2, 3 &amp; 4

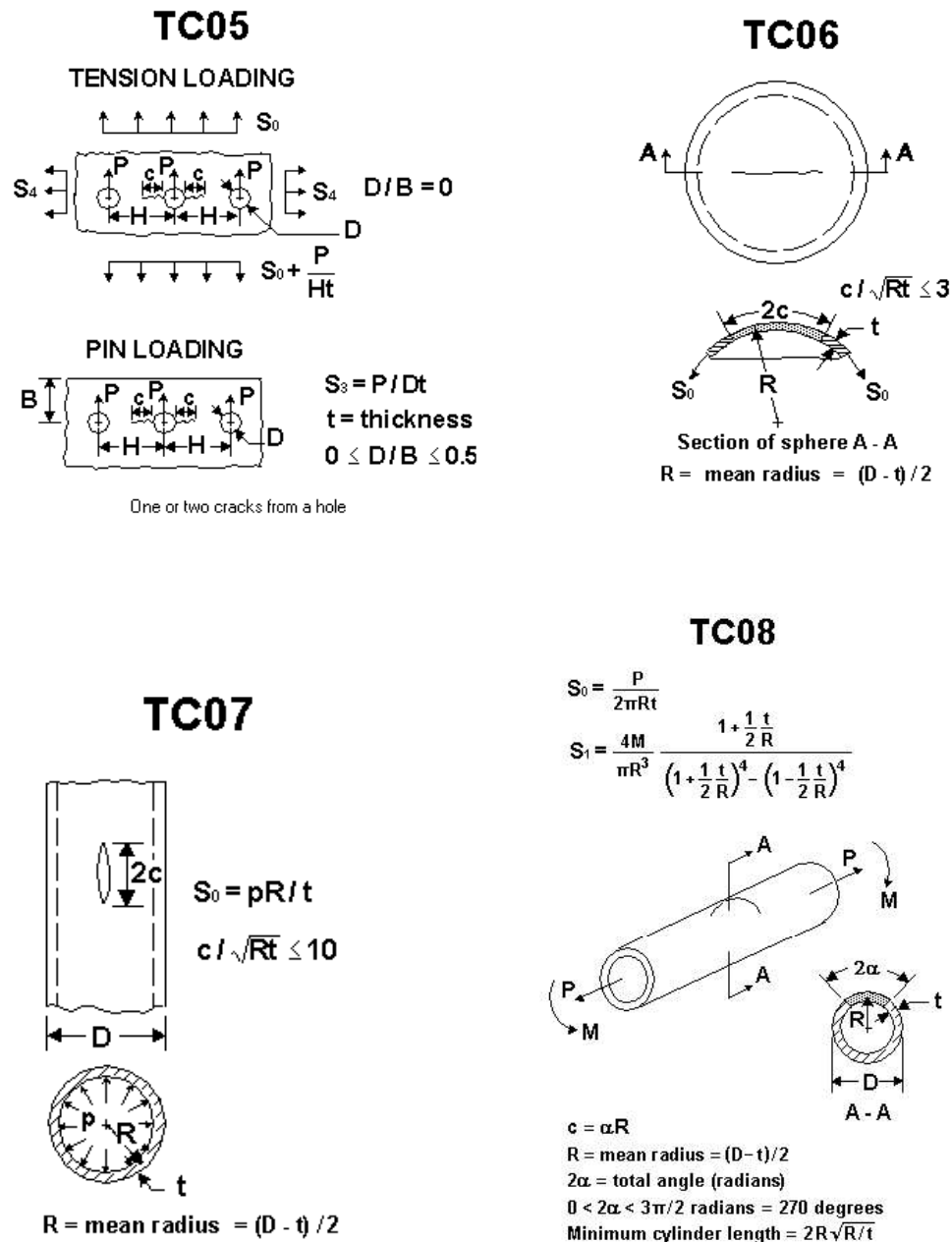


Figure 17 – Through crack cases 5, 6, 7 &amp; 8

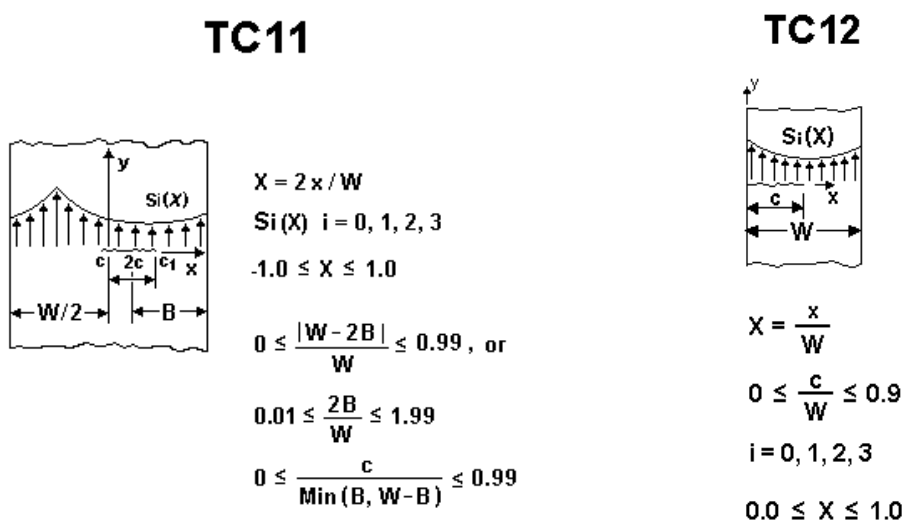
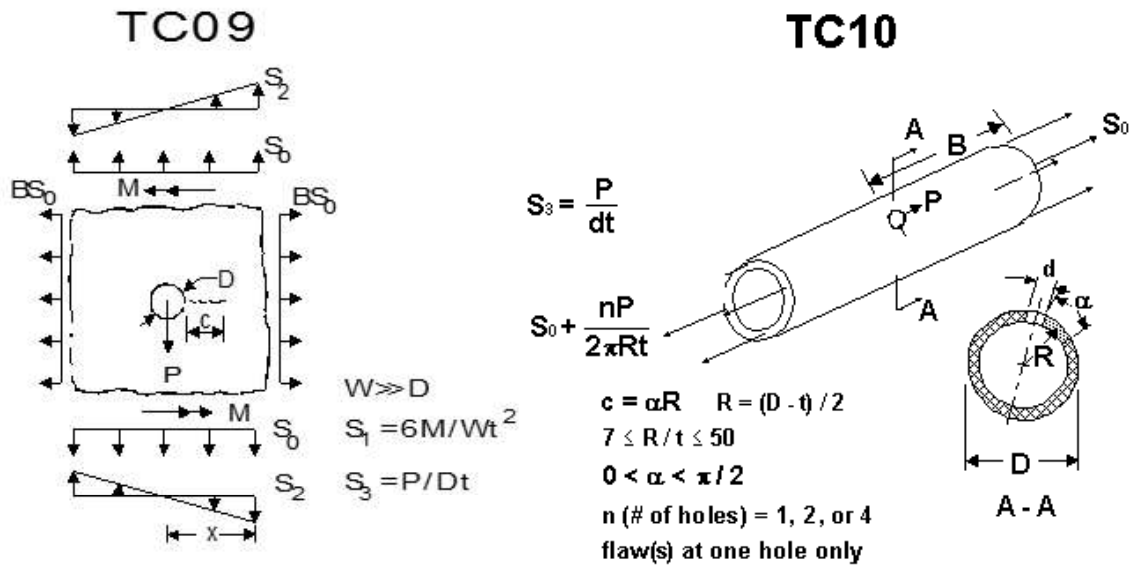


Figure 18 – Through crack cases 9, 10, 11 &amp; 12

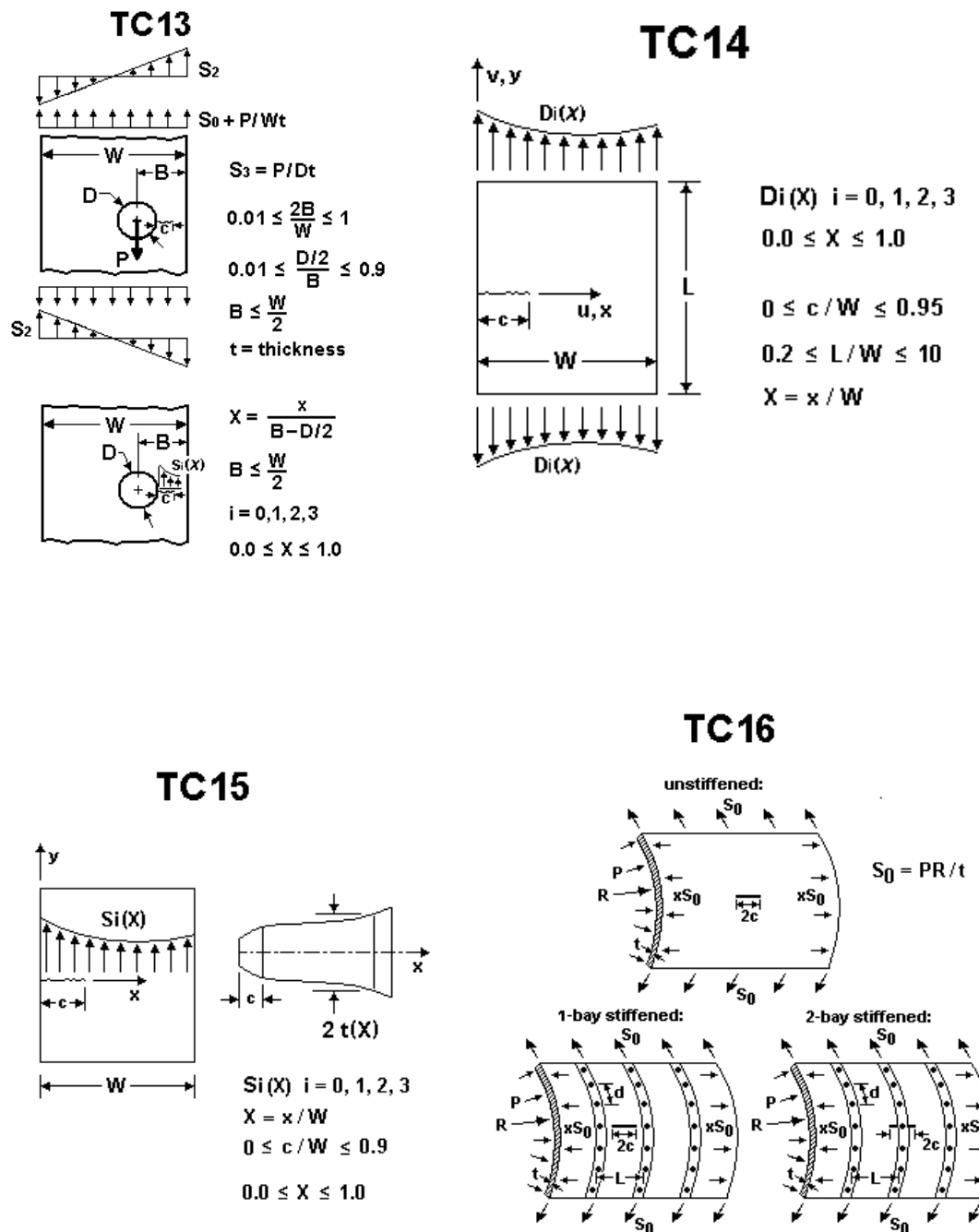


Figure 19 – Through crack cases 13, 14, 15 &amp; 16

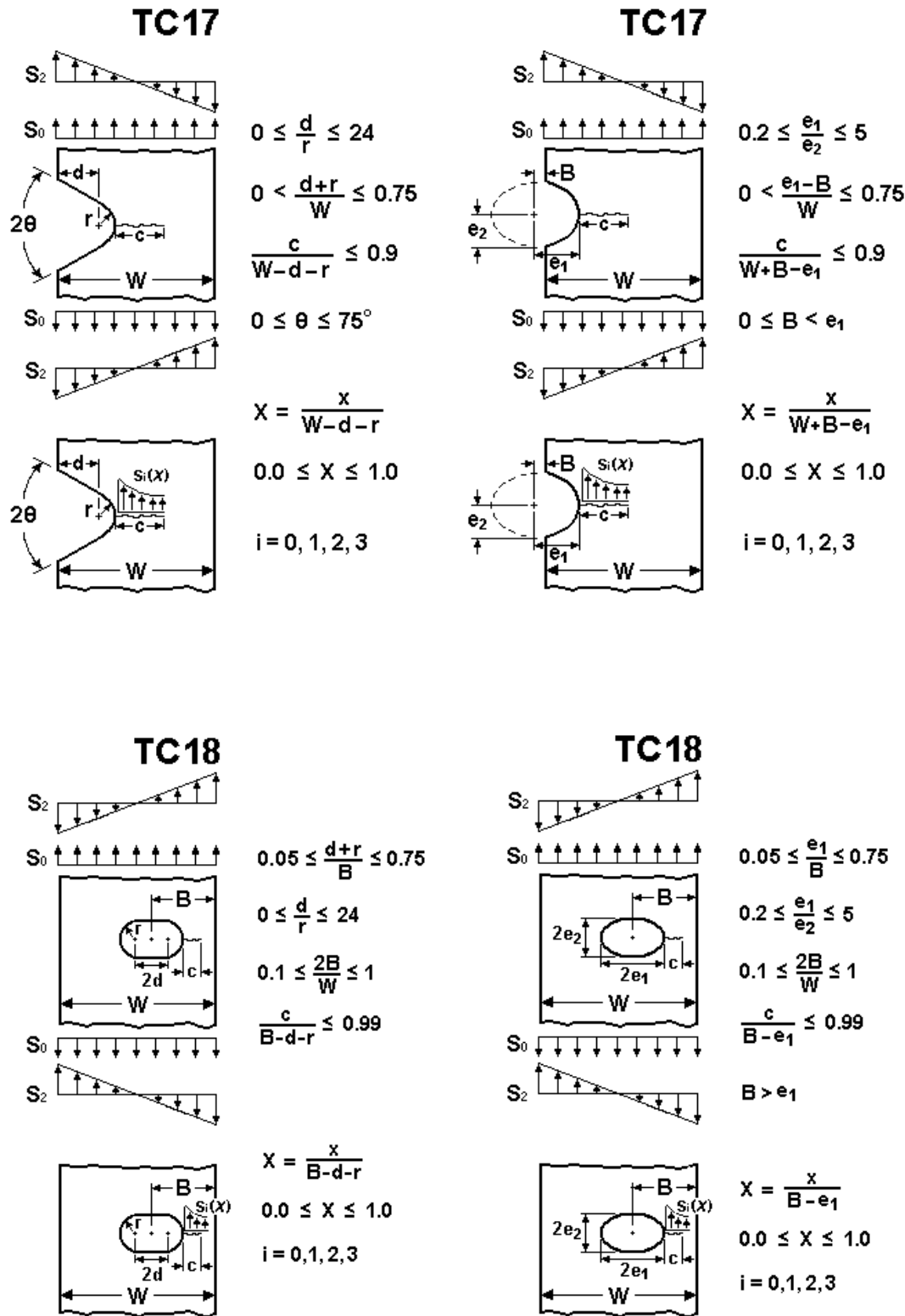
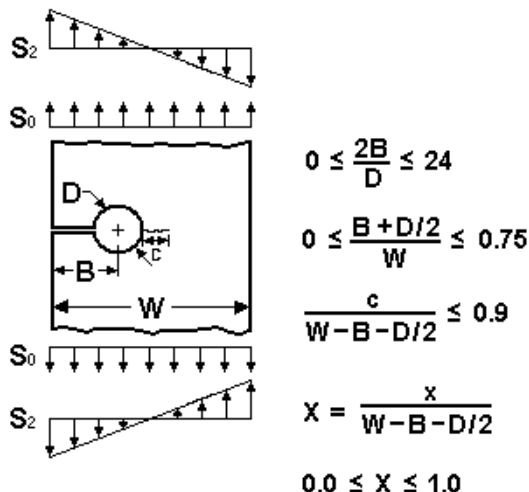
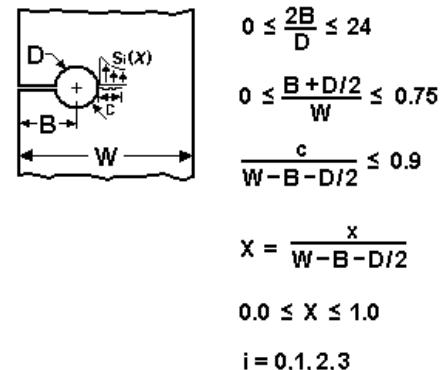


Figure 20 – Through crack cases 17 &amp;18

**TC19****TC19**

Note: The tabular stress distribution specified for the uncracked ligament assumes that the opposite ligament has failed.

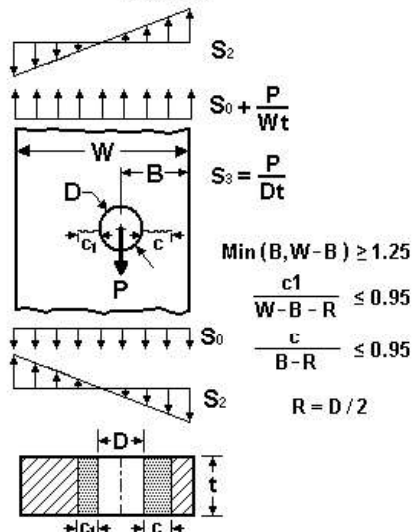
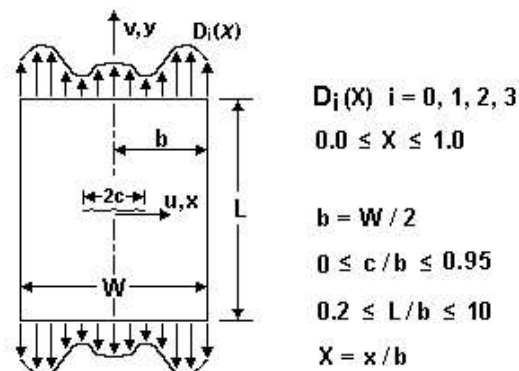
**TC23****TC24**

Figure 21 – Through crack cases 19, 23 & 24

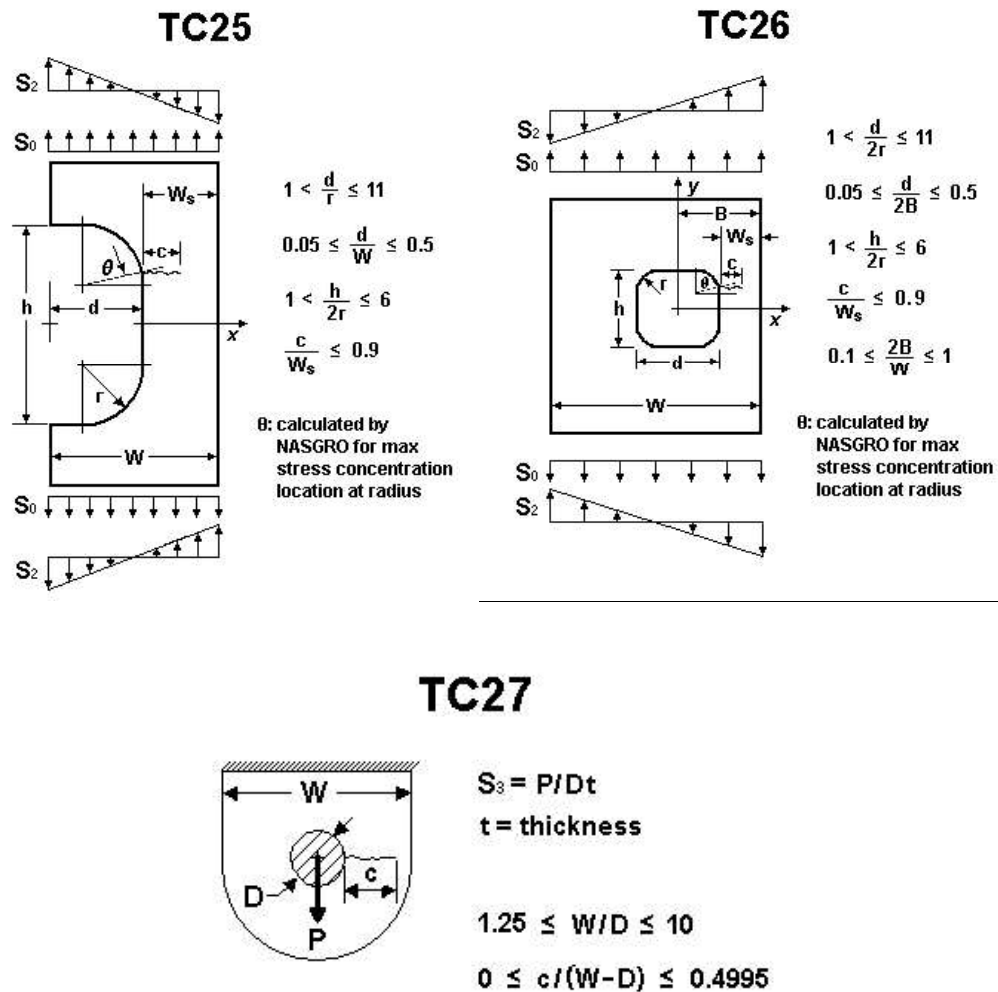


Figure 22 – Through crack cases 25, 26 &amp; 27

## 2.2 Details of Crack Growth Analysis

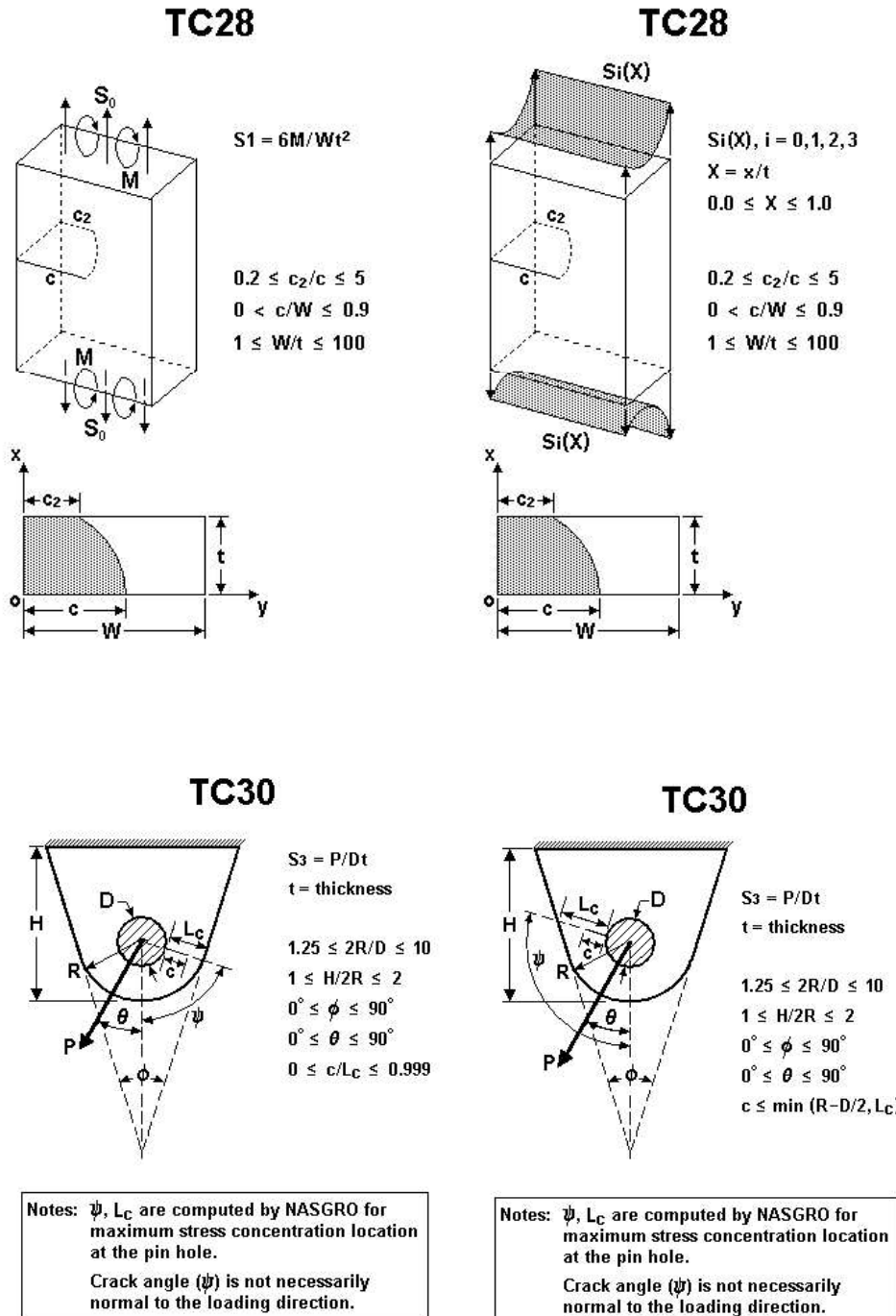


Figure 23a – Through crack cases 28 &amp; 30

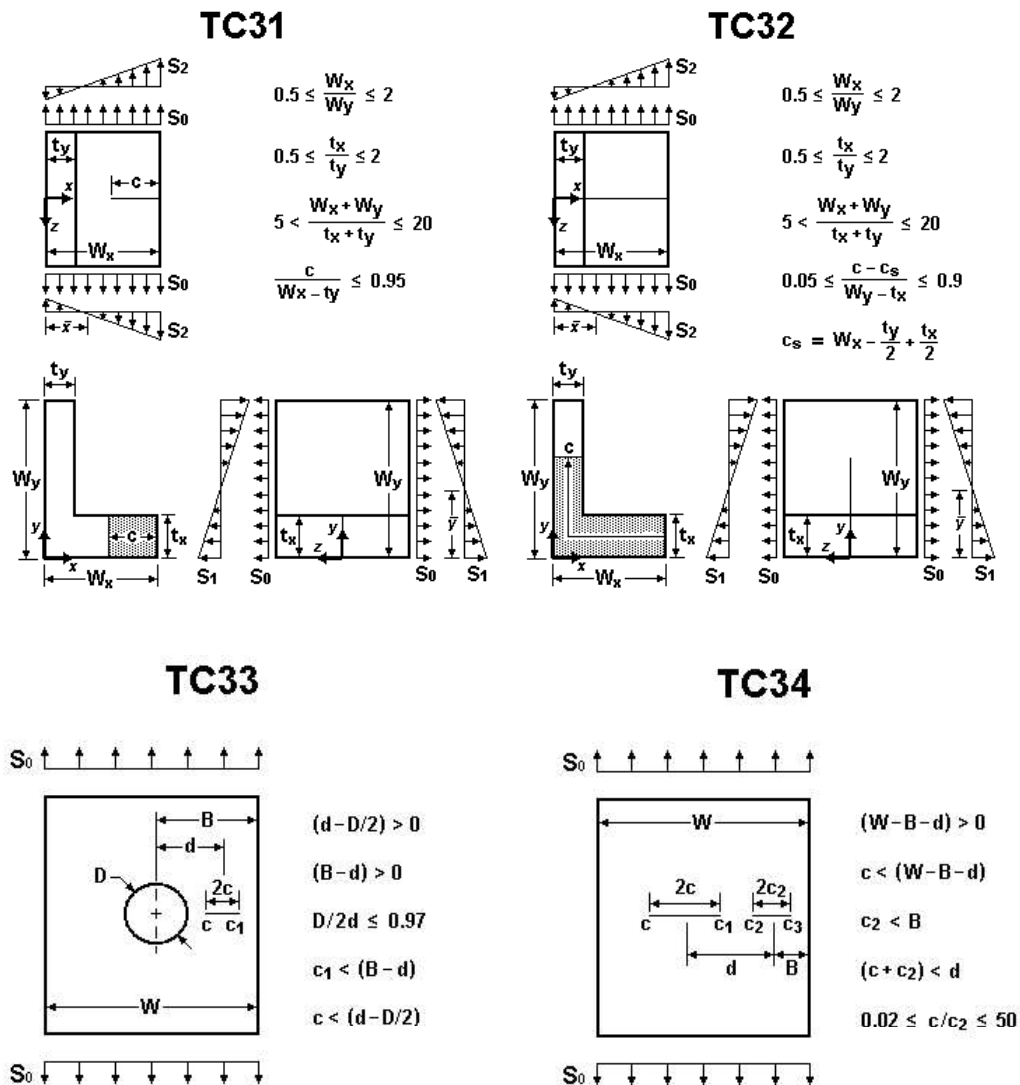


Figure 23b – Through crack cases 31, 32, 33 &amp; 34

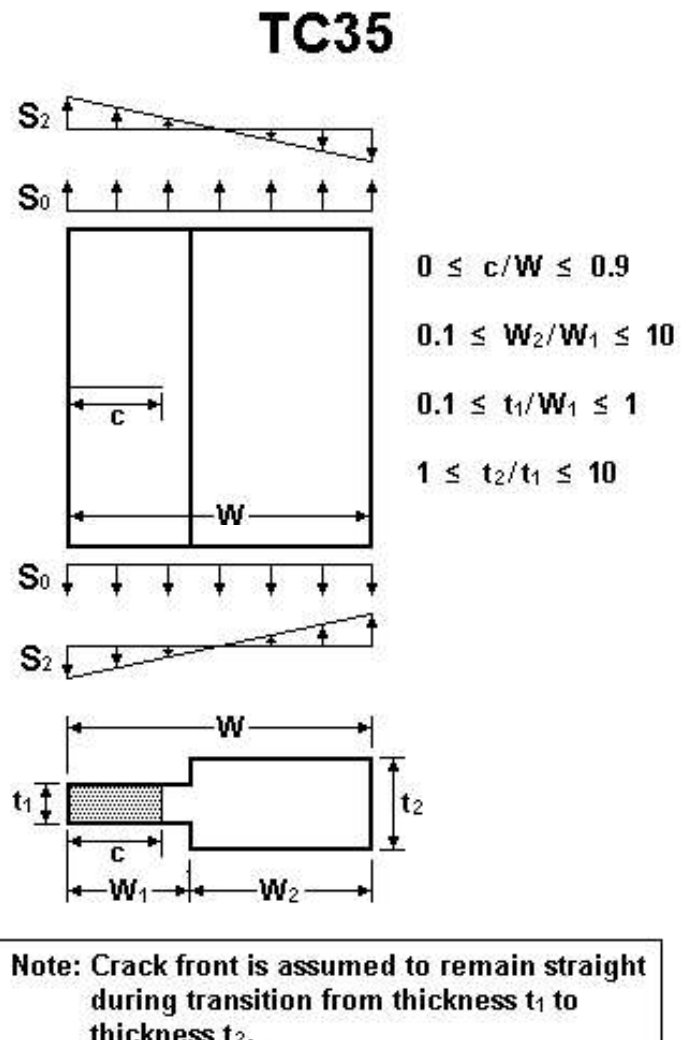
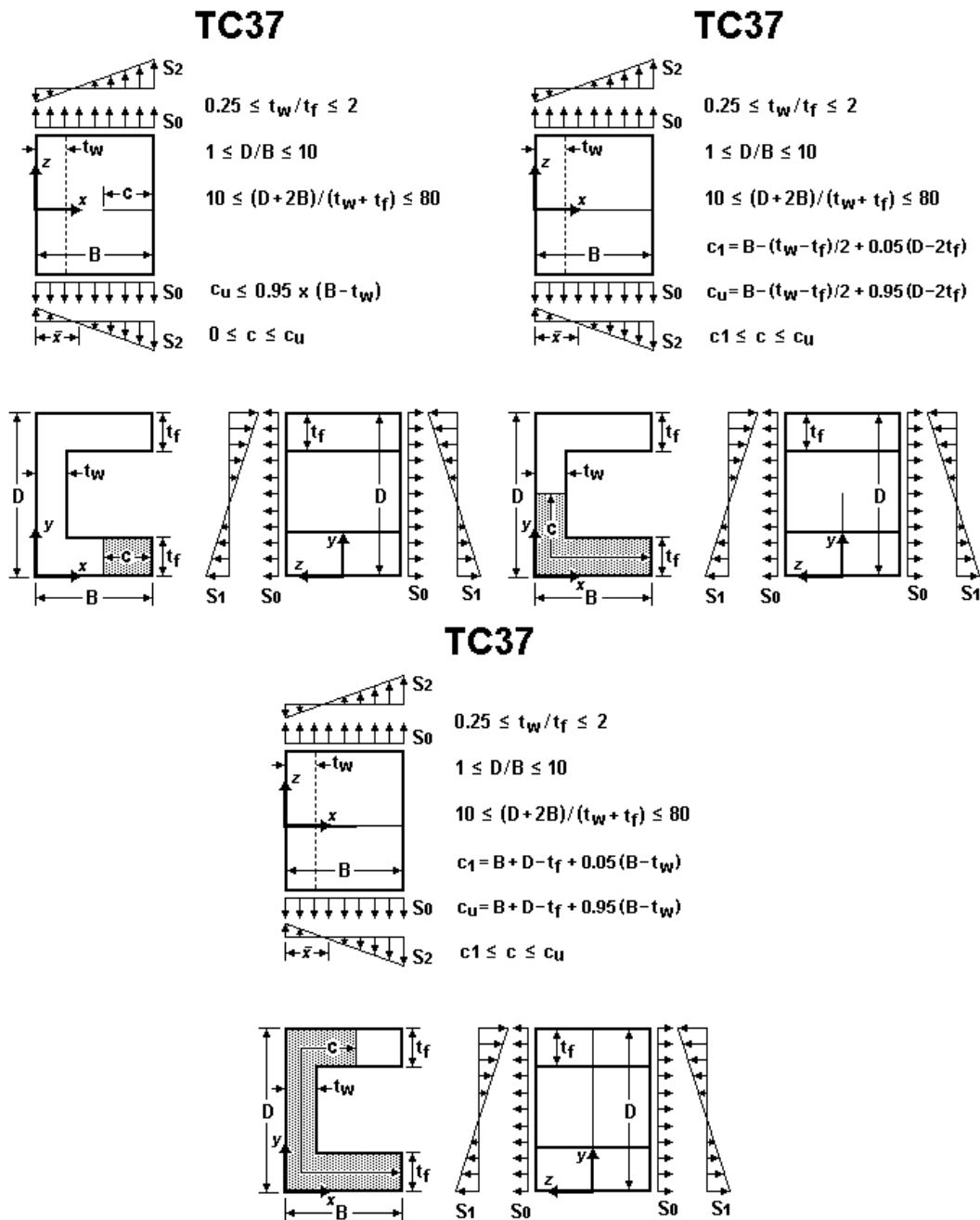


Figure 23c – Through crack cases 35



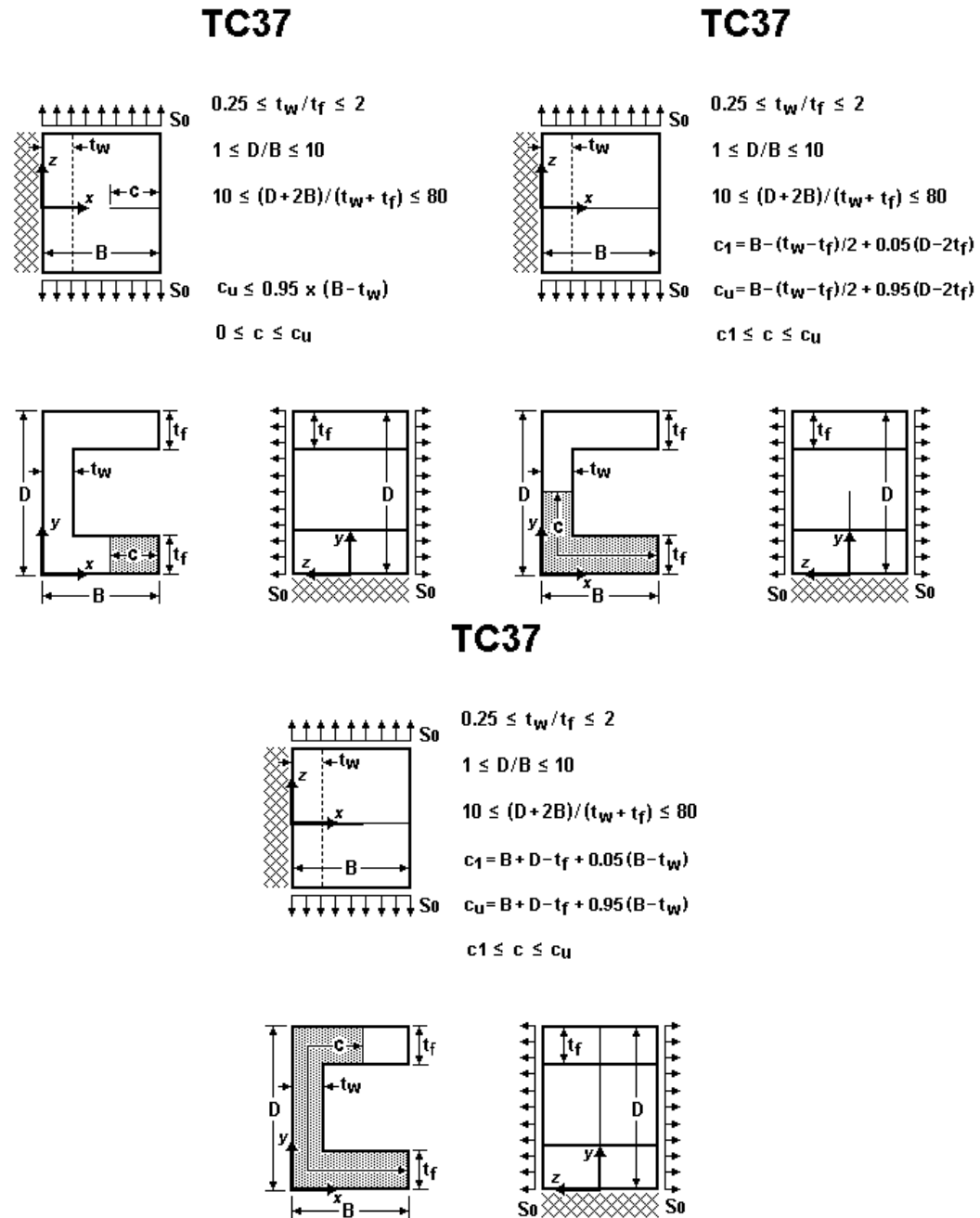
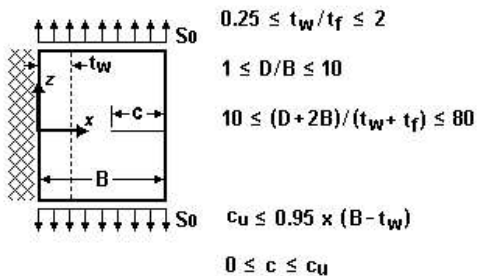
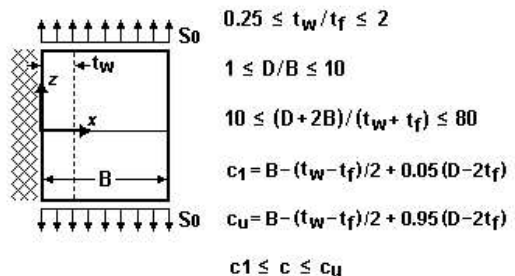


Figure 25a – Through crack 37, restrained cases

TC37



TC37



TC37

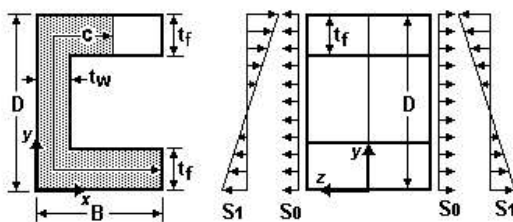
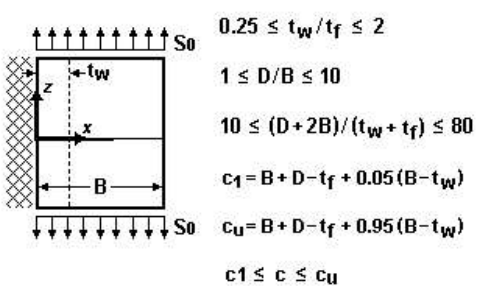
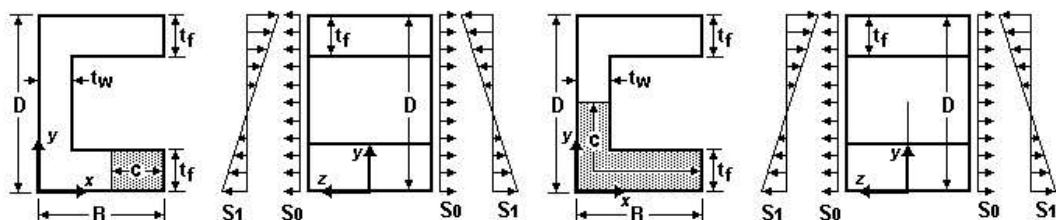


Figure 25b – Through crack 37, partially restrained cases

## 2.2 Details of Crack Growth Analysis

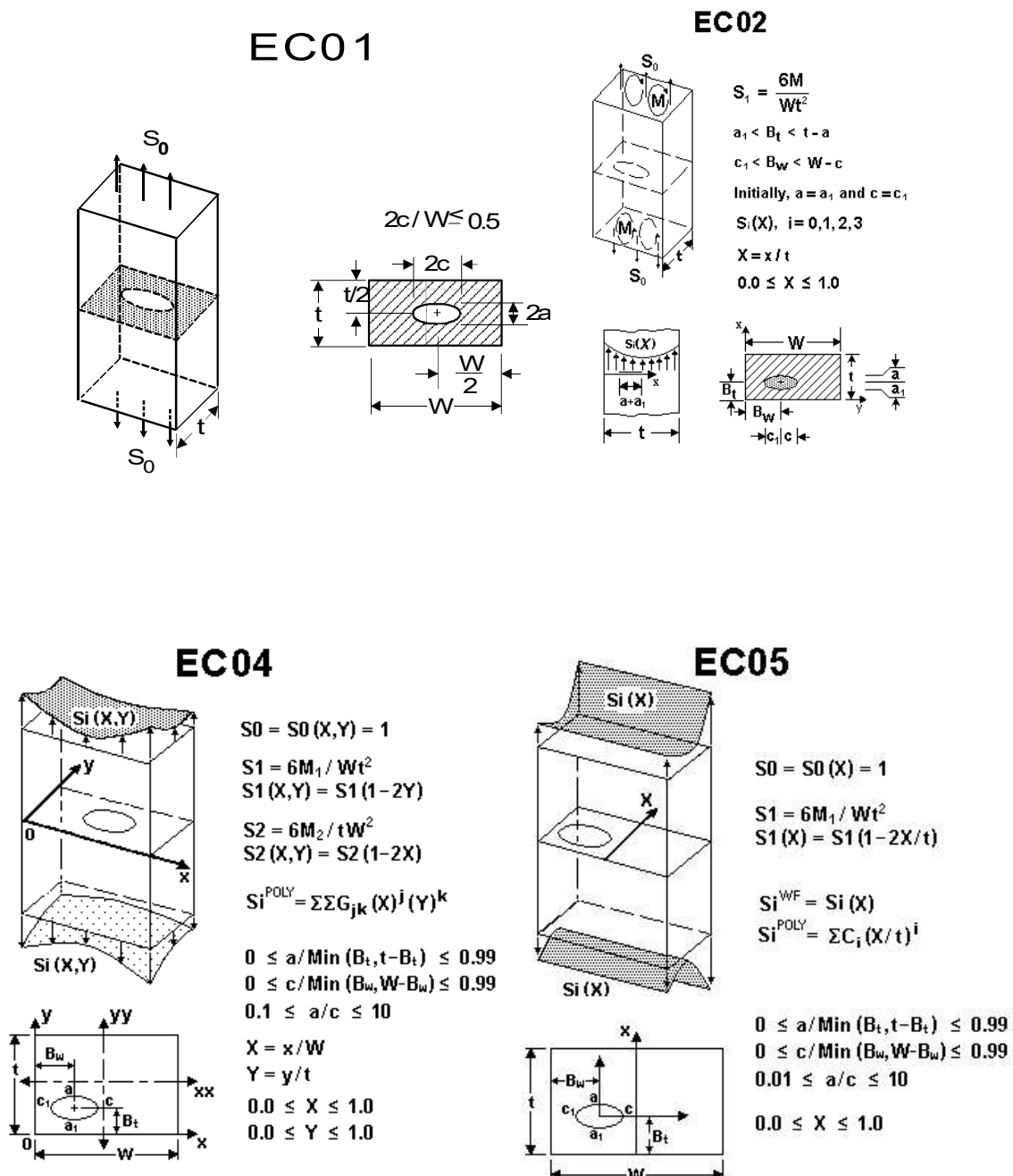


Figure 26 – Embedded crack cases 1, 2, 4 &amp; 5

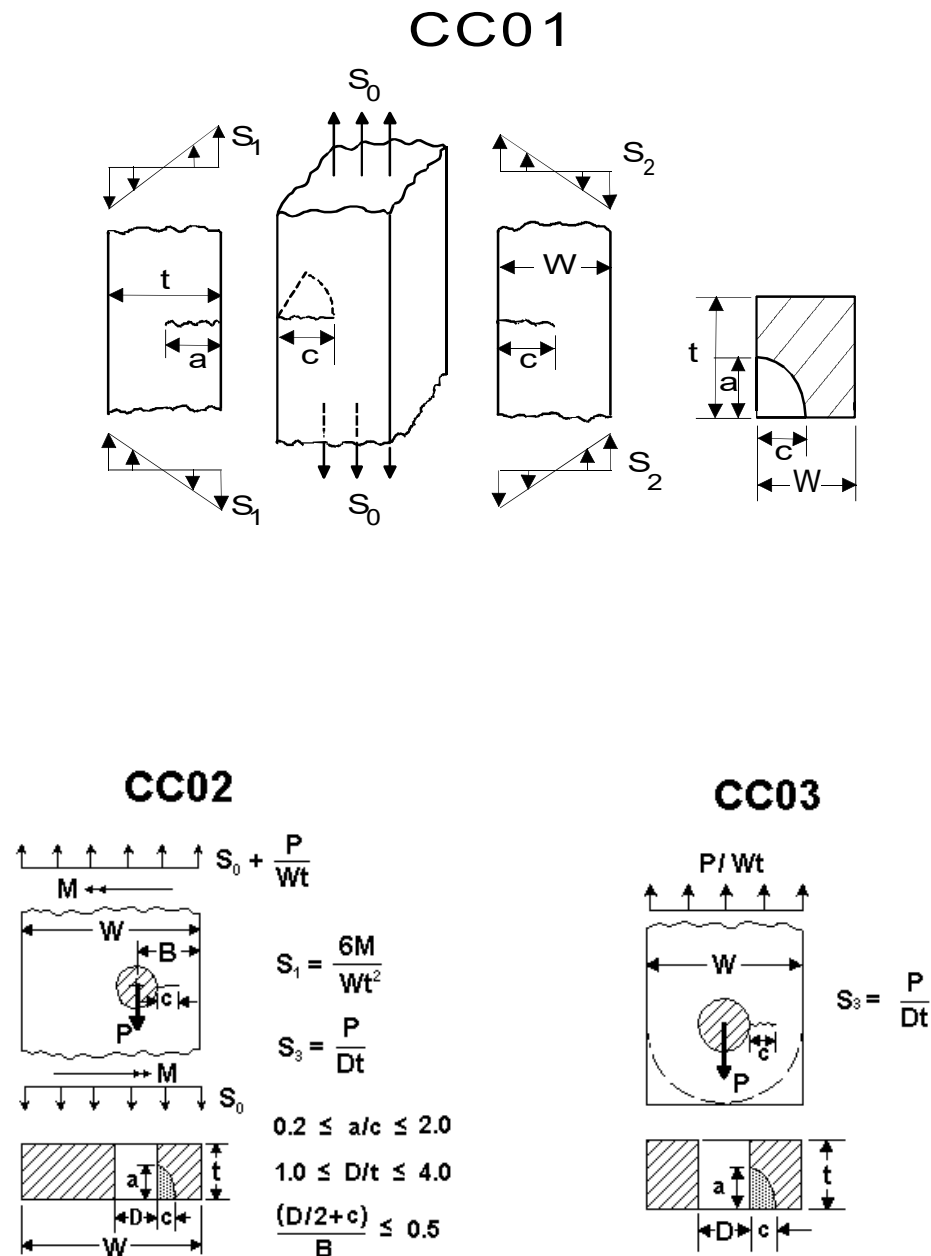
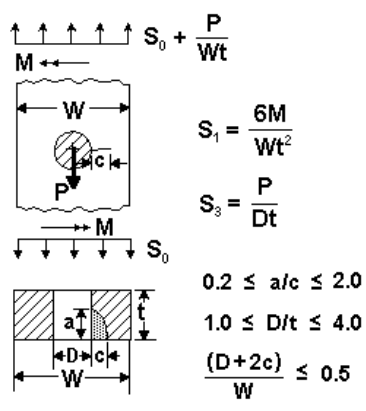
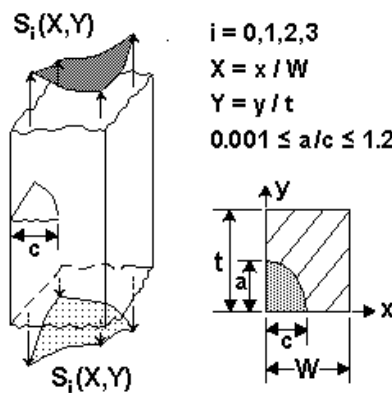
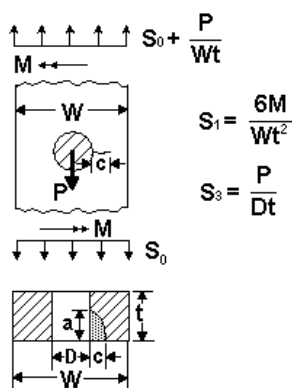


Figure 27 – Corner crack cases 1, 2 &amp; 3

**CC04****CC05****CC07**

For one corner crack under tension ( $S_0$ ) and/or pin load ( $S_3$ ) only:

$$0.1 \leq a/c \leq 2.0$$

$$0.5 \leq D/t \leq 4.0$$

For one corner crack under bending ( $S_1$ ), or two corner cracks (all load conditions):

$$0.2 \leq a/c \leq 2.0$$

$$1.0 \leq D/t \leq 4.0$$

$$\frac{(D+2c)}{W} \leq 0.5$$

Figure 28a – Corner crack cases 4, 5, 7

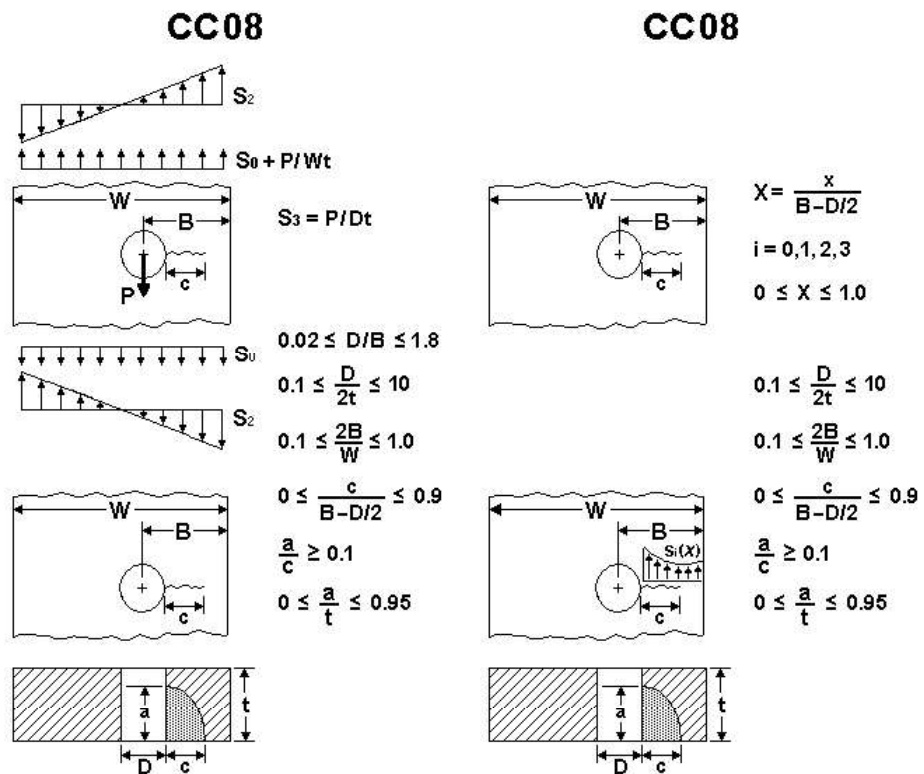


Figure 28b – Corner crack case 8

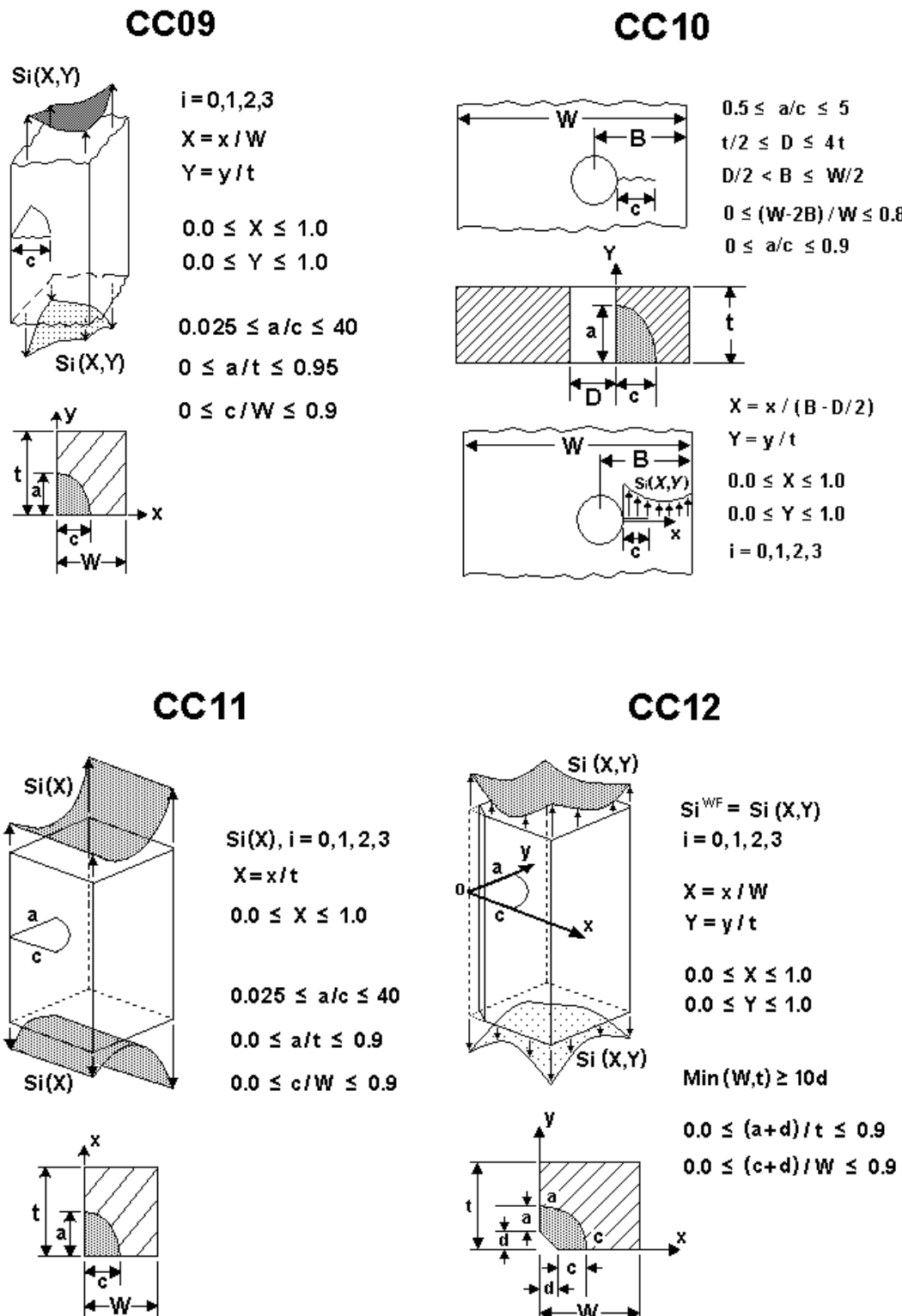


Figure 29 – Corner crack cases 9, 10, 11 &amp; 12

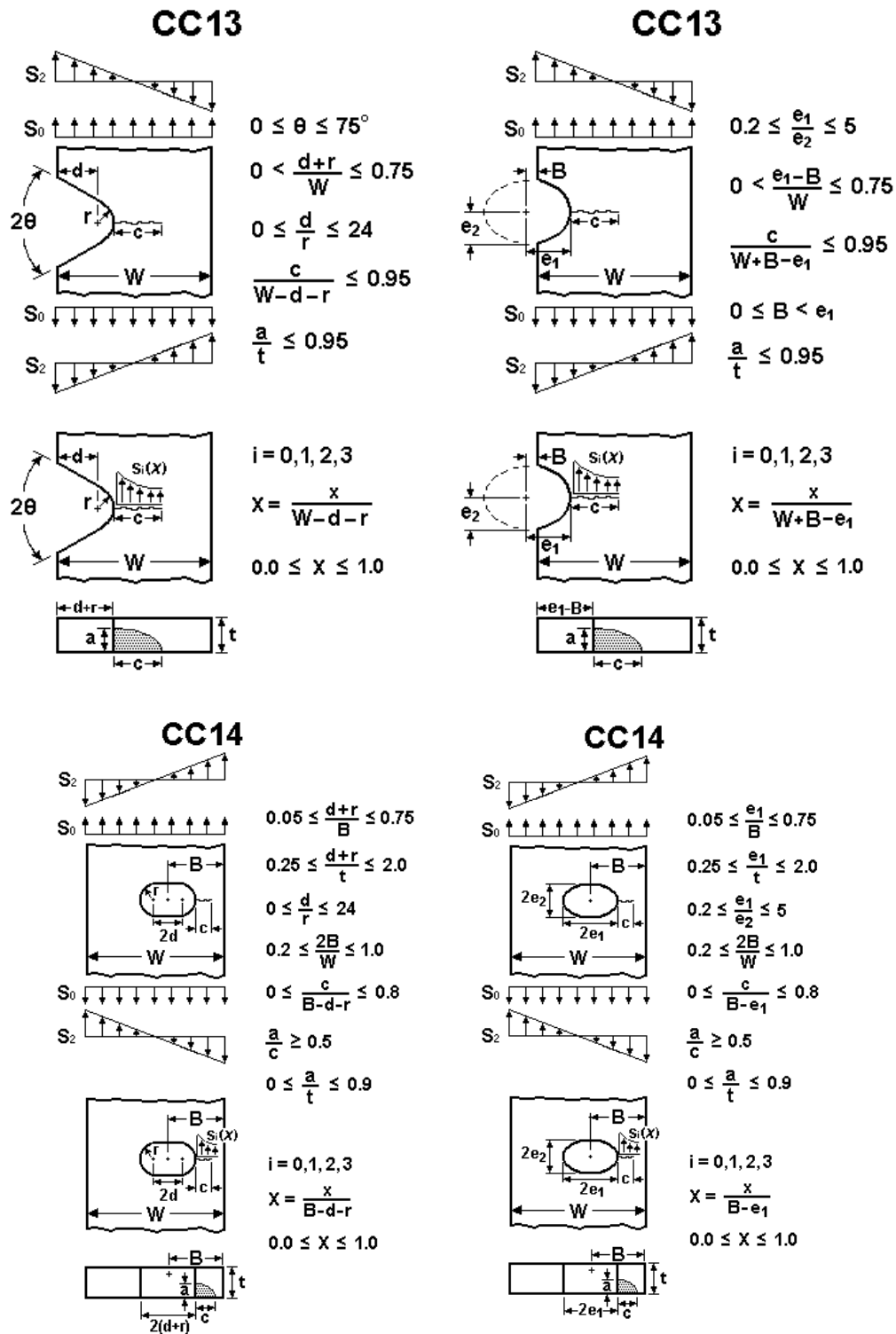


Figure 30 – Corner crack cases 13 &amp; 14

## 2.2 Details of Crack Growth Analysis

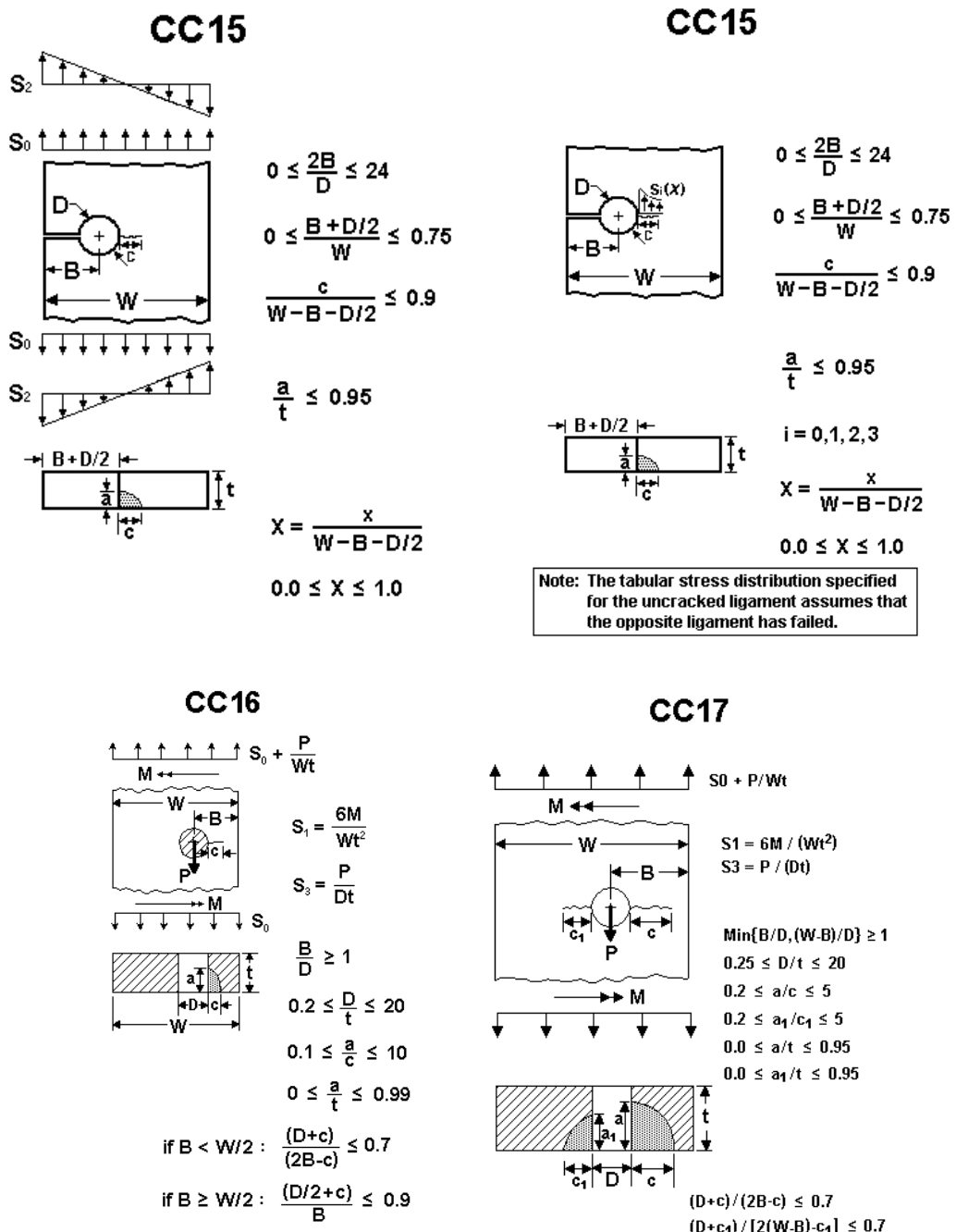


Figure 31a – Corner crack cases 15, 16 &amp; 17

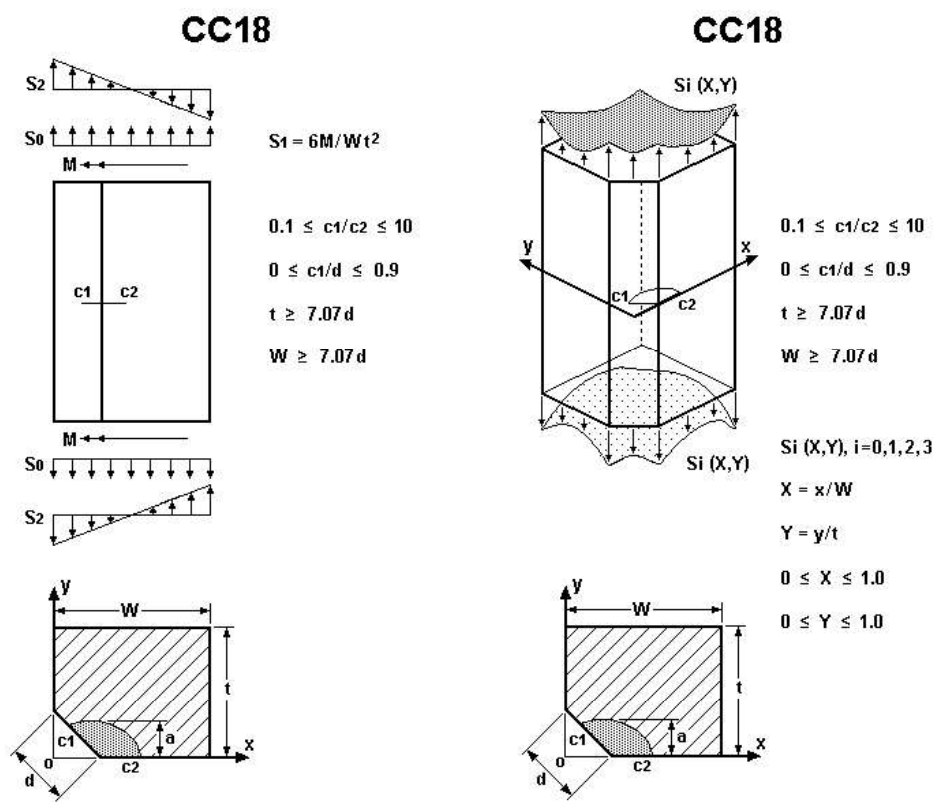


Figure 31b – Corner crack case 18

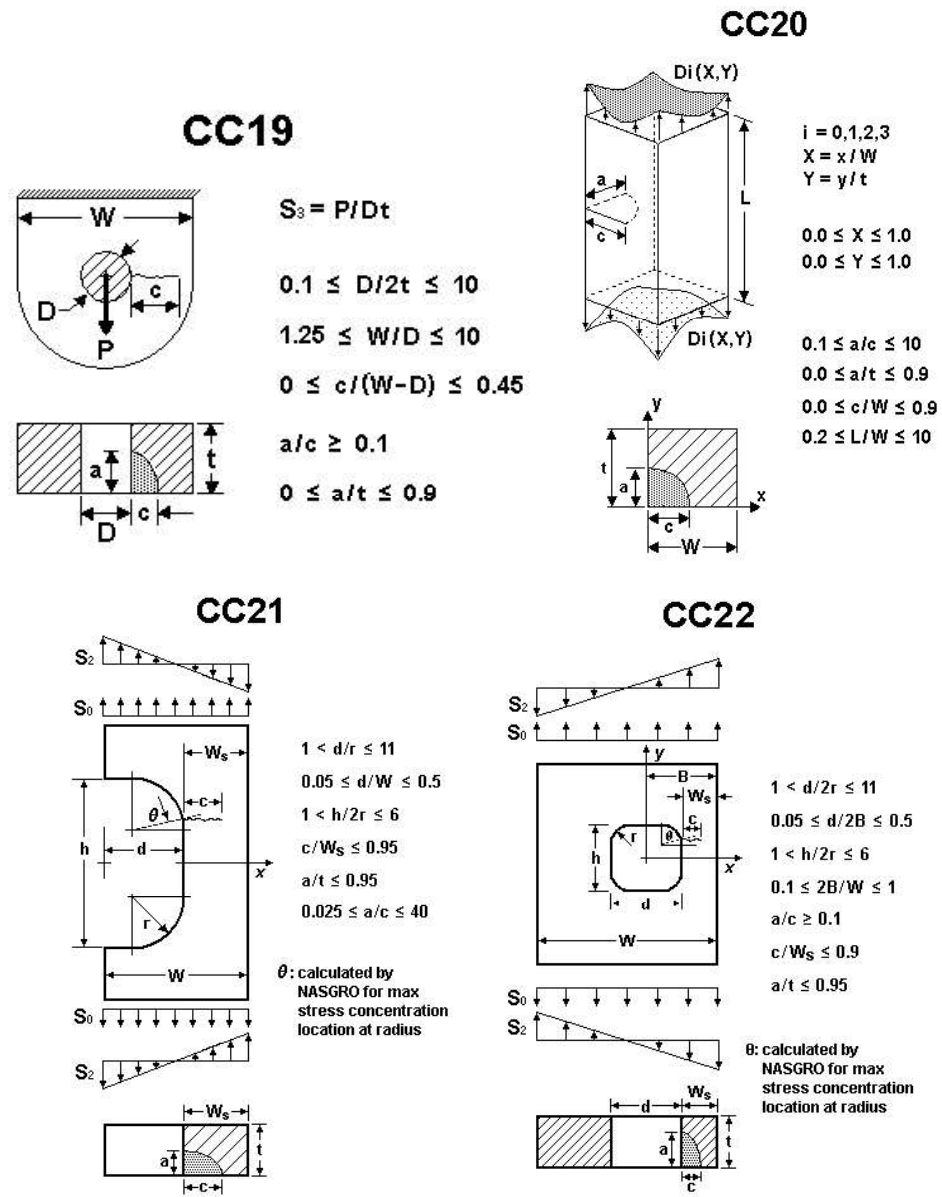


Figure 32a – Corner crack cases 19, 20, 21 &amp; 22

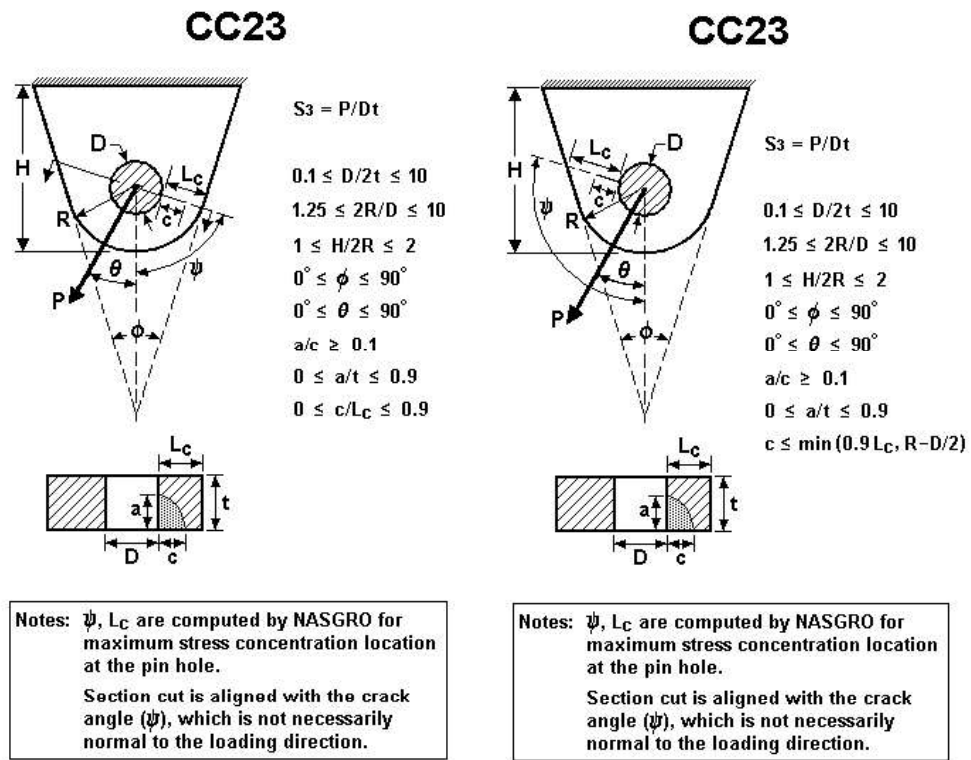


Figure 32b – Corner crack case 23

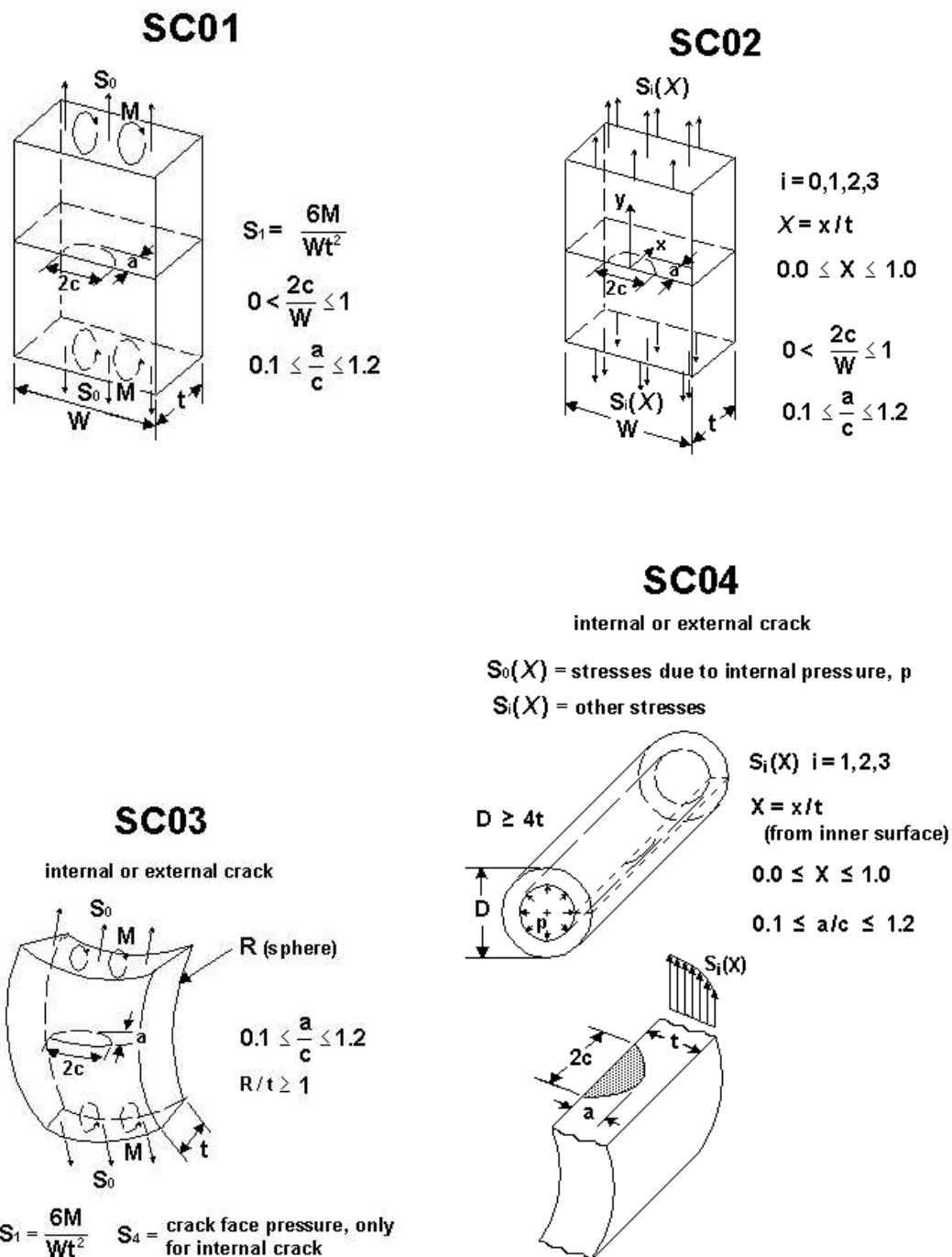


Figure 33 – Surface crack cases 1, 2, 3 &amp; 4

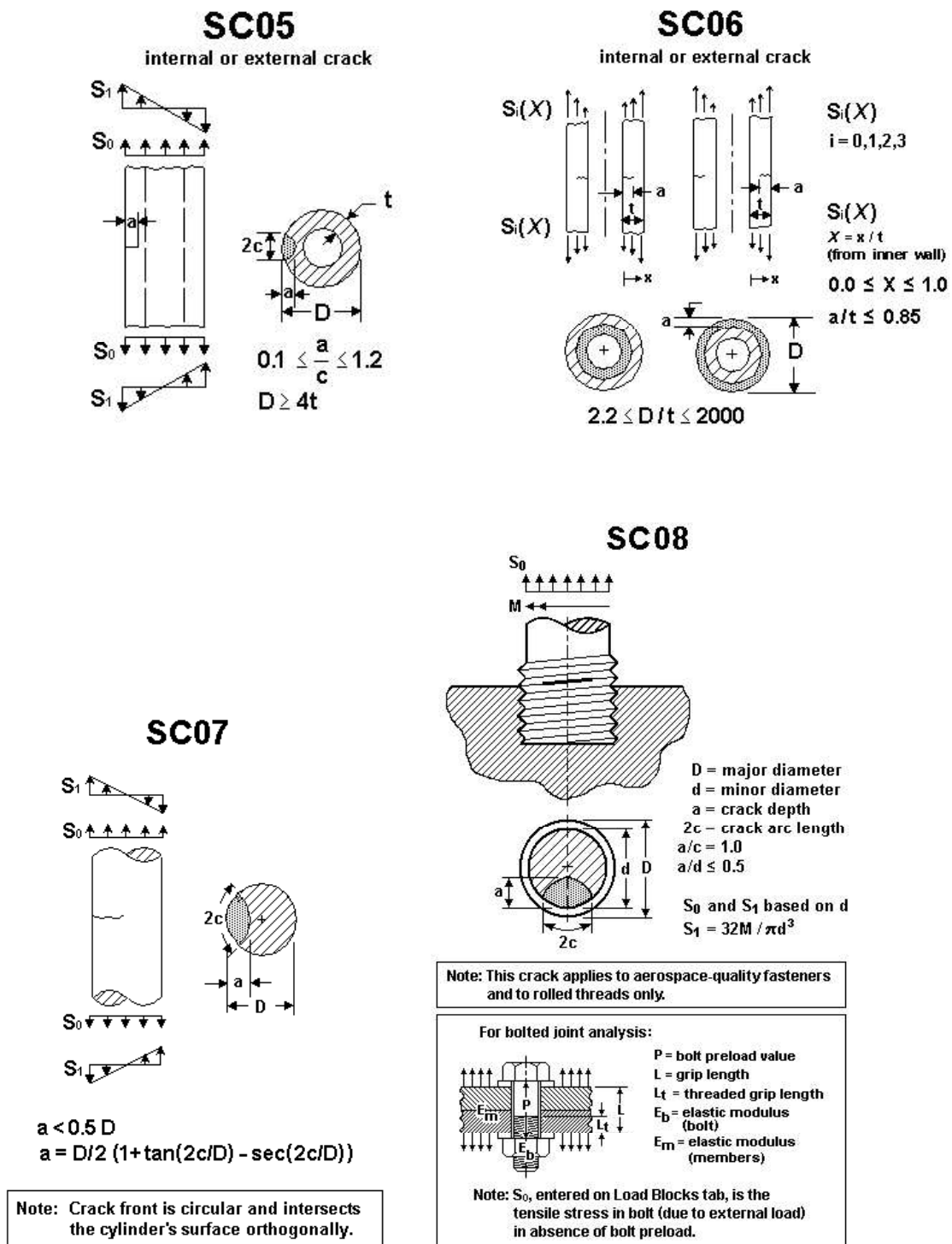


Figure 34 – Surface crack cases 5, 6, 7 &amp; 8

## 2.2 Details of Crack Growth Analysis

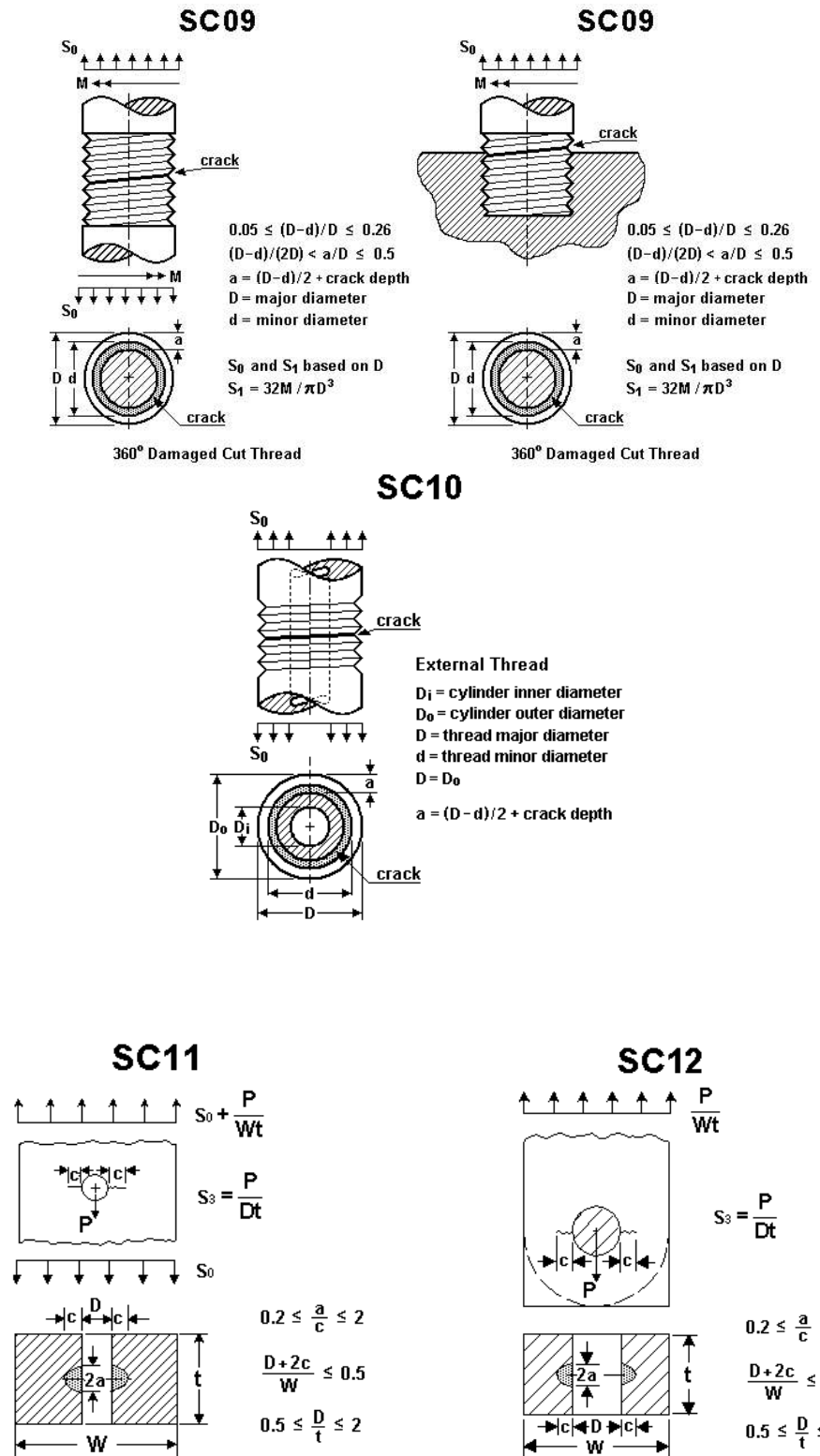


Figure 35 – Surface crack cases 9, 10, 11 &amp; 12

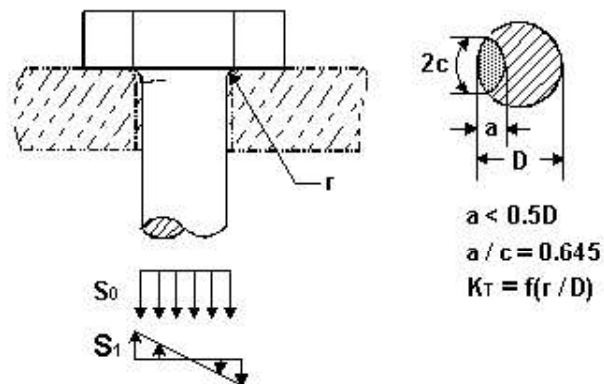
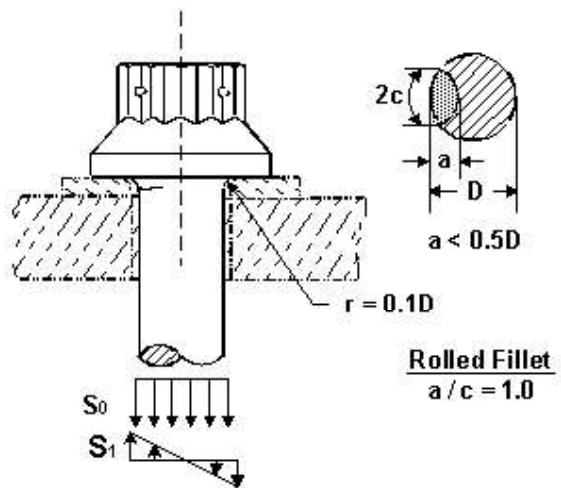
**SC13****Shear or Machine Bolt - Machined Fillet****SC14****Crack in Bolt Head Fillet**

Figure 36 – Surface crack case 13 &amp; 14

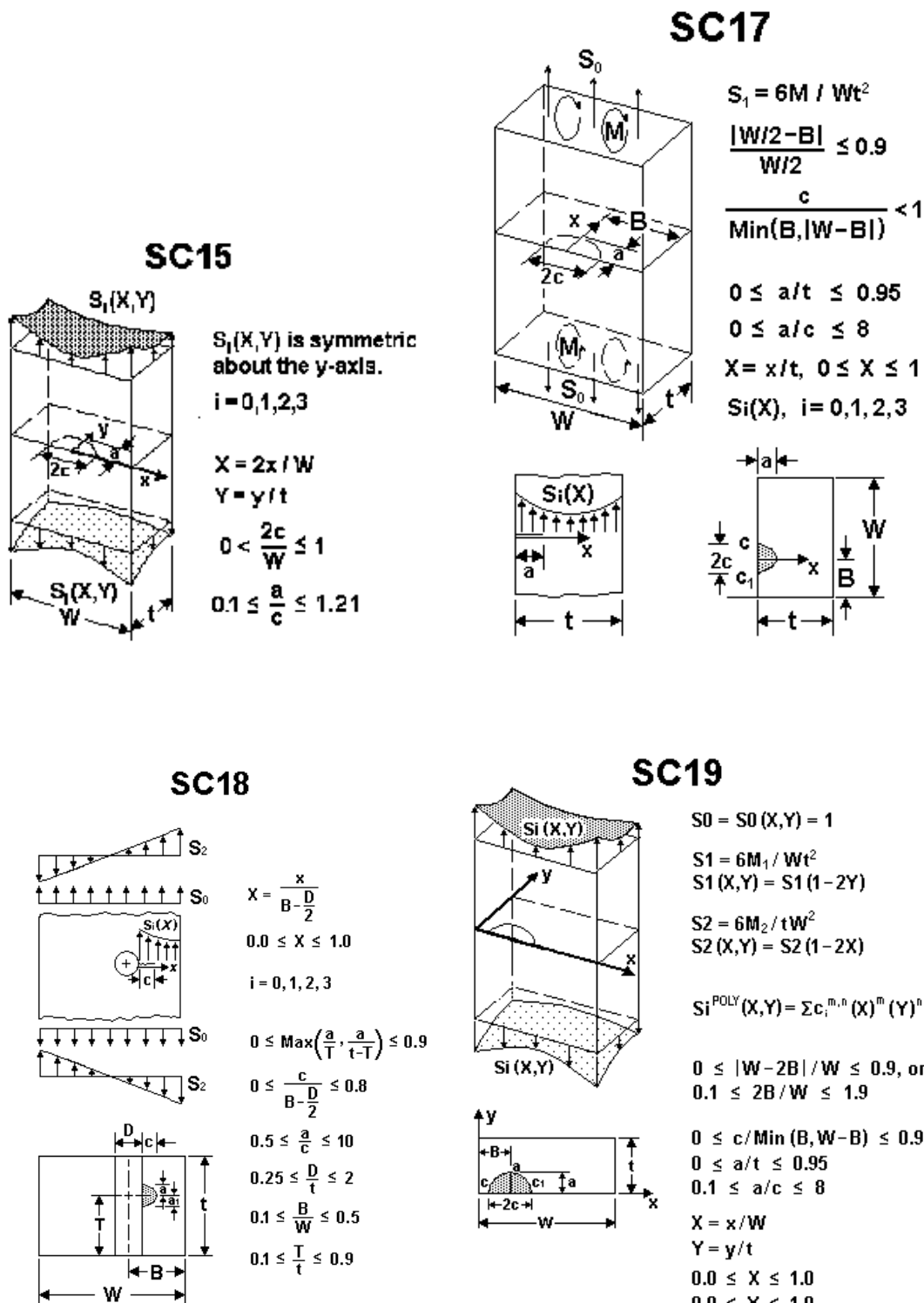


Figure 37 – Surface crack cases 15, 17, 18 &amp; 19

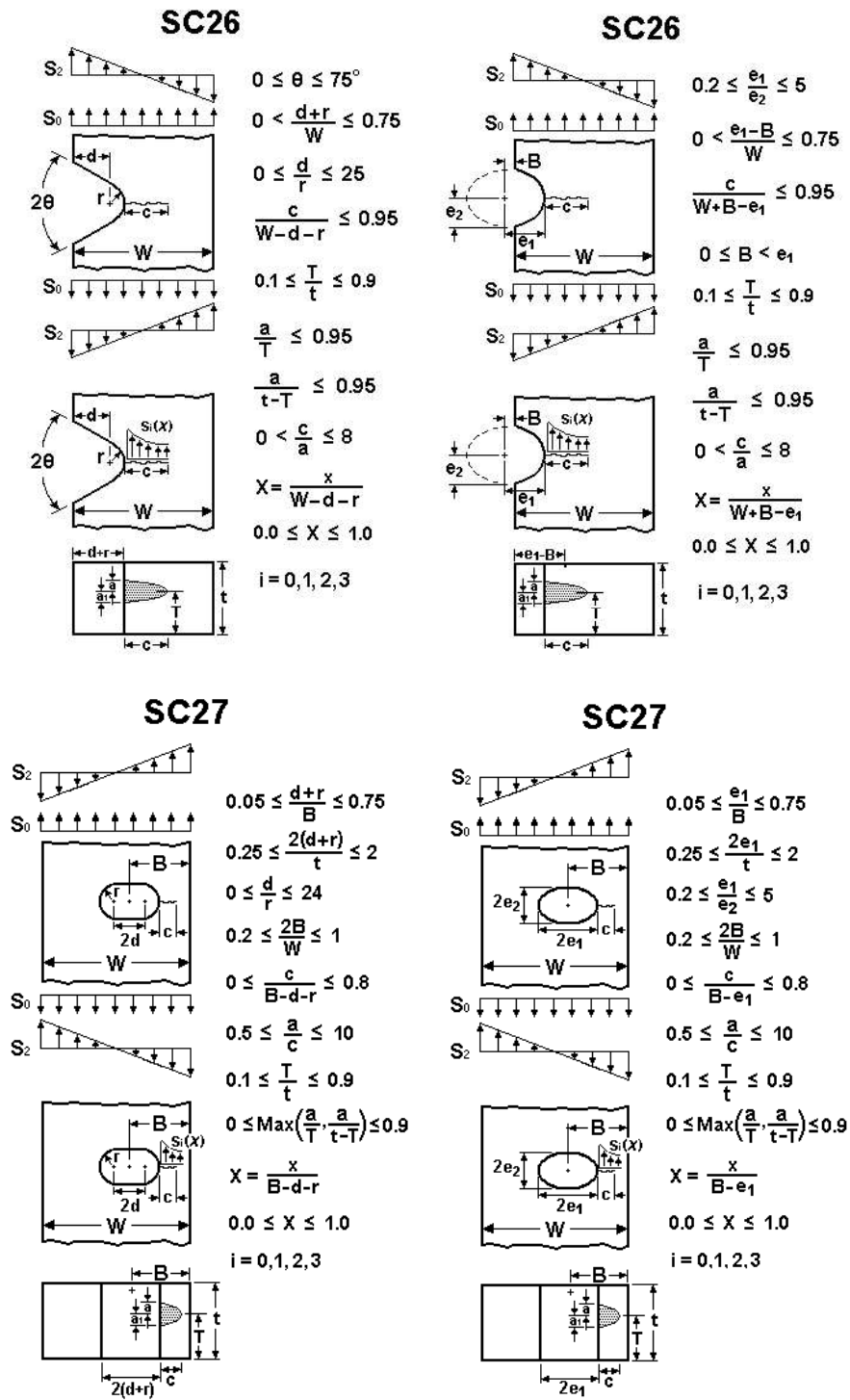


Figure 38 – Surface crack cases 26 &amp; 27

## 2.2 Details of Crack Growth Analysis

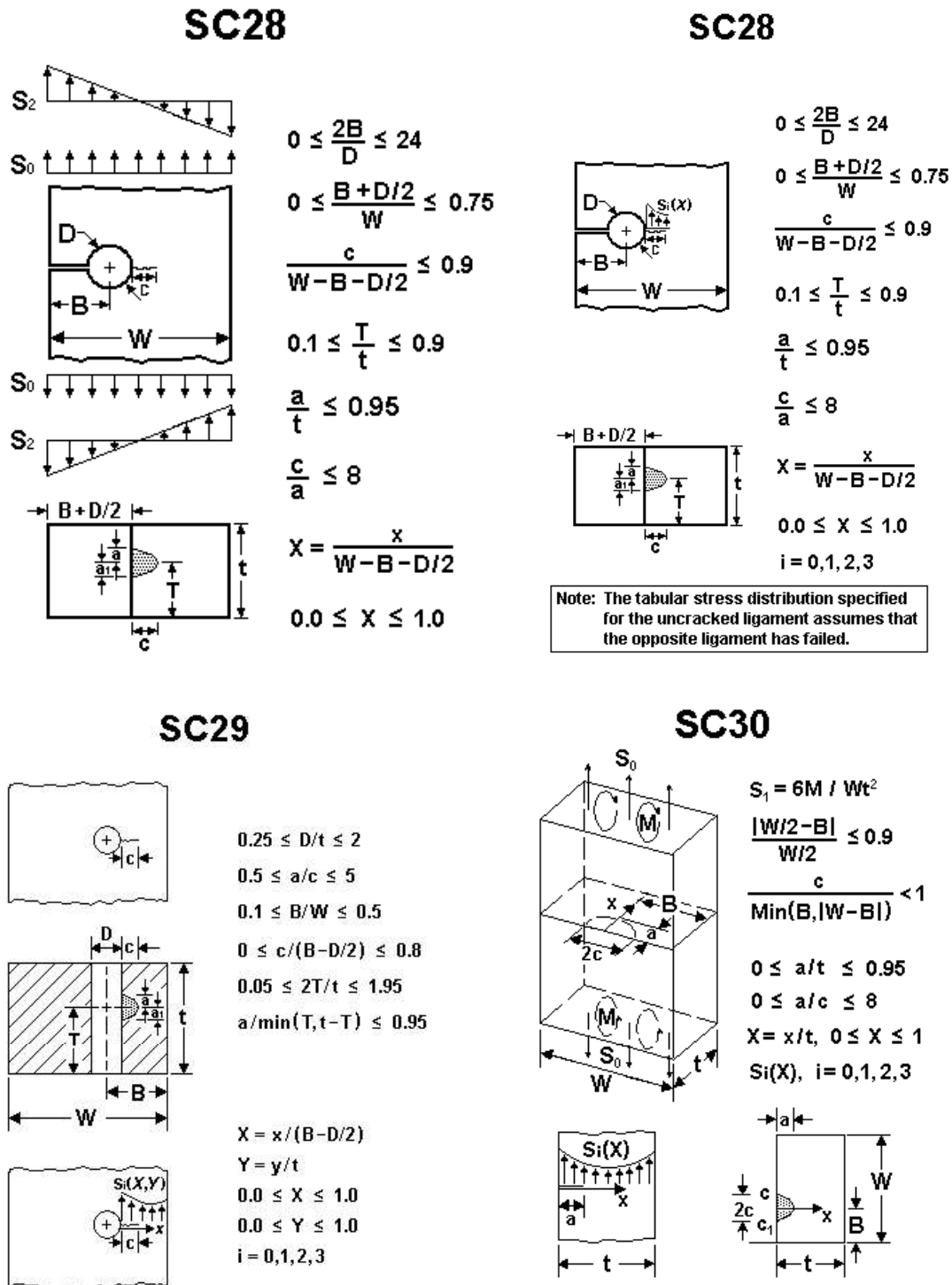


Figure 39 – Surface crack cases 28, 29 &amp; 30

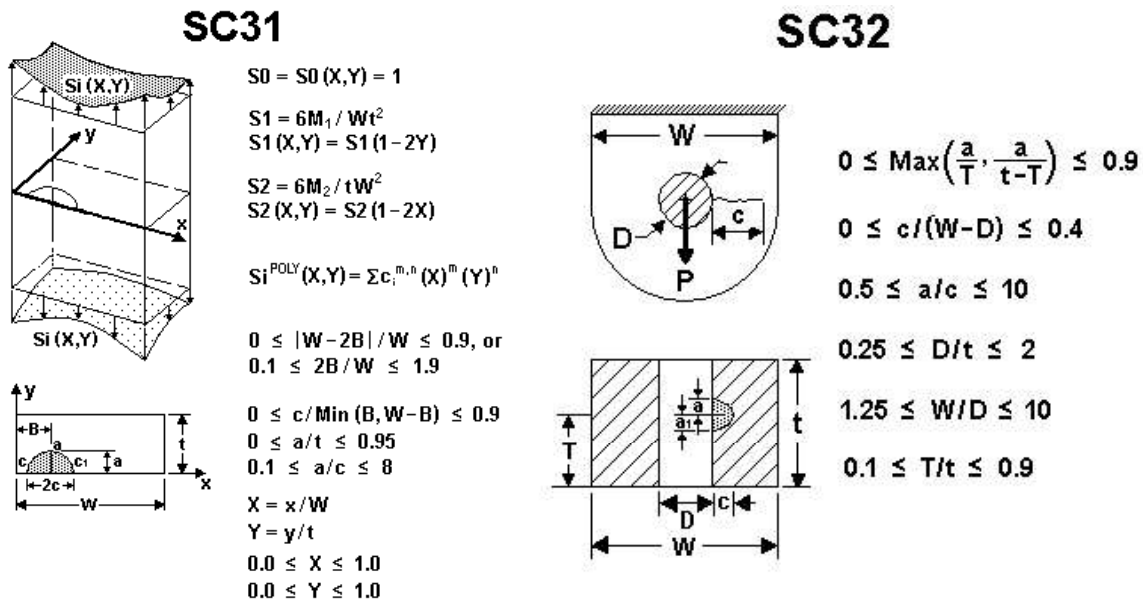


Figure 40 – Surface crack case 31 &amp; 32

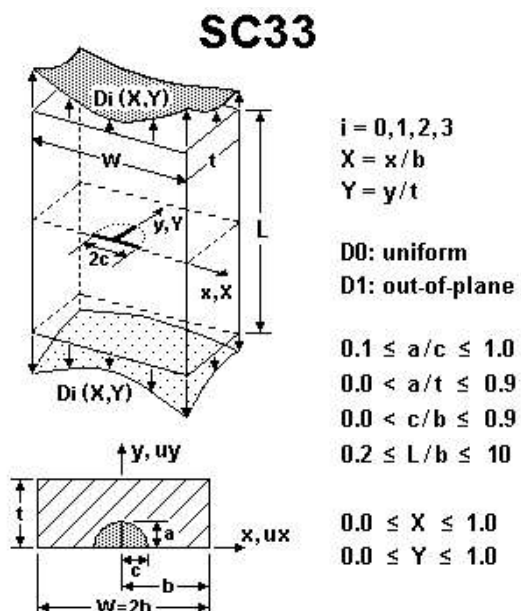


Figure 41a – Surface crack case 33

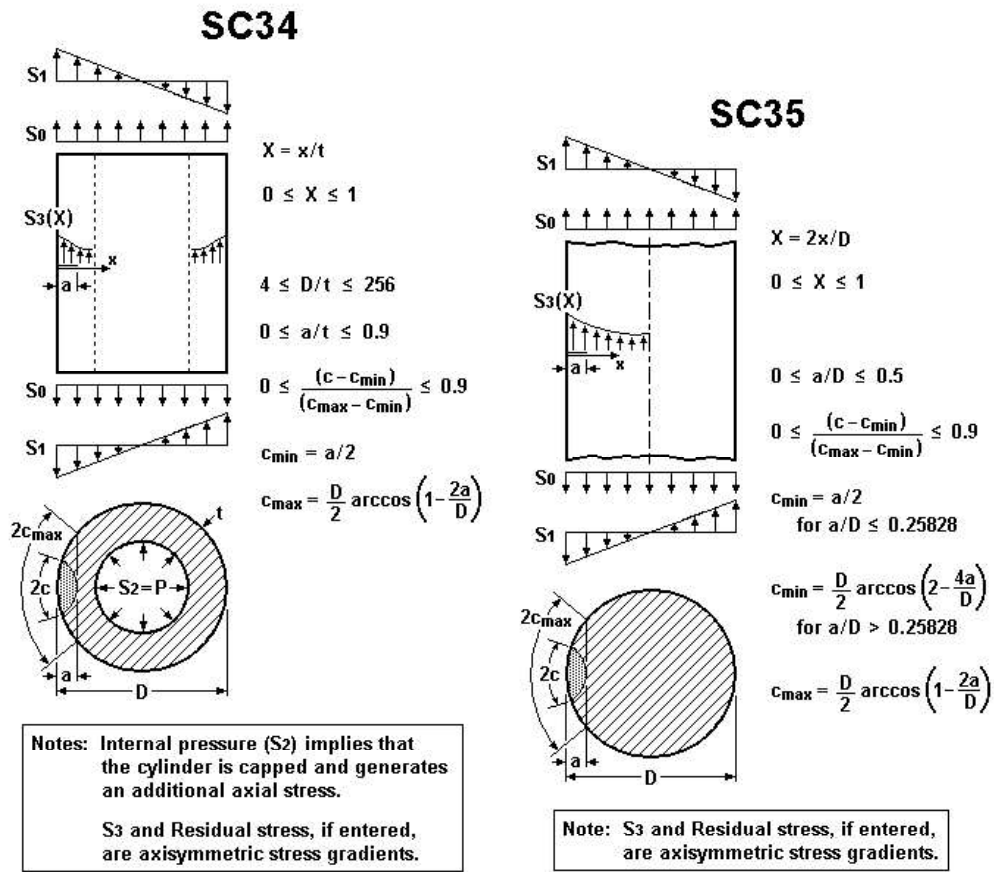
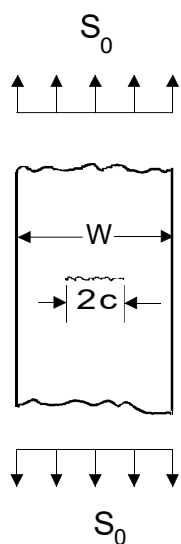
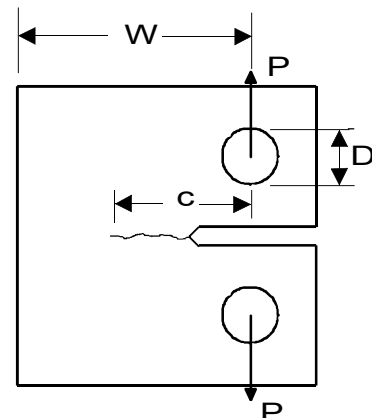
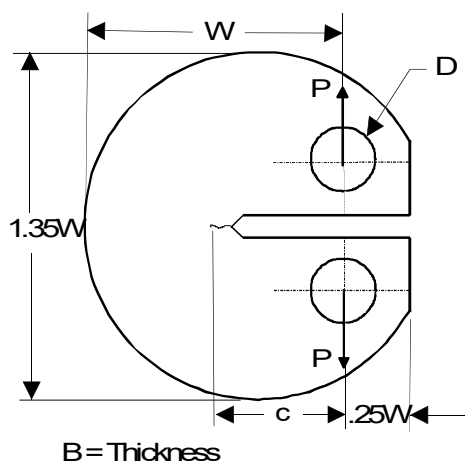
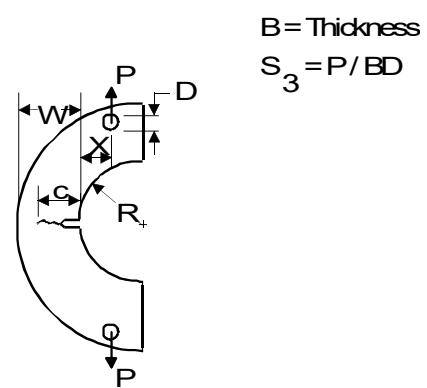


Figure 41b – Surface crack cases 34 &amp; 35

**SS01****SS02**

$$B = \text{Thickness}$$

$$S_3 = P / BD$$

**SS03****SS04**

$$B = \text{Thickness}$$

$$S_3 = P / BD$$

Figure 42 – Standard specimen crack cases 1, 2, 3 &amp; 4

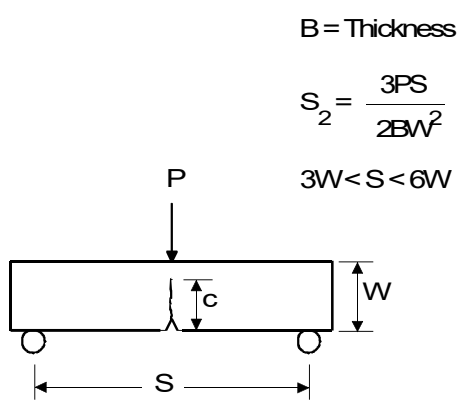
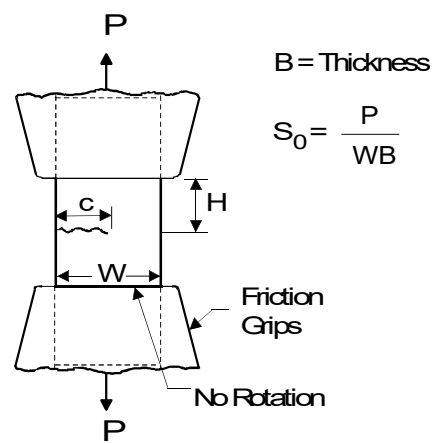
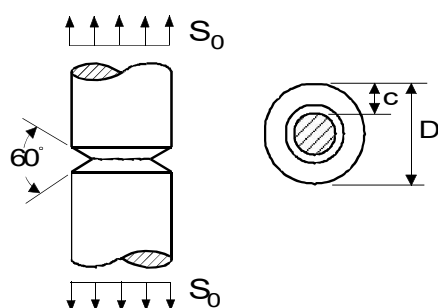
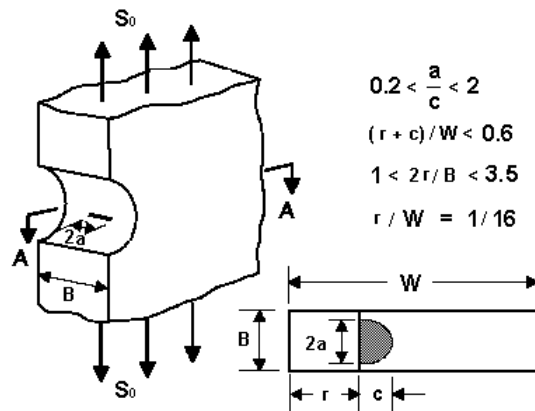
**SS05****SS06****SS07****SS08**

Figure 43 – Standard specimen crack cases 5, 6, 7 &amp; 8

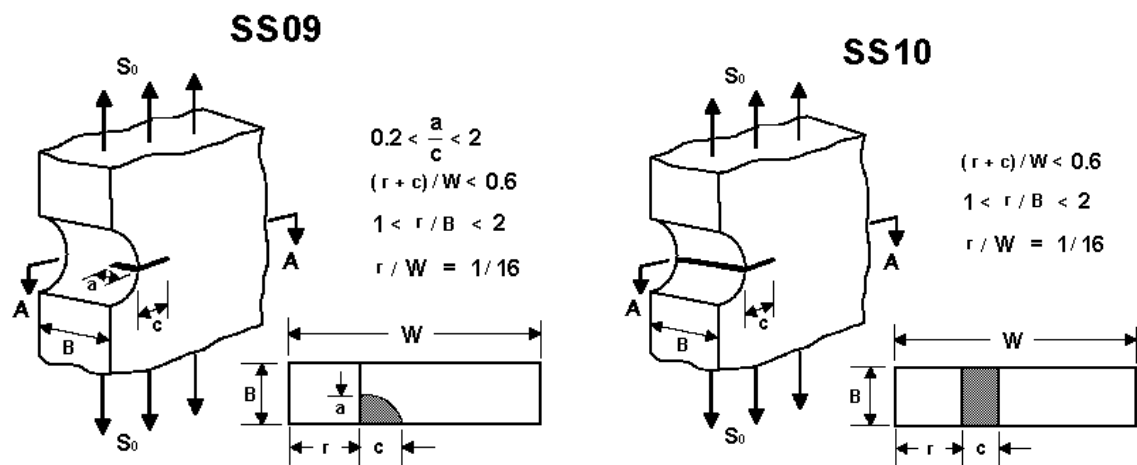


Figure 44 – Standard specimen crack cases 9 &amp; 10

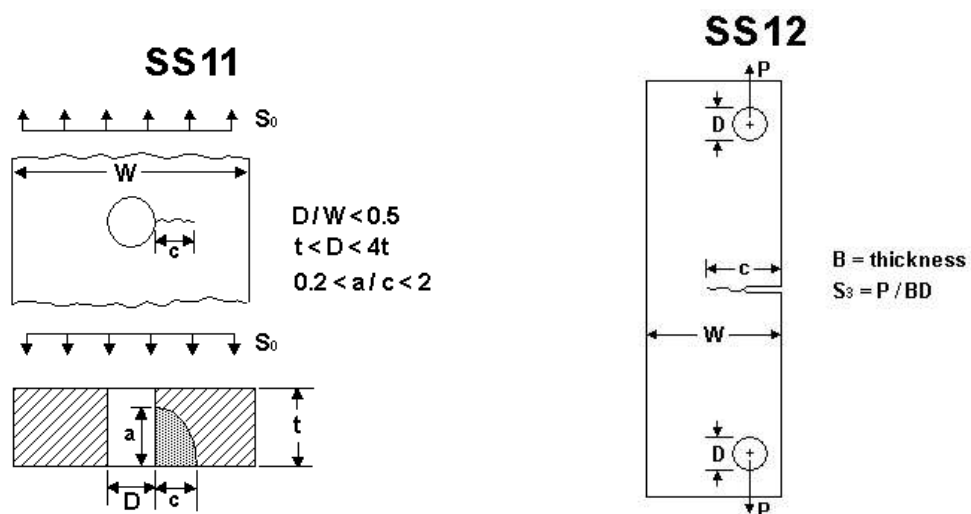


Figure 45 – Standard specimen crack cases 11 &amp; 12

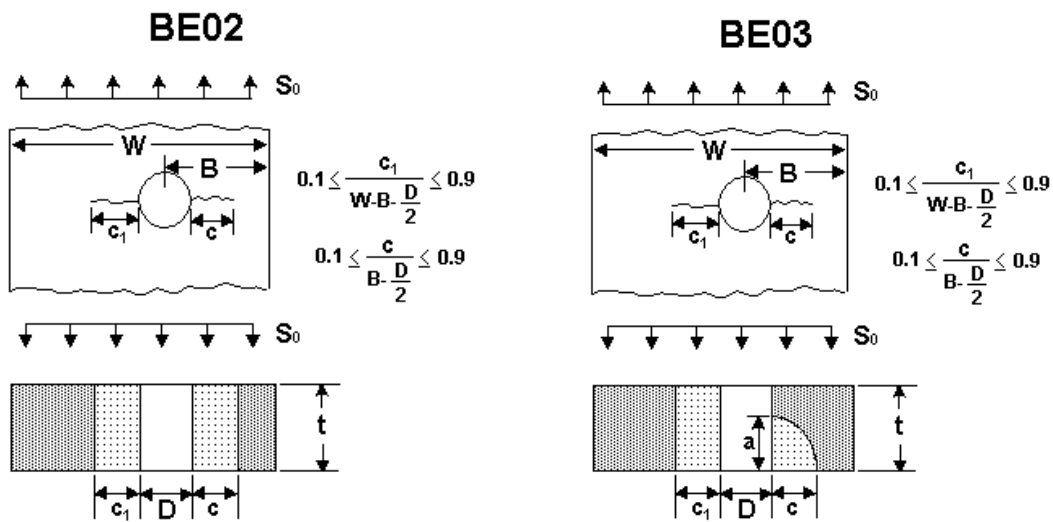


Figure 46 – Boundary Element crack cases 2 &amp; 3

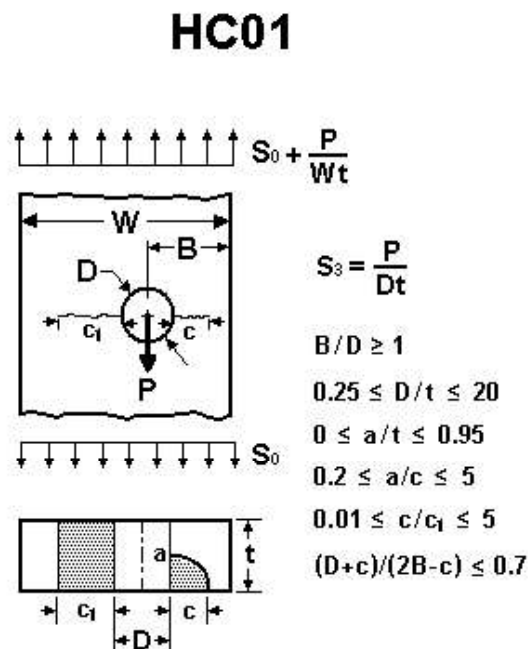


Figure 47 – Hybrid crack case 1

### 2.2.3 Entering the Initial Flaw Size

NASGRO offers two options for input of the initial flaw size:

- “User entry”: the user types the flaw size in a text box
- “NASA standard NDE”: the user selects a nondestructive evaluation (NDE) method from a list of NASA-approved methods and the initial flaw size is set automatically according to the chosen method

The “NASA standard NDE” crack size has a high probability of detection when an inspection is performed in accordance with the proper NASA specifications (as taken from the NASA NDE requirements document). From a damage tolerance point of view, the NASA standard NDE flaw size is one that may be just missed by the inspector and hence the structure should be able to withstand it for certain number of fatigue load cycles.

The current NASA NDE requirements document NASA-STD-5009 (*"Nondestructive Evaluation Requirements for Fracture-Critical Metallic Components"*) was published in 2008; this supersedes the prior requirements document, MSFC-STD-1249 (*"Standard NDE Guidelines and Requirements for Fracture Control Programs"*). The requirements document establishes the NDE specifications (including inspector qualifications, applicable methods and initial flaw sizes) for any NASA system or component, flight or ground, where fracture control is a requirement.

As of v6.0 (released 3/2009), NASGRO's list of "NASA standard NDE" initial flaw sizes and methods reflects the contents of NASA-STD-5009. The essential differences between v6.0 (NASA-STD-5009) and v5.22 (MSFC-STD-1249) in terms of NASGRO crack cases are shown in Tables 7a and 7b for US customary and SI units, respectively.

NASGRO offers information from the NASA NDE requirements as a courtesy to users. These flaw sizes may or may not be applicable to other industries or organizations. No warranty is made to the completeness or applicability of the NASGRO list to any specific application. Users are encouraged to verify the applicability of this information to their specific hardware:

- NASA users: consult your appropriate Fracture Control authority
- Non-NASA: consult your NDE personnel and/or your regulatory or approval authority

## 2.2 Details of Crack Growth Analysis

Table 7a – Changes from previous (MSFC-STD-1249) to current (NASA-STD-5009) NASA NDE standards, US Customary Units

NASGRO crack case	NDE method	Thickness	Crack size a      c		New or different in NASA-STD-5009
TC02-TC05, TC09, TC10, TC12, TC13	P	$t \leq 0.100$	-	0.100	$c = 0.150$
EC01, EC02	R	$0.025 \leq t \leq 0.107$	0.35t	0.075	1. Thickness restriction removed 2. $c = 0.7t$
	R	$t > 0.107$	0.35t	0.7t	Thickness restriction removed
	U	$t \geq 0.300$	0.065	0.065	1. Thickness restriction removed 2. Values for circular crack changed: $a = c = 0.039$ 3. Values for non-circular crack added: $a = 0.017, c = 0.087$
CC01-CC05, CC07- CC09	P	$t > 0.100$	0.100	0.100	$c = 0.150$
	U	$t > 0.100$	0.100	0.100	Method removed entirely
SC01-SC03, SC11, SC12, SC15, SC17	R	$0.025 \leq t \leq 0.107$	0.7t	0.075	Lower thickness limit removed
SC04, SC05	R (ext and int)	$0.025 \leq t \leq 0.107$	0.7t	0.075	Lower thickness limit removed
SC06	R (ext and int)	$0.025 \leq t \leq 0.107$	0.7t	-	Lower thickness limit removed

Notes: P=dye penetrant, R=radiographic, U=ultrasonic.

Red = item or value that has changed, green = new value.

Table 7b – Changes from previous (MSFC-STD-1249) to current (NASA-STD-5009) NASA NDE standards, SI Customary Units

NASGRO crack case	NDE method	Thickness	Crack size a      c		New or different in NASA-STD-5009
TC02-TC05, TC09, TC10, TC12, TC13	P	$t \leq 2.540$	-	2.540	$c = 3.810$
EC01, EC02	R	$0.635 \leq t \leq 2.718$	0.35t	1.905	1. Thickness restriction removed 2. $c = 0.7t$
	R	$t > 2.712$	0.35t	0.7t	Thickness restriction removed
	U	$t \geq 7.62$	1.651	1.651	1. Thickness restriction removed 2. Values for circular crack changed: $a = c = 0.991$ 3. Values for non-circular crack added: $a = 0.432, c = 2.210$
CC01-CC05, CC07- CC09	P	$t > 2.540$	2.540	2.540	$c = 3.810$
	U	$t > 2.540$	2.540	2.540	Method removed entirely
SC01-SC03, SC11, SC12, SC15, SC17	R	$0.635 \leq t \leq 2.718$	0.7t	1.905	Lower thickness limit removed
SC04, SC05	R (ext and int)	$0.635 \leq t \leq 2.718$	0.7t	1.905	Lower thickness limit removed
SC06	R (ext and int)	$0.635 \leq t \leq 2.718$	0.7t	-	Lower thickness limit removed

Notes: P=dye penetrant, R=radiographic, U=ultrasonic.

Red = item or value that has changed, green = new value.

Current NASA Standard NDE methods and initial flaw sizes (NASA-STD-5009), used in NASGRO versions 6.0 and beyond, are shown in Tables 8a and 8b for US customary and SI units, respectively.

The obsolete NDE methods and flaw sizes (MSFC-STD-1249), used in NASGRO versions 5.2 and prior, are retained in the NASGRO documentation in Tables 9a and 9b (for US customary and SI units, respectively) for reference in the event that users need to perform an analysis in accordance with the previous standard.

It is recommended to use the new standard rather than the old standard in all NASA applications, since it represents the current best knowledge and capabilities. For NASA applications, specific issues with the new NDE flaw sizes and methods should be taken up with the appropriate Fracture Control authority. Non-NASA users should consult their own NDE personnel and/or their regulatory or approval authority for applicability of these initial flaw sizes to their own specific applications.

Note that for a surface crack in a solid circular section (case SC07), the crack depth,  $a$ , is a function of  $c$  and  $D$  and can be calculated from:

$$a = \frac{D}{2} \left( 1 + \tan\left(\frac{2c}{D}\right) - \sec\left(\frac{2c}{D}\right) \right) \quad (2.43)$$

where  $D$  is the major diameter. Alternatively, the surface crack length,  $c$ , may be calculated from the following expression:

$$c = \frac{D}{2} \arctan\left( \frac{a(D-a)}{D\left(\frac{D}{2}-a\right)} \right) \quad (2.44)$$

which is valid for  $a < D/2$ .

## 2.2 Details of Crack Growth Analysis

Table 8a – Current NASA Standard NDE Flaw Sizes, US Customary Units  
(NASA-STD-5009)

Crack Case	NDE Inspection Technique or Flaw Size Criterion	Thickness Range (in.)	***Crack Size (in.)	
			a	c
TC01, TC06, TC07, TC08 (open surface), TC11, TC16	EC	$t \leq 0.050$	–	0.050
	P	$t \leq 0.050$	–	0.100
	P	$0.050 < t \leq 0.075$	–	0.15-t
	MP	$t \leq 0.075$	–	0.125
TC02 (edge), TC12, TC14, TC15	EC	$t \leq 0.075$	–	0.100
	P	$t \leq 0.100$	–	0.150
	MP	$t \leq 0.075$	–	0.250
TC03, TC04, TC05, TC09 (hole), TC10, TC13	EC	$t \leq 0.075$	–	0.100
	P	$t \leq 0.100$	–	0.150
	MP	$t \leq 0.075$	–	0.250
	HPD – driven rivet	any thickness	–	0.005
	HPD – other holes	$t \leq 0.050$	–	0.050
EC01, EC02, EC04, EC05	R	any thickness	0.35t	0.7t
	U (circ crack)	any thickness	0.039	0.039
	U (non-circ crack)	any thickness	0.017	0.087
CC01 (edge), CC05, CC09, CC11	EC	$t > 0.075$	0.075	0.075
	P	$t > 0.100$	0.100	0.150
	MP	$t > 0.075$	0.075	0.25
CC02, CC03 (hole), CC04, CC07, CC08, CC10	EC	$t > 0.075$	0.075	0.075
	P	$t > 0.100$	0.100	0.150
	MP	$t > 0.075$	0.075	0.25
	HPD – not driven rivet	$t > 0.050$	0.050	0.050
SC01, SC02, SC03 (open surface), SC11, SC12, SC15, SC17, SC18, SC19	EC	$t > 0.050$	0.020	0.100*
	P	$t > 0.075$	0.050	0.050**
	MP	$t > 0.075$	0.025	0.125*
	R	$t \leq 0.107$	0.075	0.075**
	R	$t > 0.107$	0.7t	0.075
	U	$t \geq 0.100$	0.030	0.150*
			0.065	0.065**
SC04, SC05	EC (ext and int)	$t > 0.050$	0.020	0.100*
	P (ext)	$t > 0.075$	0.050	0.050**
	MP (ext)	$t > 0.075$	0.025	0.125*
	R (ext and int)	$t \leq 0.107$	0.075	0.075**
	U (ext and int)	$t > 0.107$	0.038	0.188*
		$t \geq 0.100$	0.075	0.125**
			0.030	0.075
			0.065	0.150*
			0.065	0.065**
SC06	EC (ext and int)	$t > 0.050$	0.020	–
	P (ext)	$t > 0.075$	0.025	–
	MP (ext)	$t > 0.075$	0.038	–
	R (ext and int)	$t \leq 0.107$	0.7t	–
	U (ext and int)	$t \geq 0.100$	0.030	–
SC07	EC	–	Eq 2.43, 2.44	0.050
	P	–	Eq 2.43, 2.44	0.075
	MP	–	Eq 2.43, 2.44	0.125
SC08 (rolled threads), SC13 (machined fillet), SC14 (machined or rolled fillet)	P	–	–	0.075
	EC (for SC08 only)	–	–	0.050
SC09, SC10 (machined threads)	max machining defect size	–	thd depth +0.005	–

Notes:

EC = eddy current

R = radiographic

P = dye penetrant

U = ultrasonic

\*minimum crack depth

\*\*maximum crack depth

MP = magnetic particle

HPD = hole preparation defect (max)

\*\*\*1 in. = 25.4 mm

Table 8b – Current NASA Standard NDE Flaw Sizes, SI Units  
 (NASA-STD-5009)

Crack Case	NDE Inspection Technique or Flaw Size Criterion	Thickness Range (mm)	***Crack Size (mm) a                    c	
TC01, TC06, TC07, TC08 (open surface), TC11, TC16	EC	$t \leq 1.270$	—	1.270
	P	$t \leq 1.270$	—	2.540
	P	$1.270 < t \leq 1.905$	—	3.81-t
	MP	$t \leq 1.905$	—	3.175
TC02 (edge), TC12, TC14, TC15	EC	$t \leq 1.905$	—	2.540
	P	$t \leq 2.540$	—	3.810
	MP	$t \leq 1.905$	—	6.350
TC03, TC04, TC05, TC09 (hole), TC10, TC13	EC	$t \leq 1.905$	—	2.540
	P	$t \leq 2.540$	—	3.810
	MP	$t \leq 1.905$	—	6.350
	HPD – driven rivet	any thickness	—	0.127
	HPD – other holes	$t \leq 1.270$	—	1.270
EC01, EC02, EC04, EC05	R	any thickness	0.35t	0.7t
	U (circ crack)	any thickness	0.991	0.991
	U (non-circ crack)	any thickness	0.432	2.210
CC01 (edge), CC05, CC09, CC11	EC	$t > 1.905$	1.905	1.905
	P	$t > 2.540$	2.540	3.810
	MP	$t > 1.905$	1.905	6.35
CC02, CC03 (hole), CC04, CC07, CC08, CC10	EC	$t > 1.905$	1.905	1.905
	P	$t > 2.540$	2.540	3.810
	MP	$t > 1.905$	1.905	6.35
	HPD – not driven rivet	$t > 1.270$	1.270	1.270
SC01, SC02, SC03 (open surface), SC11, SC12, SC15, SC17, SC18, SC19	EC	$t > 1.270$	0.508	2.540*
	P	$t > 1.905$	1.270	1.270**
	MP	$t > 1.905$	0.635	3.175*
	R	$t \leq 2.718$	1.905	1.905**
	R	$t > 2.718$	0.7t	3.175*
	U	$t \geq 2.540$	0.762	4.755*
			1.651	3.175**
SC04, SC05	EC (ext and int)	$t > 1.270$	0.508	2.540*
	P (ext)	$t > 1.905$	1.270	1.270**
	MP (ext)	$t > 1.905$	0.635	3.175*
	R (ext and int)	$t \leq 2.718$	1.905	1.905**
	U (ext and int)	$t \geq 2.540$	0.965	4.755*
SC06	EC (ext and int)	$t > 1.270$	0.508	3.175**
	P (ext)	$t > 1.905$	0.635	3.175*
	MP (ext)	$t > 1.905$	1.905	1.905**
	R (ext and int)	$t \leq 2.718$	0.7t	4.755*
	U (ext and int)	$t \geq 2.540$	1.905	3.175**
SC07	EC	—	0.7t	3.175**
	P	—	0.7t	3.175*
	MP	—	0.7t	1.905
			0.762	2.540*
			1.651	1.651**
SC08 (rolled threads), SC13 (machined fillet), SC14 (machined or rolled fillet)	P	—	—	1.905
	EC (for SC08 only)	—	—	1.270
SC09, SC10 (machined threads)	max machining defect size	—	thd depth +0.127	—

## Notes:

EC = eddy current

P = dye penetrant

\*minimum crack depth

R = radiographic

U = ultrasonic

\*\*maximum crack depth

MP = magnetic particle

HPD = hole preparation defect (max)

\*\*\*1 in. = 25.4 mm

## 2.2 Details of Crack Growth Analysis

Table 9a – Obsolete NASA Standard NDE Flaw Sizes, US Customary Units  
(MSFC-STD-1249)

	Crack Case	NDE Inspection Technique or Flaw Size Criterion	Thickness Range (in.)	***Crack Size (in.)	
				a	c
Obsolete -- Obsolete -- Obsolete -- Obsolete -- Obsolete	TC01, TC06, TC07, TC08 (open surface), TC11	EC	$t \leq 0.050$	—	0.050
		P	$t \leq 0.050$	—	0.100
		P	$0.050 < t \leq 0.075$	—	0.15-t
		MP	$t \leq 0.075$	—	0.125
	TC02 (edge), TC12	EC	$t \leq 0.075$	—	0.100
		P	$t \leq 0.100$	—	0.100
		MP	$t \leq 0.075$	—	0.250
		HPD – driven rivet	$t \leq 0.075$	—	0.100
	TC03, TC04, TC05, TC09 (hole), TC10, TC13	P	$t \leq 0.100$	—	0.100
		MP	$t \leq 0.075$	—	0.250
		HPD – driven rivet	any thickness	—	0.005
		HPD – other holes	$t \leq 0.050$	—	0.050
	EC01, EC02	R	$0.025 \leq t \leq 0.107$	$0.35t$	0.075
		R	$t > 0.107$	$0.35t$	$0.7t$
		U	$t \geq 0.300$	0.065	0.065
		EC	$t > 0.075$	0.075	0.075
	CC01 (edge), CC05, CC09	P	$t > 0.100$	0.100	0.100
		MP	$t > 0.075$	0.075	0.25
		U	$t > 0.100$	0.100	0.100
		EC	$t > 0.075$	0.075	0.075
	CC02, CC03 (hole), CC04, CC07, CC08	P	$t > 0.100$	0.100	0.100
		MP	$t > 0.075$	0.075	0.25
		U	$t > 0.100$	0.100	0.100
		HPD – not driven rivet	$t > 0.050$	0.050	0.050
	SC01, SC02, SC03 (open surface), SC11, SC12, SC15, SC17	EC	$t > 0.050$	0.020	0.100*
		P	$t > 0.075$	0.050	0.050**
		MP	$t > 0.075$	0.025	0.125*
		R	$0.025 \leq t \leq 0.107$	0.075	0.075**
	SC04, SC05	R	$t > 0.107$	0.038	0.188*
		U	$t \geq 0.100$	0.075	0.125**
		EC (ext and int)	$t > 0.050$	0.020	0.100*
		P (ext)	$t > 0.075$	0.050	0.050**
	SC06	MP (ext)	$t > 0.075$	0.025	0.125*
		R (ext and int)	$0.025 \leq t \leq 0.107$	0.075	0.075**
		U (ext and int)	$t > 0.107$	0.038	0.188*
			$t \geq 0.100$	0.075	0.125**
	SC07	EC (ext and int)	$t > 0.050$	0.020	—
		P (ext)	$t > 0.075$	0.025	—
		MP (ext)	$t > 0.075$	0.038	—
		R (ext and int)	$0.025 \leq t \leq 0.107$	0.075	—
	SC08 (rolled threads), SC13 (machined fillet), SC14 (machined or rolled fillet)	U (ext and int)	$t \geq 0.100$	0.030	—
		EC	—	Eq 2.43, 2.44	0.050
		P	—	Eq 2.43, 2.44	0.075
		MP	—	Eq 2.43, 2.44	0.125
	SC09, SC10 (machined threads)	EC	—	Eq 2.43, 2.44	0.075
		P	—	Eq 2.43, 2.44	0.075
		MP	—	Eq 2.43, 2.44	0.075
		U	—	Eq 2.43, 2.44	0.075
	max machining defect size	EC	—	thd depth +0.005	—
		P	—	thd depth +0.005	—
		MP	—	thd depth +0.005	—
		U	—	thd depth +0.005	—

Notes:

EC = eddy current

R = radiographic

MP = magnetic particle

P = dye penetrant

U = ultrasonic

HPD = hole preparation defect (max)

\*minimum crack depth

\*\*maximum crack depth

\*\*\*1 in. = 25.4 mm

Table 9b – Obsolete NASA Standard NDE Flaw Sizes, SI Units  
(MSFC-STD-1249)

	Crack Case	NDE Inspection Technique or Flaw Size Criterion	Thickness Range (mm)	***Crack Size (mm)	
				a	c
TC01, TC06, TC07, TC08 (open surface), TC11	EC	$t \leq 1.270$	—	1.270	
	P	$t \leq 1.270$	—	2.540	
	P	$1.270 < t \leq 1.905$	—	3.81*t	
	MP	$t \leq 1.905$	—	3.175	
TC02 (edge), TC12	EC	$t \leq 1.905$	—	2.540	
	P	$t \leq 2.540$	—	2.540	
	MP	$t \leq 1.905$	—	6.350	
TC03, TC04, TC05, TC09 (hole), TC10, TC13	EC	$t \leq 1.905$	—	2.540	
	P	$t \leq 2.540$	—	2.540	
	MP	$t \leq 1.905$	—	6.350	
	HPD – driven rivet	any thickness	—	0.127	
	HPD – other holes	$t \leq 1.270$	—	1.270	
EC01, EC02	R	$0.635 \leq t \leq 2.718$	0.35t	1.905	
	R	$t \geq 2.718$	0.35t	0.7t	
	U	$t \geq 7.620$	1.651	1.651	
CC01 (edge), CC05, CC09	EC	$t > 1.905$	1.905	1.905	
	P	$t > 2.540$	2.540	2.540	
	MP	$t > 1.905$	1.905	6.35	
	U	$t > 2.540$	2.540	2.540	
CC02, CC03 (hole), CC04, CC07, CC08	EC	$t > 1.905$	1.905	1.905	
	P	$t > 2.540$	2.540	2.540	
	MP	$t > 1.905$	1.905	6.35	
	U	$t > 2.540$	2.540	2.540	
	HPD – not driven rivet	$t > 1.270$	1.270	1.270	
SC01, SC02, SC03 (open surface), SC11, SC12, SC15, SC17	EC	$t > 1.270$	0.508	2.540*	
			1.270	1.270**	
	P	$t > 1.905$	0.635	3.175*	
			1.905	1.905**	
	MP	$t > 1.905$	0.965	4.755*	
			1.905	3.175**	
SC04, SC05	R	$0.635 \leq t \leq 2.718$	0.7t	1.905	
		$t > 2.718$	0.7t	0.7t	
	U	$t \geq 2.540$	0.762	1.270*	
			1.651	1.651**	
	EC (ext and int)	$t > 1.270$	0.508	2.540*	
SC06	P (ext)	$t > 1.905$	1.270	1.270**	
	MP (ext)	$t > 1.905$	0.635	3.175*	
	R (ext and int)	$0.635 \leq t \leq 2.718$	0.965	4.755*	
		$t > 2.718$	1.905	3.175**	
	U (ext and int)	$t \geq 2.540$	0.7t	1.905	
SC07	EC (ext and int)	$t > 1.270$	0.508	—	
	P (ext)	$t > 1.905$	0.635	—	
	MP (ext)	$t > 1.905$	0.965	—	
SC08 (rolled threads), SC13 (machined fillet), SC14 (machined or rolled fillet)	R (ext and int)	$0.635 \leq t \leq 2.718$	0.7t	—	
		$t \geq 2.540$	0.762	—	
	U (ext and int)	$t \geq 2.540$	0.762	—	
SC09, SC10 (machined threads)	EC	—	Eq 2.43, 2.44	1.270	
	P	—	Eq 2.43, 2.44	1.905	
	MP	—	Eq 2.43, 2.44	3.175	
				1.905	
SC09, SC10 (machined threads)	P	—			
	max machining defect size	—	thd depth +0.127	—	

Notes:

EC = eddy current

R = radiographic

MP = magnetic particle

P = dye penetrant

U = ultrasonic

HPD = hole preparation defect (max)

\*minimum crack depth

\*\*maximum crack depth

\*\*\*1 in. = 25.4 mm

### 2.2.4 Selecting the Material Properties

The fracture mechanics data which have been curve fit for this release of NASGRO are contained in a database that includes approximately 6000 sets of fracture toughness data and about 3000 sets of crack propagation data [31]. References for the fracture mechanics data included the 1978 and 1982 editions of Hudson's Compendium [32, 33] and the Damage Tolerant Design Handbook [34]. The remaining references were taken from miscellaneous published reports and journal articles. Some of the data was generated at the NASA Johnson Space Center. Curve fit constants to Eq 2.1 were generated for over 300 different material-environment conditions and have been entered into the NASGRO material files (NASMFC and NASMFM).

The curve fit constants for the materials are entered into the NASMFC and NASMFM materials files in an encrypted form. The materials are listed in Table G in Appendix G. *The constants supplied in the database are normally typical or least squares statistical fits to data, i.e. not minimum or design allowable properties.* Also, in many cases, the tensile, threshold, and toughness properties are estimated or averaged over a fairly wide range of values. Factors of safety on life (e.g. 2 or 4) are then used to achieve adequate conservatism in analysis. Many of the curve fits are for a laboratory air (LA) condition, which is an acceptable assumption for most space hardware, which are not exposed to wet environments. In some cases, when environmental effects are minimal, data for other environments, such as dry air, high humidity air, or saltwater, have been included in the curve fit. In other cases, a separate curve fit has been generated for a specific environment. Some material/environment combinations are susceptible to frequency effects, and the frequency range for which data were available is listed with the curve fits.

Each particular curve fit applies only for the orientation(s) specified. If no crack orientation is specified, the curve fit should be assumed to apply to any orientation except S-T, S-L, C-R, C-L, and R-L. Figure 48 shows the nomenclature of the crack plane configurations for both rectangular and round product forms [35].

After selecting the total number of materials, the user selects the crack growth interaction model to be used. This may be any one of the five models: non interaction, Generalized Willenborg, Modified Willenborg, Walker-Chang, Strip Yield or Constant Closure model. Once the model is selected, the type of crack growth properties to be entered for that model needs to be selected. The default choice is input from NASGRO materials files, in which case properties are picked up from appropriate files automatically. There is also a button to choose from a list of favorite materials. Such a list is created in a previous run by saving the favorite material to an internal list. The other options are to get the material properties either from user-defined file or to enter new data from scratch. Next, the data format is selected from one of the following: NASGRO eqn., Walker eqn, 1-D table or 2-D table.

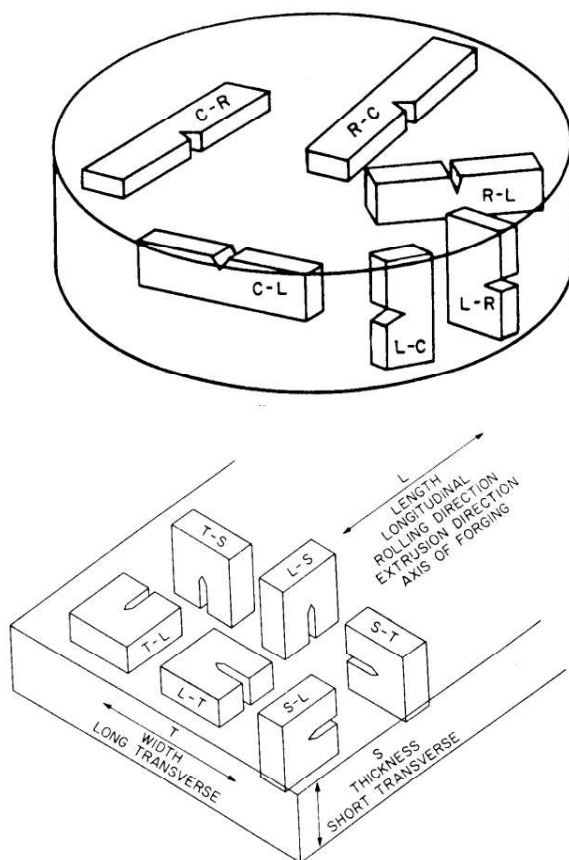


Figure 48 – Crack plane orientations

If the new data option for input of material properties is selected, one may enter 1-D or 2-D tables of  $da/dN-\Delta K$  data or supply the constants appearing in Eq 2.1. If a 1-D or 2-D table is specified, NASGRO uses an interpolation routine to compute  $da/dN$  values for a given crack growth analysis. Additional information regarding the interpolation routines that are used by NASGRO may be found in Appendix F.

Please note that while entering the 1-D table, for all models except strip yield, you would enter the usual (unmodified)  $da/dN-\Delta K$  values. For strip yield model, it is required that you enter the  $da/dN-\Delta K(\text{effective})$ . Effective values are those corrected for crack closure.

Two-dimensional tables are especially applicable to problems that include fatigue spectra with multiple stress ratios and environmentally accelerated crack growth that cannot be analyzed by Eq 2.1. The format for the tabular input is shown in Table 10. Here, the  $\Delta K_c(R)$  values are the critical stress intensity factor ranges that cause fracture. For computational purposes, these values are assumed to correspond to data points having a growth rate of 25.4E-1 mm/cycle (1.0E-1 in/cycle), or any other higher growth rate value entered in the first row of the table. In a similar manner, the last row of data should contain the  $\Delta K_{th}(R)$  values for no growth corresponding to points with a growth rate of 25.4E-8 mm/cycle (1.0E-8 in/cycle), or less.

In the graphical user interface, when the user right-clicks on the cells, there is an option to enter a user-defined equation for crack growth as a function of  $\Delta K$  and R in symbolic form. Any algebraic expression including standard functions such as Sine, Cosine etc., are allowed. The GUI then computes the 2D table of  $\Delta K$  values for selected R ratios. Once the table is filled, it can be saved for future use just as in the case of manually entered table of data.

Properties that are entered manually may be saved in the user-defined material files (USRMFC, USRMFM, etc.,) and may be accessed in future crack growth analyses.

Table 10 – Two-dimensional Interpolation Table

da/dN mm/cycle (in/cycle)	$\Delta K$				
	R	...	...	...	...
25.4E-1 (1E-1)	$\Delta K_c(R)$	...	...	...	...
...	...	...	...	...	...
...	...	(No gaps permitted; all cells must be filled)			...
...	...	...	...	...	...
...	...	...	...	...	...
25.4E-8 (1E-8)	$\Delta K_{th}(R)$	...	...	...	...

Another method of entering a 2-D table has also been provided. In this method, the da/dN values may be different for each of the R ratios. Here too, the first da/dN value should be at least 0.1 in/cycle. If not, the first value will be set to 0.1in/cycle and the user input will be placed in the next row of the table. Once the input is complete, the table is internally converted to the form shown in Table 10, and then computations proceed as usual.

#### 2.2.4.1 Entering Material Properties Data from File

To use the properties from the NASGRO materials files (NASMFC and NASMFM) in your crack growth analysis, just accept the default option. The curve fit constants for Eq 2.1 will be selected for the material that you specify. The materials are arranged in files according to the following code system:

L N LL EN LL NN ( L stands for a letter and N stands for a number, E stands for either letter or number)

- **Letter** to identify material category or group.
- **Number** to identify alloy group
- **Two letters** to identify alloy and heat treatment
- **Two numbers** to identify product form and crack orientation OR a **Letter and number** for weld type and crack orientation
- **Two letters** to identify the environment
- **Two numbers** to identify the temperature.

The program proceeds step by step by means of drop down lists, through the category, alloy group etc. until the final selection is made. All the constants are then displayed on the screen one in each text box. A “view curve fit” icon can be clicked to plot the curve fit along with the data used for fitting. Comparison plots with other raw data for various R ratios are also available from this selection. Any of the values displayed on the screen can be altered to suit the user’s needs. Choose option to select 1-D or 2-D da/dN- $\Delta K$  tables or Eq 2.1 curve fit constants that have been previously saved to the user-defined materials files. A menu system similar to that used for the NASGRO materials files has been enabled for the user-defined files also.

#### 2.2.4.2 Entering Material Properties Data Manually

To enter material properties manually, choose the “new data” radio-box choice. The material header information is entered by first selecting the alloy category and group from the drop-down boxes and then by filling the various text boxes for the alloy code and the heat-treatment code. The other required parameters are:  $\sigma_{ult}$ ,  $\sigma_{ys}$ ,  $K_{Ic}$ ,  $K_{Ie}$ ,  $A_k$ , and  $B_k$  are also to be provided. Once values for these constants have been entered, depending upon the format choice made earlier, the appropriate equation constants or tabular data will need to be entered into the text boxes presented.

Use the NASGRO option if you have the curve fit data using the procedure described in section 6.2 and want to use the constants for the crack growth analysis and/or save them in a user-defined materials file. The program prompts for  $C$ ,  $n$ ,  $p$ ,  $q$ ,  $\Delta K_1$ ,  $C_{th}$ ,  $\alpha$ , and  $S_{max}/\sigma_0$ . Similarly, if the Walker equation was chosen, the constants  $C$ ,  $n$ ,  $m$ ,  $q$  etc., will need to be entered.

The parameters used in the NASGRO equation have practical and/or theoretical limits. Many also have default or typical values that can be a good starting point when fitting material data in NASMAT and characterizing it in NASFLA. The table below summarizes the limits and typical values or ranges for each of the parameters in the NASGRO equation. The table is separated into three sections, with the NASGRO equation parameters in the top section, the near-threshold parameters below those, and the fracture toughness and strength parameters at the bottom.

**NASGRO Equation Parameter Limits**

Parameter	Minimum	Typical	Maximum
C	0	---	---
n	0	---	---
p	0	0.5 - 1.0	2
q	0	0.5 - 1.0	2
alpha	1	2.0 - 2.5	3
Smax/So	0	0.3	1
dK1	0	---	---
Cth+	-0.5	0.5 - 2.0	10
Cth-	-0.5	0.0 - 0.5	3
dK1f	0	---	---
Fth+	-0.5	0 - 3	8
Fth-	-1	(-0.3) - (-0.2)	0
Alpha_th	1	2.0 - 2.5	3
SmaxRatio_th	0	0.3	1
K1c	0	---	---
K1e	0	---	---
Ak	0	0.75 - 1	---
Bk	0	0.5 - 2.0	---
UTS	0	---	---
Fty	0	---	---

The threshold fanning parameters Cth+ and Fth+ define the slope of the threshold value ( $\Delta K_{th}$ ) against R in the NASGRO equation for positive stress ratios. If the user selects the default (Cth) option for defining threshold slopes and then switches to the alternate (Fth) option, NASGRO determines appropriate Fth parameters from the Cth parameters. However, in v9.1 and earlier, if the user selected a Cth+ value below zero, the calculated value of Fth+ was below its minimum of zero. This caused NASGRO to change all three threshold parameters (DK1f, Fth+, and Fth-) to zero and made the user unable to translate the values back to Cth. In order to resolve this issue, the minimum value of Fth+ was decreased to -0.5 as of NASGRO v9.2.

To enter a one-dimensional table of da/dN- $\Delta K$  values for a single stress ratio, select the corresponding radio box choice and a grid will appear with two columns for da/dN and DeltaK. Right-clicking on the grid cells presents many useful options for convenient data entry. Similarly the 2-D data tables can be chosen and data entered for various R ratios.

#### 2.2.4.3 Entering the Environmental FCG Factor

In order to provide some flexibility in entering the fatigue crack growth properties, an additional factor that multiplies into the computed crack growth rate has been added in this version. The default value is set to unity. It is the users' responsibility to enter a suitable value. An example of usage of this factor may be to account for the environment in which crack

growth takes place. This factor is available for all material models except for the sustained-load crack growth in glass-like materials.

### 2.2.5 Entering the Load Spectrum

The largest unit of load repetition is a schedule. A schedule comprises of several blocks. The concept of the “load schedule” is used in NASGRO to provide more flexibility by allowing the user to repeat blocks and/or combine different blocks together. This is especially useful for analyses of parts that are subjected to both pre-flight testing and flight loads. In addition, the load schedule method provides a means for entering larger spectra.

Figure 49 shows an example of a load schedule and the associated terms. A load schedule is created by filling up to 99,999 blocks with different block cases. Up to 40 different block cases can be combined, ordered, and/or repeated within these available blocks. Each distinct block case can contain up to 2000 load steps when stored in the BLOCKS file, where a load step is defined as any number of cycles (up to 999,999,999.99) of stress alternating between two specified limits. Option to input long blocks (with unlimited number of steps) such as those occurring in aircraft applications is also available in NASGRO. In such a case, each block is stored in a separate file either in standard NASGRO format or in sequential form. In the example shown in Figure 49, blocks 1 through 4 of the load schedule contain block case 1, which is a single cycle. Block case 2, which is constructed of one load step that has 5 cycles, has been put in blocks 5 and 7. Finally, block 6 of the load schedule contains block case 3, a more complicated case that has 7 load steps.

To enter the fatigue load spectrum, click on the tab “Load Blocks” which displays all the necessary choices and text boxes to enter data. To define the block cases, first select the number of block cases that will be defined by right-clicking on the numbers shown in the slider box. You may choose up to 40 distinct block cases to be combined to form the load schedule. Then each block is defined using one of the five choices available. A check box allows choice of either equivalent flights or equivalent flight hours. Once selected, the same choice is applicable to all the blocks. The number of flights or flight hours each distinct block represents can be specified for each of the blocks. Just as the total cycles are shown in the output, the cumulative flights or flight hours are also computed and shown in the output.

### 2.2.5.1 Defining the Block Cases

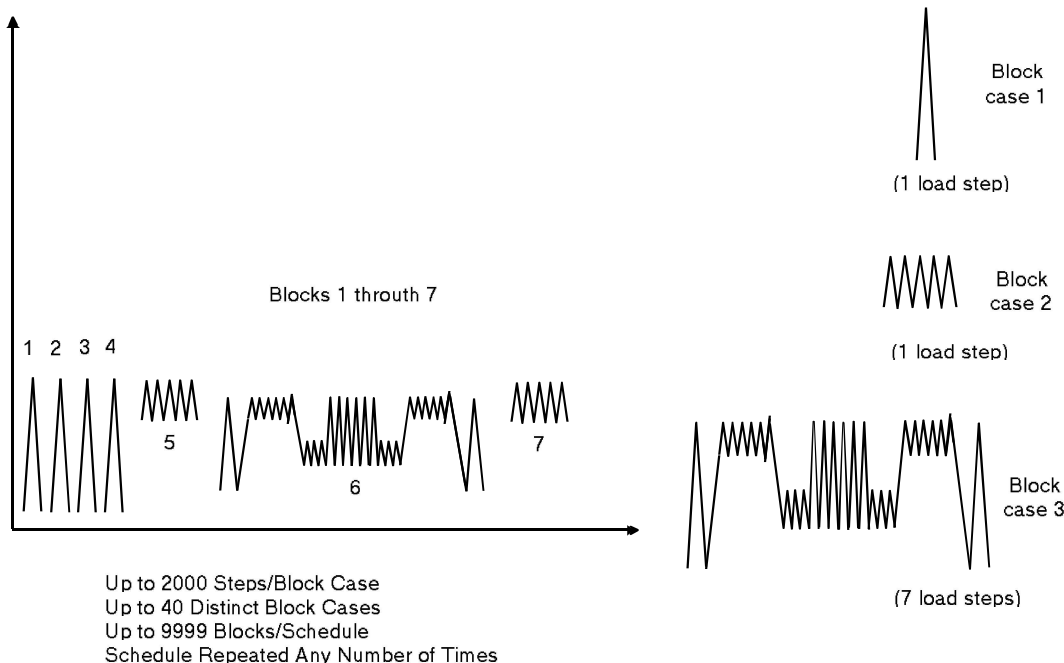


Figure 49 – Load schedule example

Using the radio box choice select one of the following:

- Use predefined block (BLOCKS database)
- Input cycles and stresses manually
- Select file(s) containing long block(s)
- Generate a standard long block
- Generate acceptance vibration block

To enter a block that has been saved in the file “BLOCKS”, choose the first option. The loading spectrum for payloads that experience stresses associated with the launch and landing of the Space Shuttle, named GSFC, is one of the stored blocks. It is shown in Table 11. The number of cycles at each stress level for the combined launch/ascent and landing/descent condition is tabulated in the column labeled “Total”. This spectrum was developed at the Goddard Space Flight Center (GSFC) and is reported in reference [36]. It is appropriate for analyzing:

- primary load-carrying payload structure in the Space Shuttle Orbiter payload bay
  - pay-loads with a fundamental (first mode) frequency below 50 Hz.
- Payloads that have a fundamental frequency above 50 Hz may be analyzed by applying the following multiplication factors to the *number of cycles* of the GSFC flight spectrum:

Table 11 – Launch and Landing Spectrum for STS Payloads

Load Step	Cycles/flight			Cyclic Stress (% limit value)	
Number	Launch	Landing	Total	Minimum	Maximum
1	1	1	2	-100	100
2	3	1	4	-90	90
3	5	3	8	-80	80
4	12	3	15	-70	70
5	46	3	49	-60	60
6	78	3	81	-50	50
7	165	13	178	-40	40
8	493	148	641	-30	30
9	2229	891	3120	-20	20
10	2132	1273	3405	-10	10
11	2920	2099	5019	-7	7
12	22272	6581	28853	-5	5
13	82954	8701	91655	-3	3

fundamental frequency	multiplication factor
0-50 Hz	1
50-100 Hz	2
100-200 Hz	4
200-300 Hz	6

The combined launch and landing spectrum has been saved as a block on file. Note that this is only a convenience for the analyst, and the actual requirements are to be obtained from relevant NASA documents or appropriate authority. NASGRO also includes an option to change the mean stress of block cases that have been saved on file. Below the grid showing the available blocks cases that have been stored previously in the BLOCKS file, the program presents a check box:

Change the block's mean stress by adding a constant value to  
the stress quantities at t1 and t2?

If one checks this box, text boxes to enter the constant values that need to be added to increase or decrease the mean stress of each of the stress quantities are displayed. Note that the value entered should have the same units as those quantities stored in the file.

The users can add their own spectra to the BLOCKS file by modifying it. Users should use the format of the existing blocks such as GSFC. The first eight characters of the first line are reserved for the name and the rest of the first line is for a descriptive title. The BLOCKS file is located in xxxxxxx/nasfla/progdata folder, where xxxxxxx is the path of the NASGRO installation on your computer. Special characters like tabs should not be added anywhere.

To enter a block case manually, select the second radio box and the program will present a grid to enter cycles and stress values. The grid has a check box in the first column to mark the

choice of checking for the Keac being exceeded, the second column is the number of cycles and the remaining columns are for appropriate stress quantities ( $S_0$ ,  $S_1$ ,  $S_2$ ,  $S_3$  and/or  $S_4$ ) at times (t1) and (t2) for that particular load step.

Remember that if you want to zero out one or more of the stresses (e.g. no tension), you will still be allowed to scale the stresses later (see section 2.2.4.3) and you can set scale factor to zero for the appropriate stress quantities.

Option 3 in the menu is meant to input long aircraft type of spectra (created by means of spectrum generation software, etc.). The essential feature of this option is that there is no limit to the size of the block (other than the disc space limit). When using this option, the following format options are available for reading the blocks from files.

### **1. Standard NASGRO Format** (same as in BLOCKS file).

Since all stress quantities are present in this format, only one file is required per block.

Line 1: A title line up to eighty characters.

Line 2 onwards: Each line should have nine numbers:

Cycles     $S_0(t_1)$      $S_0(t_2)$      $S_1(t_1)$      $S_1(t_2)$      $S_2(t_1)$      $S_2(t_2)$      $S_3(t_1)$      $S_3(t_2)$   
 (as many lines as the number of steps)

Example:

#### **Sample load spectrum - standard NASGRO format 1**

**1000 20.0 2.0 20.5 0.0 20.0 0.0 40.0 0.0**

**..... as many lines as needed**

**2. Peak-Valley Format :** There are two types of files that can be used with this format. The GUI will automatically detect which type it is. One file is needed for each stress quantity.

2(a). Northrop format (as furnished by SwRI)

The load values input in this format should be in integer form. The input values are internally divided by 100.

Line 1: A title line up to eighty characters.

Line 2: Flight no., Number of values in this flight (max.= 1000) , Load values (in free format)

Line 3 onwards: Continued load values (as many lines as needed)

Example:

#### **Sample load spectrum – peak valley format 2 (a)**

**1 102 1728 395 922 435 1216 395 1106 395 1261 339 798 395 1728 79**

**223 103 302 ..... continued until 102 values are entered**

2(b) General format (values as percentages)

The load values input in this format can be in integer or real number form. The input values are internally divided by 100 as in the above format.

Line 1: A title line up to eighty characters.

Line 2: Flight no., No of load values in this flight(max.=1000) ( in free format)

Line 3 onwards: Load values (in free format, i.e., any number of real values per line with as many lines as needed).

Example:

**Sample load spectrum – peak valley format 2 (b)**

```
1 10
10.5 11.9 6.2 12.1 15.2 18.2 30.2 11.0 23.0 11.2
```

Any number of flights can be input in one file.

### 3. Single Block <S(t1), S(t2), Cycles> Format

This is a common aircraft spectrum format that was originally provided by Boeing. The file is converted by the GUI internally to standard NASGRO format. This format can have up to four title lines followed by any number of lines each with (max., min., cycles) or (min, max, cycles) values. It is assumed that all stress quantities will use the same (t1), (t2) values within each load step. The (t1), (t2) refer to the two time instants in a fatigue cycle. Note that each line is interpreted as a step in NASGRO.

Line 1: Title line up to eighty characters

Line 2: Optional title line or <Max., Min., Cycles>

Line 3: Optional title line or <Max., Min., Cycles>

Line 4: Optional title line or <Max., Min., Cycles>

Line 5 onwards: <Max., Min., Cycles>

Example:

**Sample load spectrum – <max, min, cycles> format 3**

**Title line 2 - optional**

**Title line 3 - optional**

**Title line 4 - optional**

```
11.9 6.2 1000
```

```
22.0 11.0 2000
```

..... as many lines as desired

### 4. Multi-Block <S(t1), S(t2), Cycles> Format

This is a commonly used flight-by-flight (or block-by-block) format where the steps are grouped by flights (or blocks), all within the same file. The flights (blocks) are sequentially numbered and do not generally have the same number of steps. The first line should be a title line. This is followed by a line defining the first block and its number of steps, followed by each step in the block on an individual line in the order <S(t1), S(t2),

Cycles>. The (t1) and (t2) refer to the two time instants in the fatigue cycle and can be either max-min or min-max with cycles being one or greater.

```

Title line
<Block number, number of steps in block>
<S(t1), S(t2), cycles>
<S(t1), S(t2), cycles>
as many lines as there are steps in the 1st block
.
.
<Block number, number of steps in block>
<S(t1), S(t2), cycles>
<S(t1), S(t2), cycles>
as many lines as there are steps in the 2nd block
.
.
etc. (repeated for each block)

```

## 5. Time-Mean-Range Format

This format allows the user to specify a frequency (cycles/sec) that multiplies a time (hours) present in the file to compute cycles. Stresses are provided in terms of the mean stress and range for each time interval. One file is needed for each stress quantity. The stresses from the different files, along with the calculated number of cycles, are consolidated and written to a single long block file in NASGRO format. This file is named "tmr0.lb".

The frequency is input via a GUI box and the Time-Mean-Range file format is as follows:

```

column 1 - ignored
column 2 - hours
column 3 - ignored
column 4 - ignored
column 5 - ignored
column 6 - mean stress
column 7 - stress amplitude
column 8, etc. - ignored

```

The number of cycles is obtained by multiplying column 2 by 3600 and the frequency. Smax is computed by adding column 7 to column 6. Smin is computed by subtracting column 7 from column 6. All other columns are ignored.

In the case of format choice 2, Peak-Valley format, each consecutive pair of loads is interpreted as a single cycle and the crack growth proceeds as a cycle-by-cycle analysis. Also, as indicated above, the applied load spectra for each stress quantity (tension, bending, pin load etc.,) can be different. The user will be prompted to enter as many file names as the

number of stress quantities for the crack case being analyzed. These files are consolidated into a new file named xxx.NAS that will be created where xxx is the first portion (up to eight characters) in the name of the first block file. This file is written in the standard NASGRO format for future use. The scale factors can, of course, be different for different stress quantities.

The fifth choice, Time-Mean-Range format, is an option to generate spectra commonly used in the aircraft industry. Currently there are three spectra available: TWIST, MINI-TWIST, and FALSTAFF. The generated spectra are automatically stored in the *NASGRO* format in the files *FULTWIST*, *MINTWIST*, and *FALSTAFF*, respectively, but the file size can be quite large. The spectrum peak stress is automatically scaled to a value of 100; for the TWIST spectra this gives a mean stress of 38.46. This can be adjusted to the actual requirements by means of the scale factor, which is specified in later input. Finally, the TWIST spectra also have an option to clip cycles at values relative to the mean stress.

As the final choice, *NASGRO* provides spectrum entry to include automated block generation from vibration test data. It should be noted that each block case should contain only one vibration test type. The following choices will appear:

- Narrow Band Sine Sweep Test Spectrum
- Wide Band Sine Sweep Test Spectrum
- Sine Dwell Test Spectrum
- Random Vibration/Acoustic Test Spectrum.

When generating a block case for a vibration test block, the program will first prompt for the data needed to calculate the number of equivalent cycles, and then will prompt for the stress quantities appropriate for the current crack model. Information regarding how the number of equivalent cycles for each of these vibration test types is calculated may be found in Appendix H. If you choose option 1, you are prompted for the sine sweep rate, the amplification factor, the resonant frequency, and the notch factor. Also, you must choose whether to apply an up sweep only or both up and down sweeps. If option 2 is selected, the program prompts for the sine sweep rate, the two frequencies that define the wide band, and whether to apply an up sweep only or both up and down sweeps. For option 3, the sine dwell test, you are only asked for the time duration and the frequency of the test. Finally, option 4 is used for either random vibration or acoustic vibration tests, since the analysis method is the same. If both tests are performed, this option must be chosen twice so that one block case will be defined for the random vibration test and one block case will be defined for the acoustic vibration test. When selecting this option, you must enter the time duration of the test and the resonant frequency. After both the vibration test information and the stresses have been entered, the block menu will reappear.

### **2.2.5.2 Setting the K<sub>eac</sub> Check**

For some crack growth analyses, it will be necessary to enter the appropriate value for the critical stress intensity for environmental crack growth, K<sub>eac</sub>. The purpose of this input is to ensure that K<sub>max</sub> does not exceed K<sub>eac</sub> for material and environmental combinations that could

cause sustained stress or environmentally-assisted crack propagation. This is applicable to pressure vessels or other metallic components that are exposed to propellant fluids, gaseous hydrogen, high temperature air, or other severe fluid-material combinations. Since many parts are exposed to environments that have low  $K_{eac}$  values for only a portion of the entire spectrum, the  $K_{eac}$  check is designated at the end of the input of each block type, and  $K_{max} < K_{eac}$  is only checked for the load steps that you specify. If you want to set the  $K_{eac}$  check, check the box in the first column. Whenever the  $K_{eac}$  check is selected, the appropriate  $K_{eac}$  value needs to be entered also. In the case of long blocks, since the number of steps are too many, this check can be selected for the entire block but not for individual steps.

A materials file for  $K_{eac}$  data has not been developed because  $K_{eac}$  is often variable with temperature and environment. Table 12 lists  $K_{eac}$  data for several material-environment conditions which were obtained from experimental programs associated with the development of the Apollo and Space Shuttle vehicles, and that may be useful in the analysis of other space flight hardware. The main assumption in using  $K_{eac}$  is that the fatigue crack growth rate below  $K_{eac}$  is the same as it is in laboratory air. This is not always the case, but has been considered to be acceptable for the material/environment combinations listed in Table 12, taken from Reference [49].

Table 12 –  $K_{eac}$  Values for Several Metals

Alloy	Environment	Temp		$K_{eac}$	
		°F	°C	ksi-in <sup>1/2</sup>	MPa-mm <sup>1/2</sup>
Ti-6Al-4V (STA, forg.) (base metal, weld, HAZ)	Nitrogen tetroxide (N <sub>2</sub> O <sub>4</sub> )	75	(24)	40	(1390)
	"	100	(37)	36	(1251)
	"	125	(52)	31	(1077)
	"	150	(66)	25	(869)
	Monomethyl hydrazine (MMH)	75	(24)	40	(1390)
	"	100	(37)	38	(1320)
	"	125	(52)	34	(1181)
	"	150	(66)	30	(1042)
	Hydrazine	75	(24)	40	(1390)
	"	100	(37)	39	(1355)
	"	125	(52)	38	(1320)
	"	150	(66)	37	(1286)
	Aerozine-50 (A50)	75	(24)	40	(1390)
	"	100	(37)	38	(1320)
Distilled water (DW)	Distilled water (DW)	75	(24)	42	(1459)
	"	100	(37)	37	(1286)
	Isopropyl alcohol	75	(24)	40	(1390)
	Trichlorotrifluoroethane	75	(24)	30	(1042)
	"	100	(37)	27	(938)
Ti-6Al-4V (STA, forg.) (weldline)	Trichlorotrifluoroethane	75	(24)	22	(764)
	"	100	(37)	19	(660)
Inconel 718 (STA) (base metal and weldline)	Air	850	(454)	50	(1737)
	"	1000	(538)	13	(452)
	"	1250	(677)	10	(348)
	500-5000 psi (3.45-34.5 MPa)	-100	(-73)	24	(834)
	Gaseous Hydrogen (GH2)	75	(24)	20	(695)
A286 steel (STA)	Gaseous Hydrogen (GH2)	75	(24)	85	(2954)
	Air	1000	(538)	25	(869)
Inconel 706 (STA)	Air	1200	(649)	10	(348)

### 2.2.5.3 Scaling the Stresses

For each of the block cases, the boxes for the scale factors need to be filled. As many scale factors as the number of stress quantities will be asked. When the crack case includes more than one stress quantity, you will need to enter all of the necessary scaling factors. At least one of the scale factors has to be nonzero. If you do not want to apply any of the stress quantities (e.g., there is no bending), set the corresponding scale factor to zero. After all the scaling factors for block case 1 have been set, the program continues by giving an option to set the limit stresses (see section 2.2.5.4) for the same block case before allowing you to input data for the next block case. This process should be continued until data for each of the block cases have been entered.

### 2.2.5.4 Setting the Limit Stress Checks

For some crack growth analyses, a check is required to ensure that the residual strength of the structure is not exceeded by a seldom-occurring, severe load, such as a limit load, which is greater than the maximum load in the fatigue spectrum. This load corresponds to a stress called the “limit stress” in NASGRO. Since this load may occur at any time within a block, failure due to the limit stress is checked at every increment of crack growth. As described in section 2.1.5, failure is assumed to occur if the stress intensity factor corresponding to the limit stress exceeds  $K_c$  for the specified material or if the net-section stress exceeds the flow stress.

After entering the scaling factors for each of the block cases, you will able to check the following box:

Check throughout this block for crack instability and net-section failure at limit stresses?

If you check the box, you will be asked for the limit stresses for each of the stress quantities for the crack case (or scale factors for limit stresses, if crack plane stresses are specified). Limit stresses will be used only to check against failure criteria, but not for crack growth.

There is also an additional option to completely bypass the net-section stress failure criterion. If this box is checked, only the crack instability criterion will be operative and no warning or failure message pertaining to net-section stress will be used. This option applies to all the blocks.

### 2.2.5.5 Combining the Block Cases to Form a Schedule

Once the distinct blocks are defined and their respective scale factors and limit stresses have been entered, the user inputs the load schedule in the “Build Schedule” tab. The first column in the grid is used for the block case number and the second column for the number of repetitions. By right-clicking on the first column, several user-friendly options are presented including filling the grid from a file. The file containing the block-mix has the following formats.

The input file contents for a simple case are shown below:

*Testing 1 - file for format type 1.*

```
1 1
2 1
3 1
4 3
```

In each line, the first number refers to the block case number and the second number is the number of times that block should be repeated in one schedule.

If format type 2 is chosen, the block repetition is done by giving the actual block numbers as they occur. The same example as above will now look like:

*Testing 2 - file for format type 2*

```
6
1 2 3 4 4 4
```

The first number is the total number of blocks and the remaining are block case numbers in the same sequence as they occur in the schedule. This format is useful when the file is automatically generated.

At this point, entry of the load schedule has been completed. This schedule can be saved using the button “Add schedule to frequently-used list” and can be retrieved later using the “Show list of frequently-used schedules” button on the “Load Blocks” tab. Since the block definition is dependent on the number of stress quantities, each such saved schedule is available to only the specific crack model.

## 2.2.6 Spectrum Generation and Editing

Several features have been incorporated in NASGRO to enable creation and editing of load spectrum files used in crack growth analyses:

- Spectrum Generation
- Clipping (Spectrum Editing)
- Truncation (Spectrum Editing)
- Randomization (Spectrum Editing)

Additionally, the cycle counting options have been moved to the spectrum editing dialog window.

These new features are covered in references [37, 38].

The definitions of some of the terms widely used in this section follow:

Time series of points – a sequence of loading points, which may contain sequentially increasing and/or sequentially decreasing loading points.

Filter level – a range threshold used to eliminate undesired peaks and valleys in spectrum generation routine

Spectrum – a sequence of loading points in peak-valley formats

Peak-Valley format – each point defined in the sequence coincides with a reversal in loading. Thus each point is a local minimum or local maximum.

Clipping – limiting cycles in the spectrum to a maximum load value and/or a minimum load value. For cycles exceeding the prescribed maximum or minimum value, the cycle is clipped to coincide with the prescribed values. Note: cycles will be removed if both points in the cycle are outside the clipping level.

Truncation – removing cycles in the spectrum with loading ranges ( $\Delta S = \text{abs}(S(t2) - S(t1))$ ) less than a prescribed loading range values.

#### 2.2.6.1 Spectrum Generation from Time Series Data

The spectrum file generator allows the user to convert load data, given as a time series of points, into a standard NASGRO long block spectrum file suitable for use in fatigue crack growth calculations. The spectrum file generator identifies turning points (points where the slope changes sign in the time series of points) and removes both intermediate points (non-turning points) and points associated with load pair ranges below a user defined threshold (filter level).

The spectrum generation dialog window is accessed through the Tools menu on the NASFLA GUI by selecting *Spectrum File Generator*. The format for the time series of points input is

Line 1: Title (up to 80 characters)

Line 2: Load value

... continue to end of load values.

The user selects the input file by choosing the *Select Input* button on the *Spectrum File Generator* dialog box (Figure 50). The output file name is input by choosing the *Select Output* button on this dialog box. The user may also prescribe a filter level to remove data from the spectrum with a range below the filter level threshold (Figure 51). The solid circles in this figure represent accepted peaks and valleys and the unfilled circles represent rejected points. The NASGRO long block spectrum file is created by choosing the *Generate File* button on the dialog box (Figure 50).

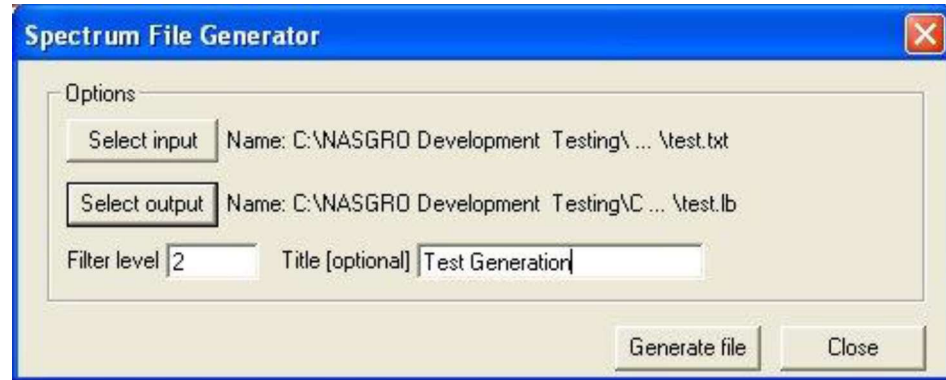


Figure 50: Spectrum File Generator dialog box

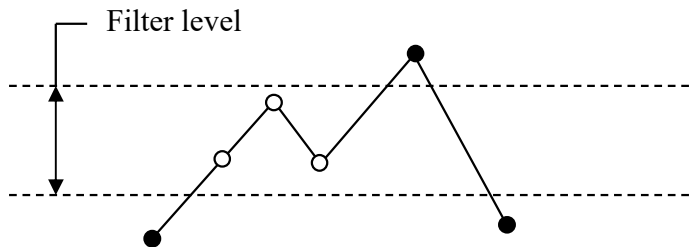


Figure 51: Time series of points evaluated using filter level threshold.

The resulting long block output is strictly the turning points identified by the spectrum generation algorithm. No spectrum counting is performed during the spectrum generation process.

### 2.2.6.2 Long Block Spectrum Editing

The spectrum editing functions are accessed by selecting the *Edit Spectrum* button located within the *Load Blocks* tab (Figure 52). The *Edit Spectrum* button is only displayed when the *Select file(s) containing long block(s)* radio button is selected.

It is important to note that a non-zero scale factor must be input for spectrum editing to function.

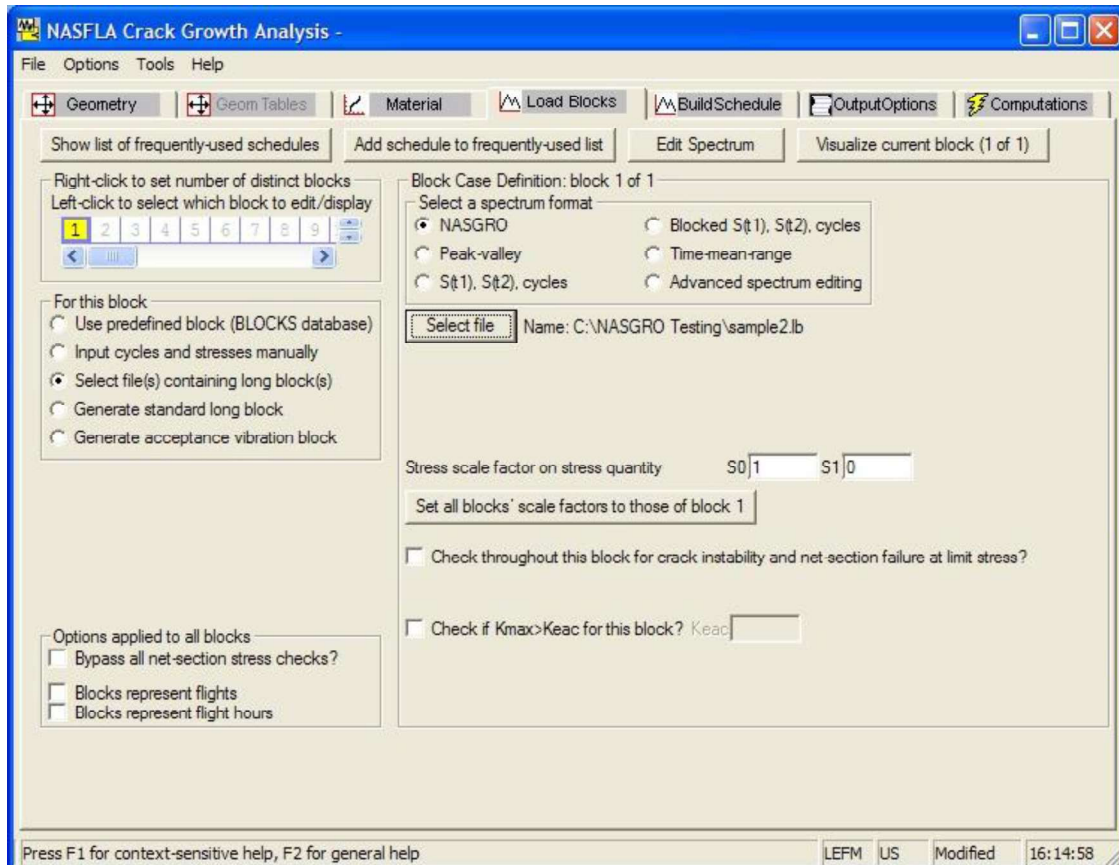


Figure 52 - Screen shot of Load Blocks tab with Edit Spectrum button

Current limitations on spectrum editing are:

- Spectrum must be defined as single-cycle steps.
- In the case of crack geometries with multiple loading options, spectrum editing is performed only on the S0 load. The edited file output is written with S0 data in all stress quantity columns.

Since spectrum editing is dependent on the order of operation, the spectrum editing function allows one operation to be performed for each spectrum edit requested.

Clipping contains several options to enable the user to perform operations on the first point in the cycle, S(t1), or second point in the cycle, S(t2), independently. Clipping can be

performed based on a percentage of the highest peak and/or lowest valley in the spectrum, or a user specified threshold for high peak and/or lowest valley. Additionally, a user-specified limit on the number of cycles clipped is available and can be independently defined for  $S(t_1)$  and  $S(t_2)$ . In conjunction with a user-specified limit, the minimum and maximum load values can be ordered (lowest to highest for minimum load values and highest to lowest for maximum load values) prior to clipping. The load point ordering option enables clipping to be performed in decreasing order of the absolute value of distance from prescribed load point to the clipping bounds.

If clipping is performed based on percentages, NASGRO searches the spectrum file to find the highest peak and lowest valley. The maximum clipping level is then defined as the user-defined maximum percentage multiplied by the highest peak. In the case of user-defined values, the maximum clipping level and the minimum clipping level are directly input by the user. The maximum value in each ordered cycle pair is then evaluated against the prescribed maximum clipping level. Similarly, the minimum clipping level is defined as the user-defined minimum percentage multiplied by the lowest valley. The minimum value in the ordered cycle pair is then evaluated against the prescribed minimum clipping level. If both points in a cycle are above the maximum or below the minimum clipping level, that cycle will be removed from the edited spectrum (Figure 53).

Truncation can be performed based on the percentage of the largest stress range in the spectrum or a user specified threshold for minimum stress range. Additionally, a user-specified limit on the number of cycles truncated is available to limit the maximum number of cycles removed from the spectrum. In conjunction with a user-specified limit, the cycles can be ordered from smallest stress range to largest stress range prior to truncation. The cycle ordering option enables the smallest stress range cycles to be truncated before the larger stress range cycles identified by the truncation algorithm. If truncation is performed based on percentages, NASGRO searches the spectrum file to find the cycle with the largest stress range. The truncation value is then calculated as the user-defined percentage multiplied by the largest stress range in the spectrum. Cycles with stress ranges less than the threshold value are removed, up to a user defined limit on truncated cycles, and the truncated spectrum is output with remaining cycles in their original order.

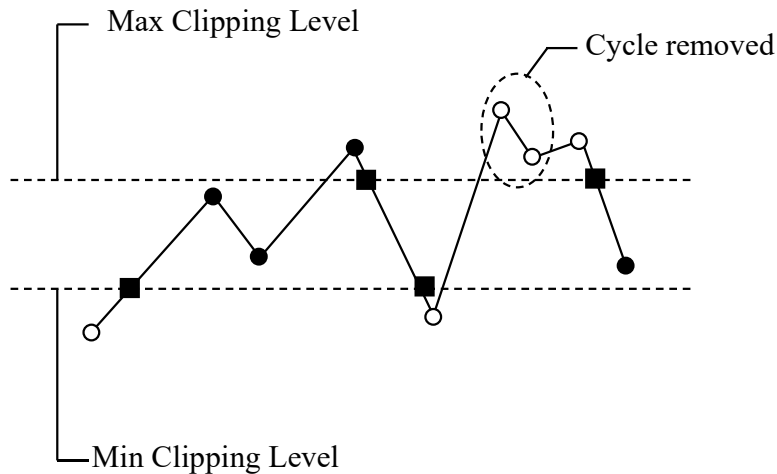


Figure 53 – Schematic of cycle removal in clipping algorithm.

The solid circles in Figure 53 represent original peak-valley data which remain unmodified by the clipping algorithm, the unfilled circles represent original peak-valley data clipped or removed by the clipping algorithm, and the solid squares represent the modified values for the clipped spectrum.

Spectrum ordering has been added to the available spectrum editing methods. Spectrum ordering can be performed in ascending or descending order on  $S(t_1)$ ,  $S(t_2)$ , or stress range ( $\text{abs}(S(t_2)-S(t_1))$ ). In the current implementation, ordering is only performed on the  $S_0$  values. A screen shot of the spectrum file editor dialog box for ordering is in Figure 54.

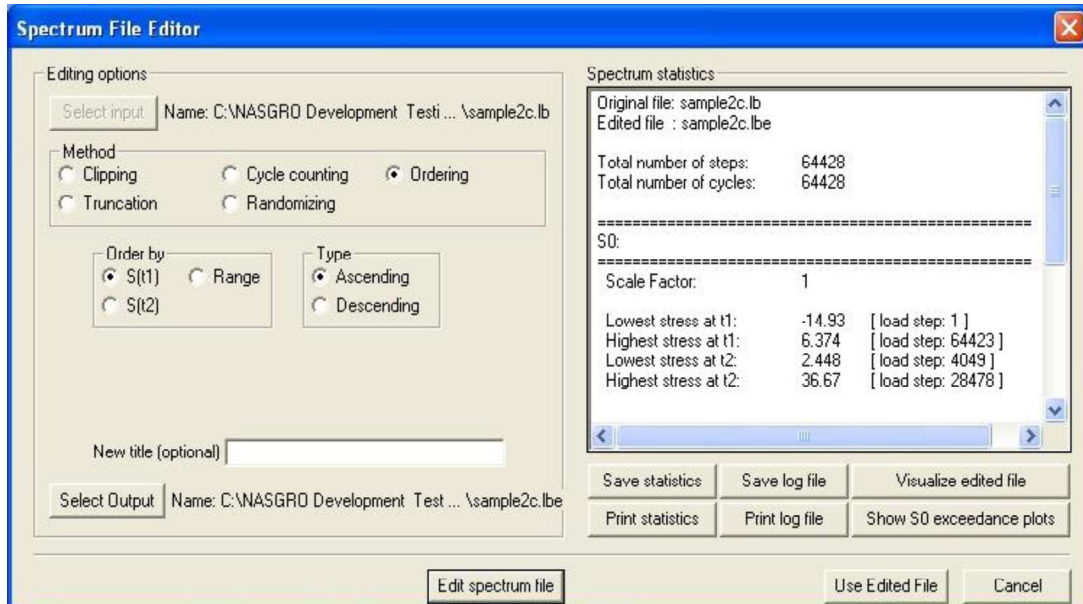


Figure 54 – Spectrum File Editor dialog window for ordering options

Randomization can be performed to create a new spectrum file by rearranging the cycles defined in the original spectrum in a new random order. No cycles are added or removed during the randomization process.

Cycle counting (pairing using rainflow or range-pair methods) is also available through the spectrum editing dialogue window. Several different cycle counting options are available, as shown in Figure 55 (note that these options were relabeled and some were revised in NASGRO v9.1).

The GUI distinguishes between methods intended for repeating or non-repeating histories. The “ASTM rainflow” method for repeating histories reproduces exactly the method described in ASTM Standard Practice E1049. This method was labeled as “Downing Algorithm I” in earlier versions of NASGRO. This method also gives the same result as the ASTM range-pair method for repeating histories. The “Modified ASTM rainflow” method for repeating histories uses exactly the same pairing algorithm as “ASTM rainflow” for repeating histories, but rearranges the paired cycles to maintain the original order of the maximum time points (since this order may be significant if load interaction models are used).

The rainflow and range-pair methods for non-repeating histories are similar to the corresponding methods described in ASTM E1049, but they are not an exact match because the ASTM methods allow half-cycles to be retained and NASGRO does not. The examples in ASTM E1049 can also be confusing when compared to NASGRO because the spectrum in the ASTM examples starts with an odd number of time points, whereas NASGRO spectra always have an even number of time points. The modified rainflow and modified range-pair methods for non-repeating histories rearrange the paired cycles to maintain the original order of the maximum time points.

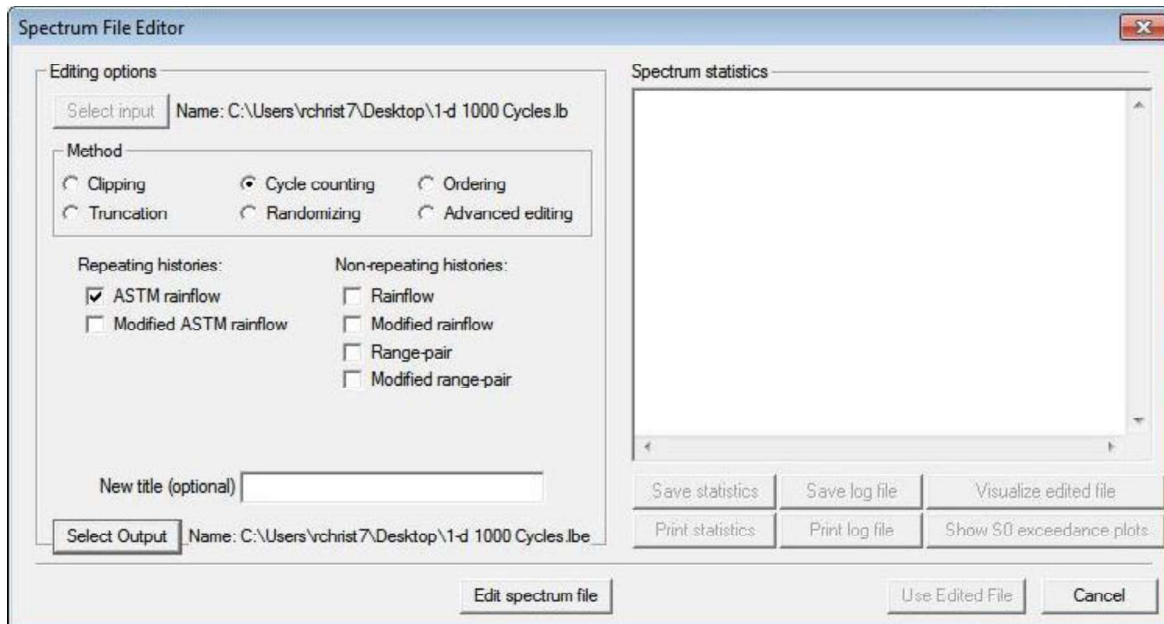


Figure 55 – Spectrum File Editor dialog window for cycle counting options

Since the cycle counting operation can sometimes result in spectra with sequentially increasing and/or sequentially decreasing points (i.e., some points are not turning points). Therefore, the cycle-counted spectrum is checked for these non-turning points and they are removed if found. This operation may result in a reduction in the total number of cycles compared to the original spectrum.

Note that only blocks with single-cycle steps can be cycle counted. The stress spectra can be in either min-max or max-min order, as long as each block is internally consistent (all min-max or all max-min).

### 2.2.6.3 Examples of Spectrum Clipping and Truncation

Prior to performing any spectrum edits, a spectrum analysis of the original spectrum is performed to view some important spectrum characteristics: number of cycles, largest peak, lowest valley, minimum stress range and maximum stress range. The NASGRO output of the spectrum analysis for sample2.lb is shown in Figure 56. From output shown in Figure 56, a table of some important spectrum characteristics is summarized in Table 13. The results shown in Table 13 will be compared with spectrum edits using clipping and truncation.

Table 13 - Summary of spectrum characteristics for sample2.lb

Spectrum File	sample2c.lb
Number of Cycles	64427
Largest Peak	36.67
Lowest Valley	-14.93
Maximum Stress Range	36.07
Minimum Stress Range	0.004

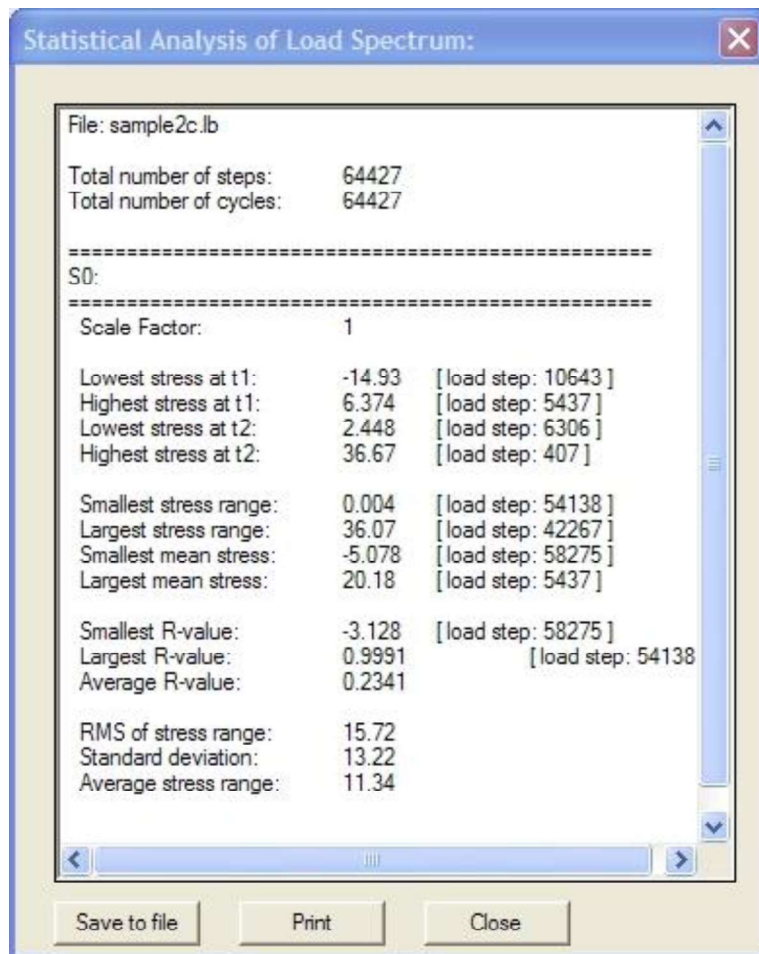


Figure 56 - Spectrum analysis for sample2c.lb spectrum file

### 2.2.6.3.1 Clipping

In this example, clipping is performed on both the minimum and maximum points in the cycle pair. The clipping values are prescribed as 30 for the maximum value and -10 for the minimum value. The first example will use the *By value* option to clip. A screen shot of the clipping *By value* example is shown in Figure 57. In Figure 57, the *Clipping* radio button is selected under *Edit spectrum file*. The *By value* option is selected and the prescribed minimum and maximum values are input by the user. For this example, there are no limits on the number of cycles clipped. No limits on the number of cycles clipped can be input either by placing -1 in the input boxes for *Limits on number of cycles clipped* or by leaving the input boxes empty. In this example, the -1 input option was used for both the Min and Max values. At this point, the *Edit spectrum file* button is pressed to perform the clipping. Upon completion, spectrum statistics are displayed for the edited file and the file is written to the same directory as the original file with an *.lbe* extension. In this example, the edited file was output as *sample2.lbe*. Reviewing the spectrum statistics for the clipping in Figure 57, the lowest valley is now -10 and the highest peak is 30.

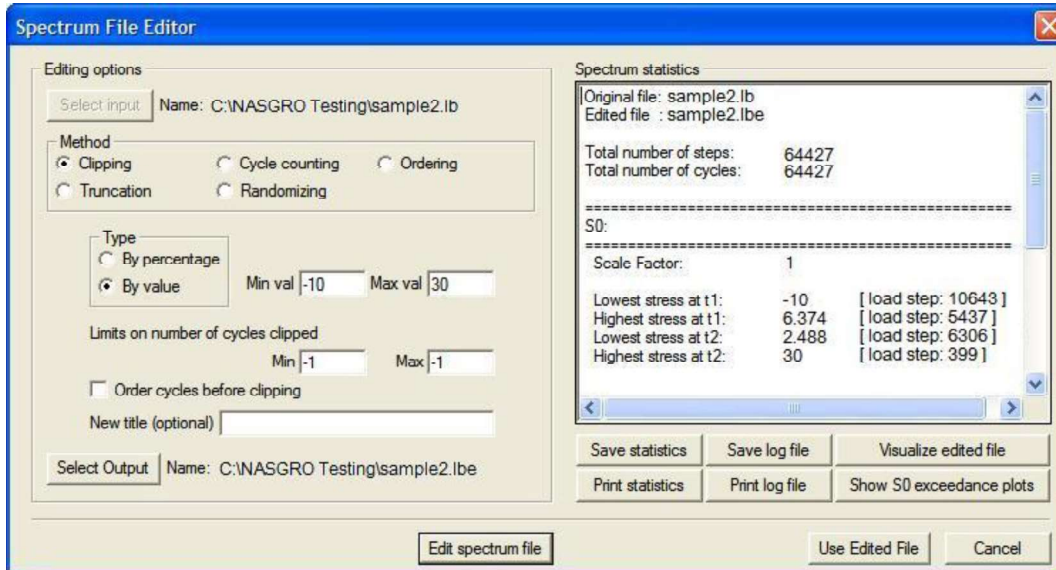


Figure 57 - Screen shot of clipping by value with spectrum statistics for edited file.

The exceedance diagrams are also available to provide a visual comparison of the edited spectrum versus the original spectrum by selecting the *Show exceedance plots* button. The exceedance plots for this example are shown in Figure 58. The original spectrum is shown in red and the edited spectrum is shown in blue on the exceedance diagrams. The plot in the upper left hand corner (sample2.lb: S0 at t1) shows the exceedance plot for the minimum value of the cycle pairs in both spectrums. The minimum clipping is visually evident with the minimum value of the edited spectrum displayed as -10. The plot in the upper right hand corner (sample2.lb: S0 at t2) shows the exceedance plot for the maximum value of the cycle pairs in both spectrums. The maximum clipping is visually evident with the maximum value of the edited spectrum displayed as 30. As noted earlier, the clipping also has an effect on the range and mean values as compared to the original spectrum.

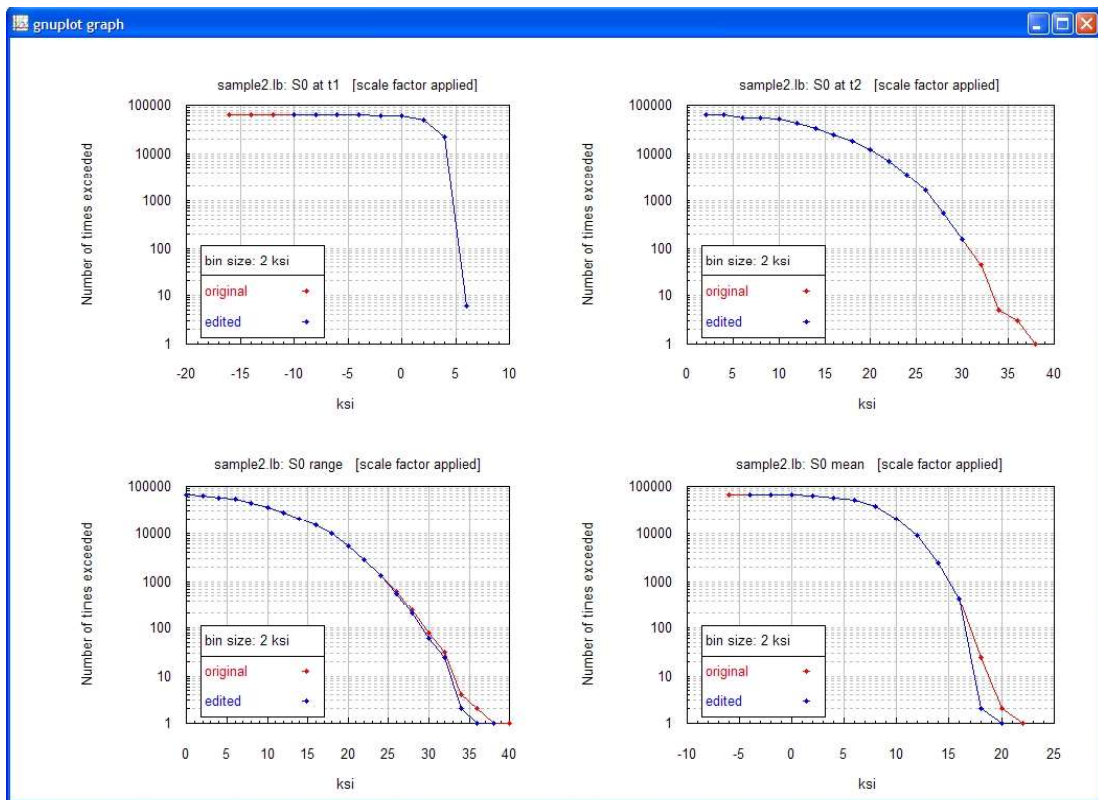


Figure 58 – Exceedance plots for clipping by value example (sample2c.lb)

The same analysis can also be carried out using clipping *By percentage*. Reviewing Table 13, the largest peak is 36.67 and the lowest valley is  $-14.93$ . Using the same clipping values of 30 for the maximum and  $-10$  for the minimum, we can define the percentages as 81.811% ( $30./36.67$ ) for the maximum and 66.99% ( $-10./-14.97$ ) for the minimum. The *Edit spectrum* screen with spectrum statistics is shown in Figure 59 and the exceedance plot is shown in Figure 60. As expected, the results for the clipping *By percentage* are the same as the results for clipping *By value*.

## 2.2 Details of Crack Growth Analysis

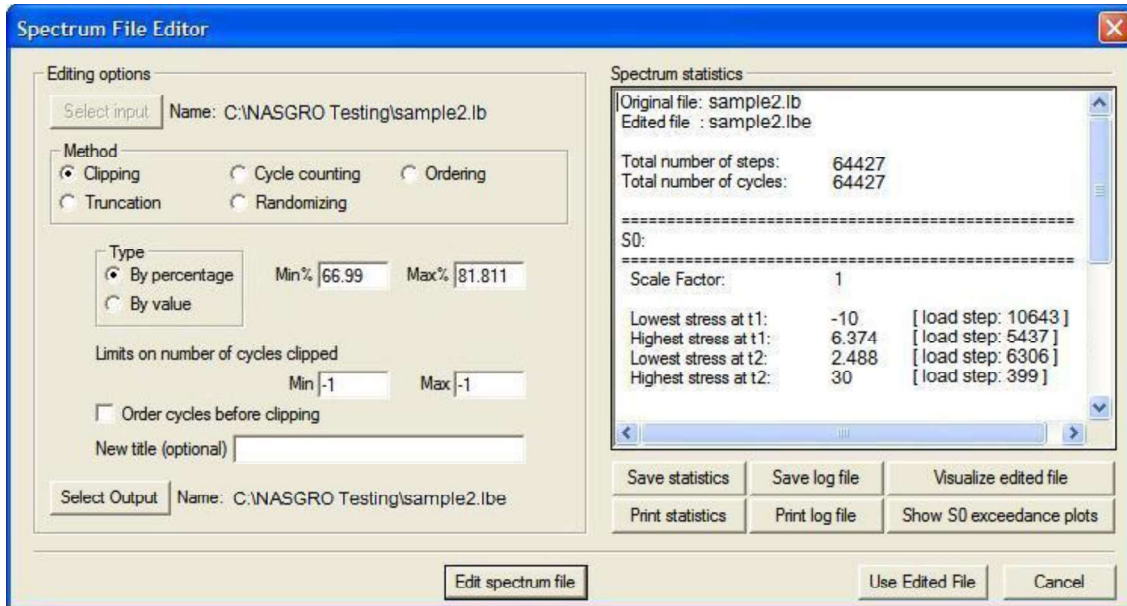


Figure 59 – Screen shot of clipping by percentage with spectrum statistics for edited file.

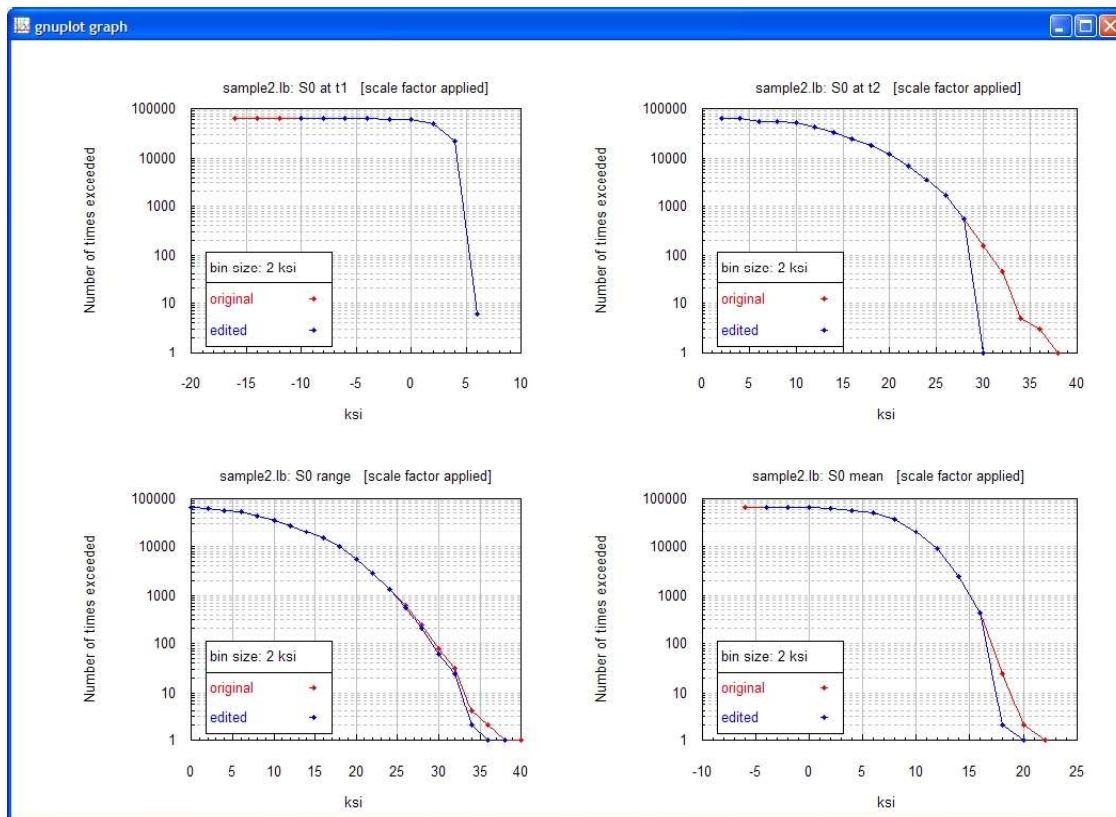


Figure 60 – Exceedance plots for clipping by percentage example (sample2c.lb)

### 2.2.6.3.2 Truncation

In the example, truncation by value is used to remove cycles with a stress range less than 5 in the spectrum file sample2c.lb. Reviewing the spectrum characteristics provided in Table 13, the maximum stress range is 36.07, the minimum stress range is 0.004, and the spectrum contains 64427 cycles. For this example, there are no limits on the number of cycles truncated. No limits on the number of cycles clipped can be input either by placing -1 in the input boxes for Limits on number of cycles clipped or by leaving the input boxes empty. In this example, a value of -1 is input in the input box for *Limit on number of cycles truncated*. A screen shot for the truncate *By value* example with the edited spectrum statistics is shown in Figure 61.

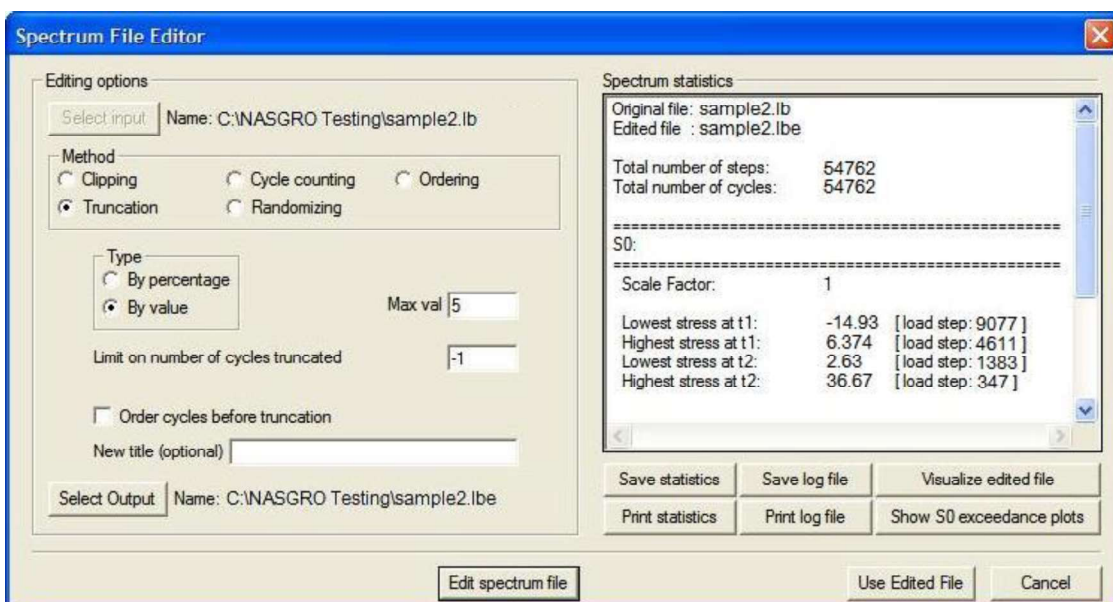


Figure 61 – Screen shot of truncation by value with spectrum statistics for edited file.

The exceedance plot for the truncation *By value* example is shown in Figure 62. The plot in the lower left hand corner (sample2.lb: S0 range) shows that the truncation removed a large number of cycles (~11000) from the original spectrum. In the exceedance plots, bins of 2 units are used to count the number of exceedances and the results for each bin are plotted at the lowest point for each bin. For this truncation example, the lowest value of the bin containing the spectrum data is 4. Therefore, the exceedance count shown at 4 includes stress values from 4 to 6. The correct truncation level is further validated in the spectrum statistics, which shows the smallest stress range of 5.044, which is larger than the user-defined value of 5.

## 2.2 Details of Crack Growth Analysis

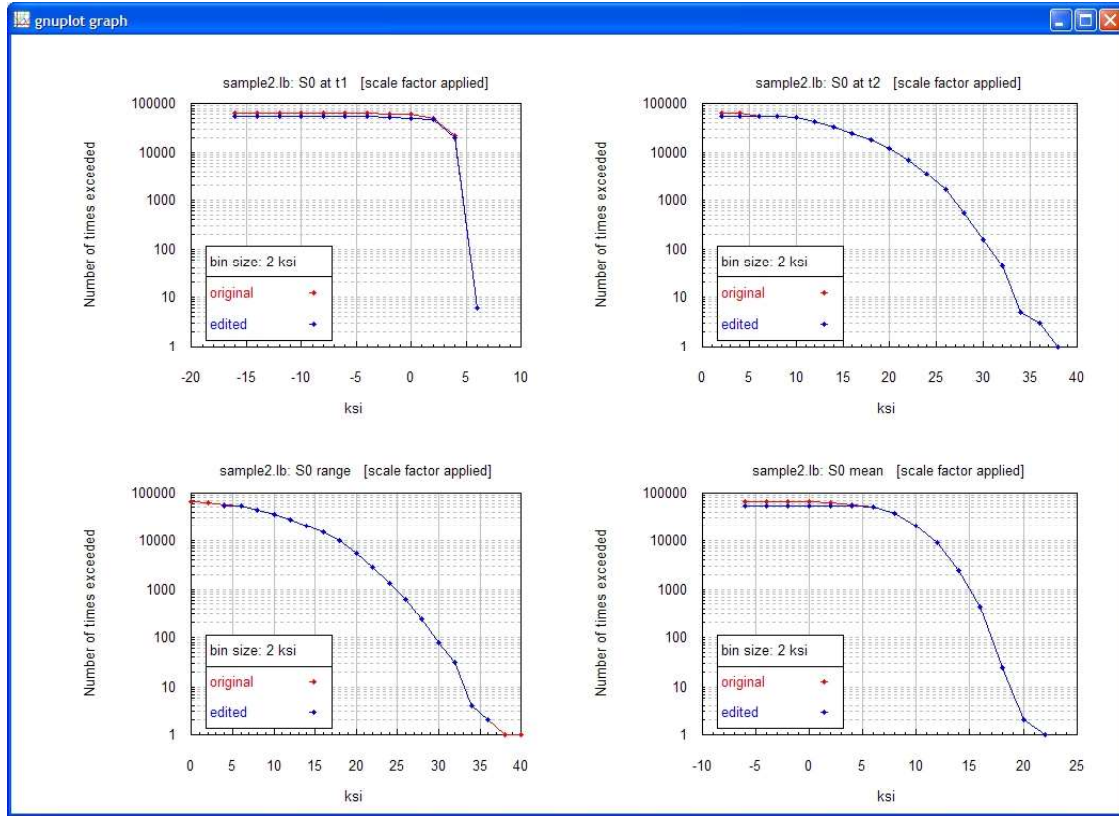


Figure 62 – Exceedance plots for truncation by value example (sample2c.lb)

### 2.2.7 Advanced Spectrum Editing

The advanced spectrum editing feature is used to identify and remove cycles (in a spectrum) that contribute negligible damage during a fatigue crack growth analysis. The technical details of the advanced spectrum editing feature are provided in Appendix S. This section discusses how to perform an analysis using the advanced spectrum editing algorithm in the NASFLA GUI.

The advanced spectrum editing method uses a special spectrum format labeled *Advanced spectrum editing* on the *Load Blocks* tab when *Select file(s) containing long block(s)* option is chosen. The format details are discussed in Section 2.2.5.1 and the default file extension is .lbd. Currently, the advanced spectrum editing method can only be used in conjunction with Strip Yield crack growth analyses. Also, the crack case can currently only be loaded with the S0 stress quantity; all other stress quantities (S1 - S3) are assumed to be 0. Finally, the spectrum must be defined with only 1 block. If multiple blocks exist, the blocks must be merged into one block prior to analysis. After the analysis is completed, a new NASGRO long block file is created, in which the negligible damage cycles have been removed. This process is divided into two parts: (1) creating the advanced spectrum editing format from a standard NASGRO long block file and (2) performing an advanced spectrum editing analysis.

### 2.2.7.1 Conversion of NASGRO Long Block Spectrum to Advanced Editing Format

The GUI includes a file conversion utility to convert the S0 components of a standard NASGRO long block file into the advanced spectrum editing format. The utility is located in the cycle counting section of the spectrum editing dialog box. The spectrum editing dialog box can be accessed by selecting the *Edit Spectrum* button after choosing the *Select file(s) containing long block(s)* option and the *NASGRO* spectrum format on the *Load Blocks* tab (Figure 63) and setting the S0 scale factor to a non-zero value.

Once the *Edit Spectrum* button is depressed, the spectrum editing dialog window is displayed. The advanced spectrum editing utility is located in the cycle counting portion of the spectrum editing window. Figure 64 shows a portion of the spectrum editing window with the *Advanced spectrum editing* option selected under cycle counting

The output file name is selected by depressing the “Select Output” button on the spectrum editing window (Figure 64). After selection, a file selection dialog box is displayed with the file name pre-seeded using the original file name and the file extension pre-seeded with the default .lbd value (Figure 65). The NASGRO file 1-d 1000 Cycles.lbd is selected as the input file.

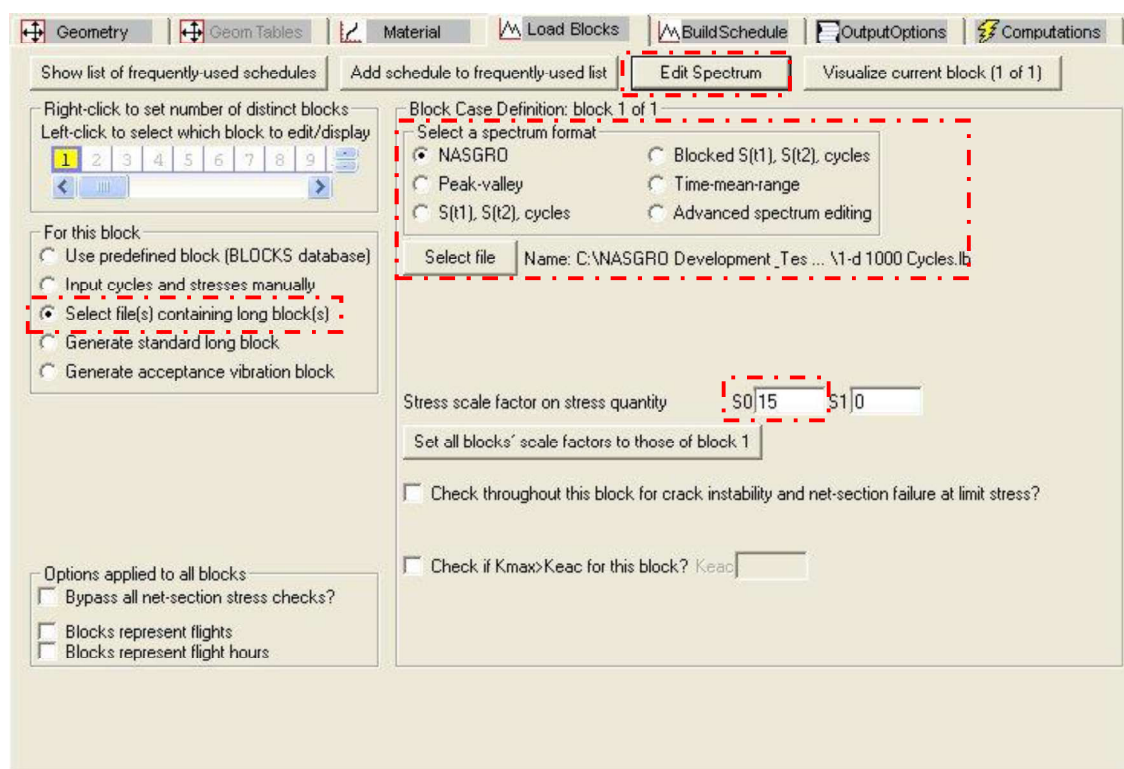


Figure 63 – Screen shot of *Load Blocks* tab with *Edit Spectrum* button

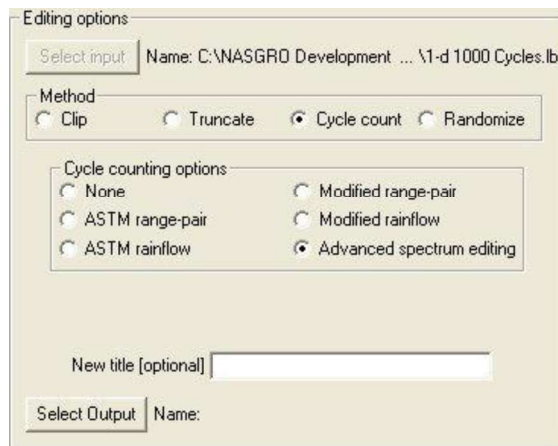


Figure 64 – Screen shot (portion) of *Advanced spectrum editing* under *Cycle counting options*

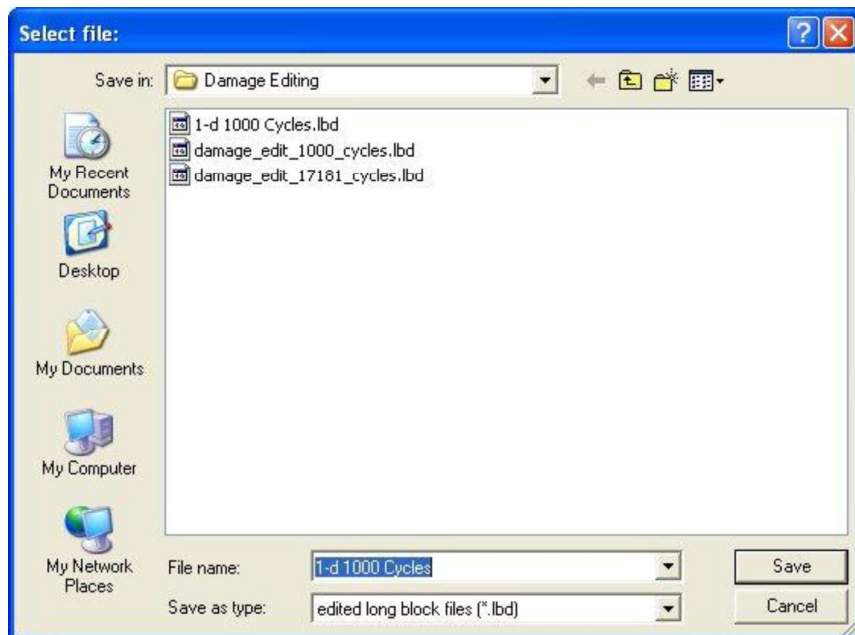


Figure 65 – File selector for output filename – Advanced spectrum editing selected as Cycle counting option

After selecting the output filename, the advanced spectrum editing file can be created by selecting the *Edit spectrum file* button on the *Spectrum File Editor* dialog box (Figure 63). At this point, the advanced spectrum editing spectrum file is created, and the spectrum statistics are displayed in the spectrum editing dialog box (see again Figure 66). If the *Use Edited File* button is selected, the spectrum format option on the *Load Blocks* tab will be updated to *Advanced spectrum editing* and the newly created advanced spectrum editing spectrum file will be set as the default filename (Figure 67).

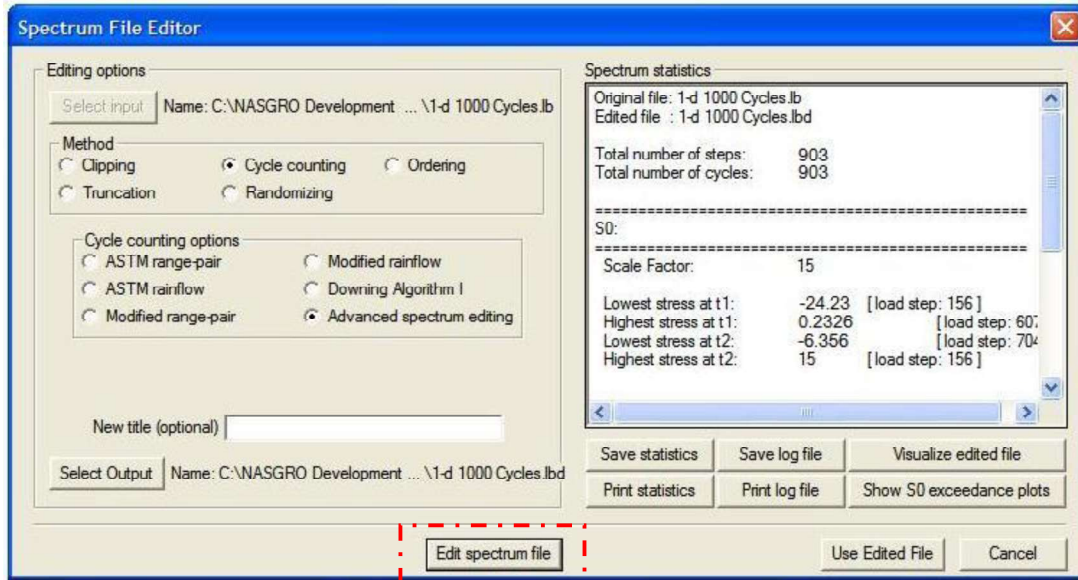


Figure 66 – Spectrum statistics for advanced spectrum editing cycle counting

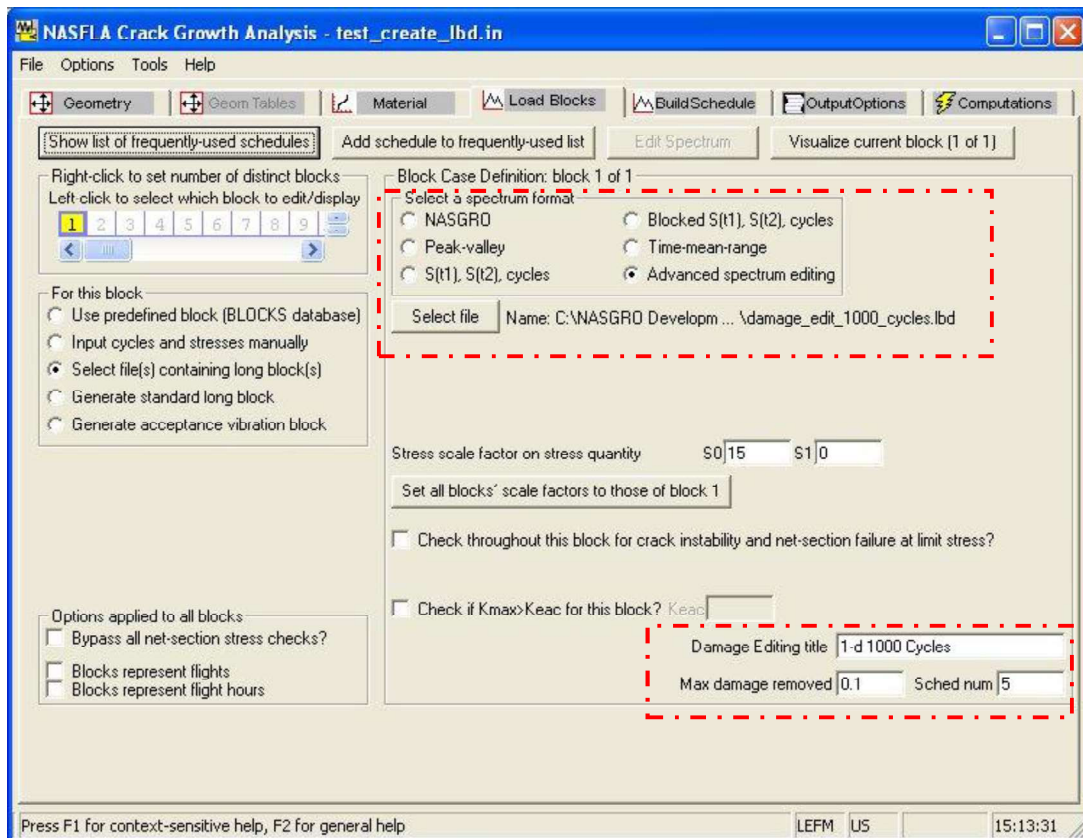


Figure 67 – Screen shot of Load Blocks tab – Advanced spectrum editing selected as spectrum format

### 2.2.7.2 Performing Advanced Spectrum Editing Analysis

Setting up a crack growth analysis that includes advanced spectrum editing requires a few additional user inputs to define the editing options. When the *Advanced spectrum editing* format is selected on the *Load Blocks* tab, three additional user input boxes are displayed (Figure 67): *Damage Editing title*, *Max damage removed*, and *Sched num*. The damage editing title is the filename used for the output files produced by the advanced spectrum editing algorithm.

*Max damage* is the maximum damage removed specified as a percentage of total damage (expressed in decimal format). Note: the advanced spectrum editing algorithm has logic to retain cycles that are identified as important minima or paired with retained cycles, so in instances where the user set a high damage percentage target, the actual damage percentage removed may be significantly lower due to the retained cycles. The experience of the developers of this algorithm has been that significant reductions in the number of cycles can be achieved by specifying relatively small damage removal fractions (such as 0.01, or even smaller). However, limited experimental studies indicated that large damage removal fractions (such as 5%) could remove more damage than was intended. Further studies are planned.

*Sched num* is the prescribed schedule pass after which the edit is performed. The damage edit is based on the cumulative damage through the prescribed editing pass. *Sched num* must be greater than one pass through the spectrum in order to allow crack closure levels to stabilize.

There are no changes to the remainder of the user input Tabs (Build Schedule, Output Options, and Computations) and they should be completed, as they would be for standard NASGRO crack growth analyses. The advanced spectrum editing algorithm is integrated into the crack growth calculation and starts when the *Save+Run* button is selected on the *Computations* tab. As such, the run times for advanced spectrum editing can be significantly greater than the other editing options (clipping and truncation) available in the spectrum editing dialog box.

After the user defined schedule is completed, the advanced spectrum editing routine outputs the following files:

(Damage editing title).lb  
Advanced spectrum editing resulting spectrum in NASGRO format

(Damage editing title).txt  
Advanced spectrum editing resulting spectrum in peak-valley format

(Damage editing title) cycle damage content.txt  
Cycles output in descending damage order

(Damage editing title) diagnostic output.txt  
Diagnostic output for advanced spectrum editing algorithm

(Damage editing title) removed damage content.txt

Identifies cycle removed and associated damage, summarizes total damage percentage removed

The *Advanced Spectrum Editing* feature creates a new long block spectrum with fewer cycles but total damage content that is theoretically the same as (or less by a specified percentage than) the original long block spectrum. Although the damage editing algorithm has been validated through limited laboratory coupon testing, this feature must be regarded as developmental in nature at the present time, and the results should be used with caution. Users are encouraged to share their experience using this feature with the NASGRO development team. Further information is available in Appendix S.

### 2.2.8 Output Options

Now click on the tab “output options”. The output file will be stored in the same folder as the input file, and uses the same name stem as the input file. For direct crack growth analysis, this tab also shows radio box choices so that output can be selected based on schedule/block/step basis or based on a certain crack growth increment. If the crack growth increment basis is chosen, you need to enter the size of the interval. In the GUI environment, the user can select the desired level of detail for the output and view it as well as print it as described in the next section.

In the case of text-based input such as in DOS or Unix environments, if the schedule/block/step basis is chosen, you would enter those numbers. If you enter 0, 0, 0 the program will print only the final results, either when the entire schedule has been repeated the desired number of times or if the crack goes critical sooner. The final results specify whether the crack has reached the critical size or not, the crack size, and the current cycle, load step, block, and schedule numbers. In addition to the final results, you may specify a block interval for printing a short line summary, which includes the current crack size and stress intensity values. For part-through cracks,  $a$ ,  $c$ ,  $K_{max}$  at the a-tip, and  $K_{max}$  at the c-tip are printed. As an example, if you enter 1, 10, 0 the program will print a line of results at the end of every tenth block case in every schedule repetition. Similarly, if you want the program to print the results only at the end of every fourth schedule, you should enter 4, number of blocks in schedule, and 0. If you need more detailed results for specific block cases, you can specify a block interval for printing the results for every load step. For example, if you enter 2, 5, and 3 the program will print a short summary at every fifth block of every other schedule and a full printout of the results at each load step for every third block of every other schedule.

### 2.2.9 Computations and Postprocessing Output

In the next tab “computations and output”, Run and Stop buttons are provided. Once the run is completed, one can choose post-processing of output to be displayed. The available items are: schedule, block, step and cycle count, crack sizes (a, c), maximum stress intensity factor within a step or block, the geometry correction factors, the flights or flight hours, the  $da/dN$ ,  $dc/dN$ , the threshold DK value, ratio of threshold DK to max DK, and the ratio  $U = DK(\text{eff})/DK$ . While the max K is the max value encountered within the step or block (and doesn't necessarily correspond to the crack size it is printed with), all other values correspond to the crack size printed (i.e. the crack size at the end of the print interval). Also, DK(eff) stands for Kmax-Kopen, and the "D" in "DK" stands for "Delta". The displayed output can be printed using the “Print Window” button. By clicking on the “save window to file” button, the output can be saved to a chosen file. You can also choose to plot the “a vs N” results by clicking on the button. Once the plot is displayed on the screen, by right-clicking on the plot, one has option to send the plot to a printer to get the hard copy. Another useful feature recently added is the button “Export computed data” which can be used to create a .CSV file that stores the various columns of output in the Microsoft Excel format. Once the file is saved, it can be opened using the Excel spreadsheet program.

### **3.0 Critical Crack Size (CCS) Calculations**

---

NASGRO provides the capabilities for determining critical crack size and threshold crack size based on fracture mechanics, net section stress, or fatigue crack growth threshold. Critical crack size is the crack size below which the cracked structure will not fail. Threshold crack size is the crack size below which none of the crack tips of the cracked structure will propagate under a specified fatigue loading.

#### **3.1 Critical Crack Size**

Critical crack size is determined based on stress intensity factor or net section stress. Generally, stress intensity factor ( $K$ ) and net section stress ( $S_n$ ) are non-linear implicit functions of crack size, and can be expressed by

$$K = f(a, L, \sigma) \quad (3.1)$$

$$S_n = g(a, L, \sigma) \quad (3.2)$$

where  $a$  is generalized crack size,  $L$  represents generalized geometric parameters, and  $\sigma$  denotes generalized loading.

The critical crack sizes are determined by letting the stress intensity factor and the net section stress equal to their critical values, i.e. fracture toughness ( $K_{cr}$ ) and critical stress (yield strength or flow strength,  $\sigma_{cr}$ ), respectively,

$$f(a_{cr}^{SIF}, L, \sigma) - K_{cr} = 0 \quad (3.3)$$

$$g(a_{cr}^{NSY}, L, \sigma) - \sigma_{cr} = 0 \quad (3.4)$$

where  $a_{cr}^{SIF}$  denotes the critical crack size determined by stress intensity factor, and  $a_{cr}^{NSY}$  is the critical crack size controlled by net section stress. The two critical crack sizes compete, and the smaller one is the final critical crack size we seek, i.e.

$$a_{cr} = \min(a_{cr}^{SIF}, a_{cr}^{NSY}) \quad (3.5)$$

Generally speaking, eqs. (3.3) and (3.4) are implicit, non-linear equations of crack size. Numerical methods have to be used to solve them.

#### **3.2 Threshold Crack Size**

Threshold crack size is the crack size below which none of the crack tips of a cracked structure will propagate under a given fatigue loading. To determine threshold crack size is to solve the following equation:

$$\Delta K - \Delta K_{th} = 0 \quad (3.6)$$

where  $\Delta K$  is the range of stress intensity factor, which is a function of crack geometry, fatigue loading, and crack size.  $\Delta K_{th}$  is fatigue crack growth threshold, a function of the effective stress ratio experienced at the crack tip. It is also a function of crack size.

Generally speaking, eq.(3.6) is an implicit, non-linear function of crack size. Numerical methods have to be employed to solve it.

For a crack subjected to constant amplitude loading, which has only one distinct load step, the threshold crack size can be obtained by solving eq.(3.6) by means of iteration procedures. For variable amplitude loading, in principle, we can obtain the threshold crack size under each load step. The smallest value is the final threshold crack size for the load schedule. But for a long variable amplitude loading, which consists of a number of load steps, it seems impossible to solve the threshold crack size for all the load steps.

In order to speed up the solution under variable amplitude loading, the following procedures are used:

(1) Collect distinct load steps. Only distinct load steps are analyzed.

(2) Determine the most severe load step.

Stress intensity factor range can be expressed by

$$\Delta K = \overline{\Delta S} \cdot \left( \sum_{i=1}^n f_i \right) \cdot \sqrt{\pi a} \quad (3.7)$$

Where  $f_i$  is correction factor under the  $i$ th stress component, and  $n$  is the number of applied stresses.  $\overline{\Delta S}$  denotes generalized stress range.

Combining eqs. (3.6) and (3.7) yields

$$\left( \sum_{i=1}^n f_i \right) \cdot \sqrt{\pi a} - \frac{\Delta K_{th}}{\overline{\Delta S}} = 0 \quad (3.8)$$

The first term in eq.(3.8) is a strong increasing function of crack size. The second term is also a function of crack size, but it has a weak dependence on crack size. Therefore this term ( $\gamma = \Delta K_{th} / \overline{\Delta S}$ ) is a good parameter to measure load severity. Calculate it under all distinct load steps with a reference crack size. The load step with the smallest value of  $\gamma$  is very likely to be the most severe load step.

(3) Obtain threshold crack size under the most severe load step by solving eq.(3.6) by means of iteration procedures.

(4) Sort distinct load steps in terms of load severity ( $\gamma$ ).

(5) Check if crack will propagate under the other load steps. If yes, compute/update threshold crack size.

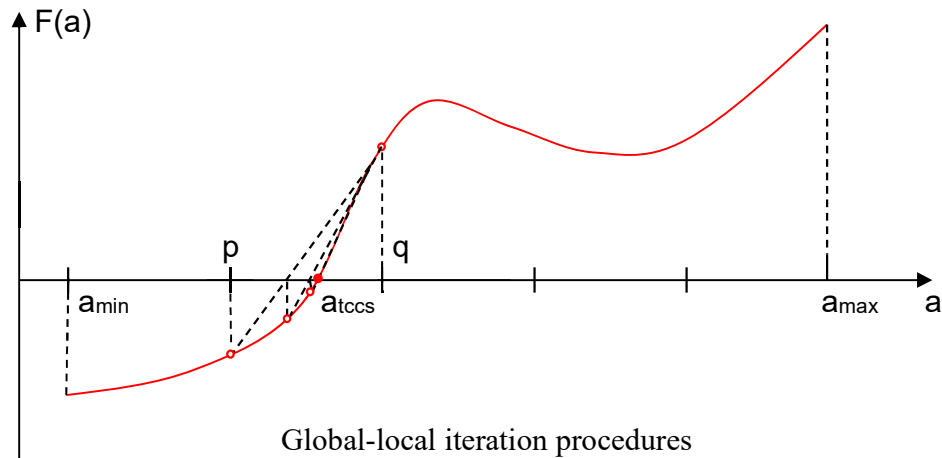
The above procedures imply that no load interaction be considered in threshold crack size determination.

### 3.3 Iteration Procedures

An essential task in critical crack size calculation is to solve an implicit, non-linear equation, i.e. eq. (3.3), (3.4) or (3.6). For a crack case with one degree of freedom, those equations have only one independent variable, i.e. crack size ‘ $a$ ’. For crack cases with more than one degree of freedom, additional assumptions are applied:

- For crack cases with two degrees of freedom: crack aspect ratio ‘ $a/c$ ’ is specified and fixed.
- For crack cases with three degrees of freedom: crack aspect ratio ‘ $a/c$ ’ is specified and fixed, and  $c_1=c$  except for BE03, where  $c/c_1$  is specified and fixed too.
- For crack case with four degrees of freedom: crack aspect ratio ‘ $a/c$ ’ is specified and fixed,  $c_1=c$ , and  $a_1=a$ .

In order to solve the implicit, non-linear equations of critical crack size, a global-local approach is used. First the whole region  $[a_{\min}, a_{\max}]$  of crack size is divided into a number of subdivisions (say 10), where  $a_{\min}$  and  $a_{\max}$  are the minimum and maximum physically or computationally allowed crack sizes. Then find the initial root bracket  $[p, q]$  for iteration. The initial root bracket  $[p, q]$  is the first subdivision with opposite values at the two ends of the subdivision. Once the initial root bracket is determined, the solution of the implicit non-linear equation can be obtained locally within the initial root bracket  $[p, q]$  by iteration. The global-local approach can help us locate the root in an efficient manner because iteration will be conducted only within the initial root bracket  $[p, q]$ , instead of the whole region of crack size  $[a_{\min}, a_{\max}]$ .



Regula Falsi method and the secant method of iteration are employed to obtain the solution for the sake of reliability and computational efficiency. Since Regula Falsi method is more reliable, it is first employed. If it does not converge, the code will automatically switch to the secant method. The tolerance used in convergence check is one thousandth (0.1%).

### ***Regula Falsi Method of Iteration***

The below figure (a) shows the procedure of regula falsi method of iteration to solve a non-linear equation,  $F(x)=0$ .

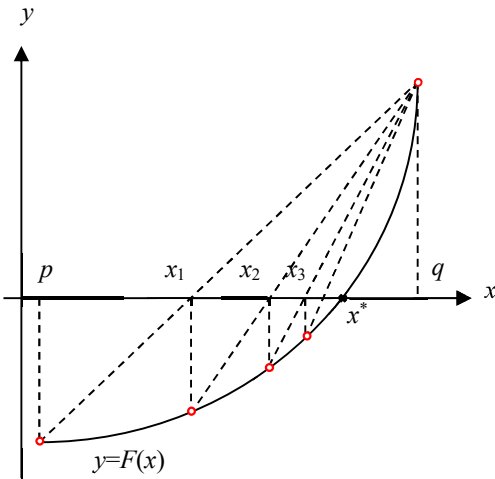
- [1] Find an initial root bracket  $[p, q]$ , which brackets the root of the equation  $F(x)=0$ . Calculate  $F(p)$  and  $F(q)$ . They are of opposite signs.
- [2] At each step of iteration, draw a line through  $(p_i, F(p_i))$  and  $(q_i, F(q_i))$ , the  $x$ -value ( $x_i$ ) of the intersection between this line and  $x$ -axis is the next approximate of the root. It is calculated by the following formula:

$$x_i = q_i - \frac{F(q_i)(q_i - p_i)}{F(q_i) - F(p_i)}$$

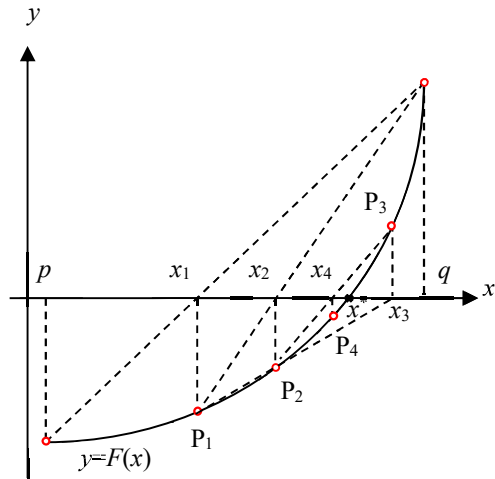
Initially  $[p_1, q_1] = [p, q]$ .

- [3] Calculate  $F(x_i)$ .
- [4] Convergence check:
  - If  $|F(x_i)| / V_{cr} \leq \varepsilon$ , stop iteration, where  $\varepsilon$  is the tolerance of iteration (0.1%).
  - If  $|F(x_i)| / V_{cr} > \varepsilon$ , construct new root bracket for next step of iteration: If  $F(p_i)F(x_i) > 0$ ,  $[p_{i+1}, q_{i+1}] = [x_i, q_i]$ . Otherwise  $[p_{i+1}, q_{i+1}] = [p_i, x_i]$ .

[5] Repeat steps 2 to 4 till convergence.



(a) Regula Falsi Method



(b) Secant Method

### Secant Method of Iteration

The above figure (b) shows the procedure of secant method of iteration to solve a non-linear equation,  $F(x)=0$ .

- [1] Find an initial root bracket  $[p, q]$ , which brackets the root of the equation  $F(x)=0$ . Calculate  $F(p)$  and  $F(q)$ . They are of opposite signs.
- [2] At each step of iteration, draw a line through  $(x_{i-2}, F(x_{i-2}))$  and  $(x_{i-1}, F(x_{i-1}))$ , the  $x$ -value ( $x_i$ ) of the intersection between this line and  $x$ -axis is the next approximate of the root. It is calculated by the following formula:

$$x_i = x_{i-1} - \frac{F(x_{i-1})(x_{i-1} - x_{i-2})}{F(x_{i-1}) - F(x_{i-2})}$$

- [3] Calculate  $F(x_i)$ .

- [4] Convergence check:

- [5] If  $|F(x_i)|/V_{cr} \leq \varepsilon$ , stop iteration, where  $\varepsilon$  is the tolerance of iteration (0.1%). If  $|F(x_i)|/V_{cr} > \varepsilon$ , repeat steps 2-4 until convergence.

In critical-crack-size determination, crack size ( $a$ ) is the independent variable ( $x$ ) in the above.  $F(x) = f(a, L, \sigma) - K_{cr}$  and  $V_{cr} = K_{cr}$  if the critical crack size is computed through stress intensity check, and  $F(x) = g(a, L, \sigma) - \sigma_{cr}$  and  $V_{cr} = \sigma_{cr}$  if through net-section-stress check.

### 3.4 How to Run NASCCS

NASCCS is a relatively easy-to-use module in NASGRO. After NASCCS is launched, the geometric parameters are input in the geometry menu. For weight functions cases, the load distributions are also input in the geometry menu. The mechanical properties like the critical stress intensity and the critical stress, as well as stress scale factors, are specified in Output Options menu. Also the criterion for calculating critical crack size is specified in this menu. Depending on crack case, the following options can be selected as the basis for critical crack size determination:

For cracks with one degree of freedom:

- K and NSY
- K only
- NSY only
- Fatigue crack growth threshold

For cracks with two degrees of freedom:

- Max K and NSY
- Max K
- K at a-tip only
- K at c-tip only
- NSY only
- Fatigue crack growth threshold

For cracks with three degrees of freedom:

- Max K and NSY
- Max K
- K at a-tip only
- K at c-tip only
- K at c1-tip only
- NSY only
- Fatigue crack growth threshold

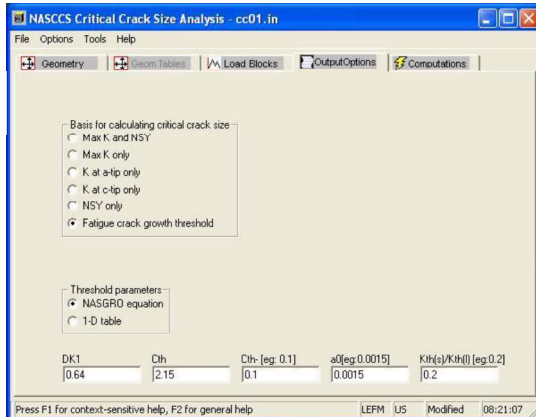
For cracks with four degrees of freedom:

- Max K and NSY
- Max K
- K at a-tip only
- K at c-tip only
- K at a1-tip only
- K at c1-tip only
- NSY only
- Fatigue crack growth threshold

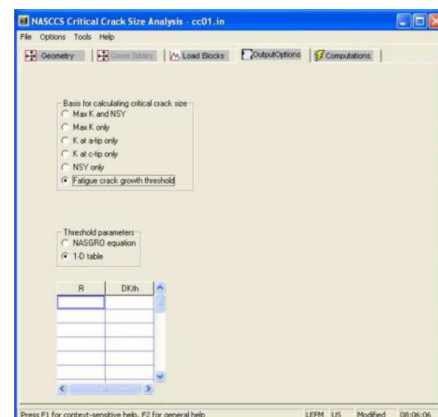
If “Max K and NSY” option is selected, the critical crack sizes will be calculated independently based upon the maximum stress intensity among all the crack tips and net section stress. The final critical crack size is the smaller of the two critical crack sizes. If “Max K” option is selected, the critical crack size will be computed by the maximum stress intensity among all the crack tips. If “K at  $x$ -tip only” option is selected, the critical crack size will be obtained by checking stress intensity factor at the  $x$ -tip only, where  $x$  can be  $a$ ,  $c$ ,  $a_1$ , or  $c_1$ , depending on the crack case. If “NSY only” option is selected, the critical crack size will be calculated by

checking net section stress solely. If an option rather than “fatigue crack growth threshold” is selected, critical stress intensity factor and critical stress need to be specified.

“Fatigue crack growth threshold” option is for threshold crack size determination. For this purpose, two kinds of information need to be provided: threshold properties of the materials of interest, and the fatigue load spectrum. Two options are provided to define threshold properties, i.e. NASGRO equation and 1-D table. The first option allows a user to enter threshold parameters (see the figure below), which are used to calculate  $\Delta K_{th}$  by NASGRO equation. The second option allows a user to enter directly  $\Delta K_{th}$  values under a series of effective stress ratio ( $R$ ).

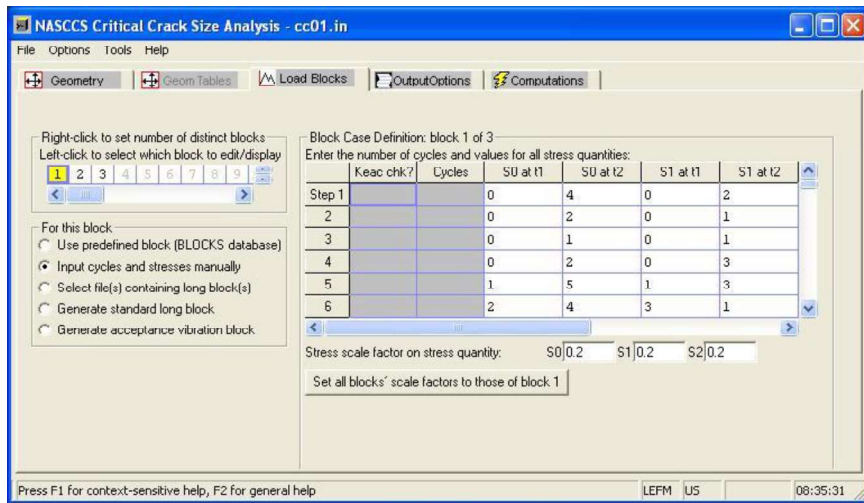


(a) by NASGRO equation



(b) by 1-D table

Definition of fatigue threshold properties



Definition of fatigue load spectrum

Fatigue load spectrum is specified in “Load Blocks” menu, which is transplanted from NASFLA GUI. Fatigue load spectrum in threshold CCS analysis can be input in the same way as in the NASFLA except that the two columns, “Keac check?” and “cycles”, are not needed.

## 4.0 Stress Intensity Factor Calculations

---

### 4.1 Theoretical Background

The stress intensity factor (SIF) is a measure of the severity of a crack in an elastic solid and is closely related to the stress field in the vicinity of the crack tip. There is a direct relationship between the SIF and the energy release rate that governs the criticality of a crack. Since the range of SIF ( $\Delta K$ ) during a fatigue loading cycle governs the crack growth rate, knowledge of the SIF for a given crack geometry is essential in any fatigue crack growth computation.

For the crack configurations described in section 2.2.1, and shown in Figures 16 through 44, a compilation of the equations or tables used in computing the SIF is given in Appendix C. The appropriate references that document the details of the solutions are also provided. Unique nonlinear interpolation routines were developed for accurate and efficient table lookup of the tabular solutions. Since most tables are multi-dimensional (e.g., variables of  $a/c$ ,  $a/t$ ,  $2c/w$ , as in SC02 shown in Figure 33), preprocessing is performed after entry of geometric dimensions to derive a two-dimensional table for a specific problem. Spline coefficients are calculated for this reduced table and reordered into a one-dimensional array for use in the crack growth analysis. This special preprocessing and dimensional array reduction results in computer run times approximately one-twentieth of those required for direct multi-dimensional and nonlinear interpolation procedures.

Stress intensity factor solutions for other geometries may be obtained by running a boundary element analysis using the NASBEM module (see Chapter 7) and then using the tabular data in crack case DT01. There are two new crack cases BE02, BE03 that are based on the boundary element solution.

### 4.2 How to Run a Stress Intensity Factor Calculation

To compute stress intensity factors, choose the relevant option from the NASFLA main menu to run the K solution module. The GUI has pull down menus to input the crack case to be used and the necessary geometric dimensions, usually the thickness and width, radius, or diameter. Under the computing options tab, display of the following radio box choices will appear:

Compute Stress Intensity Factors  
Compute Correction Factors

The first option is used for calculating the stress intensity factor(s) for a specific crack case or for plotting the variation in stress intensity factors with respect to geometry. The second option is used to calculate whichever correction factors  $F_0$ ,  $F_1$ ,  $F_2$ ,  $F_3$ , and  $F_4$  apply to a particular crack case. The stress and crack size information can also be entered from a text box. An example of how to solve for the correction factors in order to determine the proof pressure required for a glass window is given in the software.

### 4.2.1 SIF Calculations Using Linear Stresses

If you select option to compute the stress intensity factors, the program will prompt you for the material's yield strength (see tables G1 and G2 in Appendices G1 and G2) and the appropriate applied stresses. Then the following choices will be presented:

- Tabulate solutions
- Plot solutions.

If you choose tabulation, you will be prompted for crack lengths for the K calculations. For one-dimensional cracks, enter  $a$  or  $c$  values only; for two-dimensional cracks enter both the  $a$  and  $c$  values for which you want  $K(a)$  and  $K(c)$  calculations. If you choose to plot, it displays the following menu of options for choosing the x-axis and curve-defining variables:

	x-axis variable	Curve defining variable (= constant on each curve)
1	$c$	$a/c$
2	$a$	$a/c$
3	$a/c$	$c$
4	$a/c$	$a$
5	$c$	$a$
6	$a$	$c$ .

The plotting routine allows you to obtain plots of  $K(a)$  and  $K(c)$  vs. a variable along the x-axis (choose from the first column) for several curves of a constant variable (choose from the second column). The plots may then be further non-dimensionalized (e.g. with respect to thickness  $t$  or width  $w$ ). For options 1 and 2, you are given the choice to non-dimensionalize  $a$  or  $c$  by the filling the following box:

NAME of x-axis non-dimensionalizing variable

For options 3 and 4, you are given the choice to normalize the curve defining variable,  $c$  or  $a$ , by the filling the following box:

NAME of non-dimensionalizer for curve defining variable

For options 5 and 6, you are given both choices. You can non-dimensionalize  $a$  and/or  $c$  by  $a$ ,  $c$ ,  $t$ , or  $W$ .

Next the maximum and minimum limits for the x-axis variable need to be input and then the number of curves desired. Up to 5 curves of the constant variable are permitted. Finally, the program needs to know the maximum and minimum limits for the curve-defining variable. If more than 2 curves were selected, they are evenly distributed between the maximum and minimum values specified. If you have selected screen mode as the plotting device, the plot will be displayed on your screen. If you have selected postscript as the plotting device, you

will need to send the resultant NASPLT file to the printer, using an appropriate command. An example of how the plotting routine works is shown in the software.

### 4.2.2 SIF Calculations Using Nonlinear Stresses

Several of the stress intensity factor solutions (TC11, TC12, TC13, CC08, EC02, SC02, SC04, SC06, SC17 and SC18) allow nonlinear stresses across the thickness or width to be applied. Two other cases SC15, and CC05 allow stress variation in both the thickness and width directions. The method to input these stresses is given in more detail in Appendix-C. After entering the yield strength of the material, the user chooses the number of stress distributions to be included in the analysis. Some of the cases (TC11, TC12, EC02, SC17 and SC18) Up to four stress distributions are permitted for each crack case. For the SC04 crack case, the program allows you to enter the internal pressure and automatically generates stresses through the thickness of the pressure vessel. You may indicate that you want this option by clicking on the radio box showing

Generate stresses due to Unit (1 ksi or 1 MPa) Internal Pressure (Yes or No)

For crack cases SC02, SC06, SC10, and if you choose not to generate stresses for the SC04 case, the program will prompt you for the nonlinear stresses:

Enter values of Nondimensional Position ( $x/t$ ) and Stress  
(For linear case, 2 locations (e.g.  $x/t = 0$  and 1) are sufficient).

Actual stress values or scaled stresses may be entered for up to 50 different non-dimensional positions through the thickness of the plate or cylinder. There is also an option to plot the nonlinear stresses you have just entered as a function of the non-dimensional thickness. If yes, the program will ask for the graphics device number, x-axis and y-axis labels, and a title for the plot. Then you are permitted to choose whether the axes should be drawn linear-linear or log-log. Note that if you are plotting to a hard copy device, the program creates a file called NASPLT.XXX, which may later be sent to your printer using an appropriate command. Next, the following dialog box is displayed:

Tabulate solutions  
Plot solutions.

If you choose tabulation, you will be prompted for both the  $a$  and  $c$  values that you want to use for the K(a) and K(c) calculations.

If you previously entered no to indicate that you did not want to plot the stress distribution as a function of  $x/t$ , you are only given the option to tabulate the K(a) and K(c) values.  $S_n$  and  $S_n/\sigma_{ys}$  values, if available, are listed for each crack size. Otherwise, the columns will contain zeros. After the table is completed, there will be an opportunity to flag the table for printing.

## **5.0 Sustained Stress ( $da/dt$ ) Analysis of Glass (NASGLS)**

---

The strength of a glass surface is governed by the distribution of cracks present and the growth of these cracks under sustained stresses [38]. The amount of crack growth depends on crack size and geometry, the amount of sustained stress, and the environment (mainly humidity and temperature) to which the glass structure is exposed. The NASGRO NASGLS module provides the capability for performing sustained stress analyses for glass structures, such as optical lenses or windows, which contain cracks that may be accidentally introduced during handling. These analyses are carried out in a manner similar to the crack growth analyses of metals (see section 2.2), but the crack growth is a function of time instead of cycles. Ref. [45] gives the NASA requirements for structures made of glass-like materials.

It is expected that NASGRO will include the ability to model crack propagation simultaneously as a function of time and the number of fatigue cycles. This capability is necessary for an accurate modeling of environmental crack growth in metallic materials.

### **5.1 Theoretical Background**

In performing sustained stress analyses, the governing variable is time and therefore,  $da/dt$  is the operative variable for crack growth rather than  $da/dN$ . NASGRO provides two models for calculating crack growth. One formulation is the following exponential equation proposed by Wiederhorn [39]:

$$\frac{da}{dt} = V_0 e^{BK} \quad (5.1)$$

and the other is a Paris-type model that is expressed by:

$$\frac{da}{dt} = AK^n \quad (5.2)$$

At crack growth rates below approximately 1  $\mu\text{in}/\text{h}$  (25  $\text{nm}/\text{h}$ ), the exponential equation provides a more conservative approach than Eq 5.2 and should be used in all sustained stress analyses for NASA space hardware. However, although verification tests are needed, it is believed that the Paris-type equation will provide more accurate predictions in this region. At intermediate crack growth rates, the two equations are comparable, and the exponential equation produces only slightly less conservative values than the Paris-type model. Figure 68 shows a comparison of sustained stress data for borosilicate glass UBK7 in a high humidity air condition with curve fits to Eq 5.1 and 5.2.

### **5.2 How to Run a Sustained Stress Analysis**

An example of how to run a sustained stress analysis of a glass window may be found in the software. Begin by selecting sustained load analysis option from the NASGRO radio box choices. As with the other options, you will be prompted for the units and for an output file name. Next, enter a title for the calculation and the crack case that you want to evaluate.

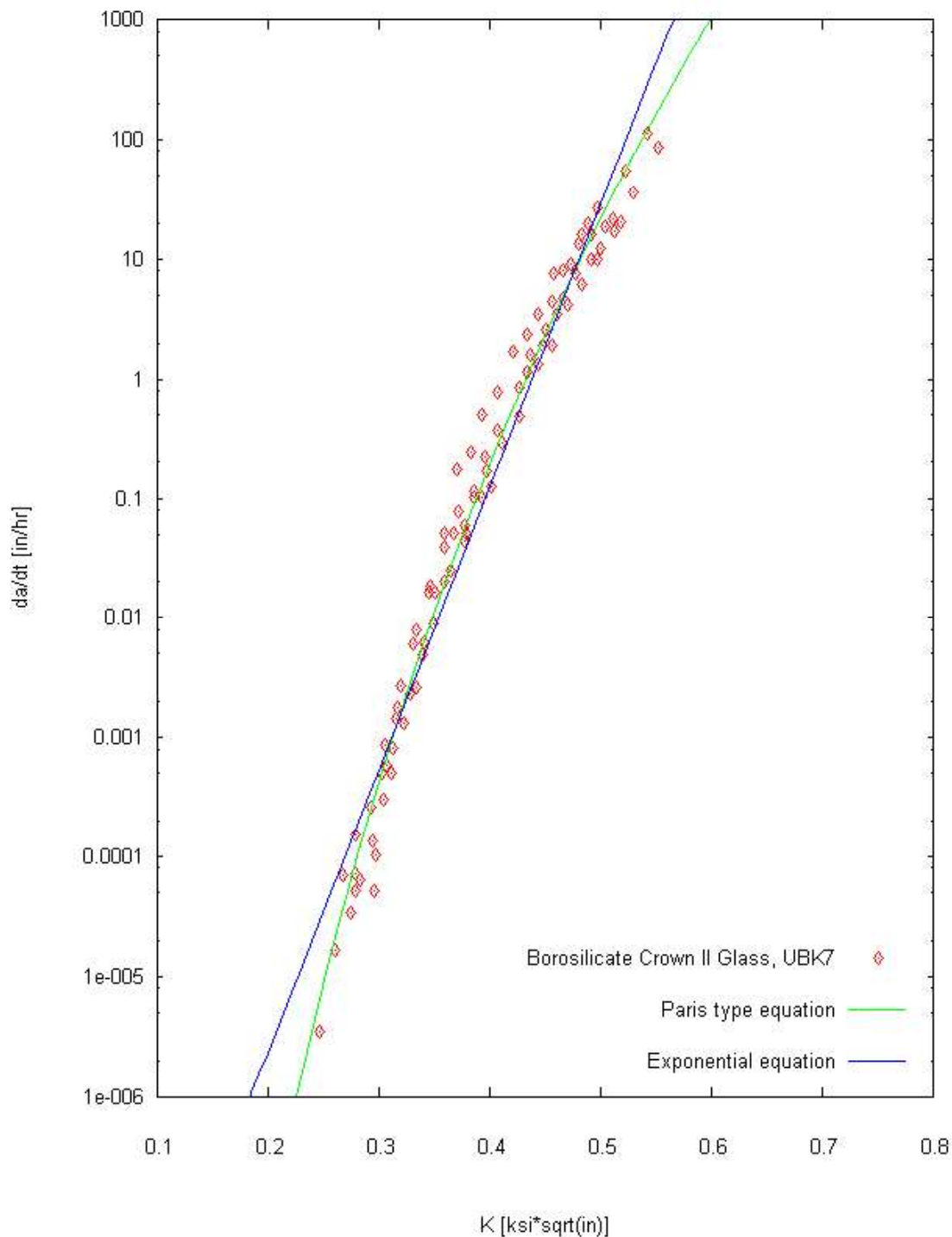


Figure 68—Sustained stress data with curve fits

### 5.2.1 Material Properties

Crack growth data for various glass materials were obtained from references [39-44] and curve fit with Eq 5.1 and 5.2. Tables 14 & 15 list constants stored in NASGLC (US units) and NASGLM (SI units) files. They are in  $(in/h)/(ksi \sqrt{in})^n$  [ $(mm/h)/(MPa \sqrt{mm})^n$ ] for A; dimension-free for n;  $in/h$  [mm/h] for  $V_0$ ;  $1/(ksi \sqrt{in})$  [ $1/(MPa \sqrt{mm})$ ] for B; and  $ksi \sqrt{in}$  [MPa  $\sqrt{mm}$ ] for  $K_{Ic}$ . Most fits are for high humidity air (HHA) or distilled water (DW) environments, yielding conservative values for space hardware. Identification codes are in accordance with Section 2.2.4, but unneeded for program input.

Table 14 – Sustained Stress Constants (US Units)

Material	Code	A	n	$V_0$	B	$K_{Ic}$	SD
Soda-Lime Glass, LA	W1AA10AB1A1	0.132E07	20.05	0.128E-10	50.47	0.670	0.034
Borosilicate Glass, C7740, HHA	W1AB10AD1A1	0.135E11	28.54	0.430E-14	75.04	0.675	0.024
Borosilicate Crown I Glass, BK7, HHA	W1AB10AD1A2	0.158E08	20.93	0.530E-10	51.99	0.643	0.022
Borosilicate Crown II Glass, UBK7, HHA	W1AB10AD1A3	0.497E08	21.13	0.471E-10	54.27	0.656	0.009
Lead Glass, SF1, HHA	W1AC10AD1A1	0.874E10	21.83	0.246E-10	68.41	0.775	0.021
Aluminosilicate Glass, C1723, HHA	W1AD10AD1A1	0.288E08	27.54	0.161E-13	59.37	0.697	0.016
Aluminosilicate Glass, C0317, DW	W1AD10WA1A2	0.201E10	23.70	0.107E-10	61.60	0.661	0.013
96 Silica Glass, C7900, HHA	W1AE10AD1A1	0.193E11	29.16	0.295E-14	75.38	0.798	0.015
96 Silica Glass, C7913, HHA	W1AE10AD1A2	0.128E12	32.84	0.908E-16	80.50	0.810	0.015
Fused Silica, C7940, HHA	W1AF10AD1A1	0.492E11	34.44	0.113E-16	79.91	0.574	0.018
Fused Silica, DW	W1AF10WA1A1	0.510E14	35.89	0.341E-17	96.79	0.574	0.018
Fused Silica, C7940, DW	W1AF10WA1A2	0.332E15	38.70	0.331E-17	94.86	0.658	0.014
Fused Silica, C7980, DW	W1AF10WA1A3	0.185E15	38.40	0.326E-17	94.12	0.655	0.007
Sapphire r-plane, DW	W1AS10WA1A1	0.289E-09	21.03	0.169E-18	20.23	2.284	0.109
Sapphire a-plane, DW	W1AS10WA1A2	0.533E-10	30.80	0.724E-25	32.76	2.066	0.110
ALON (Aluminum Oxynitride), DW	W1AO10WA1A1	0.827E-04	36.00	0.432E-15	26.80	1.880	0.060

Table 15 – Sustained Stress Constants (SI Units)

Material	Code	A	n	$V_0$	B	$K_{Ic}$	SD
Soda-Lime Glass, LA	W1AA10AB1A1	0.426E-23	20.05	0.326E-09	1.45	23.29	1.18
Borosilicate Glass, C7740, HHA	W1AB10AD1A1	0.363E-32	28.54	0.109E-12	2.16	23.46	0.82
Borosilicate Crown I Glass, BK7, HHA	W1AB10AD1A2	0.224E-23	20.93	0.135E-08	1.50	22.33	0.76
Borosilicate Crown II Glass, UBK7, HHA	W1AB10AD1A3	0.343E-23	21.13	0.120E-08	1.56	22.80	0.32
Lead Glass, SF1, HHA	W1AC10AD1A1	0.495E-22	21.84	0.672E-09	1.97	26.91	0.73
Aluminosilicate Glass, C1723, HHA	W1AD10AD1A1	0.268E-33	27.54	0.408E-12	1.71	24.22	0.54
Aluminosilicate Glass, C0317, DW	W1AD10WA1A2	0.154E-25	23.70	0.272E-09	1.77	22.96	0.44
96 Silica Glass, C7900, HHA	W1AE10AD1A1	0.580E-33	29.16	0.748E-13	2.17	27.73	0.51
96 Silica Glass, C7913, HHA	W1AE10AD1A2	0.806E-38	32.84	0.231E-14	2.32	28.14	0.51
Fused Silica, C7940, HHA	W1AF10AD1A1	0.107E-40	34.44	0.287E-15	2.30	19.95	0.28
Fused Silica, DW	W1AF10WA1A1	0.649E-40	35.89	0.865E-16	2.79	19.95	0.28
Fused Silica, C7940, DW	W1AF10WA1A2	0.195E-43	38.70	0.839E-16	2.73	22.88	0.49
Fused Silica, C7980, DW	W1AF10WA1A3	0.316E-43	38.40	0.828E-16	2.71	22.77	0.24
Sapphire r-plane, DW	W1AS10WA1A1	0.288E-40	21.03	0.428E-17	0.58	79.37	3.79
Sapphire a-plane, DW	W1AS10WA1A2	0.468E-56	30.80	0.184E-23	0.94	71.78	3.83
ALON (Aluminum Oxynitride), DW	W1AO10WA1A1	0.706E-58	36.00	0.110E-13	0.77	65.10	2.20

After entering the number of sets of glass properties to be used for input in the analysis, the program will show radio box choices to select from the following glass properties input options:

- Manual input
- Input from NASGRO glass properties file

NASGRO requires input of material properties in the form of constants for Eq 5.1 and 5.2. This may be accomplished manually (option 1) or automatically by using the constants in the glass properties file (option 2).

To enter the constants manually, select option 1. The program will prompt you for the constants, and after they are entered, the glass properties menu will reappear if more materials are to be entered. Otherwise the program will continue.

To enter the constants from the NASGRO materials file, select option 2. Curve fit constants and  $K_{Ic}$  values for fifteen glass/environment combinations are available in the NASGRO file. Then you should input the type of fit for the da/dt data. Choose the appropriate radio box choice for Paris-type equation (Eq 5.1), or the Exponential equation (Eq 5.2).

### 5.2.2 Entering the Sustained Load Schedule

The sustained stress data are entered in a manner similar to that in which the load schedule for a crack growth analysis (see section 2.2.4) was entered. However, since most sustained loads are fairly simple, a repeatable schedule is not actually built by combining blocks, and there are no options for saving the sustained stress blocks to a file.

The number of load steps in a block and the total number of blocks will be prompted for. This is followed by the stress scaling factors. If you use SSF = 1,  $S_0$  will be the actual tensile stress. You will then be prompted for scaling factors  $S_1$ ,  $S_2$ , and  $S_3$  (whichever are applicable for the chosen crack case). These scaling factors are applied to the entire block.

To enter a block manually, the program will prompt for load step number, material number, duration of sustained stress in hours, and the stress(es). This input process will be repeated until all load steps in the block are defined. The block menu will reappear. Choose option 1 to define more blocks or option 0 to continue. The graphical user interface provides tabs for geometry, material, spectrum and print options as well as one for execution. For the most part, the input process is fairly self-explanatory.

## 6.0 Crack Growth Data Analysis

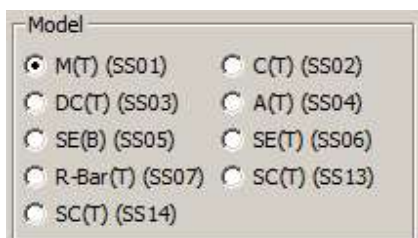
---

This section describes the software module NASMAT used to store and curve fit the crack growth rate data and fracture toughness data. Sections 6.1 and 6.2 describe the process of entering crack growth data and obtaining the constants for either the NASGRO fatigue crack growth equation, the Walker equation, or the coefficients of a cubic spline fit. The graphical user interface is self-explanatory and so the description given here is brief. The first screen provides four choices: NASA database or user database for crack growth data and NASA or user database for fracture toughness. There are two files (NASADATA.DAT, NASAHEAD.DAT) supplied with the software that contain the NASA database for crack growth data and one file (NASA KCDTA.DAT) that contains the NASA toughness database. These files are encrypted so that users cannot alter them. When new crack growth data are entered by a user, they are saved in a file named USERHEAD.DAT that stores the header information, and USERDATA.DAT that contains the data. These files constitute a small-scale database, and are updated whenever changes, additions, or deletions are made by the users. Similarly, the new toughness data is stored in the file USERKCDTA.DAT. Section 6.3 describes the entry and processing of fracture toughness data.

### 6.1 Entering Crack Growth Data for Curve Fitting

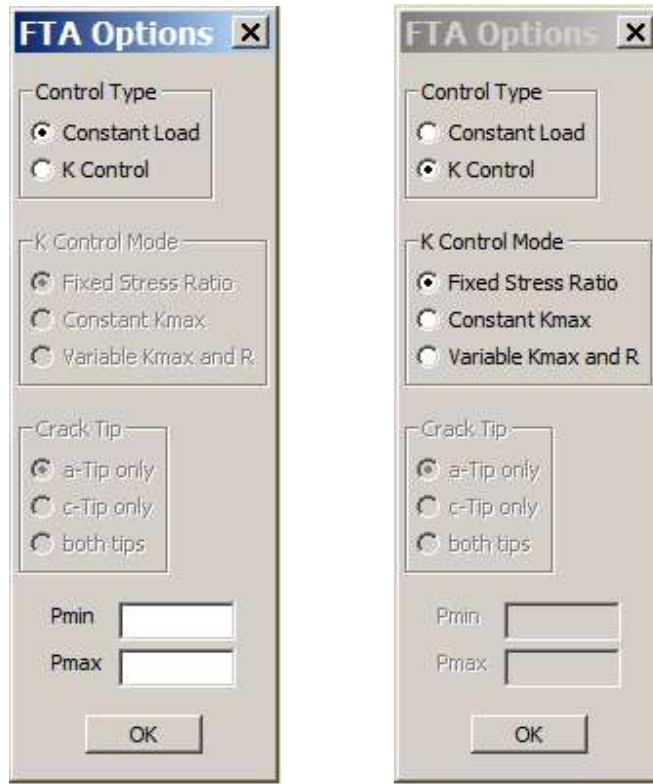
If fatigue crack growth data need to be curve fit, the first step is to enter the data. From NASGRO 6.0 onwards, the entry of data has been split into two pages. The Enter da/dN Delta K tab can be used to enter user data from any of the user's sources into the user database (i.e., into the file: USERDATA.DAT) while the Enter a vs. N tab is intended for entering data that must first be converted by NASMAT into da/dN versus Delta K data before storing them in the user database.

If the Enter a vs. N page is chosen, the user is directed to choose a standard specimen from the following list of models:



The first seven crack cases are one-dimensional models while the last two: SS13 and SS14, are two-dimensional crack cases. Upon choosing a model and entering details of the desired geometry, the following pop-up menu appears [previous to NASGRO 6.0, only *Constant Load* data were convertible by NASMAT] allowing the user to choose the *Control Type* that has been used to generate the data. The possible choices of *K Control Mode* are shown below, when either of the choices for Control Type is made: *Constant Load* or *K Control*.

## 6.1 Entering Crack Growth Data for Curve Fitting



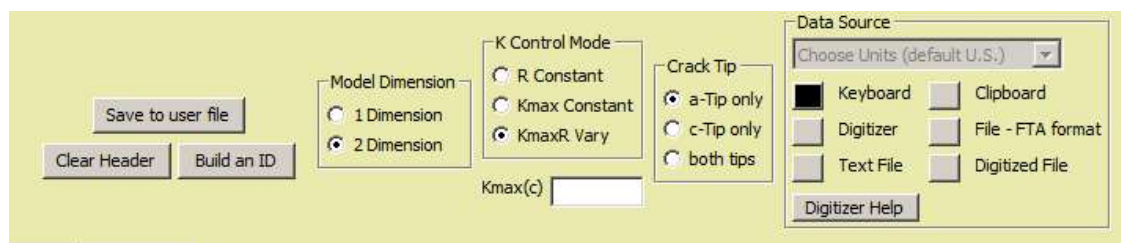
The next step in the process allows data to be entered via the following grid in the Enter a vs. N page, the required columns of which are activated by the program depending upon the chosen crack case and control type.

This screenshot shows the 'Enter a vs. N' data entry interface. It features a grid for entering crack growth data, with various controls and status indicators.

- Header Info:** A section on the left containing dropdown menus for 'Save to user file', 'Choose Standard Specimen', 'da/dN computing options' (set to 'Secant'), and 'Data Source' (set to 'Choose Units (default U.S.)').
- Data Grid:** The main area contains a table with columns labeled 'a', 'c', 'N', 'Pmin', 'Pmax', and 'Reserved'. The 'a' column has 17 rows numbered 0 to 16. The 'Pmin' and 'Pmax' columns are currently empty.
- Buttons:** At the bottom of the grid are buttons for 'Convert to da/dc/dN vs Delta K', 'Plot data set', and 'Clear Data'.
- Message Boxes:**
  - A message box at the bottom left says: 'Reference will be shown here when the reference cell is RIGHT clicked in the grid.'
  - A message box at the bottom center says: 'Largest No Letter: [ ] Largest C Ref: C292'
- Save Changes:** A 'Save Ref Changes' button is located at the bottom left of the message boxes.

Following entry of data, the button below the data grid labeled “Convert to da(dc)/dN vs Delta K” allows the user to convert the data, after which the converted data may be saved in the user database. Prior to saving the data, checks are made by NASMAT to verify that the converted data are indeed of the type originally chosen: *Fixed Stress Ratio* or *Constant Kmax*, by the user. Data whose variations are within a 2% band of the mean are accepted as “constant” data, but data with a variation greater than 2% are labeled *Variable Kmax and R* in the database and the user is so informed.

If the user wishes to use the Enter da/dN Delta K page to enter data directly into the user database, radio boxes that allow the user [from NASGRO 6.0 onwards] to choose *Model Dimension* and *K Control Mode* are provided as shown:



The radio boxes for *K Control Mode* and *Crack Tip* (for two-dimensional models) are programmed to ensure that the user makes valid data choices, disallowing those that are physically meaningless, for example, disallowing *Kmax Constant* data at both crack tips.

When saving data, it is not necessary to define an identification code that is as complicated as those listed in tables G1 and G2. However, it is necessary that the last character in the ID code be reserved for the number of stress ratios for which data are available and that the total number of characters be 11 or less. Assistance for building an ID code that is consistent with the NASA convention can be obtained by clicking on the Build an ID button. Header data may be entered in the grid provided. The header information consists of: the alloy name, heat treatment, product form, test environment, specimen type, crack orientation, specimen thickness and width, yield strength, ultimate strength, test frequency, and the reference number. Any of the entries may be omitted except for the ID and thickness. Units that will be used for the data may be chosen from the choice box at the top of the page. If U.S. units are used, da/dN data must be entered in in/cycle. If data are being entered in metric units, two sets of units are available. It should be noted, however, that the data are always stored in ksi-in<sup>1/2</sup> and in/cycle.

The data source radio box allows the user to choose the method of entry. The choices for entering data are: from keyboard, NASA lab file (FTA format), text file, clipboard, and digitizer. For keyboard input, data pairs are entered in cells in a data grid. If Text File input is chosen, the user will be prompted to define the file by giving the columns that contain da/dN and Delta K data, the number of lines to skip before the data begins (header lines), and the delimiter between columns (comma, spaces, etc). The FTA format is a format created by analysis software written by Fracture Technology Associates and its format is known by the program.

An example of the FTA format follows:

```
Index,,,CrackLength,CycleCount,,dadN,,,DK,,,,,
2,,,1.105331,63989,,0.00000E+0,,0.00000,,,
4,,,1.153600,648375,,7.38420E-8,,3.66869,,,
6,,,1.193821,1262353,,5.34757E-8,,3.37734,,,
8,,,1.224542,1975012,,3.61946E-8,,3.14259,,,
10,,,1.254578,2940978,,2.76397E-8,,2.84757,,,
16,,,1.334230,5943490,,2.33985E-8,,2.67716,,,
19,,,1.360040,7448188,,1.73501E-8,,2.44890,,,
22,,,1.386243,8941345,,1.48279E-8,,2.34292,,,
25,,,1.404470,10444523,,1.12072E-8,,2.25016,,,
28,,,1.419936,11947701,,8.53138E-9,,2.14776,,,
34,,,1.442857,14944036,,8.10812E-9,,2.08193,,,
37,,,1.456418,16447214,,6.42525E-9,,2.00719,,,
40,,,1.462109,17940370,,4.41646E-9,,1.96086,,,
43,,,1.469651,19443548,,3.70972E-9,,1.93171,,,
46,,,1.473262,20946726,,0.00000E+0,,0.00000,,,
```

Data may be pasted from the clipboard that has been copied there from any text editor or other program (e.g. Microsoft Excel). Simply clicking on the button labeled Clipboard. Clicking the button labeled Digitizer will execute the Engauge Digitizer, written by Mark Mitchell. Instructions on its use may be obtained by clicking the button labeled Digitizer Help. After a file has been digitized, clicking the button labeled Digitized File loads the data. It is necessary that the correct R values are enabled before the file is loaded. Once the data is entered it can be saved and curve-fitted.

## 6.2 Obtaining the Constants

The fitting process in NASMAT fits crack growth data with an equation to be picked from the following three available choices: NASGRO, Walker or spline. The algorithms use least-squares minimization of error in the Log-Log domain to obtain the corresponding constants.

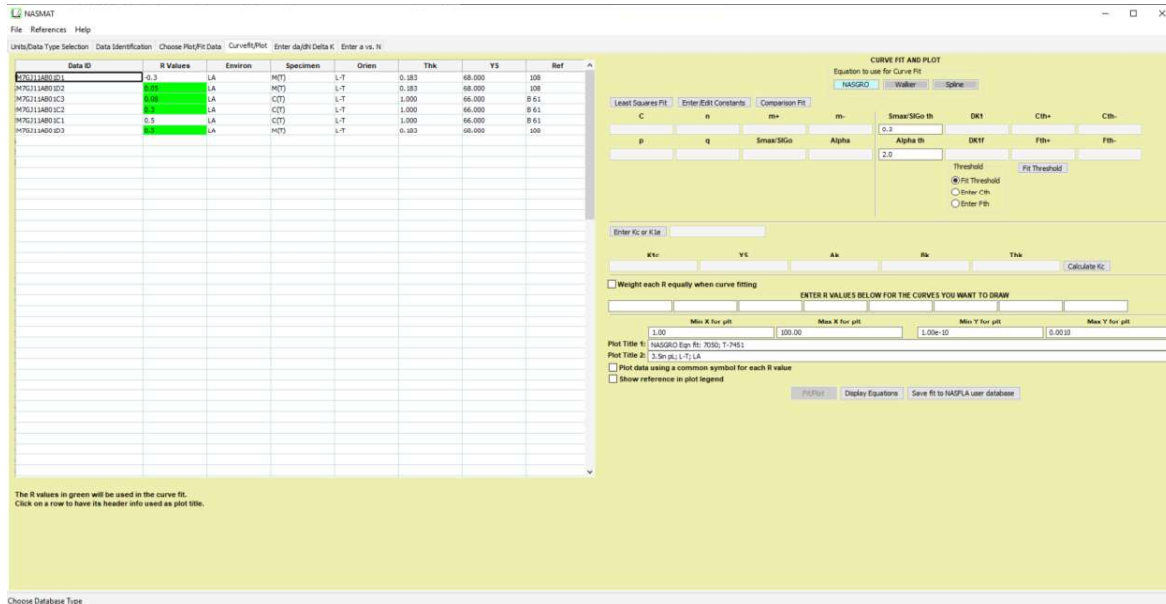
Data ID	K control Values	Alloy	Cond/H/T	Form	Environ	Specimen	Orien	Thk	Width	YS	UTS	Freq	Ref	Mac
M7GJ11AB01A	R=0.1	7050	T73651	.1" PLT	LA	C(T)	L-T	0.750	1.500	70,000	80,500	25	C 86	0.1
M7GJ11AB01B	R=0.1	7050	T73651	3.15" PLT	LA	C(T)	L-T	1.000	7.400	65,600	76,600	5-10	C 20	0.1
M7GJ11AB01C	R=.05,R=.03,R=.08	7050	T73651	4" PLT	LA	C(T)	L-T	1.000	8.900	66,000	76,000	6	B 61	0.08
M7GJ11AB01D	R=.03,R=.05,R=.05	7050	T-7451	.35" pl	LA	M(T)	L-T	0.183	6.300	68,000	78,000	UNK	108	R=.03
M7GJ11AB01E	R=.03,R=.05,R=.05	7050	T7451	3.5" Plt	LA	COP	L-T	0.390	3.900	68,000	78,000	UNK	108	R=.03
M7GJ11AB01F	R=.03,R=.05,R=.05	7050	T7451	UNK	LA	M(T)	L-T	0.390	3.900	68,000	78,000	UNK	108	R=.03
M7GJ11AB01G	R=.03,R=.05,R=.05	7075	T-7451	PLT	LA	M(T)	L-T	0.200	6.300	68,000	78,000	UNK	108	R=.03
M7GJ11AB01H	R=.005,R=.025,R=.05	7050	T7451	UNK	LA	SE(B)	L-T	1.000	2.000	68,000	78,000	UNK	108	R=.005
M7GJ11AB01I	R=.1,R=.4,R=.7,R=.8	7050-T7451 PT	-T7451	.6" Plt	IAR AIR	C(T)	L-T	0.910	3.000	67,000	77,000	50	1	R=.1
M7GJ11AB01J	R=.05	7050	T7451	0.25" Plt	Lab Air	M(T)	L-T	0.250	3.150	68,000	78,000	472	R=.05	
M7GJ11AB01K	R=.1,R=.66,R=.33,R=.0=R=.55	7050	T7451	0.5" Plt	LA	M(T)	L-T	0.250	3.900	10	D 17	R=.1		
M7GJ11AB01L	R=.02	7050	T7451	.2" Plt	LA	M(T)	L-T	0.250	3.800	72,000	78,000	10 - 15	D 18	R=.02
M7GJ11AB01M	R=.01,R=.04,R=.07,R=.08	7050	T7451	.5" plate	Lab Air	SE(B)	L-T	0.240	2.500	73,000	77,000	70	1	R=.01

First select source of the data set that you want to curve fit. The data may be from NASA database [46] or user database. The data ID can be partially entered or built from a series of menus. The user then clicks on the Show Data Sets button to display available data. Each of the available data sets that match the ID entered is displayed. You then click on the ID(s) of interest and click the Load Selected Data button. Available R values are shown and check boxes are provided to choose data for plotting only (P) or for plotting and fitting (F).

Data ID	Alloy	Cond./HT	Prod Form	Envir	Spec Type	Orien	Thk	YS	Ref
M7GJ11AB01C	7050	T73651	4" PLT	LA	C(T)	L-T	1.000	68,000	B 61
R=0.5	<input checked="" type="checkbox"/> Plot <input type="checkbox"/> Fit	R=0.3	<input type="checkbox"/> Plot <input checked="" type="checkbox"/> Fit	R=0.08	<input type="checkbox"/> Plot <input checked="" type="checkbox"/> Fit				
M7GJ11AB01D	7050	T-7451	.35" pl	LA	M(T)	L-T	0.183	68,000	108
R=-0.3	<input checked="" type="checkbox"/> Plot <input type="checkbox"/> Fit	R=0.05	<input type="checkbox"/> Plot <input checked="" type="checkbox"/> Fit	R=0.5	<input type="checkbox"/> Plot <input checked="" type="checkbox"/> Fit				

Once the data sets are chosen for fitting, click on the “plot/curve fit” button and the next screen provides all the necessary choices and text boxes for entry of parameters. Curve fitting crack growth data is an iterative process which consists of entering choices for some of the constants, specifying a data set for a least squares fit if desired, and plotting the data at varying R values with the curve fit at each stress ratio. The process is repeated by changing the values of the constants slightly until the best fit to the experimental data is obtained. The curve fit constants and material properties on this page can be saved to the NASFLA user data base by clicking the button labeled “Save fit to NASFLA user database”. A dialog box will be presented that will allow the user to supply any missing parameters (e.g., K1e, UTS) and save to USRMFC and/or USRMFM in the current NASGRO installation.

## 6.2 Obtaining the Constants



If the NASGRO equation (described in detail in section 2.1.1)

$$\frac{da}{dN} = C \left[ \left( \frac{1-f}{1-R} \right) \Delta K \right]^n \frac{\left( 1 - \frac{\Delta K_{th}}{\Delta K} \right)^p}{\left( 1 - \frac{K_{max}}{K_c} \right)^q} \quad (6.1)$$

is chosen, the fitting algorithm obtains the constants  $C$  and  $n$  after the user supplies the various input parameters needed. Some of the salient parameters needed for the NASGRO equation curve fit are:  $S_{max}/\sigma_0$  ratio, toughness value, constraint parameter  $\alpha$  and threshold information.

Fitting threshold data is generally the first step, which may be done by first entering threshold values of  $S_{max}/\sigma_0$  and  $\alpha$  (identified by the postscript  $th$ ) for which commonly used values are 0.3 and 2.0, respectively, and then pressing the *Fit Threshold* button. This opens a separate window for entry of a table of threshold values and R. After data are entered and the OK button is pressed, values of  $\Delta K_1$ ,  $C_{th}^p$  and  $C_{th}^m$  and of the alternative set of threshold variables  $\Delta K_{1f}$ ,  $F_{th}^p$  and  $F_{th}^m$  (described in Section 2.1.3) are obtained by the program and the corresponding text boxes are filled in the main fitting window.

Additional information about the use of the parameter  $S_{max}/\sigma_0$  ratio may be found in section 2.1.2. Discussion on the constraint factor  $\alpha$  may be found in sections 2.1.1 and 2.1.2. Since the least squares routine uses all of the data points, sometimes it does not provide desirable values of  $C$  and  $n$  that work for all the stress ratios. In this case, you may want to input values for  $C$  and  $n$  manually. You can also choose to plot up to nine curves for various R

values on the plot. The stress ratio values for which you want curves drawn are input into text boxes.

You also need to enter the fracture toughness value  $K_C$ . You may either enter  $K_C$  directly (e.g., if the data are from part-through specimens and  $K_{Ic}$  is known) or  $K_C$  can be calculated based on  $K_{Ic}$ ,  $\sigma_{ys}$ ,  $A_k$ ,  $B_k$ , and the specimen thickness. Additional theoretical information on fracture toughness may be found in section 2.1.4. There are also text boxes provided to enter values for  $p$  and  $q$ . The constants  $p$  and  $q$  control the shape of the asymptotes in the threshold and critical crack growth regions, respectively. Refer to Section 2.2.4.2 for more information on the limits for each parameter in the NASGRO equation.

If the Walker equation fit (akin but not identical to that used by the Chang-Willenborg model, discussed in section 2.1.7.3)

$$\frac{da}{dN} = C \left[ \frac{\Delta K}{(1-R)^{1-m}} \right]^n \quad (6.2)$$

is chosen, the fitting algorithm uses a three-stage numerical procedure to obtain the constants,  $C$ ,  $n$ , and  $m$ . In the first stage, the Paris constants for the multiple- $R$  data are obtained ignoring the dependence on  $R$ . The second stage uses a coarse trial-and-error process along trial intervals centered around the initially obtained values to obtain improved values of  $C$  and  $n$ , and a first estimate of  $m$ . In the third stage, the Newton-Raphson technique is used to solve the non-linear set of error minimization equations and obtain final, accurate values of  $C$ ,  $n$ , and  $m$ . Using the first two priming stages ensures that the N-R technique is robust and converges to the correct results.

The Walker fit algorithms work best when the crack growth data are drawn from many different  $R$  values, and will not work at all unless at least two different  $R$  values are used. Since separate values of the exponent  $m$ ,  $m^+$  and  $m^-$ , are obtained for positive and negative values, respectively, of  $R$ , obtaining accurate values of  $m^+$  and  $m^-$  requires that crack growth data be supplied for both positive and negative values of  $R$ .

If the spline fit option is chosen, the algorithm divides the  $\log[\Delta K]$  domain into a sequence of intervals and fits piecewise cubic polynomials that minimize the sum of the square of the errors,

$$e_n = \log[da/dN_n] - \sum_{j=0}^3 A_{I,j} \log[\Delta K_n]^j \quad (6.3)$$

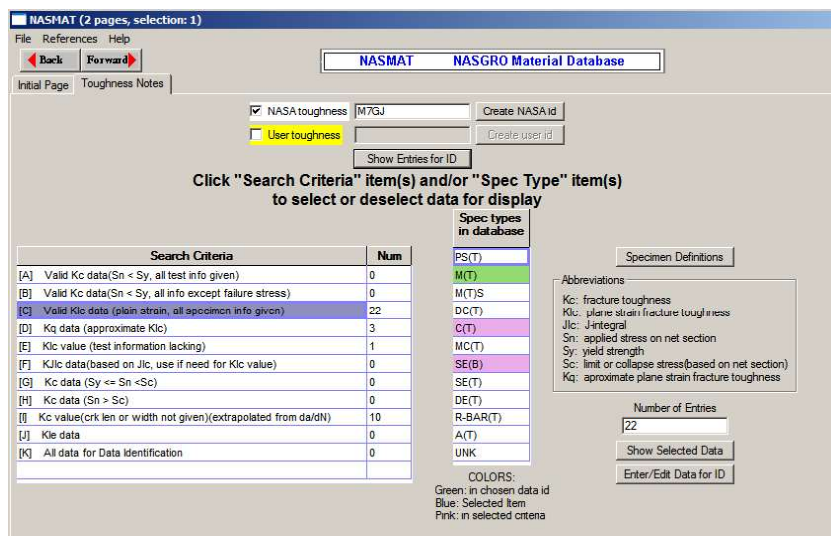
over all the data sets.  $A_{I,j}$  in the equation above are the coefficients of the cubic polynomial for the  $I$ th interval; and the index  $n$  refers to the  $n$ th data pair. The piecewise polynomials constructed are based on a modification of the standard rules for splines: functional and first derivative continuities are imposed at the knots between intervals, but no conditions are imposed on the second derivatives, at either the knots or the end points. These modified

splines avoid the problem (noticed in standard splines) of fits being affected by non-local variations in data, and thereby reduce the overall fitting error. An over-determined system of equations, in which there are more equations than unknowns, is finally obtained, which is solved by a least-squares technique. As programmed, the algorithm can be used to fit any curve. A default value of 4 is used for the number of intervals, but other values, depending on the amount and variation of data, can be used to enhance the goodness of fit.

If satisfactory curve fit constants have been obtained, you may obtain a hardcopy of the plot. If the curve fit that was plotted is not acceptable, the program allows you to start over with different parameters or constants and refit.

### 6.3 Entering and Processing Fracture Toughness Data

Once the fracture toughness database is selected from the opening screen, the next screen prompts for a data ID input. For the NASA database, the ID can be built from a sequence of text boxes by selecting the alloy type, etc. Then, by clicking on the notes/specs. button, the user can select the desired criteria and the specimen type for which available data will be displayed. Once the data is displayed, curve fitting to determine the constants in Eq. 2.12 can be done. The fit and the data can also be plotted for comparison purpose. The plot can be redone using different limits on x and y axes. Selected toughness data can also be averaged. The graphical user interface helps to screen the data using various criteria and process it as desired. The screen capture below shows the selection criteria.



The search criteria are chosen by clicking on the line(s) that has(have) a number of entries greater than zero (Line C in the above example). The grid labeled “Spec types in database” shows that for the chosen criterion the toughness data was obtained using specimen types of C(T) and SE(B). Descriptions of specimen types can be viewed by clicking on the button labeled “Specimen Definitions”. Clicking on the button labeled “Show Selected Data”, will display the following screen:

Initial Page | Toughness Notes | Toughness Data |

Data ID	N	Matl. Desc. and Heat Treat	Env	Type	Thk	W	a	2c	YS	UTS	On	S	Tough
M7GJ11AA07A	C	7050-T73651 PH(1")~ NA	-65F	C(T)	1.000	2.000	1.030	NA	75.70	NA	L-T	NA	35.100
M7GJ11AA08A	C	7050-T73651 PH(1")~ NA	OF	C(T)	1.000	2.000	1.030	NA	73.40	NA	L-T	NA	37.200
M7GJ11AA10A	C	7050-T73651 PH(1")~ NA	250F	C(T)	1.000	2.000	1.030	NA	64.40	NA	L-T	NA	37.300
M7GJ11AB01I	C	7050-T73651 PH(1")~ NA	75F	SE(B)	1.000	2.000	1.000	NA	73.80	NA	L-T	NA	37.000
M7GJ11AB01H	C	7050-T73651 PH(3.5")~ NA	75F	C(T)	1.500	3.000	1.450	NA	67.40	NA	L-T	NA	31.000
M7GJ11AB01G	C	7050-T73651 PH(4")~ NA	75F	C(T)	1.250	2.500	1.250	NA	67.20	NA	L-T	NA	34.500
M7GJ11AB01F	C	7050-T73651 PH(4")~ NA	75F	C(T)	1.500	3.000	1.500	NA	65.00	NA	L-T	NA	28.000
M7GJ11AB01E	C	7050-T73651 PH(6")~ NA	75F	C(T)	1.000	2.000	1.000	NA	61.20	NA	L-T	NA	29.500
M7GJ11AB01D	C	7050-T73651 PH(5")~ NA	75F	C(T)	2.000	4.000	2.000	NA	63.70	NA	L-T	NA	25.500
M7GJ11AB01D	C	7050-T73651 PH(5")~ NA	75F	C(T)	2.000	4.000	2.000	NA	60.30	NA	L-T	NA	29.000
M7GJ11AB01C	C	7050-T73651 PH(5")~ NA	75F	C(T)	1.000	2.000	1.000	NA	59.00	NA	L-T	NA	31.000
M7GJ12AA07A	C	7050-T73651 PH(1")~ NA	-65F	C(T)	1.000	2.000	1.030	NA	75.00	NA	T-L	NA	30.200
M7GJ12AA08A	C	7050-T73651 PH(1")~ NA	OF	C(T)	1.000	2.000	1.030	NA	72.70	NA	T-L	NA	31.200

**NOTE**  
Average toughness and standard deviation will be calculated using the selected toughness values.  
>> Click on a toughness value to toggle selection of it.  
>> Click on the "Tough" column label to toggle selection of all values.

Instructions and prompts are provided on this screen that will allow the user to calculate an average toughness and standard deviation for any number of the entries in the grid. A plot of Kc vs. Thickness can be obtained for the chosen toughness values by clicking on the button labeled “Plot Kc vs Thickness”.

## 6.4 Files created by NASMAT

*All the files listed below except for the user named files are written to the DATAFILES sub folder of NASMAT. The path to the DATAFILES/NASMAT directory is set during installation.*

1. SCREEN.OUT: A log file that shows all the prompts from the Fortran curve fit program and the response read from the input file (INDATA.CF) that was created by the NASMAT GUI.
2. INDATA.CF: The input file created by the NASMAT GUI when a curve fit is requested. It contains the header information, da/dN and delta K data, and all the flags that indicate options for the Fortran curve fit program.
3. NMDADK\_fth/cth-x.PLT: A file generated by the Fortran curve fit program that contains commands for the Gnuplot plot program. The file is named either “\_fth” or “\_cth” to differentiate between the Fth and Cth data. The x in the file name is either s, p, or c to indicate that the file is to be used for screen plot, postscript file, or cgm file, respectively.
4. DADNDK.BAS: This file contains the da/dN vs. delta K test data that is to be plotted on a curve fit plot.
5. DADNDK.FIT: This file contains curve fit data to plot the curve(s) on a curve fit plot.
6. THRESH.PLT: A file generated by the Fortran threshold program that contains commands for the Gnuplot plot program. It is created when a threshold plot is done for the calculation of Cth, DK0, and DK1.
7. THRESH.BAS: This file contains the R value and DKth test data that is plotted on a threshold plot.
8. THRESH.FIT: This file contains curve fit data to plot the curve on a threshold plot.
9. GNUSCRPT and GNUPOD: Files that contain commands for the Gnuplot plot program. These files are generated by the NASMAT GUI at different places in the program and used when plotting data only (i.e., no curves).
10. DADK.BAS: This file contains the da/dN vs. delta K test data that is to be shown on a “data only” plot.
11. KCPLOT.PLT: This file contains commands for the Gnuplot plot program and is generated in the toughness part of the NASMAT GUI. It is used to plot thickness vs. Kc.
12. TEMP.PLT: A file created by the NasPlot routine that contains title information entered on the plot dialog box.
13. THKKC.BAS: This file contains thickness and Kc values to be plotted.
14. THKKC.FIT: This file contains data to plot the curve for a thickness vs. Kc plot.
15. NASTMP and NASMAT.OUT: These files are created by the Fortran curve fit program when a fit for da/dN vs. delta K data is done. They contain header data information and the curve fit constants.
16. User named file for toughness data: This file is a copy of the grid that shows toughness values along with header data (e.g. id, thk, width, environment, etc.). It is written in a comma delimited format that is compatible with Microsoft Excel. If it is saved with a .csv extension, it will be associated with Excel by the Windows system.

The user may write the file by clicking on the button labeled “Write Data To File” when the toughness data is displayed.

17. User named file for da/dN and delta K data: This file will be written when one of the buttons labeled “Write all data” or “Write this R val” is clicked. These buttons are on the dialog box that shows detailed information (i.e., header data and da/dN delta K values for each R value) for a data set. This dialog box will be displayed by clicking on a data id button that is displayed on the notebook page labeled “Choose Plot/Fit Data”. The file is written in a comma delimited format that is compatible with Microsoft Excel.

## 7.0 Boundary Element Method Analysis

This chapter describes the use of the NASBEM (*NASA Boundary Element Method*) computer program, a tool for fracture mechanics and stress analysis of two-dimensional elastic bodies of arbitrary geometry and loading, with or without cracks, and multiple zones of different materials. This module can be particularly useful for generating stress-intensity factor solutions for complex crack configurations not found in NASGRO's built-in library; these solutions can then be imported into NASFLA (via the Data Tables crack case) for fatigue crack growth calculations.

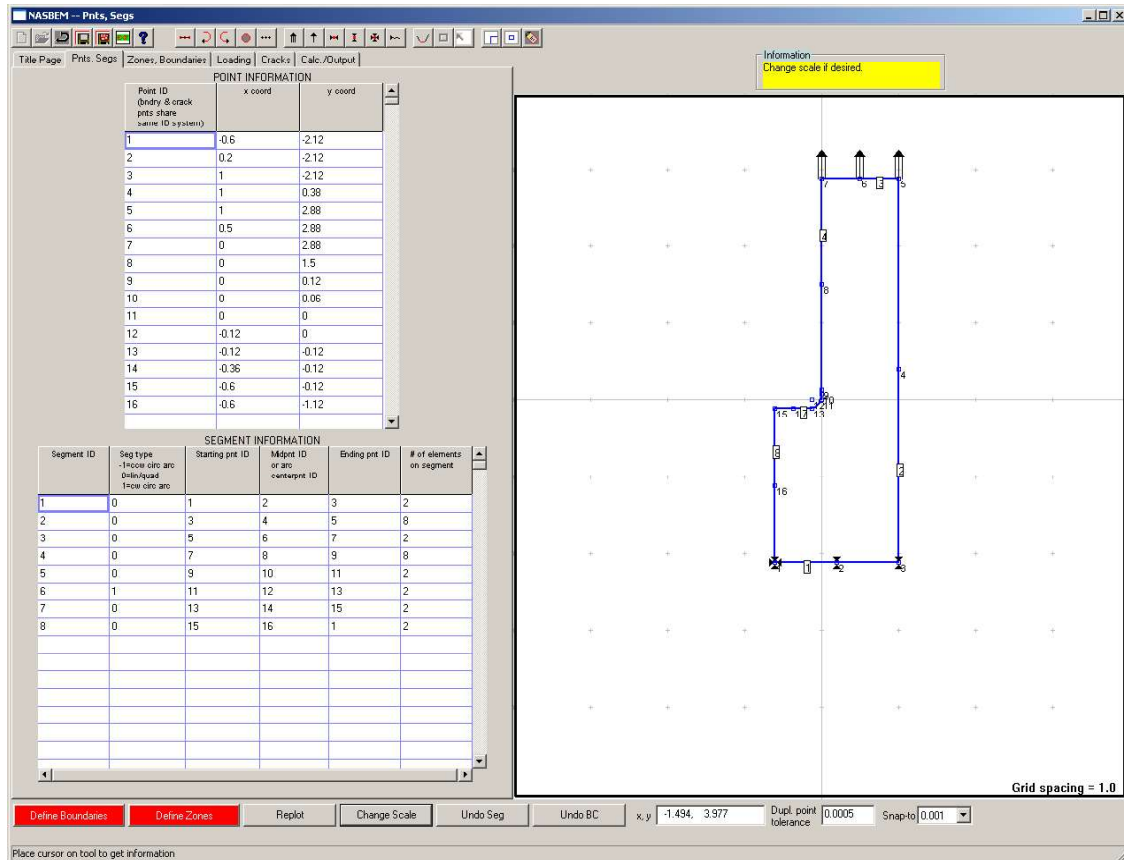
Although transparent to the user, NASBEM consists of three parts: a user-friendly data input interface, the boundary element method (BEM) computational engine which also contains the stress-intensity factor calculation and crack profile calculation codes, and a post-processing stress analysis component with optional graphical output. The data input interface, crack profile and stress analysis codes were developed at NASA's Johnson Space Center and their use is described in this chapter. The boundary element computational engine was furnished by researchers at the University of Texas as part of their FADD (Fracture Analysis by Distributed Dislocations) computer code; in this development of the BEM, cracks are modeled by point dislocations and external and internal boundaries by conventional boundary elements. Please see reference [46] for the theoretical basis, and Appendix T for example problems.

*Note: the ability to specify a problem as being of infinite domain has been temporarily disabled pending resolution of an internal coding problem. Due to the expected temporary nature of this process, this chapter has not been updated to reflect this change.*

### 7.1 The Data Input Interface

The data input interface for NASBEM, shown in the figure below, consists of two parts. On the right side is a drawing surface where the BEM model can be constructed graphically by using the built-in drawing tools; these tools are available on the button toolbar at the top of the interface. On the left side is a series of "notebook" pages, each containing tables with detailed information on particular basic components of the model (boundaries, loads, materials, cracks, etc). These tables are updated automatically as components are created graphically with the drawing tools, but they can also be edited manually to correct or fine-tune values or even to create a model or its components without the use of the drawing tools. When manually editing tables the drawing is not updated until the user clicks on the "Replot" button at the bottom of the interface.

A fundamental aspect of this user interface is that one can quit the program before input for a particular problem is complete (first saving the entered data to file, of course), and then resume input and perform computations at a later time.



## 7.2 The Philosophy of Building a NASBEM Model

The underlying principle of building a model in NASBEM is that it is similar to the levels of a pyramid. One starts at the bottom by defining the most basic building block, the point. The second level in the pyramid is to create boundary segments by connecting these points. The next level is to assemble boundaries from boundary segments. Similarly, crack segments are built from points, cracks from crack segments, and material zones by identifying which boundaries and cracks are contained within each zone. Finally, one attaches boundary conditions (the boundary loads and displacements) to segments. There are specialized tools to aid in building some common, but more complicated parts of a model such as lugs or pin-loaded holes.

This section describes the philosophy of building a model by defining these building blocks and specialized tools. A subsequent section outlines their practical use in building a model, including restrictions and caveats.

All the aforementioned building blocks are automatically assigned id numbers, i.e. numeric labels, by the program to aid in defining which segments are built from which points, which boundaries are built from which segments, etc. These id numbers start with “1” by default and numbering proceeds sequentially, but they can be modified by the user by editing the tables.

This can be especially useful for identifying particular groups of building blocks, e.g. all the segments belonging to a particular boundary, by giving them an easily identifiable range of id numbers. Care must be taken, though, to edit all the tables where the particular item's id number shows up; for example, id numbers for points are present in the point definition table, the boundary segment definition table, the crack segment definition table, and the point load definition table.

In some sections ***bold italic*** font is used to draw attention to additional tasks required of the user when building blocks are created by manually editing the tables. For example: when defining a segment by adding segment endpoints to the segment table, the user must ensure that the points referenced in that table are also defined in the points table. The drawing tools are designed to relieve the user from such tasks; however, if editing the tables manually the user is responsible for seeing those tasks completed.

### 7.2.1 Points

Points represent prominent locations in the model, such as:

- boundary segment endpoints and midpoints in the case of linear or curved segments, or endpoints and arc center points in the case of circular arc segments,
- crack segment endpoints (and arc center points in the case of circular arc segments) for the general crack case (see subsequent section),
- crack endpoints for the special crack case (see subsequent section),
- concentrated load locations,
- hole centers in the case where internal hole boundaries are entered as special case boundaries (see subsequent section)
- a point within an infinite body where displacements are fixed to eliminate rigid body motion (note: such a point cannot lie on a crack or a boundary within that body)

If the drawing tools are used to create building blocks, points are defined automatically by the tools from the coordinates where the user placed the building block, for example from the endpoints of a boundary segment or from the centerpoint of a hole.

***Note: If any tables are edited manually to add building blocks, then the user must ensure that any points referenced in a particular table are also defined in the Point Information table, adding them manually if necessary.***

### 7.2.2 Boundary Segments

Segments connect these points to form part of a boundary. A segment is defined as a portion of the boundary over which both the geometry and the loading distribution vary smoothly. This means that a section of a boundary can be considered a segment as long as the following are satisfied:

- that section's geometry can be adequately defined by a segment's three defining points (endpoints and midpoint for linear segments; endpoints and arc centerpoint for curved arc segments), and

- the boundary conditions along that segment can be adequately defined by specifying their values at the segment endpoints and midpoint.

For example, a linear section of the boundary that has a distributed load acting over only a portion of this section must be split into several linear segments: one spanning the portion with the distributed load, and one or more spanning those portions without a load. Accordingly, boundary discontinuities such as corners/kinks or boundary intersections with cracks must fall on segment endpoints.

Available boundary segment types are linear and circular arcs (both clockwise/counter-clockwise arcs). Uniformly spaced quadratic elements are generated internally on each segment; element size is governed by the number of elements specified per segment. Some notes about element size and spacing:

- for boundary segments intersecting an edge crack: in the vicinity of the intersection the size of the elements on the boundary should be of the same order of magnitude as those on the crack
- for crack tips near a boundary: the size of the elements on the boundary should be of the same order of magnitude as those on the crack
- for point loads near a boundary: the size of elements near the point load should be of the same order of magnitude as the distance between the point load and the boundary
- it is advisable to use denser element spacing on boundary segments near stress concentrations, stress discontinuities, and crack tips

The term “near a boundary” is a subjective term and cannot be adequately quantified in general terms; however, it is the stress gradients in the vicinity of such points that must be adequately captured by the element distributions.

*Note: If the Segment Information table is edited manually, then the user must ensure that any points referenced in that table are also defined in the Point Information table, adding them manually if necessary.*

One of the attractive features of this BEM is that it generally requires fewer elements in the model than other BEM implementations. However, the user is urged to experiment with element density and distribution and, as with all boundary/domain discretization analysis tools, to perform convergence studies to assure accurate results.

### 7.2.3 Boundaries

Boundaries of arbitrary shape can be assembled from the linear and circular arc segments. In the present context a boundary is considered to be a closed line in space marking the edge of a given material. Thus, there are external boundaries, internal boundaries (i.e. holes), and boundaries that share one or more segments, as in the case of a body consisting of adjoining regions (or zones, in NASBEM parlance) of differing materials where each boundary marks the extent of the material within it.

It is possible to have a geometry in which the physical external boundary is so far away from any other geometric feature of interest (e.g. a crack) that entering the actual external boundary coordinates is impractical, and for which the loading along such a boundary is uniform. In

such a case one can select the problem scale to be one with an infinite external boundary and supply the uniform remote stress, and dispense with entering any other information about the external boundary.

***Note 1: If defining zones (see next section for definition of zones) and boundaries by manually editing the tables, only finite boundaries need be assigned id numbers and counted in zone definitions.***

***Note 2: If the Ordinary Boundary Information table is edited manually, then the user must ensure that any segments and edge cracks referenced in that table are also defined, respectively, in the Segment Information and Crack Information tables, adding them manually if necessary.***

Boundaries must be defined by giving the boundary segment id numbers in sequence (important!) while traveling around the boundary, keeping the body to the left. Thus, external boundaries are generally defined in a counter-clockwise manner, while internal boundaries are generally defined in a clockwise manner, although local sense reversals are possible as in the case of a U- or C-shaped indent or bulge in a boundary.

Finally, some points to note are

- while cracks may intersect a boundary, crack segments are not included in the set of boundary segments used to define the boundary
- see the subsequent section “Special case geometries” for descriptions of simplified input of special boundary cases

#### 7.2.4 Zones

Zones are regions within the body enclosing a single material. To this end zones are bounded by boundaries, both external and internal, and may contain cracks, both edge and internal. For example, a body consisting of three distinct regions, where two regions of the same material are separated by a region of a different material, would be entered as three zones, with two zones tagged with one material and the third zone tagged with the other material. All zone interfaces are assumed to be perfectly bonded and cracks are not allowed to lie along or intersect an interface.

Multi-zone problems are useful for modeling stiffened plates, for example. The part of the plate with the stiffener underneath would be entered as a separate zone with its elastic modulus adjusted to account for the combination of stiffener and plate. Multi-zone problems by definition contain boundaries which coincide along one or more stretches. The boundary segments in these stretches need be defined only once; however, the id numbers of these segments will feature in the definition of each of the boundaries concerned. Note that multi-zone geometries are not allowed for problems with an infinite external boundary.

***Note: If the Zone Information table is edited manually, then the user must ensure that any materials, finite boundaries, cracks, and point loads referenced in that table are also defined, respectively, in the Material Information, Boundary Information, Crack Information, and Point Load Information tables, adding them manually if necessary.***

In versions of NASBEM prior to 5.11, stress analysis was possible only in zones without cracks; this required defining multiple zones made of the same material, some with cracks and some without, for cases in which one needed both SIF and stress analysis. As of this writing it is possible to perform stress analysis in zones with cracks as long as the point of interest is in the proximity of the crack line or tip. It is planned to implement complete stress analysis capability in zones with cracks in a future version of NASBEM.

### 7.2.5 Crack Segments and Cracks

Cracks are built up in the same manner as boundaries; that is, points define crack segments and crack segments define cracks. Some considerations to be noted:

- while physical cracks have top and bottom faces, this code makes no such distinction and cracks are modeled by a single line of segments only
- available crack segment types are linear or circular arc; uniformly spaced linear elements are generated internally on each segment (quadratic crack elements are planned for a future version of the code)
- crack segments and boundary segments are both called “segments” but are different kinds of segments and thus have separate id numbering sets; and while cracks may intersect boundaries (and therefore crack segments intersect boundary segments), boundaries are built from boundary segments only and do not include crack segments
- unlike segments, there is only one kind of point; that is, points on boundaries and points on cracks (along with points defining point load locations, etc) are all part of the same single point id numbering scheme
- edge cracks must intersect boundaries at boundary segment endpoints

*Note for edge cracks if editing tables manually: the user must ensure that the point id number of the crack segment endpoint and that of the boundary segment endpoint at the intersection match; however, for special case hole boundaries (described in a subsequent section) the hole’s segment generation and intersection with the crack is done internally and the user need not intervene*

- edge cracks should be defined by specifying the constituent crack segments from the edge (i.e. the crack mouth) to the crack tip
- crack segments cannot intersect or coincide with inter-zonal boundary segments
- crack loading conditions are specified as uniform normal and tangential loads over a crack segment
- for edge cracks: in the vicinity of the crack/boundary intersection the size of the elements on the boundary should be of the same order of magnitude as those on the crack
- see the subsequent section “Special case geometries” for input of special crack cases

*Note 1: If the Crack Segment Information table is edited manually, then the user must ensure that points referenced in that table are also defined in the Points Information table, adding them manually if necessary.*

*Note 2: If the Ordinary Crack Information table is edited manually, then the user must ensure that crack segments and any intersecting boundaries referenced in that table are also defined, respectively, in the Crack Segment Information table and the*

*Ordinary Boundary Information table (or in the Special Hole Boundary Information table, if applicable), adding them manually if necessary.*

*Note 3: If the Ordinary Crack Information table is edited manually, then the user must ensure that any cracks defined in that table are also appropriately referenced in other tables, adding them manually if necessary.*

### 7.2.6 Boundary Conditions and Concentrated (or Point) Loads

Boundary conditions are specified by giving the type (traction or displacement) and value at a boundary segment's endpoints and midpoint. Components in the  $x$ - and  $y$ -directions are used for linear segments, while circular arc segments require normal and tangential components.

The default boundary condition assumed for all element nodes is one of zero traction in both coordinate directions, so that only those segment midpoints or endpoints with displacement conditions or non-zero traction conditions need have their boundary conditions specified. Note that the boundary condition type and value must be specified for both coordinate directions at any point where boundary conditions are specified, regardless of whether one of those components is a zero traction.

Recall that a boundary segment is defined as a portion of the boundary over which both the geometry and the loading distribution vary smoothly. A boundary segment in fact serves as the basis for a simple mesh generator within the NASBEM computational engine. To this end, the rules for boundary condition (BC) generation along a segment are as follows:

- the BC type assigned to a segment midpoint is assigned to all element nodes on that segment except the first and last nodes (i.e. the two segment endpoints)
- the BC type assigned to a segment endpoint is valid only for the node corresponding to that segment endpoint
- the BC values for all nodes on a segment (including those two at the segment endpoints) are interpolated quadratically from the values entered by the user at all three segment points (midpoint and two endpoints)

The BC then, nominally applied at segment endpoints and midpoints, are associated with the particular segment. This means that

- the BC at a point on a segment can be interpreted to be the value obtained as one travels along that segment and approaches that point; thus it is possible for a segment endpoint that is shared by two segments to have two sets of BC, one for the first segment and another for the second segment
- mixed BC (traction in one coordinate direction, displacement in the other), such as those used to fix a body in space in order to eliminate rigid-body solution modes, should be examined carefully before being set
- in this version of NASBEM, mixed BC can be accommodated only on segments which are parallel to one of the coordinate axes, i.e. not on the following: inclined straight segments, curved segments, or circular arc segments

- care must be taken in how boundary segments are defined so that boundary conditions can be properly accommodated at the segment endpoints/midpoints and properly generated on the elements along the segment.

Any applied concentrated loads are defined independently of boundary conditions by specifying their location and their value;

***Note 1: If the Point Load Information table is edited manually, then the user must ensure that points referenced in that table are also defined in the Points Information table, adding them manually if necessary.***

***Note 2: If the Point Load Information table is edited manually, then the user must ensure that point loads defined in that table are also referenced in the Zone Information table, adding them manually if necessary.***

For point loads close to a boundary, the boundary element size in the vicinity of the point load should be of the same order of magnitude as the distance between the point load and the boundary. Point moments can be simulated by having two point loads acting in opposite directions and separated by a small distance.

It should also be noted that a body must be fixed in space in order to eliminate rigid body motion (translation and rotation) from the solution. In general, for finite bodies this can be accomplished by choosing two points on the boundary, one where both x- and y-displacements are set to zero and another point where either x- or y-displacement is set to zero. For infinite bodies this is accomplished by specifying a point within the body where both displacements are set to zero; the boundary element algorithm assumes that rotations at infinity are zero.

## 7.2.7 Special Case Geometries

NASBEM has a meshing “assistant” to facilitate input of several commonly occurring yet complex geometric components where even using the individual drawing tools to build up these components, while much easier than manually editing the tables, would be complicated and tedious.

### 7.2.7.1 Special Case Geometries: Circular Hole Boundaries

The first special case is input of circular hole boundaries with up to two collinear cracks, optional uniform internal pressure, and optional pin (or bearing) loading. Recall that a boundary segment is defined as a portion of the boundary over which both the geometry and the loading distribution vary smoothly, and that edge cracks must intersect a boundary at boundary segment endpoints only. Thus, for a first cut, potential boundary segment endpoints are the load arc endpoints as well as the crack/hole intersection(s); depending on the relative location of the bearing load and the crack intersection(s), the hole may have to be divided into several segments in order to adequately accommodate the boundary conditions and crack location(s). This task of selecting the segment distribution around a hole can quickly become tedious and prone to errors if done manually.

Rather than forcing the user to define such holes by calculating segment endpoints and boundary conditions, with this special case option one merely specifies the hole location, direction of the pin load resultant, the average bearing stress on the hole (taken as  $P/2rt$ , the ratio of pin load value per unit thickness and the hole diameter).

*Note: If the Special Hole Boundary Information table is edited manually, then the user must ensure that points and edge cracks referenced in that table are also defined, respectively, in the Points Information table and the Crack Information table, adding them manually if necessary.*

NASBEM will calculate the appropriate segment distribution, an element distribution within those segments (dependent on the crack-size-to-hole-diameter ratio, and relative crack(s) and pin load position), and nodal boundary condition values. Note that special case hole boundaries and “ordinary” boundaries differ only in the manner of input. Thus they share the same id numbering system and there should be no duplication of id numbers between the two.

A note on boundary conditions on a hole due to pin or bearing loading: a commonly-used approximation for modeling such boundary conditions is to use a cosine load distribution along 180° arc, centered about the bearing load resultant. NASBEM, however, generates quadratically varying tractions from the segment’s endpoint and midpoint traction values; the difference between this quadratic variation and the cosine distribution (equilibrated to give the same resultant) is less than 4%.

### 7.2.7.2 Special Case Geometries: a Row of Holes of Uniform Diameter

The second special case is input of a row of holes of uniform diameter; the user provides the locations of the centerpoints of the first and last holes and specifies the number of holes to be generated and their diameters. Note that the meshing assistant treats a row of holes as just a case of multiple “special case” holes but does not ask for input of internal pressure or bearing stress; these can be added by manually editing the “Special Hole Information” table.

### 7.2.7.3 Special Case Geometries: an Arc Connected to One or Two Inclined Linear Sections

The third special case is input of an arc connected to one or two inclined linear sections. This can be particularly useful in creating a model of a tapered lug. For example, the only information known about the bottom curved portion of a lug may be a point on each of the inclined sides, as well as the centerpoint of the arc connecting the two sides; the meshing assistant determines the point of intersection of the inclined faces and the circular arc, and creates the segments for the mesh.

#### 7.2.7.4 Special Case Geometries: SIF Analysis of a Single Straight Crack, Evaluated Automatically at Multiple Lengths

The fourth special case is that of SIF analysis of a single straight crack, evaluated automatically at multiple lengths. Without this meshing assistant, in order to calculate the SIF for a crack at multiple sizes, a user would need to define a new crack and then run the analysis for each length. However with the meshing assistant, one merely defines a single crack for the initial length, the final-to-initial crack length ratio and the number of lengths to calculate, and then sends the job off for analysis only once. NASBEM will calculate the appropriate crack configurations and tabulate the output as length versus SIF. These results can then be used easily in other modules of NASGRO. Note that since it is defined by its endpoints and is restricted to be straight, this type of crack is essentially a single-segment crack; separate specification of crack segments is not necessary (and, in fact, not allowed).

*Note 1: If the Special Crack Information table is edited manually, then the user must ensure that any points and intersecting boundaries referenced in that table are also defined, respectively, in the Points Information table and in the Ordinary Boundary Information table (or in the Special Hole Boundary Information table, if applicable), adding them manually if necessary.*

*Note 2: If the Special Crack Information table is edited manually, then the user must ensure that the crack defined in that table is also appropriately referenced in other tables, adding it manually if necessary.*

#### 7.2.8 Materials

This program assumes that all materials are linearly elastic and homogeneous; the user must simply provide the elastic modulus and Poisson ratio to fully define a material.

#### 7.2.9 Stress Analysis

Stress analysis is performed as a post-processing task by specifying the number of points, either individually or as falling along one of several available line types, at which to calculate stress values. As noted above, in versions of NASBEM prior to 5.11, stress analysis was possible only in zones without cracks; this required defining multiple zones made of the same material, some with cracks and some without, for cases in which one needed both SIF and stress analysis. As of this writing it is possible to perform stress analysis in zones with cracks as long as the point of interest is in the proximity of the crack line or tip. It is planned to implement complete stress analysis capability in zones with cracks in a future version of NASBEM. Note that stress analysis is not available for the special case of a single straight crack evaluated at multiple lengths due to the sequential nature of the calculations involved for this case and stress analysis being a post-processing feature.

### 7.3 The Drawing Toolbar

This section describes the toolbar in some detail as shown in the figure below. The toolbar can be found at the top of the input interface and contains buttons for various bookkeeping tasks such as loading and saving input files, as well as buttons for the built-in drawing tools. As described in an earlier section, a model can be constructed by typing details directly into the information tables or by using the drawing tools, which will populate the tables automatically. In most cases the drawing tools will provide a much quicker way to input a model's data.



Note that for purposes of illustration all the buttons in the figure above are displayed as “enabled”, i.e. available for use; during various phases of the interface’s normal operation some buttons will be disabled (“greyed out”) if their function does not apply to that particular phase of input or calculations.

#### 7.3.1 File Manipulation Buttons

Upon program start-up the drawing surface is blank, the “Title Page” notebook page is the only notebook page displayed, and all toolbar buttons are disabled (“greyed out”) except the following:

- “Create new file” – select this item to start entering data for a new problem. Selecting this enables all the notebook pages for editing information tables manually, and enables the drawing surface and the toolbar buttons for drawing the mesh and filling the tables automatically.
- “Open existing file” – select this item to load and display input data from a file created earlier. This file may have been created by the program in an earlier session and the data it contains may or may not be complete. [Alternatively, the file may have been created by using a text editor, adhering to a prescribed format (important!)...see the description for “Save file” below.] Upon loading the file, the file name is displayed in the title bar of the NASBEM window is shown in the figure above.
- “Exit” – selecting this button shuts down NASBEM after prompting the user to save any unsaved input.
- “Help” – select this item to display a pop-up box for displaying version information and a list of recent updates to the program.

Once  “Create new file” button or  “Open existing file” has been selected, additional file manipulation buttons become available:

-  “Start over” – selecting this button clears the drawing surface, all information tables in the notebook pages, and all internal data buffers, and prompts the user to save any unsaved input. The user input interface is restored to the initial start-up state.
-  “Save file” – select this item to save to file any data entered in the current session. Data sections within these files are written in a prescribed order and format, and each section begins with three comment lines (each starting with the character #) and continues with data pertaining to that section:
  - The first comment line contains a short section description.
  - The second comment line contains a description of what is written on the first data line.
  - The third comment line contains a description of the information contained in the remaining data lines.
  - Following the comment lines are the section’s data lines, where the first data line generally contains the number of items to read (e.g. how many points in the model) and subsequent data lines contain the information associated with each item (e.g. the point’s id number and coordinates).
  - Example:
 

```
#points
#line 1: no of points
#line n: pnt id no, x and y coords
4
1  -.6000      -2.120
2   .2000      -2.120
3   1.000      -2.120
4   1.000       .3800
```
  - Note: for those users who wish to manually create a data file, it is advisable to first choose the “Save file” option without having any actual data to save; NASBEM will write a data file that can serve as a template with all the data sections listed in the proper order (important!).
-  “Save file as” – selecting this performs the same action as  “Save file” with the user prompted for an optional filename change.

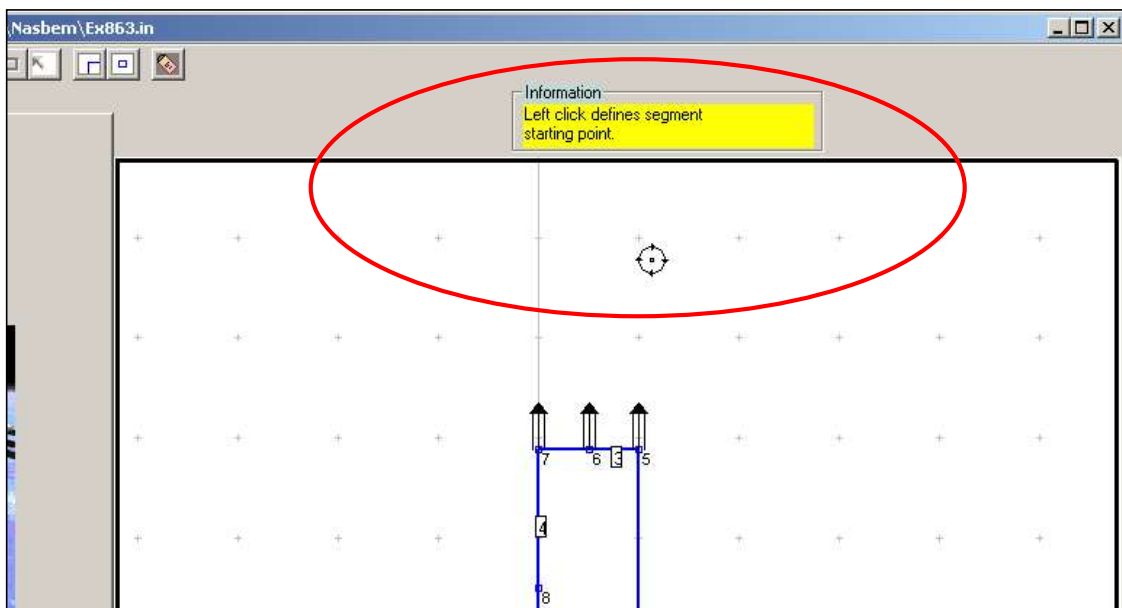
The , , and  buttons are duplicated on the “Title Page” notebook page itself and become enabled/disabled as described above.

The  and  buttons are duplicated on the “Calc./Output” notebook page and become enabled/disabled as described above.

### 7.3.2 Segment Drawing Tools and Mesh Assistants

Upon selection of the  “Create new file” button or the  “Open existing file” button, several basic segment drawing tools as well as three advanced drawing “wizards” become available for creating a model.

Note that when a drawing button is selected, the cursor changes from the standard Windows cursor to a representation of the selected tool, and that the yellow information window near the top right corner of the interface contains helpful hints about operation of the selected drawing tool, as highlighted in the figure below.



The basic drawing tools are:

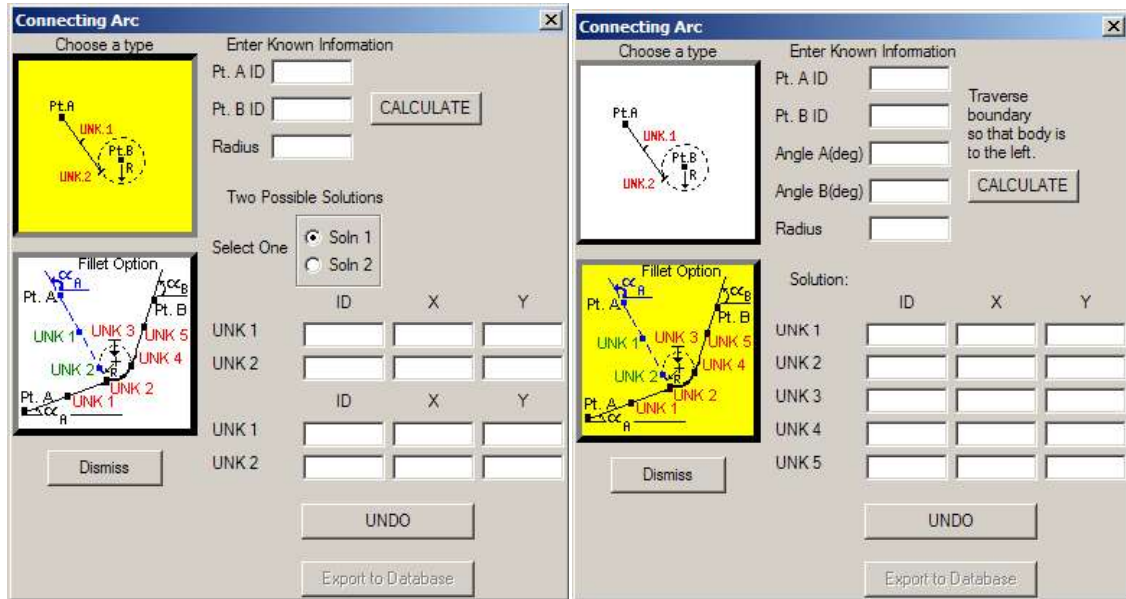
-  “Draw straight line” – select this tool to draw linear segments. After selecting this tool, a left-click on the drawing surface marks the location of the starting point (“first endpoint”) of the first segment to draw. The next left-click on the drawing surface marks the terminating point (“second endpoint”) of this segment. This drawing tool remains active until the right mouse button is clicked. While it is active the second endpoint of the segment just drawn automatically serves as the first endpoint of the next segment to be drawn; in this way consecutive linear segments can be drawn by simply left-clicking the terminating point of each segment. The interface automatically creates point definitions for the locations of the segment endpoints and segment midpoints, assigns IDs to those points, and populates the point and segment information tables.
-  “Draw clockwise arc” and  “Draw counterclockwise arc” – select these tools to draw clockwise and counterclockwise circular arcs. After selecting this tool, a left-click on the drawing surface marks the location of the starting point (“first endpoint”)

of the first segment to draw. The next left-click on the drawing surface marks the terminating point (“second endpoint”) of this segment. Finally, the arc centerpoint is then defined by a further left click on the desired location. This drawing tool remains active until the right mouse button is clicked. While it is active the second endpoint of the segment just drawn automatically serves as the first endpoint of the next segment to be drawn; in this way consecutive circular arc segments can be drawn by simply left-clicking the terminating point and the arc centerpoint of each segment. The interface automatically creates point definitions for the locations of the segment endpoints and arc centerpoints, assigns IDs to those points, and populates the point and segment information tables.

The three drawing “wizards”, or meshing assistants, are:

-  “Hole (Special Boundary)” – select this tool to activate the circular hole creation “wizard”. After selecting this tool, a left-click on the drawing surface marks the location of the hole’s centerpoint, and a pop-up input box will be displayed for specifying the hole radius, pressure, average bearing stress, and pin load direction. The interface automatically creates a point definition for the location of the hole centerpoint, assigns an ID to that point, and populates the point and Special Hole Boundary information tables. (Just prior do the calculation phase, when problem definition is complete, the interface calculates the optimum segment distribution around the hole based on pin load direction and crack location). This drawing tool remains active until the right mouse button is clicked.
-  “Rivet holes” – select this tool to activate the “wizard” to create a row of rivet holes. These holes are generated as “Special holes” (see above) but without loads or cracks; these can be specified later by manually editing the Special Hole information table. After selecting this tool, a left-click on the drawing surface marks the location of the centerpoint of the first hole in the row. The next left-click on the drawing surface marks the centerpoint of the last hole in the row, and a pop-up input box will be displayed prompting for the number of holes in the row and the holes’ radius (same radius for each hole). The interface automatically creates point definitions for the locations of the holes’ centerpoints, assigns IDs to those points, and populates the point and Special Hole Boundary information tables. (Just prior to the calculation phase, when problem definition is complete, the interface calculates the optimum segment distribution around the holes based on pin load direction and crack location). This tool does not remain active after the input boxes are dismissed.
-  “Draw connecting arc” – select this tool to activate the connecting arc creation “wizard”. This tool simplifies input of an arc connected to either one or two inclined linear sections when only limited information is known about the configuration. For example, perhaps only the vertices, fillet radius and lug angles of a tapered lug are known, but not the coordinates of some of the other points necessary for defining boundary segments. Selecting this tool from the toolbar displays a pop-up input box prompting for the known data as shown in the two figures below; the tool then calculates the unknown parameters (such as the point of intersection of the inclined faces and the circular arc), creates the segments for the mesh, and populates the point

and segment information tables. This tool does not remain active after the input boxes are dismissed.



As noted in the preceding paragraphs, some of the drawing tools remain active until the right mouse button is clicked. In practical terms this means that consecutive segments of the same type can be drawn by merely defining the segments' ending points (and arc centerpoints, if applicable) in sequence without separately having to redefine each segment's starting point.

### 7.3.3 Boundary Condition and Point Load Buttons

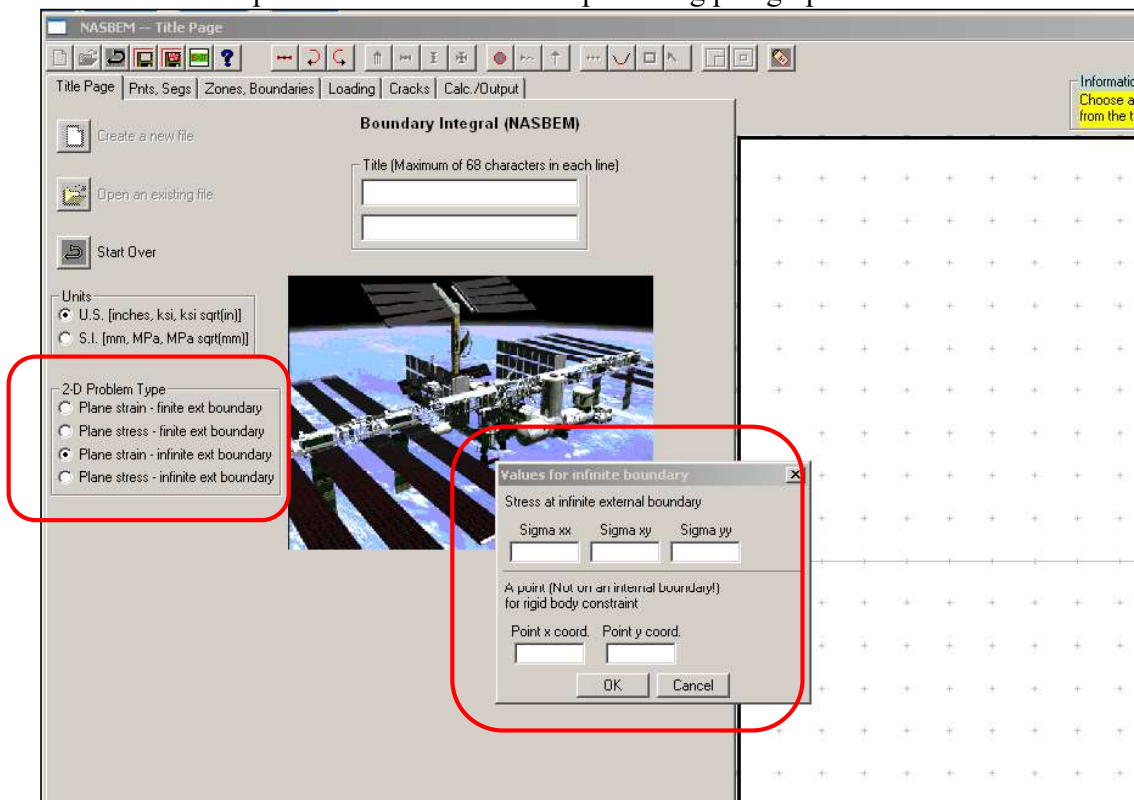
Three combinations of boundary conditions can be specified (tractions only, mixed tractions and displacements, and displacements only), as well as point loads (concentrated loads) in the interior of a body, by use of the following tools. Note that these tools remain active until the right mouse button is clicked.

- “Distributed load” – select this tool to apply tractions to any segment of a finite external or internal (i.e. hole) boundary. Recall that boundary conditions are specified at a segment’s two endpoints and midpoint. After selecting this tool, a left-click on the drawing surface at a segment endpoint or midpoint will display a pop-up window prompting for input of the  $x$ - and  $y$ -components of traction (or normal and tangential components in the case of circular arc segments). For endpoints shared by more than one segment the user must also specify which segment the boundary condition applies to. Recall also that crack segments are not part of the boundary segment set; crack face tractions are specified as part of the crack definition process.
- “Normal (x) constraint”, “Tangential (y) constraint”, and “ $x$  and  $y$  constraint” - select this tool to apply displacement constraints to any segment of a finite external or internal (i.e. hole) boundary. Recall that boundary conditions are specified

at a segment's two endpoints and midpoint. After selecting this tool, a left-click on the drawing surface at a segment endpoint or midpoint will display a pop-up window prompting for input of the  $x$ - and/or  $y$ -components of displacement (or normal and tangential components in the case of circular arc segments), depending on whether the constraint is defined in one or both coordinate directions. For constraints in one coordinate direction only (i.e. mixed mode boundary conditions), the other direction will require specification of a traction. For endpoints shared by more than one segment the user must also specify which segment the boundary condition applies to.

-  “Point load” – select this tool to define point loads (concentrated loads) acting on the interior of a body. After selecting this tool, a left-click on the drawing surface marks the location of the point load and a pop-up window will prompt for input of the point load’s  $x$ - and  $y$ -components.

For infinite domain problems, boundary conditions at infinity are specified at the time the domain is chosen to be infinite (using the “2-D Problem Type” radiobox on the “Title Page” notebook page). A pop-up input window will prompt for stresses at infinity and the point for eliminating rigid body motions, as shown in the figure below. Boundary conditions for interior boundaries can be specified as outlined in the preceding paragraphs.



### 7.3.4 Crack Definition Button

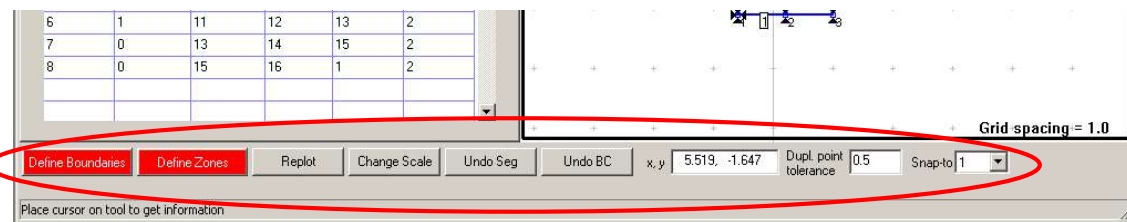
This button is not available until after zone have been defined.

-  “Crack” – select this tool to draw crack segments. After selecting this tool, a left-click on the drawing surface marks the location of the starting point (“first endpoint”) of the first crack segment to draw. The next left-click on the drawing surface marks the terminating point (“second endpoint”) of this segment. After this second click, a pop-up window will prompt the user for what kind of crack this will be: an “ordinary crack” or a “special crack” (a single straight crack evaluated at multiple sizes).
  - If a “special crack”, then a subsequent pop-up window will prompt the user for “special crack” details (crack face tractions, the number of crack sizes to calculate, and the ratio of the final to initial crack sizes).
  - If an ordinary crack, then the second endpoint of the segment just drawn automatically serves as the first endpoint of the next segment to be drawn; in this way consecutive segments can be drawn by simply left-clicking the terminating point of each segment. Right-clicking terminates the crack drawing mode and presents a pop-up window prompting the user to confirm details of all segments just drawn and to provide details of any crack face tractions.

The interface automatically creates point definitions for the locations of the segment endpoints, assigns IDs to those points, and populates the point and segment information tables. The interface will also populate boundary and zone information tables as needed with information regarding cracks intersecting boundaries and zones containing cracks.

## 7.4 Other Buttons not on the Drawing Toolbar

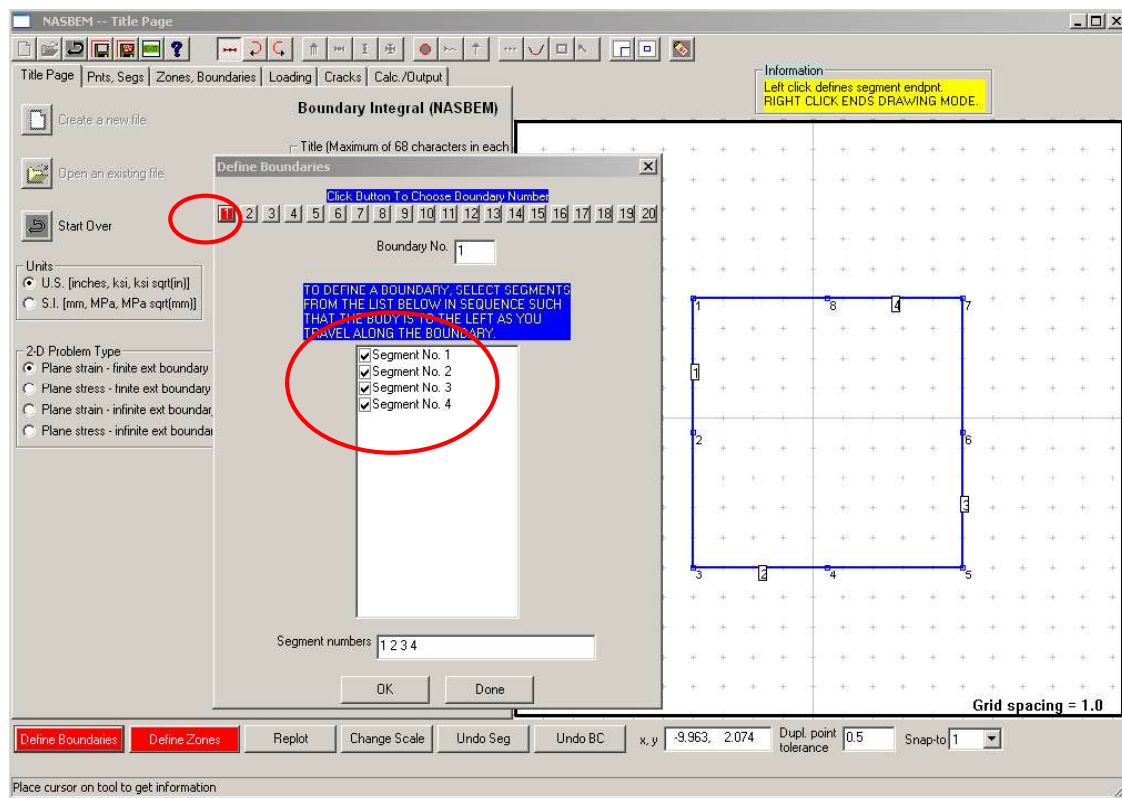
There is a row of buttons and input boxes along the bottom on the input interface below the information tables and drawing surface, as shown in the figure below. These buttons and input boxes, while necessary for creating models, are strictly speaking not drawing tools; hence they are not included in the toolbar along the top of the input interface.



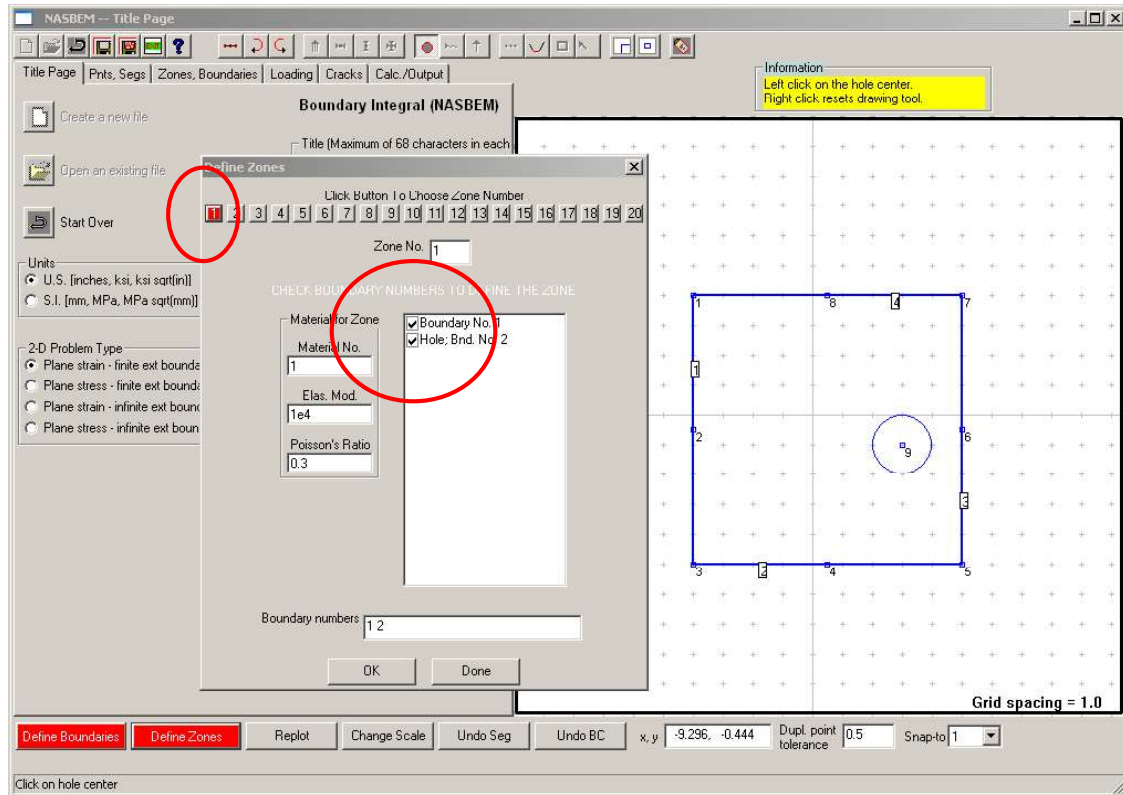
### 7.4.1 Mesh Assembly Buttons

These buttons are used to assemble the higher-order building blocks from the basic building blocks just drawn.

- **Define Boundaries** - select this tool, after the boundary segments have been defined, to specify which segments make up a particular boundary. Upon selecting this button a pop-up window will display a row of boundary ID buttons and a list of all the already-defined segments. Click the button for the desired boundary and select the appropriate segments' checkboxes in order so that the body is to the left as you travel along the boundary, as shown in the figure below. Click “OK” to store this information; the pop-up window will remain visible to allow other boundaries to be defined. Dismiss the window when done by clicking on the “Done” button.



- **Define Zones** - select this tool, after the boundaries have been defined, to specify which boundaries make up a particular zone. Upon selecting this button a pop-up window will display a row of zone ID buttons and a list of all the already-defined boundaries, as shown in the figure below. Click the button for the desired zone and select the appropriate boundaries' checkboxes —the order is not important—and supply the zone's material parameters. Click “OK” to store this information; the pop-up window will remain visible to allow other zones to be defined. Dismiss the window when done by clicking on the “Done” button.

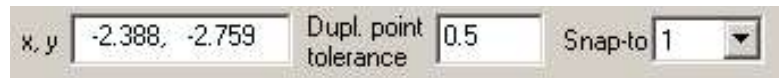


#### 7.4.2 Utility Buttons

- Replot** - select this button to refresh the drawing surface. NASBEM will update the drawing surface automatically when the drawing tools are used; this button is most useful when changes are made by manually editing the information tables.
- Change Scale** - select this button to change the minimum and maximum scale values of the drawing surfaces. NASBEM will adjust the axes to maintain a 1:1 aspect ratio between the x and y axes.
- Undo Seg** - select this button to delete segments in the reverse order that they were defined.
- Undo BC** - select this button to delete boundary conditions in the reverse order that they were defined.

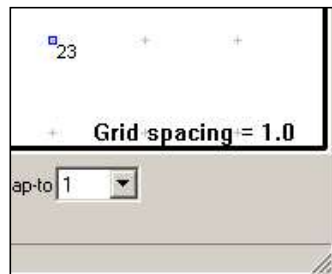
#### 7.4.3 Drawing Surface Information Windows and Settings

There are three drawing surface information windows displaying cursor location, duplicate point tolerance, and the “snap-to” tolerance, as shown in the figure below.



- The cursor location window displays the coordinates of the cursor relative to the scale of the drawing surface.
- The “duplicate point tolerance” defines how close two mouse clicks can be set before NASBEM considers them to be one and the same point. The intent of this setting is to make it easier for the user to click on a previously defined point by allowing the user to click near the point without having to hit it exactly. Note that although the duplicate point tolerance can be set independently of the snap-to value, any change to the snap-to value will automatically set the duplicate point tolerance to one half of the snap-to value.
- The “snap-to” value is a “nearness” tolerance which allows mouse clicks to mark locations on the drawing surface without having to get the mouse cursor exactly on the desired spot. For example, the default value of 1 forces the x and y coordinates of points created with the drawing tools to be “snapped” to the nearest integer relative to where the mouse was actually clicked. This setting can be changed to smaller values by factors of 10, so that a value of 0.1 forces coordinates to be “snapped” to the nearest tenth, and so on. Note that although the duplicate point tolerance can be set independently of the snap-to value, any change to the snap-to value will automatically set the duplicate point tolerance to one half of the snap-to value.

Finally, as shown in the figure below, near the bottom right corner of the drawing surface itself is a label containing the current grid spacing on the drawing surface, that is, the distance between the light grey “+” marks on the drawing surface.



## 7.5 Information Tables

As the drawing tools are used, NASBEM automatically fills in the Information Tables on the various notebook tabs. These tables contain all the information necessary to completely define the problem to be solved. At any time during the problem definition phase the contents of the Information Tables can be examined and changed by manually editing the tables. The tables have useful editing functions accessible by right-clicking the mouse on a table.

Editing could be useful, for example, to correct point coordinates if the drawing tools had difficulty getting a mouse click to correspond to the desired decimal digit. Such editing changes will cause the internal information buffers to be updated immediately; however, to see

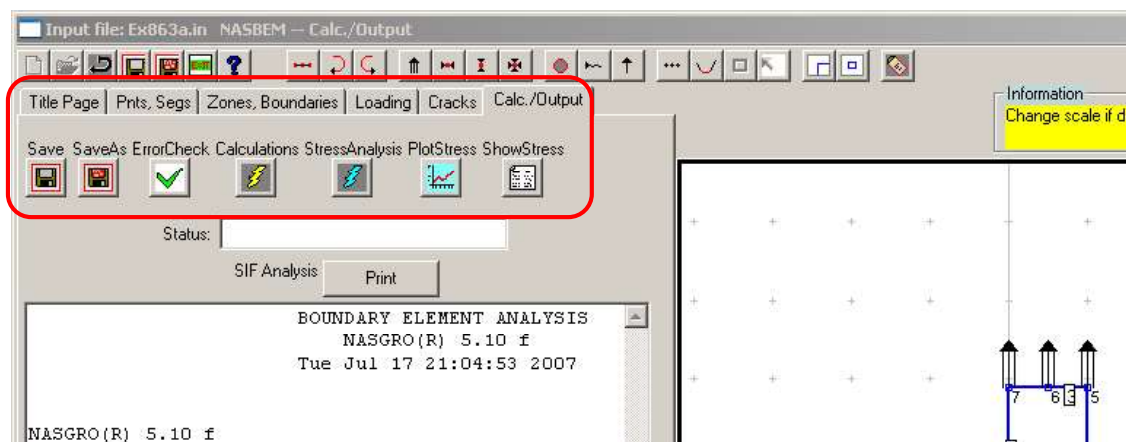
changes reflected on the drawing surface usually requires a manual refresh (see using the “Replot” button in the section on utility buttons above).

However, editing is required to change some of the default settings assigned by NASBEM during use of the drawing tools. For example, the default number of elements per segment is 2, but that number should be tailored to the problem at hand.

**Note: If any table is edited manually care must be taken that all other tables affected by that particular change are updated. For example: when defining a segment by adding segment endpoints to the segment table, the user must ensure that the points referenced in that table are also defined in the points table.**

## 7.6 The Calculations Page

When problem definition is complete, calculations are started from the “Calc./Output” notebook page. As shown in the figure below, the row of buttons at the top of this notebook page (not to be confused with the main drawing toolbar at the top of the NASBEM window) contains buttons for various bookkeeping tasks, starting the problem solution process, and performing post-processing stress calculations.



Note that for purposes of illustration all the buttons in the figure above are displayed as “enabled”, i.e. available for use, at the same time. In actuality the “Stress Analysis” button does not become enabled until the main computations are complete (or an input file is loaded that was previously used and computed, and its output files still exist). The “Plot Stress” and “Show Stress” buttons do not become enabled until a stress computation is complete (or an input file is loaded that was previously used and computed, and its output and stress files still exist).

- The “Save file” and “Save file as” buttons are duplicates of the buttons found in the main toolbar and perform the same functions.
- “Error Check” – select this button to check input data for errors, omissions, and completeness. While it is impossible to check for all possible pathologic situations,

NASBEM makes an effort to catch the most common input errors such as boundaries that are not closed, or boundary segments that are not contiguous.

-  “Calculations” – select this button when data input is complete and you wish to run the BEM to compute SIFs and/or stresses. Note that this option automatically first invokes the error check described above before launching any computations. When calculations are complete, computed stress intensity factors and crack profiles (crack opening displacements) will be displayed automatically in the upper output window, while the lower window contains the computed boundary tractions and displacements.
-  “Stress Analysis” – select this button to perform stress analysis after the main calculations are finished (as indicated in the status window below these buttons). A pop-up window will prompt the user for the manner of input of the locations at which to calculate stress (individual points, points along a straight line, or points on a circular arc) as well as any required information.
-  “Plot Stress” and  “Show Stress” – select one of these buttons to display the stresses as a plot with respect to distance along the line of interest, or in tabular form.

## 7.7 Operational issues

This section describes operational issues of interest to the user: how big can a model can be (i.e. how many points, segments, etc the model can contain), and what files are created during a run.

### 7.7.1 Numerical Limits on Input Items - how big can a model be?

The limits on array sizes (and thus problem sizes) are as follows:

- Maximum number of points = 1024
- Maximum number of boundary segments = 512
- Maximum number of boundaries = 20
- Maximum number of zones = 20
- Maximum number of crack segments = 200
- Maximum number of cracks = 20
- Maximum number of materials = 20
- Maximum number of point loads = 100
- Maximum number of segments per boundary = 512
- Maximum number of elements per boundary = 1024
- Maximum number of elements per crack = 200
- Maximum number of segments per crack = 200
- Maximum number of boundaries per zone = 20
- Maximum number of cracks per zone = 20

Note that these limits are absolute, not multiplicative. For example, the limit on the total number of cracks is 20, not the maximum allowed number of cracks per zone multiplied by the maximum allowed number of zones (20x20).

### 7.7.2 Program Output and Files Created During a Run

During a run NASBEM creates the following files:

- BEMDAT.TMP: this is an auxiliary file for use by the BEM computational engine.
- BEMDAT.OT1: this file contains SIF results (when calculated). For internal cracks SIF's are listed for the first tip and the second tip, where "first" and "second" refer to the crack tips in the order they were specified by the user. For the special case of a single-straight crack evaluated at multiple sizes, the SIF's are listed for the crack sizes corresponding to the user-specified number of calculation steps.
- BEMDAT.OT2: this file contains displacements and tractions at each boundary node and, if applicable, the displacements at each crack face node.
- BEMSIG: this file contains stress analysis results, if applicable. One can elect to do multiple stress calculations for the same problem; stress results are continually appended to this file until a new problem is started or the program is terminated.

When the user deems the analysis of a problem to be complete (either by "starting over" or by quitting the program), NASBEM will rename the aforementioned files to contain the name of the file in which the input is saved. For example, if the input file name is "test.in", then

- "BEMDAT.TMP" becomes "test.tmp".
- "BEMDAT.OT1" becomes "test.ot1".
- "BEMDAT.OT2" becomes "test.ot2".
- "BEMSIG" becomes "test.ot3".

In addition, for the special case of a single straight crack evaluated at multiple lengths, the aforementioned files (except BEMSIG, since post-processing stress analysis is not available for this case) are created for each crack size. For these three files the new names also include the label "size", followed by the sequence number of the crack size.

## 7.8 Theory of Stress Analysis

As noted in a preceding section, in versions of NASBEM prior to 5.11, stress analysis was possible only in zones without cracks; this required defining multiple zones made of the same material, some with cracks and some without, for cases in which one needed both SIF and stress analysis. As of this writing it is possible to perform stress analysis in zones with cracks as long as the point of interest is in a strip of half-width  $R$ , 2 crack-element lengths wide, on either side of the crack line and extending no farther than  $R$  beyond the crack tip. It is planned to implement complete stress analysis capability in zones with cracks in a future version of NASBEM.

Special means have been used to overcome the “boundary layer” effect [47], the decay in accuracy in stress and strain as the boundary is approached that is commonly experienced with boundary element techniques. The stress computing algorithms have been tested on several geometries and found to yield acceptably accurate values at all locations within the bodies up to and including their boundaries.

The program allows the specification of points for computing stresses in one of three ways: (a) point by point, (b) straight (or quadratic) line, and (c) circular arc subtending any angle about any point. The output is presented in tabular form or plotted as a function of distance (or angle) along the line (or arc) of interest.

In developing expressions for stresses that are valid for all locations within a body, there are three regions that have been considered: (a) the interior, (b) the boundary, and (c) a narrow boundary layer adjacent to the boundary elements. Different sets of stress expressions are employed for each of these regions. For a point in the boundary layer, stresses are obtained by interpolation between proximal boundary and interior points.

### 7.8.1 Stresses in the Interior

In the standard Boundary Integral Equation formulation, stresses in the interior of the body are obtained from the strains. The strains are obtained by taking appropriate partial derivatives of the displacements, given by

$$u_\alpha(p) = \int_{\Gamma} [t_\beta(Q)U_{\alpha\beta}(p,Q) - u_\beta(Q)T_{\alpha\beta}(p,Q)]dQ \quad (7.1)$$

Here  $p$  is the point of interest (in the interior), and  $Q$  is a generic point on the boundary  $\Gamma$ ;  $t_\beta$  and  $u_\beta$  are the boundary tractions and displacements; and  $U_{\alpha\beta}$  and  $T_{\alpha\beta}$  are the displacement and traction kernels. The kernels, (with  $\alpha=1,2$ ) are given by

$$U_{\alpha\beta} = \frac{1}{8\pi(1-\bar{v})G} [(-3 + 4\bar{v})\delta_{\alpha\beta} \ln r + r_{,\alpha} r_{,\beta}] \quad (7.2)$$

$$T_{\alpha\beta} = -\frac{1-2\bar{v}}{4\pi(1-\bar{v})r} \left[ \left\{ \delta_{\alpha\beta} + \frac{2r_{,\alpha} r_{,\beta}}{1-2\bar{v}} \right\} \frac{\partial r}{\partial n} - r_{,\alpha} n_\beta + r_{,\beta} n_\alpha \right] \quad (7.3)$$

where  $G$  is the shear modulus and  $\bar{v}$  equals  $v$  for plane strain (or  $v/(1+v)$  for plane stress) and  $v$  is Poisson's ratio;  $r$  is the distance between the source point  $p$  and the field point  $Q$ , and a comma beside the  $r$  denotes a derivative with respect to the corresponding coordinate of the field point;  $n_\beta$  denotes the components of the unit outward drawn normal (to the boundary) at  $Q$  and  $\partial r/\partial n$  is the derivative of  $r$  with respect to this normal; and  $\delta_{\alpha\beta}$  is the Kronecker delta.

In order to overcome the problem of diminished accuracy near the boundary, a consequence of the singularity in  $T_{\alpha\beta}$  as  $r \rightarrow 0$ , an alternate kernel is developed in [48]. This is expressed as

$$W_{\alpha\beta} = \frac{1}{4\pi(1-\bar{\nu})} \left[ 2(1-\bar{\nu})\phi\delta_{\alpha\beta} + \varepsilon_{\beta\gamma} r_{,\alpha} r_{,\gamma} + (1-2\bar{\nu})\varepsilon_{\alpha\beta} \ln r \right] \quad (7.4)$$

where  $\phi$  is the angle made by the join of the source and the field points with the x-axis, and  $\varepsilon_{\alpha\beta}$  here equals  $\beta-\alpha$ . Interior displacements are shown in [47] being related to this new kernel by the expression:

$$u_{\alpha}(p) - u_{\alpha}(\hat{P}) = \int_{\Gamma} t_{\beta}(Q) U_{\alpha\beta}(p, Q) - \frac{\partial u_{\beta}(Q)}{\partial s} W_{\alpha\beta}(p, Q) ds \quad (7.5)$$

where  $\hat{P}$  is the point on the boundary where a line from  $p$  parallel to the x-axis intersects it. Equation (7.5) allows a means (through its partial derivatives) of obtaining the stresses and is so used in the program. The reduced singularity in  $W_{\alpha\beta}$  (as compared to  $T_{\alpha\beta}$ ) allows accurate determination of stresses close to the boundary; the boundary layer is made thinner but not eliminated by these means. In this program, equation (7.5) is used for points farther than  $0.15l$  away from the boundary where  $l$  is the length of the proximal element.

### 7.8.2 Stresses on the Boundary

Stresses at points on the boundary are obtained from the computed boundary tractions and displacements. Referring to the normal and tangential directions at the boundary point of interest by  $\xi$  and  $\eta$ , the stress components  $\sigma_{\xi\xi}$  and  $\sigma_{\eta\eta}$  are related to the tractions by

$$\sigma_{\xi\xi} = t_1 \cos(1, \xi) + t_2 \cos(2, \xi) \quad (7.6)$$

$$\sigma_{\xi\eta} = t_1 \cos(1, \eta) + t_2 \cos(2, \eta) \quad (7.7)$$

The tangential stress component is given by

$$\sigma_{\eta\eta} = E' \varepsilon_{\eta\eta} + \nu' \sigma_{\xi\xi} \quad (7.8)$$

where  $E'$  equals Young's modulus  $E$  for plane stress ( $E/(1-\nu^2)$  for plane strain) and  $\nu'$  equals  $\nu$  for plane stress ( $\nu/(1-\nu)$  for plane strain). Finally, the tangential strain  $\varepsilon_{\eta\eta}$  is related to the boundary displacements by

$$\varepsilon_{\eta\eta} = \cos(1, \eta) \frac{\partial u_1}{\partial \eta} + \cos(2, \eta) \frac{\partial u_2}{\partial \eta} \quad (7.9)$$

Stress components in the normal and tangential directions are obtained from equations (7.6), (7.7) and (7.8), from which components in the x- and y- directions are readily obtained.

### 7.8.3 Stresses in the Boundary Layer

For locations in the boundary layer, defined in the implementation as a layer adjacent to the boundary of thickness  $0.15l$ , where  $l$  is element length, a process of interpolation between the proximal boundary and interior points is carried out. Note that as  $l$  is not, in general, uniform throughout, the thickness of the boundary layer varies as one travels along the boundary.

The process is straightforward if the point of interest is within the exclusive boundary layer of a single element. Complications arise when the point falls in the inter-elemental region common to adjacent elements.

Figure 69 shows the four types of inter-elemental boundary regions that arise depending upon the angle made by element 2 with respect to element 1 at the point of intersection  $P_0$ , elements 1 and 2 being approximately equally proximal to the point of interest. Regions I and II refer to parts of the boundary layer where the interpolation is based on boundary points located on either (but not both) of the two elements. However, if the point of interest is within any of the inter-elemental triangles:  $\Delta P_0P_1P_m$  or  $\Delta P_0P_mP_2$  (Type 1),  $\Delta P_0P_3P_a$ ,  $\Delta P_0P_aP_b$ , or  $\Delta P_0P_4P_b$  (Type 3), or  $\Delta P_0P_3P_m$  or  $\Delta P_0P_mP_4$  (Type 4), triangular interpolation is carried out to compute the stresses, the vertices of these triangles lying either on the boundary or considered to be in the interior. Note that although straight lines are used in Figure 69 to represent the elements and the boundary layer, they are not, in general, straight but are curvilinear instead. The implementation in the program takes this into account.

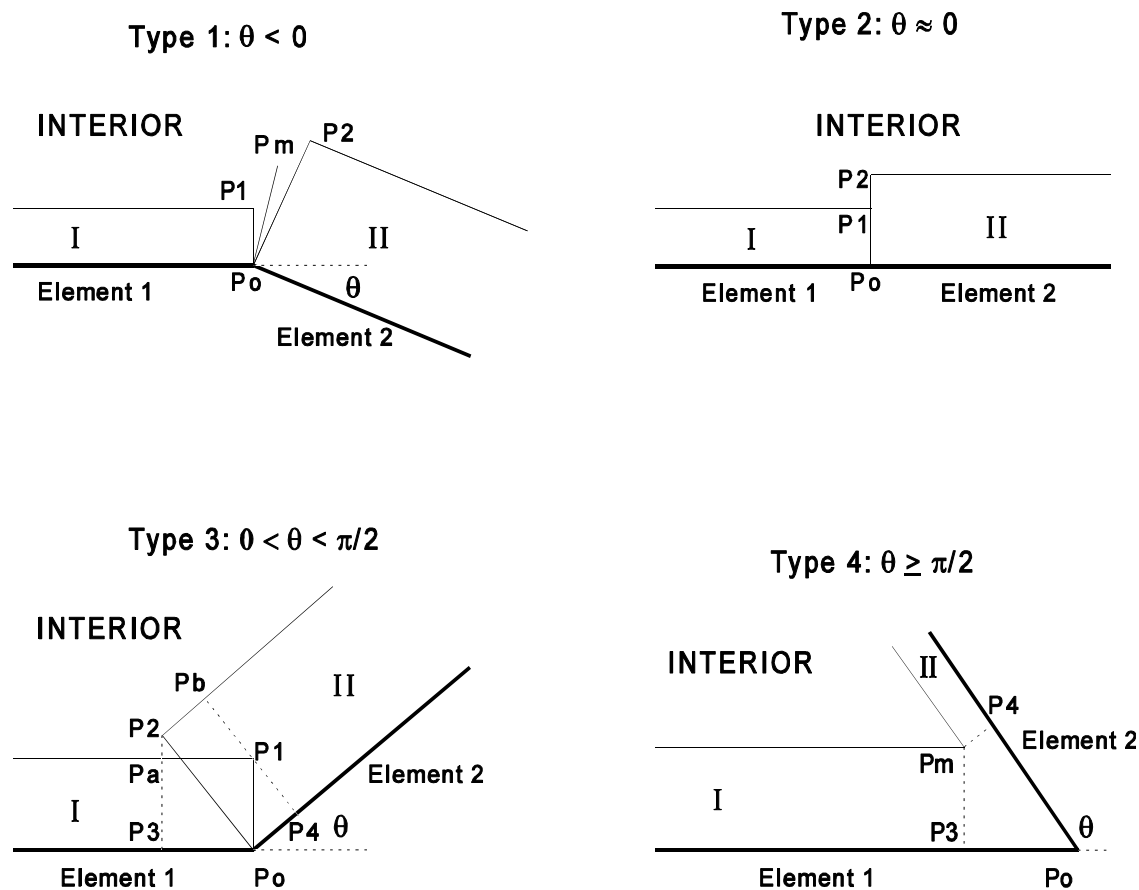


Figure 69 – Element intersection types

## **Acknowledgments**

---

The task of developing NASGRO had the participation and cooperation of many individuals working for NASA, Southwest Research Institute, the European Space Agency, the FAA, the USAF, U. S. aerospace contractors, and European aerospace contractors. The development and technical evaluation of this program have been monitored by the NASA Fracture Control Methodology Panel (formed in March 1985) the Interagency Working Group (formed 1993) and the NASGRO industrial consortium being run by Southwest Research Institute (formed in 2001).

## References

- [1] Broek, D., *Elementary Engineering Fracture Mechanics*, 4th edition, Nijhoff, 1985.
- [2] Broek, D., *The Practical Uses of Fracture Mechanics*, Kluwer Academic Publishers, 1989
- [3] Barsom, J. M. and Rolfe, S. T., *Fracture and Fatigue Control in Structures: Applications of Fracture Mechanics*, 2nd edition, Prentice-Hall, Inc., 1987.
- [4] Anderson, T. L., *Fracture Mechanics: Fundamentals and Applications*, CRC Press, 1991.
- [5] Forman, R. G., and Mettu, S. R., "Behavior of Surface and Corner Cracks Subjected to Tensile and Bending Loads in Ti-6Al-4V Alloy," *Fracture Mechanics: Twenty-second Symposium, Vol. 1, ASTM STP 1131*, H. A. Ernst, A. Saxena, and D. L. McDowell, eds., American Society for Testing and Materials, Philadelphia, 1992, pp. 519-546.
- [6] Newman, Jr., J. C., "A Crack Opening Stress Equation for Fatigue Crack Growth," *International Journal of Fracture*, Vol. 24, No. 3, March 1984, pp. R131-R135.
- [7] Newman, Jr., J. C. and Raju, I. S., "Prediction of Fatigue Crack-Growth Patterns and Lives in Three-Dimensional Cracked Bodies," *Advances in Fracture Research (Fracture 84)*, Sixth International Conference on Fracture, Vol. 3, 1984, pp. 1597-1608.
- [8] Forth, S. C., Newman, Jr., J.C., and Forman, R.G., "Evaluation of Fatigue Crack Thresholds Using Various Experimental Methods," *Fatigue and Fracture Mechanics: 33<sup>rd</sup> Volume, ASTM STP 1417*, W.G. Reuter and R.S. Piascik, Eds., American Society for Testing and Materials, West Conshohocken, PA, 2002.
- [9] Forth, S.C., Newman, Jr., J.C., Forman, R.G., "Generating Fatigue Crack Growth Thresholds With Constant Amplitude Loads," to be presented at *Fatigue 2002* Conference.
- [10] ASTM standard test method E 647, American Society for Testing and Materials, West Conshohocken, PA,
- [11] Tanaka, K., Nakai, Y., and Yamashita, M., "Fatigue Growth Threshold of Small Cracks," *International Journal of Fracture*, Vol. 17, No. 5, October 1981, pp. 519-533.

- [12] Lindley, T. C., "Near Threshold Fatigue Crack Growth: Experimental Methods, Mechanisms, and Applications," *Subcritical Crack Growth Due to Fatigue, Stress Corrosion, and Creep*, L. H. Larsson, ed., Elsevier Applied Science Publishers, New York, pp. 167-213, 1985.
- [13] Schmidt, R. A. and Paris, P. C., "Threshold for Fatigue Crack Propagation and Effects of Load Ratio and Frequency," *Progress in Flaw Growth and Fracture Toughness Testing*, ASTM STP 536, American Society for Testing and Materials, Philadelphia, 1973, pp. 79-94.
- [14] Yoder, G. R., Cooley, L. A., and Crooker, T. W., "A Critical Analysis of Grain-Size and Yield Strength Dependence of Near Threshold Fatigue Crack Growth in Steels," *Fracture Mechanics: Fourteenth Symposium -- Vol. I: Theory and Analysis*, ASTM STP 791, J. C. Lewis and G. Sines, eds., American Society for Testing and Materials, Philadelphia, 1983, pp. 348-365.
- [15] Vroman, G. A., "Material Thickness Effect on Critical Stress Intensity", Monograph #106, TRW Space & Technology Group, February 1983.
- [16] Forman, R. G. and Henkener, J. A., "An Evaluation of the Fatigue Crack Growth and Fracture Toughness Properties of Beryllium-Copper Alloy CDA172," NASA-TM-102166, 1990.
- [17] Henkener, J. A., Lawrence, V. B., and Forman, R. G., "An Evaluation of Fracture Mechanics Properties of Various Aerospace Materials," *Fracture Mechanics: Twenty-Third Symposium, ASTM STP 1189*, R. Chona, ed., American Society for Testing and Materials, Philadelphia, 1993, pp. 474-497.
- [18] Orange, T. W., Sullivan, T. L., and Calfo, F. D., "Fracture of Thin Sections Containing Through and Part-through Cracks," *Fracture Toughness Testing at Cryogenic Temperatures*, ASTM STP 496, American Society for Testing and Materials, Philadelphia, 1970, pp. 61-81.
- [19] Willenborg, J., Engle, R. M. and Wood, H. A., "A Crack Growth Retardation Model Using an Effective Stress Concept," AFFDL-TM-71-1-FBR, Wright Patterson Air Force Laboratory, January 1971.
- [20] Gallagher, J. P., "A Generalized Development of Yield Zone Models," AFFDL-TM-74-28-FBR, Wright Patterson Air Force Laboratory, January 1974.
- [21] Gallagher, J. P., Hughes, T.F., "Influence of Yield Strength on Overload Affected Fatigue Crack Growth Behavior in 4340 Steel," AFFDL-TR-74-27-FBR, Wright Patterson Air Force Laboratory, February 1974.
- [22] Newman, J. C. Jr., Private Communication, 1995.

- [23] Brussat, T. R., Private communication, May 1997.
- [24] Chang, J. B. and Engle, R. M. "Improved Damage-Tolerance Analysis Methodology," *Journal of Aircraft*, Vol. 21, 1984, pp. 722-730.
- [25] Ten Hoeve, H. J. and de Koning, A. U., "Implementation of the Improved Strip Yield Model into NASGRO Software - Architecture and Detailed Design Document," National Aerospace Laboratory (NLR) Report: NLR CR 95312L, 1995.
- [26] Paris, P.C., Gomez, M.P., and Anderson, W.P., "A Rational Analytic Theory of Fatigue," *The Trend in Engineering*, Vol. 13, 1961, pp. 9-14.
- [27] Elber, W., "The Significance of Fatigue Crack Closure," *Damage Tolerance of Aircraft Structures*, ASTM STP-486, 1971, pp. 230-242.
- [28] Dugdale, D.S., "Yielding of Steel Sheets Containing Slits," *Journal of Mechanics and Physics of Solids*, Vol. 8, 1960, pp. 100-104.
- [29] Chang, J.B., "Round-Robin Crack Growth Predictions on Center-Cracked Tension Specimens under Random Spectrum Loading," *Methods and Models for Predicting Fatigue Crack Growth under Random Loading*, ASTM STP 748, J.B. Chang and C. M. Hudson, Eds., American Society for Testing and Materials, 1981, PP. 3-40.
- [30] Ball, D., Private communication, March 2001.
- [31] Lawrence, V. B. and Forman, R. G., "Structure and Applications of the NASA Fracture Mechanics Database," *Computerization and Networking of Materials Databases: Third Volume*, ASTM STP 1140, American Society for Testing and Materials, Philadelphia, 1992.
- [32] Hudson, M. C. and Seward, S. K., "Compendium of Sources of Fracture Toughness and Fatigue Crack Growth Data for Metallic Alloys," *International Journal of Fracture*, Vol. 14, 1978, pp. R151-R184.
- [33] Hudson, M. C. and Seward, S. K., "Compendium of Sources of Fracture Toughness and Fatigue Crack Growth Data for Metallic Alloys," *International Journal of Fracture*, Vol. 20, 1982, pp. R59-R117.
- [34] Gallagher, J., *Damage Tolerant Design Handbook*, University of Dayton Research Institute, prepared for Air Force Wright Aeronautical Laboratories, Wright-Patterson Air Force Base, Ohio, December 1983.
- [35] E 616-89, "Standard Terminology Relating to Fracture Testing," *1993 Annual Book of ASTM Standards*, Vol. 3.01, American Society for Testing and Materials, Philadelphia, 1993, pp. 647-658.

- [36] Brodeur, S. J., Basci, M. I., and Latimer, M. W., "Fracture Mechanics Loading Spectra for STS Payloads," AIAA-83-2655-CP, Goddard Space Flight Center, Greenbelt, Maryland, 1983.
- [37] AE-10 Fatigue Design Handbook, 2<sup>nd</sup> Edition, Society of Automotive Engineers, 1988.
- [38] E 1049-85, Standard Practices for Cycle Counting in Fatigue Analysis, American Society for Testing and Materials, Philadelphia, 2005.
- [39] Wiederhorn, S. M., Evans, A. G., Fuller, E. R., and Johnson, H., "Application of Fracture Mechanics to Space-Shuttle Windows," American Ceramic Society, July 1974, pp. 319-323.
- [40] Wiederhorn, S. M., "Dependence of Lifetime Predictions on the Form of the Crack Propagation Equation," *Fracture* 1977, Vol. 3, 1977, pp. 893-901.
- [41] Schwartzberg, F. R., Kiefer, T. F., and Rothermel, L. J., "Strength and Fracture Behavior of MDA Window Materials," MCR-73-27, Final Report for Contract NAS8-24000, Martin Marietta Corporation, Denver, Colorado, January 1973.
- [42] Salem, J. A., and Calomino, A. M., "Slow Crack Growth and Fracture Toughness of Sapphire for The International Space Station Fluids and Combustion Facility," Draft Report, NASA Glenn Research Center, Cleveland, Ohio.
- [43] Braun, L. M., Wallace J., and Fuller, E. R. Jr., "Fracture Mechanics and Mechanical Reliability Study of Chemcor Glass," Draft Report, NIST Ceramics Division, Gaithersburg, Maryland, November 1998.
- [44] Braun, L. M., Wallace J., and Fuller, E. R. Jr., "Fracture Mechanics and Mechanical Reliability Study Comparison of Corning Code 7980 and Code 7940 Fused Silica," Draft Report, NIST Ceramics Division, Gaithersburg, Maryland, November 1998.
- [45] SSP 30560, "Glass, Window, and Ceramic Structural Design and Verification Requirements," National Aeronautics and Space Administration, Space Station Freedom Program Office, Reston, Virginia, June 1991.
- [46] Henkener, J. A. and Forman, R. G., "Fatigue Crack Growth and Fracture Toughness Data for Selected Space Systems Structural Alloys," JSC 24976, NASA Lyndon B. Johnson Space Center, Houston, Texas, March 1991.
- [47] Chungchu Chang, "A Boundary Element Method for Two Dimensional Linear Elastic Fracture Analysis", Ph.D. Dissertation, The University of Texas at Austin, December 1993.

- [48] Ghosh, N., Rajiyah, H., Ghosh, S., and Mukherjee, S., 1986, "A New Boundary Element Method Formulation for Linear Elasticity", *Journal of Applied Mechanics*, Vol. 53, pp. 69-76.
- [49] Ecord, G. M., Apollo Experience Report – Pressure Vessels, NASA TN D-6975, September 1972